Quantitative Definition of Phenotypic Variation in Land Snail Shells

Hannah Jayne Jackson

Thesis submitted to the School of Life Sciences, University of Nottingham for the degree of Doctor of Philosophy

September 2021

Abstract

The study of both animal colouration and patterning across the natural world has been imperative for understanding some of the key principles of biology throughout the past century, particularly with respect to evolution and genetics. Generally, colour and pattern have each been described qualitatively, often being binned into discrete groups relying on human perception of colour or pattern, rather than being considered in a biologically relevant context. 'Binning' traits into discrete groups has the consequence that variation within discrete morphs is often overlooked. Terrestrial gastropods, such as the selected study genera *Cepaea* and *Auriculella*, provide an ideal system for the study of polymorphisms and colour variation due to the extreme variety of morphs present across the taxa, as well as the nature of shell growth providing a complete ontogeny of an individual.

The aims of this thesis are threefold; firstly, I aimed to understand fine-scale variation within and between established banding pattern morphs in *Cepaea*, to allow inferences to be made regarding the genetic mechanisms responsible for this variation. The implementation of two quantitative methods for measuring variation in band position and width in individual shells found that individual band absence has a minor but significant effect on the position of the remaining bands, implying that the locus controlling band presence/absence acts mainly after the position of bands is determined. I establish a method which is useful for comparative studies of quantitative banding variation in snail shells, and for extraction of growth parameters and morphometrics, highlighting the importance and usefulness of gastropod shells in the understanding of how variation is established and maintained in a population.

Secondly, I aimed to understand the shell colour variation present in both *Cepaea nemoralis* and *Cepaea hortensis* by using spectrophotometry and psychophysical modelling in tandem. It was revealed that colour variation in *Cepaea hortensis* is continuous, with no detectable effects of geographic location with the exception of an association of the paleness

of yellow shells with latitude. Differences between the colour of *Cepaea hortensis* and *Cepaea nemoralis*, both in terms of exact shade and overall colour were revealed*; Cepaea hortensis* are generally paler, and less pink-toned, but slightly more brown-toned. Precise shade variation of yellow individuals from genetically diverse lineages of *Cepaea nemoralis* were also detected. The results presented have significance in furthering the understanding of the precise nature of the colour polymorphism displayed in *Cepaea* spp., and the nature of the selection which acts upon it, as well as highlighting the importance of considering colour as a continuous trait, rather than binning it into discrete groups.

Thirdly, I aimed to investigate colour variation across a number of scales in the Hawaiian land snail genus *Auriculella*, to allow inferences about the genetic architecture responsible for the variation, and to highlight the usefulness of museum collections of gastropod shells in understanding variation in extinct or endangered species. I demonstrated that there are differences in colour within single shells of *Auriculella*, similar to variation displayed by other Pacific Island snails. I described significant variation between isolated populations of the same species, and determined that there is no difference in colour variation between shells on the islands of Maui and Oahu. Finally, I demonstrated that there is no difference in colour between shell chiralities, suggesting that interchiral mating is not uncommon, and that the loci responsible for colour variation and chirality are not closely linked. By describing the variation present in *Auriculella* in a biologically relevant context, inference regarding genetic mechanisms of variation becomes possible in a taxa of conservation concern.

By achieving these aims, and synthesising conclusions drawn from their achievement, I have highlighted the importance of accurately defining phenotypes for the purposes of evolutionary ecology and genetics. Defining phenotypes and investigating variation present within morphs has allowed inferences to be made regarding the underpinning genetic mechanisms which control variation in two gastropod genera, although the principles are applicable to other taxonomic groups. Finally, and more

broadly, I have demonstrated the usefulness of gastropods as study systems, particularly where large collections of shells are available.

Acknowledgements

Thanks must also go particularly to those who have dragged me kicking and screaming over the finish line – Georgie, Nancy, Davis, Tyler, Paddy, Laura, other Laura, Ella, Charlotte, and Jack. Thanks for getting me through the absolute hellscape that has been 2021, and for still being my friends despite my writing-induced grumpiness. Also, Alex Tarr – thankyou so much for helping me stick this entire thesis together, for sorting out my chaotic formatting, and for never once saying "you should probably have thought about this earlier"…

Finally, thanks to my utterly ridiculous and completely mad family, for your never-ending support and for always pushing me to do my best. For letting me cry down the phone when it all got a bit much, and for always believing in me. Your kind words and support kept me going through the inevitable ups and downs. You are all always around for a bit of silliness, and that has made more of a difference than you can possibly imagine. Particularly you Mum, I am more grateful to you than you will ever know.

Declaration

I declare that this thesis is the result of my own work, unless otherwise stated. It has not been presented as part of any other degree.

"For observing nature, the best pace is a snail's pace"

- *Edwin Way Teale*

Table of Contents:

List of Figures:

[x]

List of Tables:

Chapter 1: Introduction

1.1 Polymorphisms

According to Darwin's theory of evolution by natural selection (1859), heritable phenotypic variation between individuals of a population is imperative for natural and sexual selection to occur. A species may be defined as polymorphic under the condition that there are multiple discrete phenotypes, or "morphs", present in a given interbreeding population, where the least common morph is present at a higher frequency than would be expected if its existence were the result of random mutation events alone (Ford 1945, Huxley 1955, Gray and McKinnon 2007). In other words, a species is polymorphic when phenotypic variation within and between populations of a single species is caused and subsequently maintained by two or more alleles, each with considerable recurrence. A polymorphism may be defined as either transient or balanced, depending on the variation of morph frequencies over time (Ford 1945, Forsman 2016). If relative morph frequencies vary consistently over time, eventually leading to monomorphism, the polymorphism is transient; if morph frequencies remain largely stable at a fixed level of equilibrium defined by selective environmental or genetic factors, the polymorphism is balanced. Transient polymorphisms are maintained only whilst a gene is spreading throughout a population; once the presence of the new mutation has surpassed the previous one, or at least reduced it to a rarity, the presence of the polymorphism in the population is effectively terminated. A transient polymorphism occurs during the interim period where an advantageous character spreads through a population, uninhibited.

A balanced polymorphism occurs when the spread of a characteristic in a population is halted at some level during its course, so as to produce a stable equilibrium (Forsman 2016). Both the favoured character and the

barrier placed upon its spread may be genetically or environmentally controlled. A species possessing a balanced polymorphism may be monomorphic in some parts of its range, and polymorphic in others, depending on local selection pressures. The temporal shift of environmental conditions and other selective processes means that, even within "true" balanced polymorphic populations, relative morph frequencies are often expected to change and oscillate in response to a varying selective environment (Ford 1945, McLean and Stuart-Fox 2014, Forsman 2016).

Balanced polymorphic species, henceforth referred to as simply "polymorphic" species, provide a tangible link between genotype and outwardly expressed phenotype, and have historically provided an ideal source of phenotypic variation with which to study selective processes (Gillespie and Oxford 1998). Genetic variability within a species is necessarily present due to alterations which are either harmful, neutral, or beneficial to the species in question. The majority of mutations are thought to be neutral, meaning they do not influence the fitness of an individual in either a positive or negative manner (Ford 1975). When mutations are either harmful or beneficial, selective forces work to increase the prevalence of, or to remove, said mutation within a population. Polymorphisms are known to have survived speciation events (Jamie and Meier 2020), therefore are unlikely to be selectively neutral, but rather to be beneficial, although it is important to note that processes such as drift and founder effects can also impact balanced polymoprhisms(Brisson 2018). This is compounded by a number of studies suggesting that the presence of a polymorphism in a population reduces extinction risk, and founder groups demonstrate better establishment success when there is a higher degree of genetically determined polymorphism present (Forsman and Hagman 2009, Wennersten et al. 2012, Forsman 2016). The lack of selective neutrality in the presence of polymorphisms suggests evidence for the role of

directional natural, or sexual, selection in the maintenance of such polymorphisms in natural populations.

The simplest forms of polymorphisms, dimorphisms, are limited to the presence of two morphs within a population and are often associated with the sex of an organism, with males and females of the same species having markedly disparate phenotypic traits (Kottler 1980b, a). It is thought that polymorphisms in general, but sexual dimorphisms in particular, often evolve in the context of complex interplay between natural and sexual selective processes (Shine 1989, Hodge et al. 2020). Ornamentation, elaborate behavioural displays, and conspicuous colouration evolve in response to mate choice, although there are likely substantial mortality costs to conspicuousness, favouring drab, inconspicuous colouration, and reduced ornamentation (Endler 1980, Andersson 1982, Clutton-Brock 2007). The interaction between these selective pressures may act to generate phenotypic variation *within* the two discrete morph types, as well as between them (Andersson 1982, Hodge et al. 2020). Behavioural, morphological, and physiological sexual dimorphisms are commonplace in the Lepidoptera (Allen et al. 2011), with several examples of elaborate male ornamentation and exaggerated traits for courtship and mate attraction. The polymorphisms present in the Lepidoptera are not exclusively intersexual dimorphisms, with several examples of within-sex polymorphisms observed across the taxa, such as female-limited mimetic colour patterns (Kemp 2007, Kunte 2009).

Polymorphisms may also be entirely more complex than a single allelic change resulting in the presence of a dimorphism. An example of a highly complex polymorphism with multiple discrete morphs can be seen in the strawberry poison frog, *Dendrobates pumilio* (Siddiqi et al. 2004). There are at least 15 discrete colour morphs of the strawberry poison frog across and within geographic localities in the Bocas del Toro region of Panama; these colour morphs include red, yellow, blue, and lime green

(Hegna et al. 2013). The colour variation across morphs is an effective signal to both conspecifics in mate choice experiments, and to predators as an aposematic warning signal (Limerick 1980, Summers et al. 1999). The dorsal colouration of *D. pumilo* tends to be less heavily saturated than the ventral colouration; dorsal colours are thought to be important in signalling to predators, and ventral colours in signalling to conspecifics (Siddiqi et al. 2004). Dorsal spots are also present in some individuals of *D. pumilo*, and the size and number of these spots varies with colour morph (Hegna et al. 2013).

Morph ratios vary clinally in many polymorphic species, with a gradual change in morph frequencies across the distributional range of a species (Takahashi et al. 2011). Clines of variation may be present in any given polymorphic population, whereby some selective influence creates gradients of change across quantitative phenotypic traits across populations of a species (Amar et al. 2014). These clines may either be concordant with discontinuities or occur along an area of seemingly homogeneous environment (Clarke 1966). Clarke argues that a morph ratio cline may be impacted due to various parameters, but that if the environment remains stable, the slope may only be influenced by the spread of mutants or recombinants (ie gene flow across populations occurring along the cline). A smooth morph ratio cline has been suggested to be the product of two conflicting forces – local selection and gene flow, which may respectively act to increase and reduce phenotypic variation in a population (Takahashi et al. 2011). Any gene which has differential effects on the selective values of allelic variation may be classified as a "modifier" of a cline, and can impact its slope in various ways such as steepening, flattening, or creating steps (Clarke 1966).

1.1.1 Maintenance of polymorphisms

As both selection and drift tend to impact genetic variation in local populations (Gray and McKinnon 2007, Takahashi et al. 2010), understanding the mechanisms of maintenance of genetic variation,

particularly in polymorphic species, presents a longstanding problem in evolutionary biology. Directional selection may act to reduce genetic variation in a population, whilst also having the ability to temporarily increase variation when a new allele is spreading through a population. Polymorphisms such as those described above may be maintained in a population by a variety of mechanisms, such as assortative mating, pleiotropy, and negative frequency dependent selection.

Assortative mating

Assortative mating is a form of sexual selection in which mate choice is non-random (Jiang et al. 2013). It can be positive, where individuals with similar phenotypes mate with one another more frequently than would be expected under random mating conditions, or negative (also referred to as disassortative mating), where the inverse is true. Positive assortative mating is hypothesised to be involved in the maintenance of the throat patch colour polymorphism in the lizard genus *Podarcis*, where over a period of six years, homomorphic male-female pairs were significantly more common than heteromorphic pairs in the wild (Pérez i de Lanuza et al. 2012). Assortative mating maintains phenotypic differences in a population by stabilising variation, which preserves genetic and phenotypic differences, particularly in the context of sympatric speciation (Fronhofer et al. 2011).

Pleiotropy

Pleiotropy refers to a scenario where a single gene effects multiple traits (Jamie and Meier 2020). Pigmentation differences are associated with pleiotropic differences in a variety of behaviour types in *Drosophila melanogaster*, including associations with courtship behaviour. A secondary sexual trait which can be displayed in *D. melanogaster* is a male-specific melanin wing spot (Yeh et al. 2006), males who possess

this wing spot exhibit differences in courtship behaviours to those individuals without. It is thought that sexual selection by differences in female mate choice maintains the two traits for a joint function, and it is likely that genetic linkage and pleiotropy function in tandem in the co-evolution of these traits (Yeh et al. 2006, Wittkopp and Beldade 2009). Outside of genetic model systems, circumstantial evidence of pleiotropy is often inferred from collinearity of traits, however these correlations could occur due to genetic linkage, shared environmental conditions, or selection pressures impacting multiple traits (Wittkopp and Beldade 2009).

Negative frequency dependent selection

Negative frequency dependent selection (NFDS) occurs when rare alleles are favoured in a population (Svensson 2017). NFDS can occur under a number of circumstances, such as preferential selection by parasites, or with visual selection by predators. In the case of parasitism, individuals with a common allele will be preferentially parasitised, and reduce in frequency (Ebert and Fields 2020). NFDS by visual selection occurs when a predator disproportionately focuses efforts on more common morphs in a population, giving rare morphs a selective advantage (Holmes et al. 2017). It is thought that NFDS is implicated in the maintenance of several polymorphisms, including the human histocompatibility polymorphisms where, counterintuitively, immunological interactions resulting from differences between the histocompatibility complex of a mother and offspring may render more viable offspring (Clarke and Kirby 1966), and the damselfly *Ischnura senegalensis* (Takahashi et al. 2010), in which females are dimorphic. Prey selection which favours a common morph causes an increase in relative frequency of the rare morph over time, until it is more common than the previous most common morph, and a cyclical process of morph frequency oscillation begins.

Several predator prey relationship systems which rely on NFDS centre around the search image hypothesis, which was first proposed by Tinbergen (1960), and suggested that perceptual processes occurring in a predator resulted in the formation of a "search image", whereby prior experience with prey types facilitates the detection of the same morphological type in subsequent encounters (Punzalan et al. 2005). A predator is likely to encounter a common morph in a given population, and if found to be palatable, form a search image for said morph, resulting in preferential predation of the common morph.

1.2 Colour variation

The study of colour polymorphisms across the natural world has been imperative for understanding some of the key principles of biology throughout the past century, particularly with respect to evolution and genetics. Early studies of colour formed the basis for understanding basic Mendelian inheritance (Hurst 1906, Wheldale 1907), and how natural and sexual selection operate in wild populations, where colour is used as a method of signalling to both conspecifics and predators (Endler 1990, Weaver et al. 2017). Colour and colour patterns may be used in thermoregulation, predator avoidance, status signalling, and mate selection.

Species which display colour variation are useful model systems for several reasons. Firstly, many colour morphs have a simple genetic basis, so colour can provide a tangible link between genotype and phenotype (McLean and Stuart-Fox 2014). The systems in which the mode of inheritance of variation is fully understood are few, but it is these systems which allow the insights into the roles of genetic architecture and genetic variation in driving specific elements of adaptation (Ożgo 2012). In the species which the genetic basis for colour polymorphism has been

elucidated, alternative morphs are often explained by simple Mendelian segregation of few alleles across limited loci (Rankin et al. 2016). Secondly, many colour polymorphic species have discrete morphs which can be scored unambiguously, providing an easy visual marker for examining selection in natural populations, allowing the tracking of morph frequencies across multiple generations to understand how allele frequencies fluctuate spatially and temporally within and between populations (Wellenreuther et al. 2014).

1.3 Pattern formation

Patterns of colouration can also provide a useful visual marker for examining selection, particularly in species where variation in pattern across morphs is present. Whilst colour patterns observed in the natural world may take varying forms, it is hypothesised that in many species, regular banding patterns may be under the control of Turing's reaction diffusion mechanism (RDM) (Turing 1952, Kondo 2002). In short, the RDM is based on the interplay between two diffusible molecules. For the autonomous creation of self-organising patterns, two molecule types are required, an activator and an inhibitor (Meinhardt and Klingler 1987). The activator molecule promotes production of both itself and an inhibitor molecule, whilst the inhibitor works to restrict the activator production (Kondo and Miura 2010). The key to the production of stable waves of molecule presence lies in a difference of diffusion rates between these molecules (Muller et al. 2012). In a single region, the concentration of the activator may be higher than in other regions due to random fluctuation of molecule presence. The self-enhancing properties of the activator will cause the concentration to increase at the centre of a given region, followed by the increase of inhibitor presence. If the diffusion rate of the inhibitor is greater than that of the activator, substantial amounts of inhibitor move towards neighbouring regions, suppressing the activator function, resulting in a decrease of activator concentration in these areas. Decrease of the activator will result in a decrease of inhibitor in the wider

regions, where the activator will become the dominant molecule, thus causing self-production of the activator. Production of the activator cause the cycle to repeat. This results in predictable expression patterns of proteins, which translate into a phenotype consisting of repeating self-organised patterns.

1.4 Signal perception

For colour and pattern variation associated with polymorphisms to be an effective signal, either to conspecifics or to predators, it must first be perceived by a receiver. Traditionally, and until recently, variation was necessarily classified according to a human perceiver. Humans are rarely drivers of the selective processes in either direction, so human perception of variation remains arbitrary (Osorio and Vorobyev 2008, Kelber and Osorio 2010). Instead, an ecologically relevant view of perception should be implemented – this view should consider the visual sensitivities, cognition, and physiology of the colour vision of a potential receiver.

Colour vision can be defined as the ability of an eye to discriminate between light stimuli of varied wavelength compositions independent of signal intensity (Harosi 1996, Jacobs 2012). Vertebrate colour vision is mediated by the presence of retinal cones, which are photoreceptor cells that possess specialised sensory pigments, or opsins (Jacobs 2009). These pigments detect light, and colour vision relies on the extraction of information regarding wavelength distribution from incident photons of this light by these sensory pigments. Wavelength discrimination requires the action of at least two photoreceptor types with spectrally disparate visual pigments (Kelber 2019), and the level of discrimination possible is proportional to the number of cone types and distribution of pigments within these. It is thought that any given preceptor of colour has between

one and five cone types (Harosi 1996), the human visual system centres around three cone types, thus humans are trichromats. Most passerine bird species have tetrachromatic vision, possessing four cone types, allowing the cognition of a broader visual spectrum than trichromats. Many bird species also possess coloured oil droplets within the retina, which selectively filter light and modify photoreceptor sensitivity (Vorobyev et al. 1998, Stavenga and Wilts 2014). Oil droplets act as cut-off filters, absorbing wavelengths below a critical value, thus narrowing the spectral sensitivity function of cones, and reducing the overall quantum catch.

In order to frame colour vision in the context of the visual systems of a perceiver, reflectance spectrophotometry and psychophysical modelling are often used in tandem. Reflectance spectrophotometry is a useful method for accurately and objectively measuring colour, as raw wavelength reflectance spectra allow for interpretation of results in a non-arbitrary way. This is achieved by converting raw data into a representation of how signals are interpreted by specific visual systems with the use of psychophysical modelling techniques (Delhey et al. 2015). Reflectance spectrophotometry relies on the channelling of broad-spectrum light through a series of bifuricating optical wires, and out of a directional probe with a small aperture. The light is reflected off of the specimen, back into the probe, and the wavelengths at which light is reflected from the specimen are recorded as a percentage reflectance across a range of wavelengths, relative to a diffuse white standard with close to 100% reflectance.

Colour vision can be modelled from an objective measure of reflectance across a range of wavelengths by the implementation of psychophysical modelling (Delhey et al. 2015). These models incorporate information on ambient light (irradiance), sensitivity functions of photoreceptors, noise-to-signal ratios of the different photoreceptors in the retina, and the

filtering effects of ocular media and coloured oil droplets found in the cones (Vorobyev and Osorio 1998, Delhey et al. 2015). The key to these models lies in the cone quantum catch of a visual system, that is the degree to which individual photoreceptors absorb and sense wavelengths. Four steps are required to give ecological relevance to objective reflectance measurements from these models (Delhey et al. 2015), firstly it is necessary to obtain cone quantum catches from reflectance spectra. Secondly, these cone quantum catches must be transformed into coordinates of visual space where Euclidean distances reflect perceptual differences. Thirdly, variation is summarised in visual space with the use of principal components analysis (PCA), whilst retaining the original perceptual units. Finally, the main axes of chromatic variation are interpreted. The implementation of these steps allows contextualisation of the colour of an organism as it may be perceived by a receiver.

1.5 The Mollusca

The term "mollusc" refers to individuals belonging to the phylum Mollusca, the second-largest phylum of invertebrate organisms, after the Arthropoda (Parkhaev 2017). There are estimated to be between 85,000-110,000 extant species of mollusc recognised (Brown et al. 2010, Rosenberg 2014), with a remarkable fossil record reaching back to the early Cambrian, 543 million years ago (Kouchinsky 2000). The Mollusca are an incredibly diverse phylum, encompassing a large range of species with enormously diverse body plans and life history strategies, from large predatory squid, to chiton, limpets, and the land snails and slugs (Lindberg 2008). The Mollusca comprises seven classes - the Bivalvia, the Gastropoda, the Cephalopoda, the Scaphopoda, the Aplacophora, the Monoplacophora and the Polyplacophora, but splitting the Aplacophora into the Solenogastres and the Caudofoveata, creating eight classes is debated (Lindberg 2008, Parkhaev 2017). Several species of mollusc, most notably several of those belonging to the

11

bivalves, are economically important as food items, such as mussels, oysters, and clams (Winter et al. 1984, Glaser 2003, Beasley et al. 2005). Molluscs are also being increasingly used as biological monitors of pollution (de Carvalho et al. 2000, Gupta and Singh 2011, El-Gendy et al. 2021).

The Gastropoda, the snails and slugs, represent one of the most diverse groups of molluscs, comprising over two thirds of species belonging to the Mollusca (Brown et al. 2010). Gastropods may inhabit marine, freshwater, or terrestrial habitats (Bouchet 1997, Lydeard et al. 2004), and generally have a single helically coiled shell, although reduction and internalisation of this shell is thought to have repeatedly independently evolved in several slug species (Tillier 1989, Wade et al. 2001, Osterauer et al. 2010, Medina et al. 2011, Johnson et al. 2019). Where a shell is present, there may be a wide range of morphologies, with variation in colour, pattern, shape, and ornamentation observed across the Gastropoda.

1.5.1 Shell colour

Colour polymorphisms appear to be relatively common in terrestrial gastropod shells (Cain and Sheppard 1954, Raffaelli 1982, Chiba 1997, Saenko and Schilthuizen 2021). These polymorphisms are maintained by a variety of selective processes, including predation pressures (Hoagland 1977, Surmacki et al. 2013). For example, shell colours which are more difficult to distinguish from a given background may not be as readily discovered by predators, thus cryptic individuals are favoured through visual selection (Hughes and Mather 1986, Reid 1987). The creation of directional selection by the formation of a search image in an avian predator may cause an increase in fitness in uncommon morphs, leading to a system where variation is maintained through negative frequency dependent selection by a predator (Clarke 1979, Chiba 1999, Johannesson and Butlin 2017). Genetic processes such as drift, founder effects, and population bottlenecks may also affect the colour variation

present in a population (Roulin 2004). In some highly diverse taxa such as *Polymita*, a genus of Cuban land snail famed for their vibrant shells, the explanation for the presence of the vast phenotypic variation remains unclear (Davison 2002, Williams 2017), although it is thought that negative frequency dependent selection by a specialist snail hawk is likely a contributing factor (Davison, pers. comms.). There is also a case for polymorphisms to be maintained by physical selection due to climate, although this is arguably less straightforward than maintenance due to predation pressures (Heath 1975, Cook and Freeman 1986). Simplistically, a lighter shell morph is less likely to overheat in a sunny, exposed environment, whereas a darker morph will warm up more rapidly, which may be advantageous in a cooler environment.

1.5.2 Shell banding patterns

Banding patterns are also a key part of gastropod polymorphisms – many species from the family Helicidae have a pattern of longitudinal bands which vary between individuals (Cook 2017). Variation within these banding patterns is likely also under the control of selective processes; the presence of a banding pattern which covers a large percentage of a light-coloured shell may functionally act as a dark shell in cold, less exposed areas where faster heating is beneficial (Rotarides 1926, Delima-Baron et al. 2017). This is exemplified in the Mediterranean land snail, *Theba pisana*, which displays shell banding pattern polymorphism, in which microhabitat selection is strongly associated with banding pattern; fully banded snails, or individuals possessing shells with heavily pigmented bands tend to migrate to shadier areas (Hazel and Johnson 1990, Johnson 2011). This difference in microhabitat choice represents a form of climatic selection which has been implicated as an important cause of differences in morph frequencies both between and within populations of *T. pisana* (Heller 1981).

A theoretical possibility for the control of banding position is that a Turing reaction-diffusion mechanism might define the position of patterns on

shells. In several land snail species, pigmentation patterns that match those on the shell can be observed on the mantle (Emberton 1963). The presence of these bands on the mantle suggests that controlling pigmentation in banding may not be as simple as variable gene expression in a single line of cells along the growing edge of a shell (Budd et al. 2014). Direct experimental evidence of the control of banding pigmentation by Turing-like systems has proved difficult to gain in gastropods, and to date there is no evidence for loci contributing solely to the determination of band position on a shell, rather than simply determining presence or absence of bands.

1.5.3 Shell chirality

Shells may also be polymorphic in terms of their chirality, being either dextral, coiling to the right, or sinistral, coiling to the left (**Figure 1.1**). Although parts of the soft tissue appear to be bilaterally symmetrical, the coiling of gastropod shells reflects a complex and asymmetric internal body structure (Kuroda and Abe 2020a). Whilst sinistral individuals are rare in most cases (Davison et al. 2020b), some gastropod taxa are chirally dimorphic in natural populations, such as species of the Hawaiian land snail genus *Auriculella* and the South East Asian land snail genus *Amphidromus* (Schilthuizen and Davison 2005, Schilthuizen et al. 2007, Yeung et al. 2020). Difficulties in inter-chiral mating usually result in a single morph persisting in a population or species, as rare reverse-coiled morphs are not favoured by frequency-dependent selection (Johnson 1982, Ueshima and Asami 2003, Schilthuizen and Davison 2005). It is possible that plasticity in mating behaviours can act to allow the persistence of a chirality dimorphism (Asami et al. 1998). High spired individuals such as *Partula* spp. may show non-reciprocal mating behaviours in which the "male" mounts the shell of the "female" in a position whereby both snails are aligned in the same direction (Lipton and Murray 1979, Asami 1993), although this is not true of *Amphidromus*.

In *Amphidromus*, it is thought that preferential mate choice for a partner with mirror-image asymmetry maintains and stabilises the dimorphism in natural populations (Schilthuizen et al. 2007).

Direction of shell coiling is determined at early stages of embryonic division, visible at the third cleavage (Davison 2020). The direction of this cleavage, whether clockwise or anticlockwise, determines the chirality of the adult snail. It is hypothesised that LR asymmetry originates in a chiral 'F-molecule' and is transmitted via a chiral cytoskeleton to the embryo. In two species of snail, formin genes are implicated in chirality differences (Davison et al. 2020b). In *Lymnaea stagnalis*, a frameshift mutation in a single copy of a duplicated cytoskeletal protein, a diaphanous-related formin, is responsible for chirality variation (Davison et al. 2020a, Kuroda and Abe 2020b). In *Bradybaena similaris*, chiral variation is also associated with formin gene duplication (Noda et al. 2019).
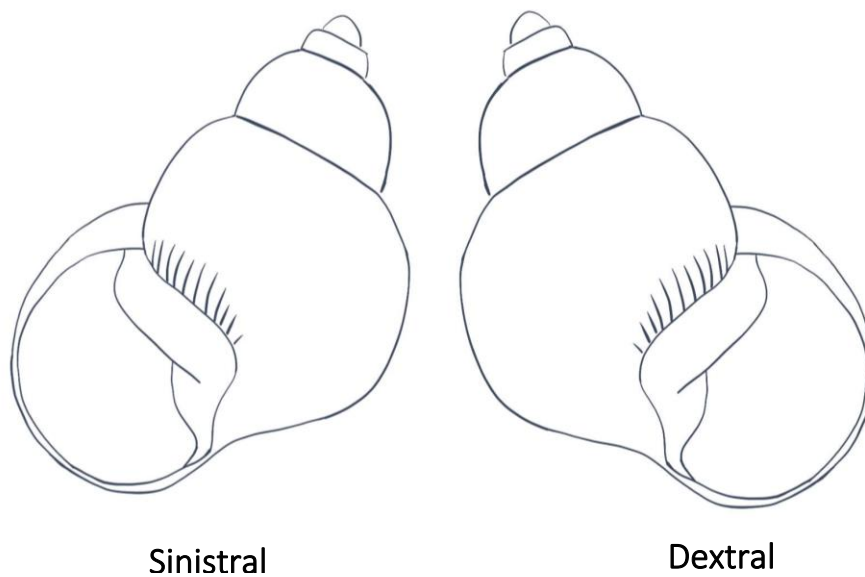
Sinistral   Dextral

Figure 1.1: Representation of variable chirality displayed in some species, sinistral shells coil to the left, and dextral to the right.

1.6 Gastropod shell formation, growth, and pattern establishment

Whilst gastropod shell morphologies are incredibly diverse in terms of colour, pattern, shape, chirality, and ornamentation, a common geometry is consistent, the logarithmic spiral which shell growth is based around. The growth of a snail shell follows a simple accretionary growth pattern, with new shell material deposited around the apertural opening in exponentially increasing dimensions along each whorl (Hutchinson 1989). A consequence of this growth pattern is that all previous whorls are retained, preserving a complete ontogeny of growth and development of every individual, from the protoconch to the final adult body whorl (Johnson et al. 2019).

Initial shell formation occurs at the end of gastrulation, a process where a single layer of cells, the blastosphere, becomes inverted at the bottom to form three germ layers, the endoderm, mesoderm, and ectoderm (Kniprath 1981, Hohagen and Jackson 2013). There is differentiation and local thickening of a group of ectodermal cells which invaginate into the blastocoel to form the shell gland. The shell gland then evaginates to form the shell field, which expands and differentiates to form the mantle, an organ which is homologous across the gastropods, and is responsible for the production of the diverse shell structures and morphologies seen across the Gastropoda (Aguilera et al. 2017). The mantle of adult and juvenile conchiferan molluscs (Cephalopoda, Bivalvia, Scaphoda and Gastropoda) is divided into distinct morphological regions which consist of highly specialised epithelial cell types which are responsible for secreting shell matrix macromolecules, which influence the formation of specific shell layers (Johnson et al. 2019). Most gastropod shells consist of three layer types, the periostracum, the prismatic, and the nacreous layers (Budd et al. 2014). The underlying calcified layer types are composed of aragonitic or calcite crystals, with structure of these layers

being determined by the assembly patterns of microstructures (Aguilera et al. 2017).

The outermost layer, the periostracum, is secreted from within a specialised mantle fold, the periostracal groove (Budd et al. 2014). The production of the central prismatic layer is controlled by genes expressed in columnar epithelial cells towards the extremities of the dorsal mantle surface (Marie et al. 2012). The third layer, the nacreous layer, is controlled by genes expressed in the inner zone of the mantle. Many of the genes expressed by these differentiated prismatic and nacreous layer forming cells have matched with changes in shell features such as structure, colouration, and patterning (Kocot et al. 2016). They have been identified and biochemically characterised with a wide range of potential functions, including increasing shell strength, catalysis of enzymatic reactions, triggering cell differentiation, and synthesis of extracellular matrix components. The mantle secretome is rapidly evolving; genomic variations are likely to underlie inter- and intraspecific differences observed in shell structure, shape, colour, pattern and strength.

To date, the only mollusc for which the expression of a gene has been found to correlate with shell pigmentation patterns is the tropical abalone, *Haliotis asinina* (Jackson et al. 2006, Jackson et al. 2007). This gene, *Sometsuke*, is expressed in regions of the mantle which lie directly underneath pigmented patches of the shell (Budd et al. 2014), which correspond to areas which are responsible for producing the prismatic layer in tubule-like structures (Checa et al. 2014). Based on this gene expression and the localisation of pigment-containing tubules to the prismatic mantle zone, it can be assumed that pigmentation is present in the prismatic shell layer. Similar structures are found in other gastropod species, suggesting that pigmentation is not controlled by individual cells, but by numerous cells which secrete products into a common duct (Budd et al. 2014).

1.7 The study systems:

1.7.1 The genus *Cepaea*

Cepaea nemoralis, and its sister species, *Cepaea hortensis*, collectively referred to henceforth as '*Cepaea*', represent the entirety of the genus *Cepaea*, which are terrestrial pulmonate gastropods in the family Helicidae (Neiber and Hausdorf 2015, Neiber et al. 2016). Previously, two other species were present in the genus, '*Cepaea*' *sylvatica* and '*Cepaea*' *vindobonensis*, but these have been reclassified as belonging to the genera *Macularia* and *Caucasotachea* respectively. The *Cepaea* polymorphism is present across both *C. nemoralis* and *C. hortensis*, and is characterised by a wide range of variation of several morphological features including shell ground colour, banding pattern, lip and band pigmentation, and whether bands are interrupted (or 'punctate') (Lamotte 1959, Cain et al. 1960, Jones et al. 1977). The inheritance of several aspects of the polymorphism is known to have a Mendelian basis (Jones et al. 1977), however simple rules of inheritance are not sufficient to describe the complexities of the system.

The polymorphism in *Cepaea* is well studied, and the inheritance of colour, banding, and other phenotypes displaying variation is well understood (Cook 1967). The presence or absence of each constituent part of the polymorphism is under the control of a multi-locus "supergene" (Richards et al. 2013, Schwander et al. 2014, Thompson and Jiggins 2014). At least nine loci have been identified as having a role in the control of phenotypic variation in *Cepaea nemoralis* (**Figure 1.2**) (Richards et al. 2013). At least five of these loci form a tight linkage group, and are inherited together as a supergene, these loci are the shell ground colour (*C*), banding (*B*), band/lip pigmentation (*P/L*), spread band (*S*), and punctate, or interrupted (*I*) (Cain and Currey 1963a, Cain et al. 1968, Richards et al. 2013). Epistatic interactions are present between both

(A)
Shell ground colour

Yellow   Pink ————————————————→ Dark brown

Presence or absence of banding:

Zero to five bands. Bands may be partially or fully suppressed.

Band pigmentation:

Band interruption
('Punctate' shown)

Spread bands
(Spread 4–5 and 1–5 shown)

Band and lip pigmentation
(Unpigmented bands and lip shown)

(B)
Supergene loci (alleles in decreasing order of dominance)

Ground Colour
C^B (brown)
C^{DP} (dark pink)
C^{PP} (pale pink)
C^{FP} (faint pink)
C^{DY} (dark yellow)
C^{PY} (pale yellow)

Band Presence
B^O (unbanded)
B^B (banded)

Band Interruption
I^I (interrupted)
I^- (continuous)

Band Spreading
S^S (spread)
S^- (unspread)

Band Pigmentation
P^N (brown bands + lip)
P^L (light brown bands + lip)
P^A (white lip + brown bands)
P^T (white lip + unpigmented bands)

Unlinked loci   **Linkage unclear**

Band Suppression
U^3 (single mid-band present)
U^- (unsuppressed)

Band Suppression
T^{345} (bands 1 + 2 suppressed)
T^- (unsuppressed)

Band Intensity
R^- (band complete)
R^D (band darkens from apex to lip)

Band Colour
O^- (black bands)
O^O (orange bands)

Figure 1.2: **A)** Variation in polymorphic traits of *Cepaea nemoralis* shells. There is considerable variation present between shells. Variation in shell ground colour, banding presence/absence, and band pigmentation patterns are shown.

B) Loci involved in the control of polymorphic shell characters. At least five of these are tightly linked with low recombination frequencies and are inherited together as a "supergene". Whilst colour and band presence form the tightest linkage group, physical order of these loci are unknown. Whilst shells displayed are all *Cepaea nemoralis*, the supergene is also found in *Cepaea hortensis*. Figure from Richards et al. (2013).

19

those loci inherited as a part of the supergene, and those which are unlinked, such as the band suppression locus.

Historically, recombination frequency estimates within the supergene suggest that the shell ground colour (C) and presence or absence of bands (B) loci are tightly linked with minimal recombination, typically towards the lower end of 0-2% (Cain et al. 1960, Cook 1967). There are some exceptions where C/B recombination rates have been estimated to be as high as ~20% (Fisher and Diver 1934). The estimate by Fisher and Diver is problematic, not least because non-virgin adults were used in crosses, so parentage cannot be assumed. The band spread, pigmentation, and punctate loci appear to be less closely linked, both to one another and to the supergene itself, and possess a characteristically higher recombination frequency, with historical estimates of between 3-15% (Cain et al. 1960, Cook 1967, Cain et al. 1968). Gonzalez et al. (2019) found no recombinants in crosses, placing upper limits of 0.8% and 1.8% on recombination frequencies respectively, suggesting a lack of evidence for recombination within the *C. nemoralis* supergene. This implies that the supergene structure may not be as has been previously supposed. Historically, it was not possible to verify putative incidences of recombination between loci within the supergene, except by continuing to breed offspring from the 'recombinant' individuals to verify genotype, which was rarely possible. It is likely, therefore, that the historical estimates are high due to 'recombination' phenotypes being a result of incomplete penetrance and epistatic interactions (Gonzalez et al. 2019). Some of the remaining, unlinked, loci which contribute to the *Cepaea nemoralis* shell polymorphism are various forms of band suppressing loci, such as the locus which suppresses all bands except the mid-band, unifasciata (U), and a second which suppresses the first two bands, trifasciata (T) (Cain et al. 1968).

There are several alleles for ground colour known, with a dominance structure of brown (C^B), dark pink (C^{DP}), pale pink (C^{PP}), faint pink (C^{FP}), dark yellow (C^{DY}), and pale yellow (C^{PY}) (Jones et al. 1977, Richards et al. 2013). A shell may have between zero and five bands, with absence of bands (Unbanded – B^O) dominant to band presence (Banded – B^B). Bands may be interrupted (I^i) in a punctate phenotype, or continuous (I^-) and may be spread (S^s) or unspread (S^-). Four alleles have been identified regarding lip and band pigmentation – normal dark brown lip and bands (P^N), light brown bands (P^L), white lip and normal bands (P^A), and white lip with transparent bands (P^T). Bands may also be fused, creating a shell phenotype which appears very different to that of an individual with unfused bands. The genetics of band fusions are poorly understood, but their presence can dramatically alter the appearance of a shell, causing a functionally dark phenotype. The origins and maintenance of this supergene however remain elusive, although avian predation and NFDS are often hypothesised as being at least partly responsible for colour variation maintenance (Clarke 1962, Jones et al. 1977, Cook 1998, 2005, Tucker 2008, Surmacki et al. 2013).

Classically, the ground shell colour phenotype is binned into one of three groups, yellow, pink, or brown, which was often sufficient for in-field classifications and citizen science projects such as the Evolution Megalab(Silvertown et al. 2011, Cameron and Cook 2012b, Worthington et al. 2012). In reality, shell colour variation in *Cepaea nemoralis* is continuous in three-dimensional colour space, albeit around three clusters which roughly correspond to the human scoring of colour (**Figure 1.3**) (Davison et al. 2019). The distribution of colour in 3-dimensional colour space in *Cepaea hortensis* is resolved in **Chapter 3**.

Figure 1.3: **A)** Examples of the three classically considered colour morphs in *Cepaea nemoralis*, from left to right: Yellow (Y), Pink (P), and Brown (B).

B) Variation present in natural populations of *Cepaea nemoralis*, showing variation in colour, banding, and lip pigmentation.

Cepaea nemoralis in particular is a species with a wide ecological tolerance, commonly occurring in areas with high levels of anthropomorphic disturbance, and it is easily accidentally spread, particularly in horticultural exports (Cameron and von Proschwitz 2020). In the last several decades, the species range has been expanding into areas previously too polluted to sustain it (Cameron et al. 2009), and has expanded largely into urban habitats to the north and east of its previous limits, extending as far east as Moscow (Ożgo 2005, Egorov 2018, Gheoca 2018). *Cepaea hortensis* is present in populations further to both the north and the east than *C. nemoralis*. Both species have a distribution which spans much of Europe and have been introduced to North America (Reed 1964, Örstan 2010, Gheoca et al. 2019, Layton et al. 2019, Gural-Sverlova and Gural 2021).

The two species of *Cepaea* are morphologically similar in shell phenotype, with the primary defining feature of the two being the characteristic brown lip of *Cepaea nemoralis* and the white lip in *Cepaea hortensis*. Where species co-occur in a single geographic region, they are often separated by topography or habitat (Carter et al. 1979). Mixed colonies occur but seem to be limited to more diverse habitats. *C. hortensis* are smaller in size in areas where populations of the two species co-exist, and there is divergence in heritable phenotypes in mixed populations (Clarke 1962). It is thought that the evolution of the supergene responsible for much of the variation present in both species of *Cepaea* predates the speciation event between *C. nemoralis* and *C. hortensis* (Cook 1998). *Cepaea*, like many members of the Helicidae, produce calcified love-darts to aid in copulation. These love darts also differ in structure between the two species, providing a potential identification tool. There are also differences in genital physiology (Jones et al. 1977), and in the arrangement of the mucous glands (Aubertin 1927).

Both species of *Cepaea* display morph ratio clines which apparently do not correspond with any environmental parameter (Clarke and Murray 1962, Cain and Currey 1963a). Areas much larger than a single panmictic population of *Cepaea* are characterised by a predominance of a few morphs, regardless of habitat; morph frequencies may fluctuate dramatically between these areas (Clarke 1966). These so called "area effects" have been attributed to cryptic differences in environment which produce changes in selective forces (Cain and Currey 1963a), and it has been argued that these area effects cannot be due to drift as the area in which differences occur is too large. It has also been suggested that the differences might be due to the founder principle (Goodhart 1963), whereby initial differences were sustained due to the evolution of balanced gene complexes. When these initial populations spread out, it was argued that the relative inavailability of hybrids between the systems resulted in the establishment of clines of variation between the initial populations, which are maintained in a state of dynamic equilibrium (Wright 1937, Goodhart 1963). These gene complexes, however, are unlikely to be of equal fitness, and therefore it is likely that a single morph would prevail (Cain and Currey 1963b). Other explanations for the "area effects" observed in *Cepaea* include genetic drift and co-adaptation (Goodhart 1963), accumulation of modifiers along morph-ratio clines (Clarke 1966), and changing uses of land creating differences in refugia (Cameron et al. 1980).

1.7.2 The genus *Auriculella*

Auriculella is a genus of terrestrial gastropod snails of the family Achatinellidae, endemic to the Hawaiian archipelago (Hartman 1888, Asami et al. 1998, Schilthuizen and Davison 2005, Holland et al. 2018). The *Auriculella* is a poorly described genus, with much of the focus on the imperilled Hawaiian land snails being directed towards the larger, more charismatic, more variable genus *Achatinella* (Yeung and Hayes 2018, Meyer et al. 2021). *Auriculella* are variable in colour and chirality in single populations; the colour of shells ranges from pale yellow, to pink, brown, and green (**Figure 4**). They are also variably chiral, with populations consisting of a combination of both sinistral and dextral individuals. Species of the genus also vary somewhat in shape and size, as well as banding patterns, where some individuals possess a "candy-striped" shell pattern (Yeung et al. 2020).

Much of the variation present in *Auriculella* spp. is likely to be related to stochastic events, including founder effects and genetic drift, as small propagules became isolated in the numerous steep-sided valleys of the Hawaiian islands, rather than variation being attributed to finely tuned adaptation (Cowie 1992). *Auriculella* are unique amongst the Hawaiian land snails in that they appear to be able to persist on non-native flora in areas where native vegetation is no longer found (Holland et al. 2017). Despite this, current estimates suggest that as many as 18 of the 32 described species of *Auriculella* are extinct (Yeung, pers. comm.), and the conservation status of those remaining extant are poorly described (Holland et al. 2017). Whilst biologically endangered, this status is not yet officially recognised by the IUCN (Holland et al. 2010, Kraus et al. 2012). Large amounts of the loss of species diversity is attributed to non-native predators, such as the rosy wolf snail *Euglandina rosea* and Jackson's chameleon *Chamaeleo jacksonii* (Hadfield and Mountain 1980, Gerlach et al. 2021).
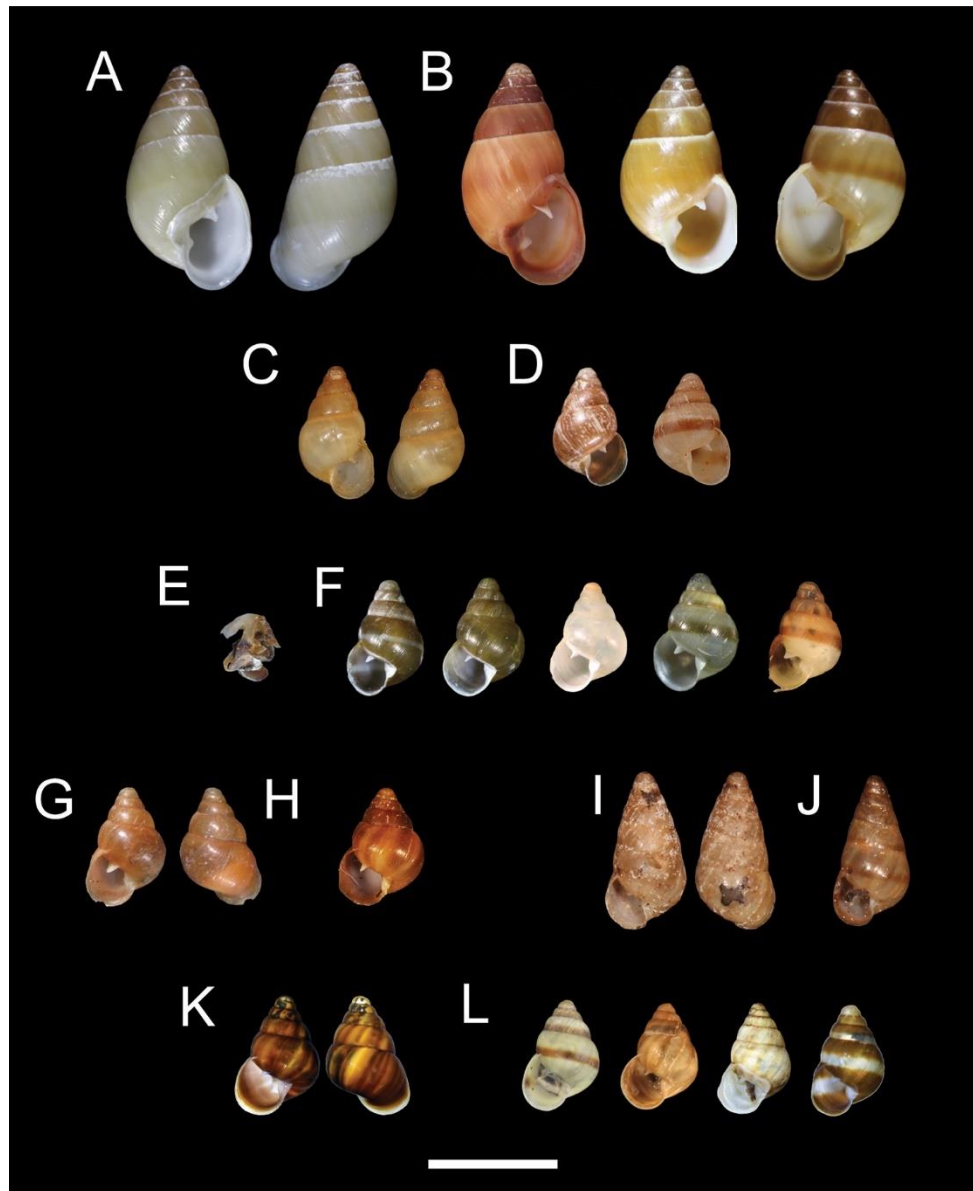
Figure 1.4: Representation of shell variation in *Auriculella* spp. All individual shells pictured are from the malacology collection of the Bernice Pauahi Bishop Museum. Scale bar is 5mm. Species are as follows: **A.** *A. auricula* neotype **B.** *A. auricula* variation **C.** *A. minuta* lectotype **D.** *A. minuta* shell variation **E.** *A. perpusilla* holotype **F.** *A. perpusilla* variation **G.** *A. perversa* lectotype **H.** *A. perversa* shell variation **I.** *A. tenella* lectotype **J.** *A. tenella* variation **K.** *A. gagneorum* holotype **L.** *A. gagneorum* variation.

Image courtesy of Norine Yeung, from Yeung et al (2021)

1.8   Thesis outline

The overarching aim of this thesis is to demonstrate the importance of accurately defining phenotypes, and to highlight the usefulness of terrestrial gastropods in aiding the understanding of how variation is established and maintained at a species level. It aims to emphasise the importance of understanding an outward-facing phenotype as a "springboard" to understanding the genetic mechanisms which underpin variation. Once said variation is understood, it is easier to establish the mechanisms, genetics, and interactions therein which may be responsible for controlling it. This aim is achieved by describing phenotypic variation using several metrics such as colour, chirality, and banding pattern across two molluscan genera, the European land snail *Cepaea*, and the Hawaiian land snail *Auriculella*.

In this thesis, I aim to address the following questions regarding the presence of polymorphic variation in terrestrial gastropod shells, using *Cepaea* and *Auriculella* as study genera:

- How do banding patterns in *Cepaea* vary both within and between phenotypes? (**Chapter 2**)
- How does the shell colour variation in *Cepaea hortensis* compare to that observed in *Cepaea nemoralis*? (**Chapter 3**)
- How does shell colour vary across a variety of scales in the relatively poorly studied Hawaiian land snail genus, *Auriculella*? (**Chapter 4**)

These aims are achieved by answering each of these questions in turn as a stand-alone study, presented as a single chapter. These three chapters are followed by a review of key findings, and suggestions for future avenues of research, as opened up by the results of each chapter.

These chapters are outlined as follows:

Chapter 2 – Banding in *Cepaea*

In Chapter 2, I demonstrate a method of quantitatively defining and measuring variation within established banding phenotypes of *Cepaea nemoralis* and *Cepaea hortensis*. The combination of empirical measures of quantitative variation and the implementation of 3-dimensional shell models aid in understanding how bands are placed on the shell, and how they interact with one another through presence or absence of other bands. Commonly found banding phenotypes were used to show that individual band absence has a minor but significant effect on the position of the remaining bands, implying that the locus controlling band presence/absence acts mainly after position of bands is established. I establish a method which may be used for comparative studies of quantitative banding variation in snail shells, and extraction of growth parameters and morphometrics, highlighting the importance and usefulness of gastropod shells in the understanding of how variation is established and maintained in a population.

Chapter 3 – Colour variation within and between *Cepaea* species

In chapter 3, I use reflectance spectrophotometry in tandem with psychophysical modelling to define the colour variation present in *Cepaea hortensis* and *Cepaea nemoralis* shells. The main aims are fourfold, to determine whether individuals of *C. hortensis* and *C. nemoralis* vary continuously across 3-dimensional colour space, to establish whether this variation is associated with geographical parameters such as latitude and longitude, to determine whether there are clusters of individuals present within single phenotypes of *C. nemoralis*, and to establish whether colour variation interacts with other

shell characteristics, such as banding pattern. It was revealed that colour variation in *Cepaea hortensis* does not appear to fall into the typically described three groups of yellow, pink, and brown when modelled according to a tetrachromatic visual system, and there are no detectable effects of geographic location with the exception of an association of the paleness of yellow shells with latitude. Differences between the colour of *Cepaea hortensis* and *Cepaea nemoralis*, both in terms of exact shade and overall colour are revealed; *Cepaea hortensis* are generally paler, and less pink-toned, but slightly more brown-toned. Precise shade variation of yellow individuals from genetically diverse lineages of *Cepaea nemoralis* is also revealed. The results presented have significance in furthering the understanding of the precise nature of the colour polymorphism displayed in *Cepaea* spp., and the nature of the selection which acts upon it, as well as highlighting the importance of considering colour as a continuous trait, rather than binning it into discrete groups.

Chapter 4 – Colour and chirality variation in the Hawaiian land snail genus *Auriculella*

In chapter 4, I use a combination of reflectance spectrophotometry and psychophysical modelling to define the variation present in four species of the Hawaiian land snail genus *Auriculella*. This variation is explored across a number of scales, ranging from small scale variation present within individual shells, to within population and within species variation, up to large-scale inter-island variation. I demonstrate that there are differences in colour within a single shell, similar to variation displayed by other Pacific Island snails. I also describe significant variation between isolated populations of the same species, and demonstrate a lack of differences present in colour variation between species. I also determine that there is no difference in colour variation between individuals on the islands of Maui and Oahu, which suggests similar selection pressures on

islands. Finally, I demonstrate that there is no difference in colour between dextral and sinistral individuals, suggesting that interchiral mating is not uncommon, and that the loci responsible for colour variation and chirality are not closely linked. By describing the variation present in *Auriculella* in an ecologically and evolutionarily relevant context, inference regarding genetic mechanisms of variation becomes possible in a taxon of conservation concern. The importance of museum collections is highlighted, as is the application of technology to enhance information which can be gleaned from historical collections.

Chapter 5 – Discussion

Finally, I synthesise findings from across chapters, and further highlight the importance of accurately defining phenotypes for the purposes of both evolutionary ecology and genetics, and conservation. To understand the internal genetic mechanisms underpinning phenotypic variation across any species further, it is important to first define the outward-facing phenotype accurately, and in a biologically relevant context. I emphasise the usefulness of quantitatively defining variation within and between phenotypes to make inferences regarding the genetic mechanisms underpinning variation, and establish phenotypic variation present both between *Cepaea hortensis* and *Cepaea nemoralis*, and in the *Auriculella* genus. More broadly, I highlight the usefulness of molluscs as a study system due to the nature of shell growth, and ease of preservation.

Chapter 2: Banding pattern variation in *Cepaea*

2.1 Abstract

The nature of shell growth in gastropods is useful because it preserves the ontogeny of shape, colour and banding patterns, making them an ideal system for understanding how inherited variation develops and is established and maintained within a population. However, qualitative scoring of inherited shell characters means there is a lack of knowledge regarding the mechanisms that control fine variation. Here, we combine empirical measures of quantitative variation and 3D modelling of shells to understand how bands are placed and interact. By comparing five-banded *Cepaea* individuals to shells lacking individual bands, we show that individual band absence has minor but significant impacts upon the position of remaining bands, implying that the locus controlling band presence/absence mainly acts after position is established. Then, we show that the shell grows at a similar rate, except for the region below the lower-most band. This demonstrates that wider bands of *Cepaea* are not an artefact of greater shell growth on the lower shell; they begin wider and grow at the same rate as other bands. Finally, we show that 3D models of shell shape and banding pattern, inferred from 2D photos using ShellShaper software, are congruent with empirical measures. This work therefore establishes a method that may be used for comparative studies of quantitative banding variation in snail shells, and extraction of growth parameters and morphometrics. In the future, studies that link the banding

phenotype to the network of shell matrix proteins involved in biomineralization and patterning may ultimately aid in understanding the diversity of shell forms found in molluscs.

2.2 Introduction

The nature of shell growth in gastropods is useful because it preserves the ontogeny of shape, colour and banding patterns, making them an ideal system for understanding how inherited variation develops and is established and maintained within a population (Johnson et al. 2019). This is particularly beneficial when considering animal colouration and patterning, both of which have been critical in understanding the key principles of evolution (Richards et al. 2013, Cuthill et al. 2017a).

Historically, the foremost gastropod species in understanding colour polymorphism and band patterning has been the European land snail *Cepaea nemoralis*, and its sister taxon *C. hortensis* (Jones et al. 1977, Ożgo 2011), partly due to their ease of collection. Also useful has been the ability to record morph frequencies, whether yellow, pink or brown, with varying numbers of bands, from zero to five (Cain and Sheppard 1950, 1952, Jones et al. 1977). A further reason is the apparent simplicity of the Mendelian inheritance of the shell colour and banding loci, many of which are inherited together in a 'supergene' (Cook 1967, Jones et al. 1977). As a result, studies on the shell polymorphism of the snail *Cepaea* have played a crucial role in establishing the role of natural selection in maintaining morphological variation, with the genus becoming a pre-eminent model for ecological genetics, alongside the peppered moth (Grant et al. 1996, Majerus et al. 2000, Cook and Saccheri 2013, Walton and Stevens 2018).

In the present day, one of the continuing benefits of working with *Cepaea* is an ability to compare the frequencies of shell morphs in historic collections against modern day samples, to infer the potential impact of natural selection and/or drift in changing shell morph frequencies (Cameron 1992, Arthur et al. 1993, Cook et al. 1999, Ożgo and Schilthuizen 2012, Cameron et al. 2013a, Ożgo et al. 2017). Of particular use, the "Evolution Megalab" project digitised a large set of 20th century samples. These records, and others deposited in museums, are now being used with modern surveys to

produce an increasing number of comparative papers (Silvertown et al. 2011, Cameron and Cook 2012b, Worthington et al. 2012, Cameron and Cook 2013). New studies on the genetics and genomics (Richards et al. 2013, Mann and Jackson 2014, Kerkvliet et al. 2017, Saenko et al. 2021) mean that *Cepaea* snails are poised once again to become a powerful system. The findings from this single genus should lead the way in understanding the diverse variety of shell patterns that are found in the wider group of snails and molluscs to which they belong.

Unfortunately, a traditional focus on the qualitative scoring of the shell characters of *Cepaea* has resulted in a lack of knowledge regarding the mechanisms that control fine variation. For example, the ground colour of *Cepaea* has traditionally been grouped into one of three categories, yellow, pink, or brown. This was necessary for field-based classifications, but recent spectroscopy and psychophysical modelling of avian visual systems has shown that the colour variation is continuously distributed, albeit around three clusters which roughly correspond to the qualitative colour groupings of yellow, pink and brown (Davison et al. 2019). Although further studies are necessary, the observation of continuous variation in colour is intriguing because the traditional theory is that, provided observed variation results from frequency-dependent selection, the underlying supergene that determines colour has evolved to prevent phenotypes from "dissolving" into continuous trait distributions. These findings raised questions about the nature of the selection that acts upon the polymorphisms.

With interest in quantitative variation in *Cepaea* colour (Davison et al. 2019), it seems appropriate to reconsider variation within and between banding patterns, which has received little attention since Rotarides (1926), who established that the proportion of shell covered by band is correlated with variation within habitat types. This, and subsequent work using similar methods (Ożgo and Komorowska 2009) have tended to focus on the proportion of the shell that is banded, and the potential effect on natural selection (Neiber and Hausdorf 2015, Neiber et al. 2016). How the position

and widths of bands might be established during shell growth has been neglected, but could provide useful insight into how banding patterns vary within individual shells over time.

In banding notation (Cain 1988), bands are numbered 1 to 5 from the top of the shell down, with modifications to recognise band fusions and interruptions (**Figure 2.1a**). A five-banded snail with bands fused on the lower part of the shell is thus 123(45), and a mid-banded is 00300. However, as with colour, the qualitative scoring of bands masks complexities. For example, a five-banded individual may possess five wide bands which are close to fused with little ground colour visible between them, or it may possess five narrow bands, with considerable visible colour between the gaps. These individuals would be scored as having the same phenotype, yet the large differences between them may affect thermoregulation, visibility to predators and resistance to crushing forces (Staikou 1999, Cook 2008, Ożgo and Schilthuizen 2012, Rosin et al. 2013, Surmacki et al. 2013). Bands are deeply integrated into the shell matrix, unlike colour which has no structural elements (Budd et al. 2014, Williams 2017). In *Cepaea*, bands are present in all three layers of shell, and their presence in the central calcareous prismatic layer is likely responsible for the increased crushing resistance displayed by banded shells relative to their unbanded counterparts (Rosin et al. 2013).
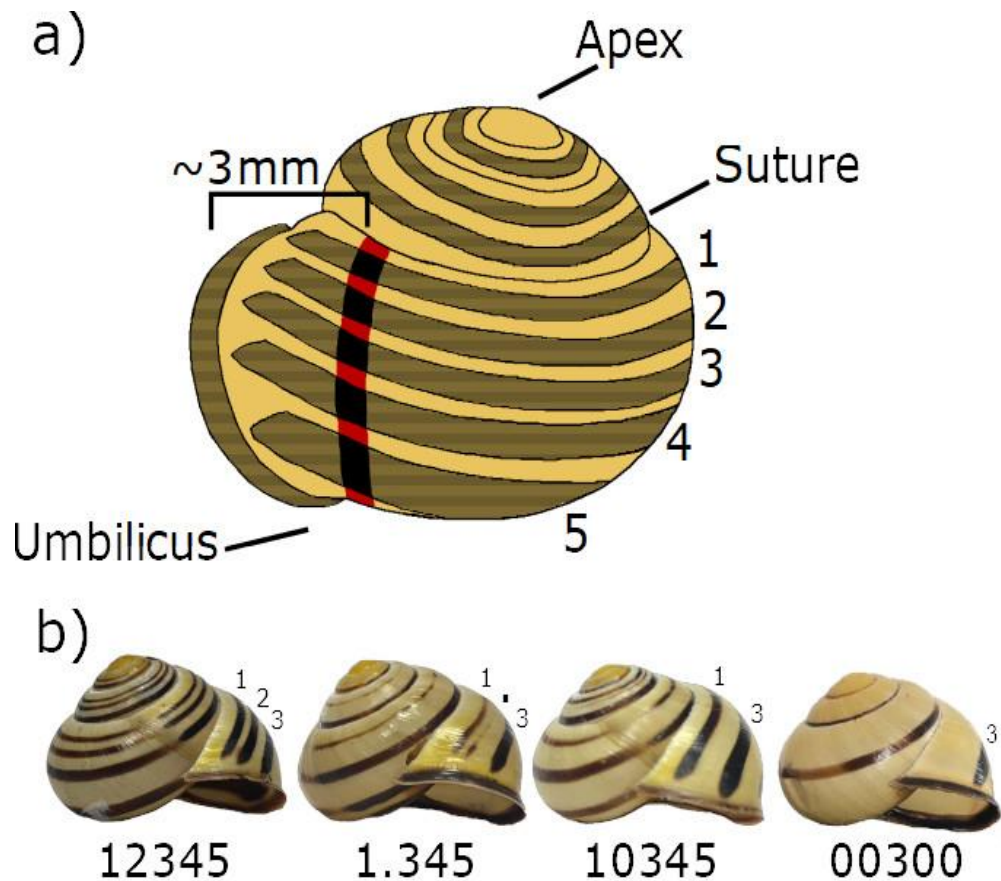
Figure 2.1. a) *Cepaea* shell showing shell characters and illustrating position for measurement of bands. **b)** Banding phenotypes, from left: five bands (12345), missing second band (10345), partial missing second band (1.345), mid-band (00300).

2.2. Band position determination

How is band position determined? The main shell loci have been characterised but not yet identified. A locus *B* determines band presence/absence, locus *U* suppresses all bands except band 3 (to make a mid-banded snail 00300), and another locus suppresses bands 1 and 2. Several other loci, including spread band *S* and punctate *I* (or 'interrupted') loci modify the nature of the band phenotype. Individuals may also have unpigmented bands, a phenotype known as hyalozonate, where bands are present and visible, but lack the usual pigmentation, suggesting that whilst these processes may interact, the laying down of bands and the

pigmentation of these bands occur independently of one another. There are also likely other loci, or environmental factors which act during growth, that exert a multifactorial effect on the phenotype, including modifiers of band width, band fusion, band colour, suppression of individual bands, and the timing of band expression (e.g. bands only on last whorl). However, these loci are not useful in understanding how bands are placed, because they mainly specify presence/absence, or character, rather than position.

One theoretical possibility behind band position control is that a Turing reaction-diffusion mechanism might define the position of patterns on mollusc shells, including *Cepaea* (Meinhardt and Klingler 1987, Kondo and Miura 2010). In the simplest form of this theory, two diffusible substances interact with each other to produce waves of consistent predictable protein expression which are then translated into morphological structures such as stripes or bands. Although direct experimental evidence has been difficult to gain, the observed patterns in zebrafish (Nakamasu et al. 2009) and a number of other organisms as well as non-biological systems, such as the origin of spiral galaxies (Torii 2012, Ball 2015) are consistent with a reaction-diffusion model. To date, however, there is no empirical evidence for this in gastropods, nor even any evidence for loci that contribute to determining band position rather than presence/absence.

To begin to understand the genetic mechanisms underpinning pattern variation in *Cepaea*, a first step is to re-evaluate the description of the banding phenotype by quantification of variation in banding patterns both between and within phenotypes, and throughout shell growth. Here, we combine empirical measures of quantitative variation within and between bands, and 3D shell models, to understand how bands are placed and interact with one another. By comparing fully banded individuals against shells lacking individual bands, we infer that the locus that controls band absence mainly acts after band position is established. We also show that the lower bands are not wider as an artefact of greater shell growth on the lower shell. They grow at the same rate as all other bands, but are wider

from their first formation. Finally, we show that the same measures may be taken from a photograph, and a 3D model inferred. Validation of these methods for shell pattern quantification provides a baseline for future analysis of shell patterning and ornamentation in gastropods. As we move towards identifying the genes involved in setting the patterns, these findings may together be used to develop a model for band placement in snail shells, set in the general context of understanding shell growth parameters.

2.3 Materials and methods

2.3.1 Snails

Individuals of both species, *Cepaea nemoralis* and *C. hortensis,* were collected by volunteers and on fieldtrips across Europe. Snails were euthanised by freezing at −80°C upon arrival at the University of Nottingham, and subsequently thawed and bodies extracted from their shell.

Shell banding and colour phenotypes were first scored qualitatively, using the scheme described in Murray (1963b), with some minor deviations where necessary (Davison et al. 2019). The main phenotypes of importance to this study were five-banded, 12345, and mid-banded, 00300 (**Figure 2.1b**). These were used to understand the impact of band absence on the position and width of band 3. In a single Spanish population, shells lacking the second band, phenotype 10345, were relatively common. This population also included some shells in which band 2 was only present in the very last part of the shell, just before the lip. Here, we describe this feature as ".", distinct from the mark used to represent punctate ":" e.g., 1.345. These shells were used to understand the impact of the absence of band 2, and also a partial suppression of band 2, upon the positions of the remaining bands.

2.3.2 Shell measurements

To measure the positions and widths of the bands on the *Cepaea* shells, a ~1 mm strip of electrical tape was wrapped around the last whorl of individual adult shells, from the suture to the umbilicus (**Figure 2.1a**). The tape was attached parallel to any growth lines, and placed ~3 mm back from the shell lip, necessary because banding phenotype often differs close to the lip. Band start and end position was then recorded by marking the tape with a super-fine permanent marker under a dissection microscope. Tape was removed from the shell, and the distances between marks measured using Vernier callipers under a dissection microscope.

The individual measures of band position were converted into proportions, standardising against the distance between the suture and the umbilicus, to enable comparison between shells of different sizes. The mid-point of the band was used to define band position, with band width considered separately. Individual measures were not used if bands were ill-defined or fused. Shell height, width and weight were also measured, to enable tests for associations with size, and shell shape (width/height).

2.3.3 Interactions between bands and band-gaps

We first checked whether other shell parameters influence band position and width. Statistical models were created, using height, weight, shape, and band position and width data, in R version 3.6.2. All full models included fixed effects of shell shape (obtained by dividing shell height by shell width), shell height (used as a proxy for shell size), and shell weight (as a proxy for shell thickness). In all models run, a random effect of population was fitted to remove this as a confounding variable and attempt to mitigate effects of location as far as possible. For model selection, a full set of models including every combination of fixed effects was generated. These models were ranked according to their Akaike Information Criterion (AIC). From a full model set, models with a value within 2 AICs of the best fitting model (value closest to zero) were considered to be equally supported, and so these were averaged. Full coefficients are quoted in the final averaged model, meaning that any terms not appearing in a given component model were assigned a coefficient of zero before averaging.

The null hypothesis was that if the deposition of pigment in each band is independent of others, then absence of individual bands in the adult shell will not impact upon the position and width of other bands. Mann-Whitney U tests were therefore performed to determine whether the position and width of band 3 varied in mid-banded individuals (00300) compared with five-banded individuals (12345) in *Cepaea nemoralis*. Similarly, multivariate

Kruskal-Wallis tests, followed by Dunn's pairwise tests with Benjamini-Hochberg adjustment, were carried out to determine whether partial or complete absence of band 2 impacted upon the position and width of the remaining bands.

Bands are established in juvenile snails, usually becoming progressively wider with each whorl of the shell. Band width is necessarily constrained by the edges – the point of contact with the suture and towards the umbilicus – and likely also interactions with other bands, and the gaps between bands. Therefore, to understand how bands grow in width and interact with one another, the edges, and the gaps between bands, we tested all possible correlations between individual band width and band-gap, focussing on the width of the gap immediately above or below each band. If bands increase in width together, a positive relationship will result between focal band width and the widths other bands at the level of an individual snail. The corollary was an expectation for a positive relationship between individual band-gap width and other band-gap widths, and a negative relationship between band width and band-gap width.

2.3.4 Comparison between species and colour

Differences in the position and width of each band between species were tested using five-banded snails and generalised linear mixed effects models (GLMMs). Each band was modelled separately. Species was fitted as the sole fixed factor, with a random effect for population in each model. The fixed term of species was removed in each model, testing the effect of deletion by comparison of Akaike Information Criterion (AIC). The AIC of the GLMM including the fixed effect was compared with that of a generalised linear model without the random terms to provide an approximate test of the importance of population, as per Davison et al. (2019). As genes for colour and banding patterns of shells may be in linkage disequilibrium (Cook 2005), GLMMs were repeated with colour as the sole fixed factor.

2.3.5 Shell growth and use of 3D models

Bands 3, 4, and 5 on a *Cepaea* shell are typically wider than bands 1 and 2. One explanation is that the wider bands are simply an artefact of greater relative growth on the lower part of the whorl. Therefore, two complementary methods were used to understand how band width varies with growth of the final whorl.

Shell segments were removed with a small circular saw, in 90° increments until an entire whorl had been removed, at each of five points, measurements of band width and position were taken as described above. In addition, shells were mounted on a flat surface with their apertures facing up, columella parallel to the surface. A photograph was also taken at each stage, ensuring that all bands were visible around the aperture. An updated version of ShellShaper software (https://github.com/jslarsson/ShellShaper; Supplementary Methods) was used to build 3D models of shells, including the positions of bands, obtained by user-defined landmarks from each of the 2D images as per Larsson et al. (2020). Models were based on three-dimensional logarithmic helicospiral growth, although using only circular apertures and no shell thickness. Band position and width were defined for a predetermined number of bands on any given shell. Widths and positions were then extracted from the model and analysed.

To determine whether growth rate was influenced by the position on the shell, GLMMs were performed on mid-banded and five-banded shells, with the response variable of growth rate, and a fixed effect of shell section, with a random factor of ID included to mitigate the potential differences between individuals. Least square means with Tukey adjustments for multiple comparisons were performed to allow direct comparison of shell areas to one another.

Comparative analysis was performed on the two methods using a Bland-Altman plot to analyse agreement between the two methods, using the

average of paired measurements of five banded individuals for reference. Differences in measurements from each method at constant locations and stages of growth across shells were analysed, and the measurement bias and 95% upper and lower confidence intervals found.

2.4 Results

Band measurements were taken for 440 individuals, 271 *Cepaea nemoralis* and 169 *C. hortensis*, across 40 populations, distributed throughout the UK and mainland Europe. Shell shape, height, or weight did not impact upon the relative position or width of any of the five-bands (**Tables 2.1, 2.2**). In each of the 10 final averaged models generated, one for each position and width of each band, no predictors were significant. Ten similar models were generated to test for associations of band position and width with shell ground colour. The sole fixed factor of colour was not a significant predictor of variance in any of the 10 models.

Table 2.1 Outcome of statistical tests (model averaged GLMMs) for the impact of shell shape, height, or weight relative position of bands. From a full model subset, models within two Akaike Information Criterion (AIC) of the best model were selected, and means of the coefficients were taken. All of the terms listed were included in all of the full models for each band position model. CI represents the Confidence Interval; Weight represents the sum of weights from models in which the variable in question appears in the final averaged model. Significant predictors are highlighted in bold.

	Predictors	*Coefficient*	*2.5% CI*	*97.5% CI*	*Weight*
Band 1	**Intercept**	**8.09**	**3.87**	**12.32**	**-**
	Shape	1.65	-3.54	6.84	0.45
	Weight	0.13	-0.24	0.50	0.53
	Height	-0.02	-0.14	0.09	0.24
	Height:Shape	-	-	-	-
	Height:Weight	-	-	-	-
	Shape:Weight	-	-	-	-

Band 2	*Intercept*	*7.88*	*-13.71*	*29.46*	*-*
	Shape	12.21	-16.63	41.05	1.00
	Weight	0.33	-0.81	1.47	0.58
	Height	0.08	-1.13	1.29	0.62
	Height:Shape	-0.24	-1.86	1.38	0.14
	Height:Weight	0.00	-0.05	0.04	0.10
	Shape:Weight	-	-	-	-
Band 3	Intercept	18.65	-6.42	43.71	-
	Shape	11.49	-21.86	44.85	1.00
	Weight	1.00	-2.72	4.71	0.71
	Height	0.04	-1.31	1.38	0.58
	Height:Shape	-0.20	-1.97	1.57	0.11
	Height:Weight	-0.01	-0.10	0.07	0.13
	Shape:Weight	-0.41	-4.55	3.72	0.10
Band 4	**Intercept**	**45.58**	**37.21**	**53.96**	**-**
	Shape	2.37	-7.10	11.85	0.32
	Weight	-	-	-	-
	Height	-0.21	-0.54	0.12	0.77
	Height:Shape	-	-	-	-
	Height:Weight	-	-	-	-
	Shape:Weight	-	-	-	-

	Predictors			
	Intercept	1.41	-102.50	105.33	-
	Shape	85.27	-49.04	219.58	1.00
	Weight	-	-	-	-
Band 5	Height	2.54	-3.56	8.64	1.00
	Height:Shape	-4.01	-11.88	3.87	0.36
	Height:Weight	-	-	-	-
	Shape:Weight	-	-	-	-

Table 2.2. Outcome of statistical tests (model averaged GLMMs) for the impact of shell shape, height, or weight relative width of bands. From a full model subset, models within two Akaike Information Criterion (AIC) of the best model were selected, and means of the coefficients were taken. All of the terms listed were included in all of the full models for each band position model, but several model averages include a reduced model with no fixed factors. CI represents the Confidence Interval; Weight represents the sum of weights from models in which the variable in question appears in the final averaged model. Coefficients in bold indicate those for which the 95% confidence interval does not include zero (therefore the effect of the predictor is not significant)

	Predictors	*Coefficient*	*2.5% CI*	*97.5% CI*	*Weight*
	Intercept	**3.64178**	**1.363071**	**5.920491**	**-**
	Shape	-0.69108	-3.48987	2.107718	0.32
	Weight	0.02701	-0.11889	0.172911	0.24
Band 1	Height	-	-	-	-
	Height:Shape	-	-	-	-
	Height:Weight	-	-	-	-
	Shape:Weight	-	-	-	-

Band 2	**Intercept**	**3.66466**	**2.231354**	**5.097974**	**-**
	Shape	-	-	-	-
	Weight	0.11351	-0.2041	0.431125	0.45
	Height	0.01142	-0.05438	0.07723	0.2
	Height:Shape	-	-	-	-
	Height:Weight	-	-	-	-
	Shape:Weight	-	-	-	-
Band 3	**Intercept**	**9.0729**	**3.36438**	**14.78146**	**-**
	Shape	-	-	-	-
	Weight	-2.1178	-6.25615	2.020602	0.56
	Height	-0.1498	-0.45856	0.158956	0.56
	Height:Shape	-	-	-	-
	Height:Weight	0.1107	-0.10496	0.326377	0.56
	Shape:Weight	-	-	-	-
Band 4	**Intercept**	**8.8122**	**5.244962**	**12.37944**	**-**
	Shape	-0.61887	-4.50273	3.264984	0.18
	Weight	0.11229	-0.32187	0.546444	0.34
	Height	-0.02817	-0.16895	0.112605	0.47
	Height:Shape	-	-	-	-
	Height:Weight	-	-	-	-
	Shape:Weight	-	-	-	-

		Intercept	10.34408	-6.14405	26.83221	-
Band 5	Shape	-6.41179	-33.1891	20.36552	0.21
	Weight	-1.35367	-7.58921	4.881867	0.39
	Height	0.22894	-0.14747	0.605343	0.82
	Height:Shape	-	-	-	-
	Height:Weight	-0.05204	-0.26841	0.164324	0.18
	Shape:Weight	2.98324	-9.43401	15.4005	0.18

2.4.1 Effect of missing bands

Mann Whitney U tests demonstrated that, in *Cepaea nemoralis*, when other bands are absent, the mid-band was shifted towards the top of the shell, albeit only ~0.9% closer (W = 6867.5, *P* = 0.0107; **Figure 2.2a**). In comparison, the mean difference between first and second measures of the same band was 0.17%, ranging between 0.004% and 0.7%. The absence of other bands did not impact upon the variability in position of the band of a mid-banded individual; Kolmogorov-Smirnov tests demonstrated that distributions were equal when shifted to centre around a single mean, suggesting that variance in band position remained constant in both phenotypes (D=0.08, *P*=0.9). The width of the bands also did not change in the absence of other bands (W = 8831, *P* = 0.7; **Figure 2.2a**). Gaussian finite mixture modelling of the distribution of widths indicated that the width of band 3 in five-banded individuals is not multimodal. Both the best model (X, univariate normal, BIC -295.4; *P* = 0.04 compared to second best model) and the next best models resolved a single cluster. As with band position, the distribution of band widths in mid-banded snails did not differ from the distribution of individuals with five-bands.
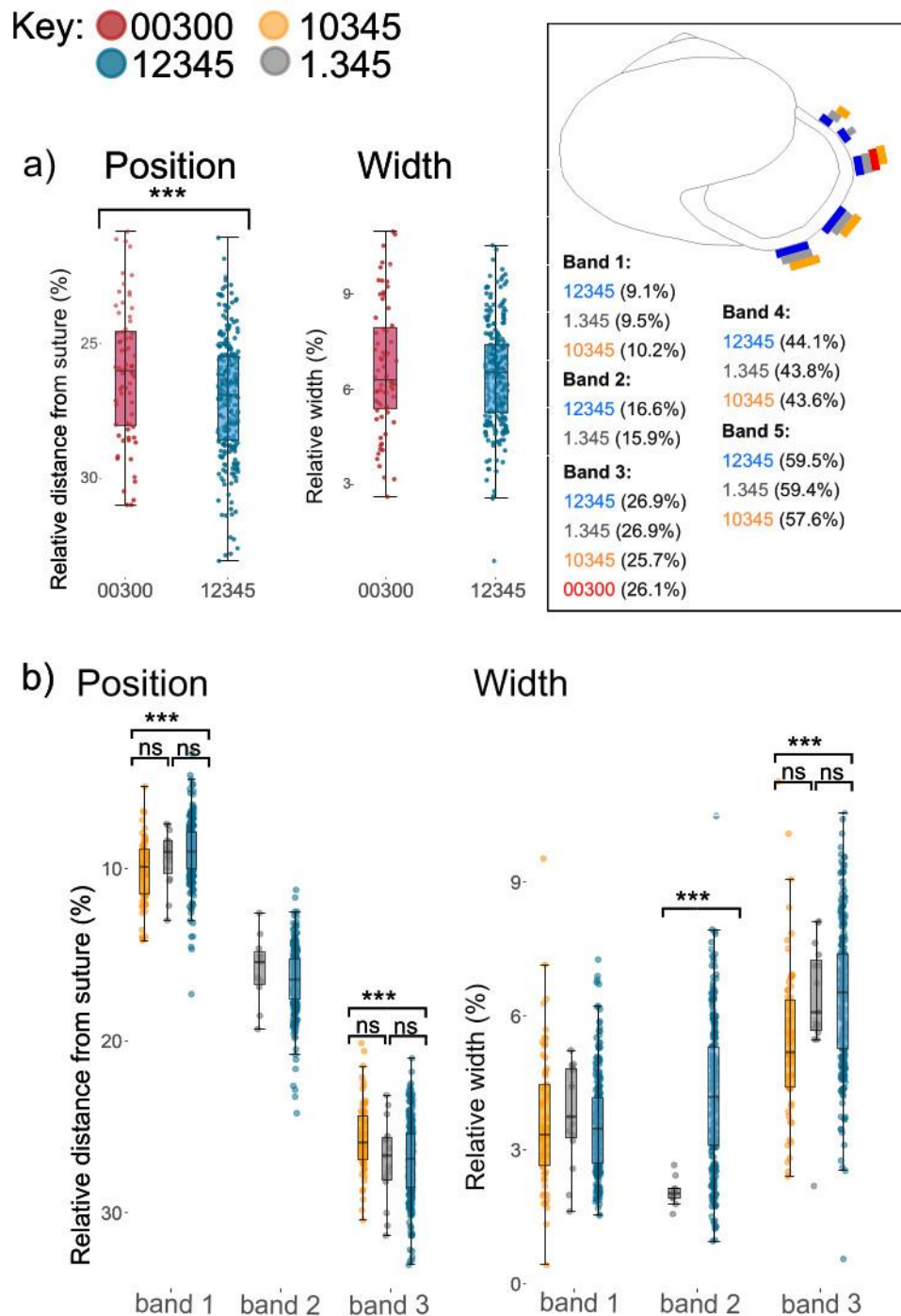
Figure 2.2. Band positions and widths in different phenotypes. **a)** Band 3 in mid-banded (00300) individuals is shifted ~ 0.9% upwards compared with the same band in five-banded (12345) snails. The width of band 3 does not differ between the same phenotypes. **b)** In shells in which band 2 is missing (10345), bands 1 and 3 are ~2.4% closer together. There are also some differences in band width, especially band 3. $P < 0.05$,*; $P < 0.0001$,***. Inset: summary of band positions in different phenotypes.

49

Similarly, Kruskal-Wallis tests indicated that when band 2 was missing or partially suppressed (**Figure 2.2b**), both bands 1 and 3 were in different positions across the three phenotypes (H = 18.05, df = 2, *P* = 0.0001; H = 17.1, df = 2, *P* = 0.0002). Specifically, bands 1 and 3 were ~2.4% closer to each other when band 2 was absent (**Figure 2.2b**). Pairwise Dunn's tests with Benjamini-Hochberg adjustments indicate that this difference was only present between the 12345 and 10345 phenotypes for both bands one and three (Z = -4.1, *P* = 0.000007; Z = -4.2, *P* = 0.0001), with the partially suppressed phenotype intermediate and non-significantly different from the bands 1 and 3 in 10345 (10345; Z = -1.4, *P* = 0.2; Z = 1.9, *P* = 0.06), and 12345 (Z = 0.6, *P* = 0.5; Z = 0.09, *P* = 0.9). Band 4 was in a consistent position, but band 5 was shifted upward, by ~1.8%, in the absence of band 2 (Z = -3.0, *P* = 0.0009); band 5 was in the same position in shells of phenotype 12345 and 1.345.

Kruskal-Wallis tests indicated that band 1 did not differ in width across the three phenotypes (H = 1.2, df = 2, *P* = 0.6), whereas band 3 width did differ (H = 23.1, df = 2, *P* = 0.00001). Pairwise Dunn's tests with Benjamini-Hochberg adjustments indicated that there was no difference between any of the phenotypes in band 1 (Z = 1.02, *P* = 0.3; Z = 1.1, *P* = 0.3; Z = -0.1, *P* = 0.9). The width of band 3 differed between 12345 and 10345 phenotypes (Z = -4.8, *P* = 0.000005), with band 3 narrower when band 2 was absent. No difference in the width of band 3 was observed between the other phenotypes (Z = 2.3, *P* = 0.06; Z = 0.05, *P* = 0.96). The width of band 2 varied significantly between the partially suppressed phenotype and 12345 individuals (H = 20.6, *P* = 0.000006).

2.4.2 Interactions between bands and band-gaps

When individual bands were larger, the corresponding gaps above the band tended to be smaller (**Figure 2.3**), with band 4 showing the strongest relationship (R = -0.5, *P* < 2.2e-16), and band 5 the weakest (R = -0.2, *P* = 0.005). The same relationship was found between the individual bands and the gap width below (**Figure 2.3**); except that band 2 showed the strongest

relationship (R = -0.6, *P* < 2.2e-16) and band 1 did not show any correlation with the band below (R = -0.01, *P* = 0.8).
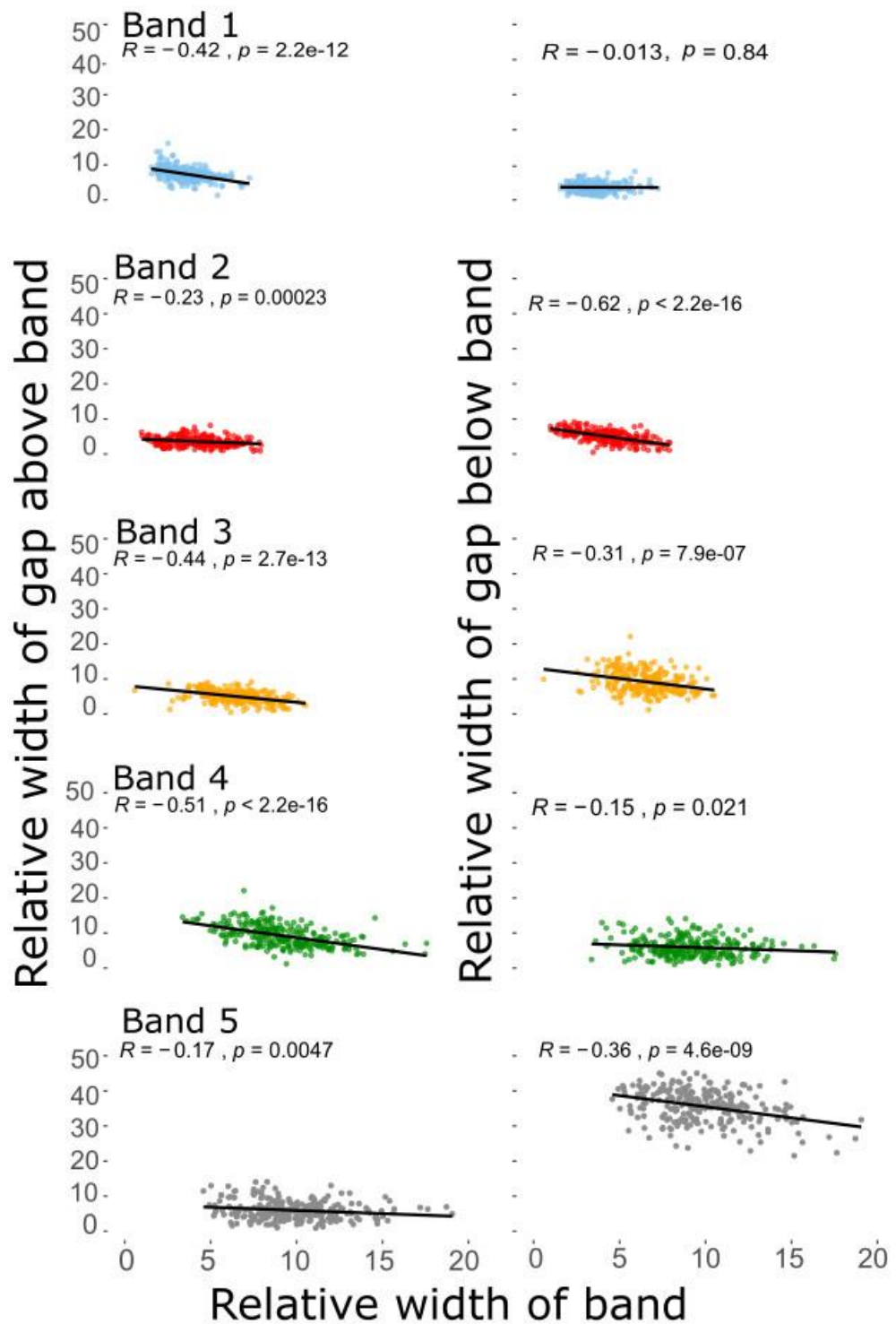
Figure 2.3. The relationship between the width of a band and the widths of the gap above and the gap (left hand side), and below (right hand side) in five banded *C. nemoralis.* Most of the correlations are significantly negative, as expected if bands expand in width by occupying the gaps in-between.

In testing all comparisons between band widths and band-gap widths, most relationships were in the expected direction, except for some of the gap-gap comparisons (**Figure 2.4**); there were unexpected negative correlations between gaps 1/2 ($R = -0.2$, $P = 0.004$), 1/5 ($R = -0.2$, $P = 0.003$), 2/6 ($R = -0.3$, $P = 0.000003$), 3/6 ($R = -0.2$, $P = 0.003$), and 5/6 ($R = -0.5$, $P < 2.2e-16$).
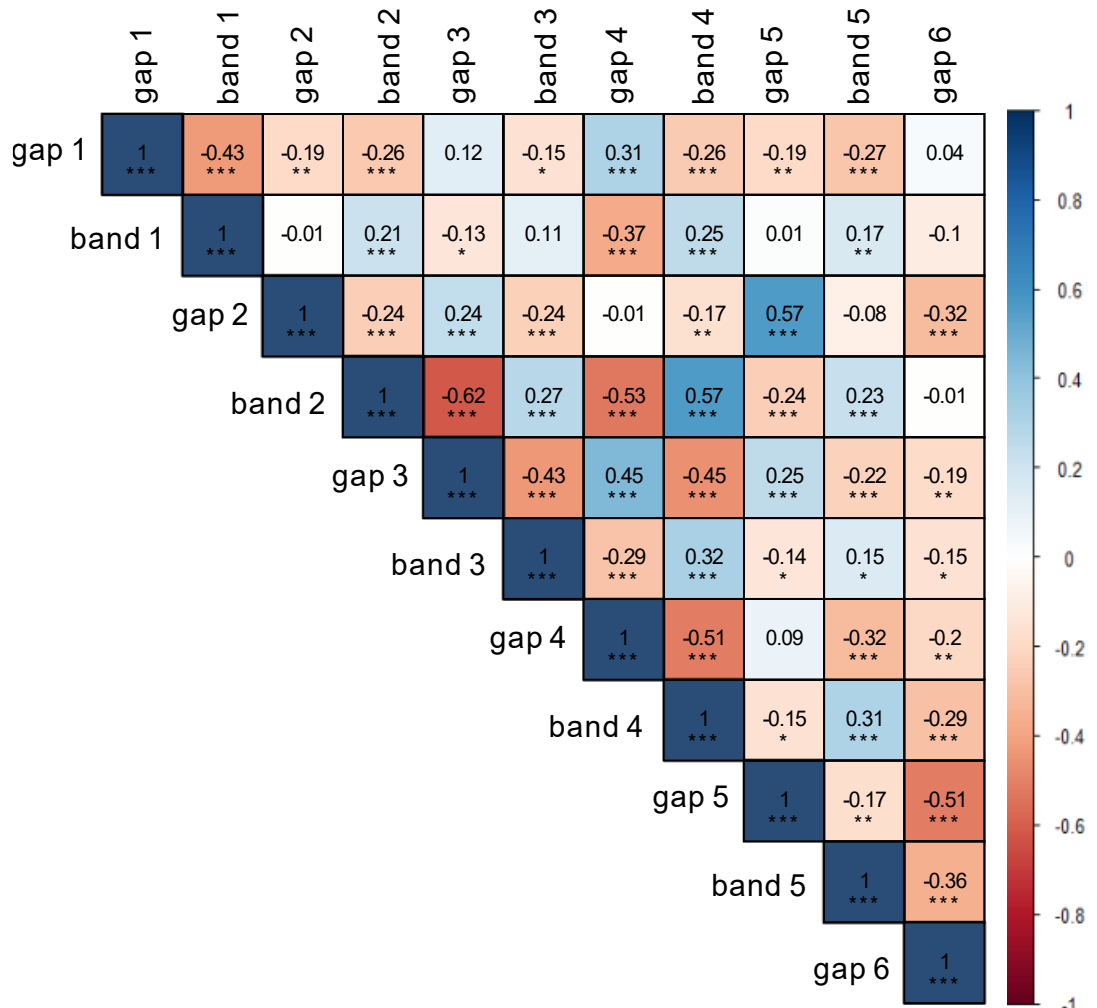
Figure 2.4. Matrix showing correlation between the width of all bands and the width of all gaps, where gap 1 is the gap preceding band 1, next to the suture. Positive relationships are shown in shades of blue and negative relationships in shades of red. $P < 0.05$, **; $P < 0.01$; *** $P < 0.001$.

2.4.3 Comparison between species

The bands had broadly similar positions and widths in the two species, with some minor, significant differences in magnitude (**Figure 2.5**). In *C. nemoralis,* band 1 was ~1% towards the base of the shell, whereas band 5 was ~3% closer to the top ($X^2 = 4.4$, df = 1, $P = 0.04$; $X^2 = 12.6$, df = 1, $P = 0.0004$). *C. nemoralis* individuals also had slightly narrower bands in positions 1 and 4 compared with *C. hortensis* ($X^2 = 18.05$, df = 1, $P = 0.00002$; $X^2 = 21.8$, df = 1, $P = 0.00003$).
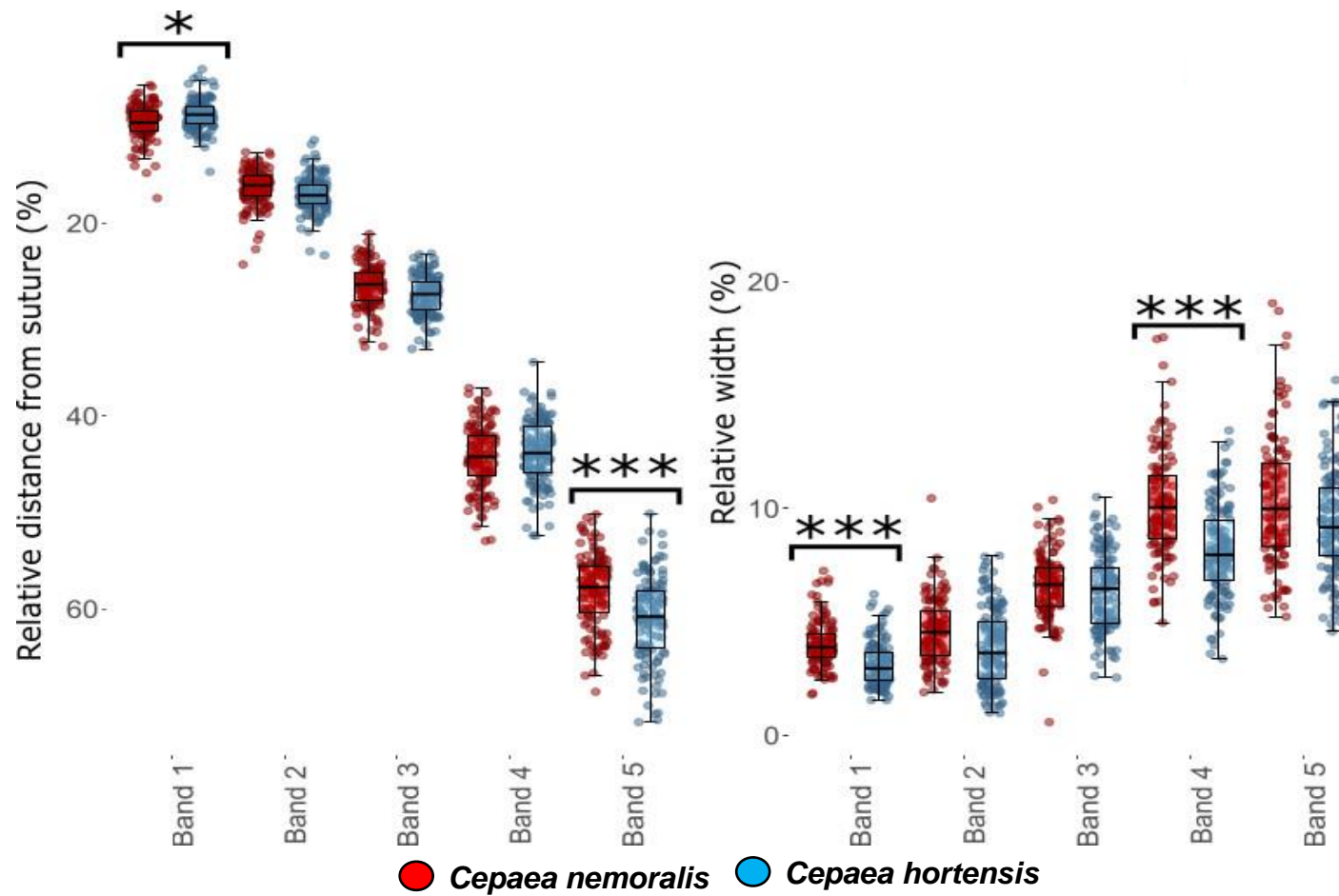
Figure 2.5. Between species comparison of the position (left) and width (right) of each of the five bands in five-banded individuals. *Cepaea nemoralis* is shown in red, and *C. hortensis* in blue. The position of the first and fifth band of a fivebanded individual varies significantly between the two species, and the width of the first and fourthband differs significantly between the two species.

2.4.4 Shell growth and use of 3D models

Bland-Altman plots of paired shell measurements (**Figure 2.6**) showed that neither the tape or computer-based method resulted in measurements which were consistently larger or smaller than the other, thus, the differences in the plots shows data points scattered evenly above and below zero. There was no consistent bias between the two methods (Bias = 0.005), and 95% of the data fell between the upper and lower limits of agreement of -2.04 and 2.05. This confirmed that whilst data is variable, the model is able to reproduce the 3D shape from a 2D photo, and also, that ShellShaper is able to extract band-measurement
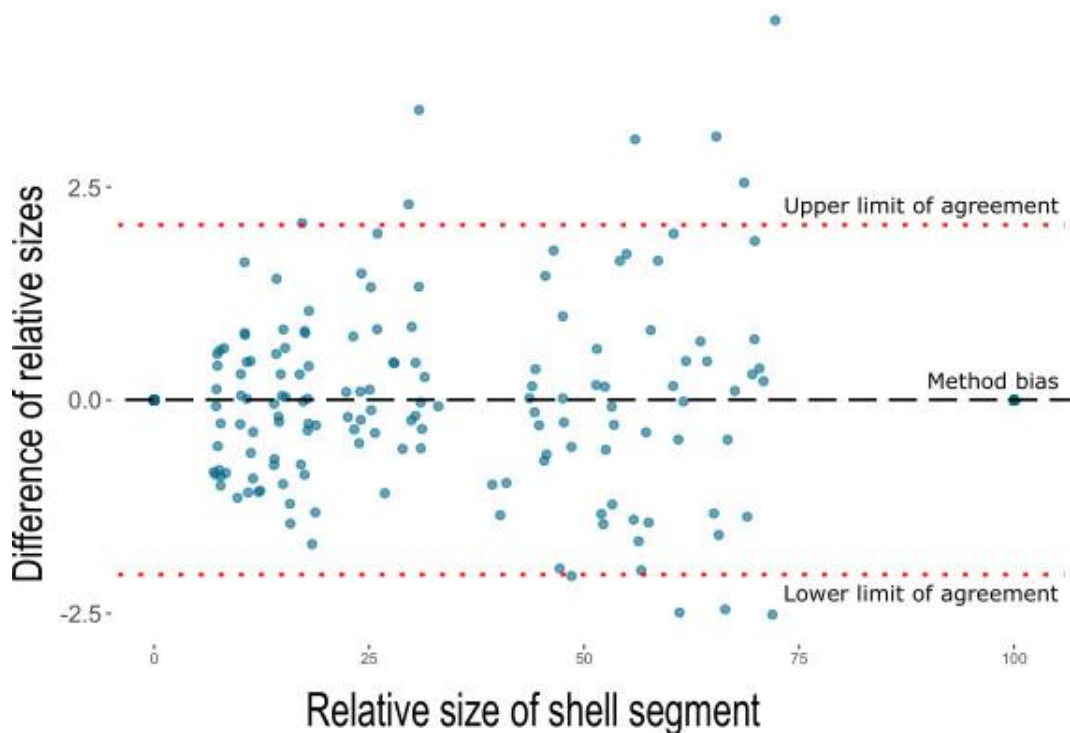
Figure 2.6: Bland-Altman plot of relative widths of shell sections of five banded individuals. X axis represents the average measure of width of shell segment taken by the two methods, and the y-axis represents the difference of measurements from this average. The line of bias (black dashed lined) and the 95% limits of agreement (red dotted lines) are shown.

56

data from a 2D image, whilst retaining information revealed by manual measurements.

Models fitted with fixed effect of shell region, and random effects for distance along the last whorl, and individual, demonstrated that regions of shell in both mid-banded and five-banded shells grow at different rates (Figure 6; $X^2 = 119.7$, df = 10, $P < 0.0001$; $X^2 = 84.9$, df = 2, $P < 0.0001$). Pairwise comparisons show that this difference is exclusively between all shell regions and the region between the last band and the umbilicus. The bottommost area grows at a faster rate than other areas of the shell, which all increase in size at an equal rate throughout growth (**Tables 2.3, 2.4**). The relative proportions of the shell covered by each region changed along the whorl, as the lowermost region of the shell expanded more rapidly than the others. All other shell regions remained at equal proportions relative to one another throughout growth (**Figure 2.7**). Models were repeated with distance along the last whorl as the sole fixed factor, with random effects for shell region and individual. These demonstrated that there is no difference in growth rates in areas of the shell across the length of the last whorl in five banded or mid banded snails (mid-banded: chi-squared = 0, df = 10, P = 1; five-banded: chi-squared = 0, df = 10, P =1). Expansion per quarter whorl in every shell section remains constant throughout the growth of the entire last whorl.

Table 2.3. Pairwise comparisons of proportionate differences in growth rates between areas of shell in mid banded individuals. Data generated by construction of 3D Shell Shaper models. Significant comparisons are highlighted in bold. The gap number refers to the number of gap in each shell, or number of bands plus one, so, here, gap 2 refers to the gap underneath the single band.

Comparison		Estimate	SE	df	t-ratio	p-value
Gap 1	Band 3	1.95	1.05	36.89	1.86	0.165
Gap 1	Gap 2	-1.33	1.05	36.89	-1.26	0.425
Band 3	Gap 2	-3.28	1.05	36.89	-3.12	**0.0009**

Table 2.4. Pairwise comparisons of proportionate differences in growth rates between regions of shell in five banded individuals. Data generated by construction of 3D Shell Shaper models. Only significant comparisons included.

Comparison		Estimate	SE	df	t-ratio	p-value
Gap 1	Gap 6	-3.43	0.79	141.62	-4.32	**0.0014**
Band 1	Gap 6	-3.18	0.79	141.62	-4.01	**0.0046**
Gap 2	Gap 6	-3.32	0.79	141.62	-4.18	**0.0025**
Band 2	Gap 6	-3.10	0.79	141.62	-3.90	**0.0067**
Gap 3	Gap 6	-3.67	0.79	141.62	-4.62	**0.0004**
Band 3	Gap 6	-3.15	0.79	141.62	-3.97	**0.0053**
Gap 4	Gap 6	-4.05	0.79	141.62	-5.10	**0.0001**
Band 4	Gap 6	-3.38	0.79	141.62	-4.26	**0.0018**
Gap 5	Gap 6	-3.65	0.79	141.62	-4.60	**0.0005**
Band 5	Gap 6	-3.06	0.79	141.62	-3.85	**0.0081**
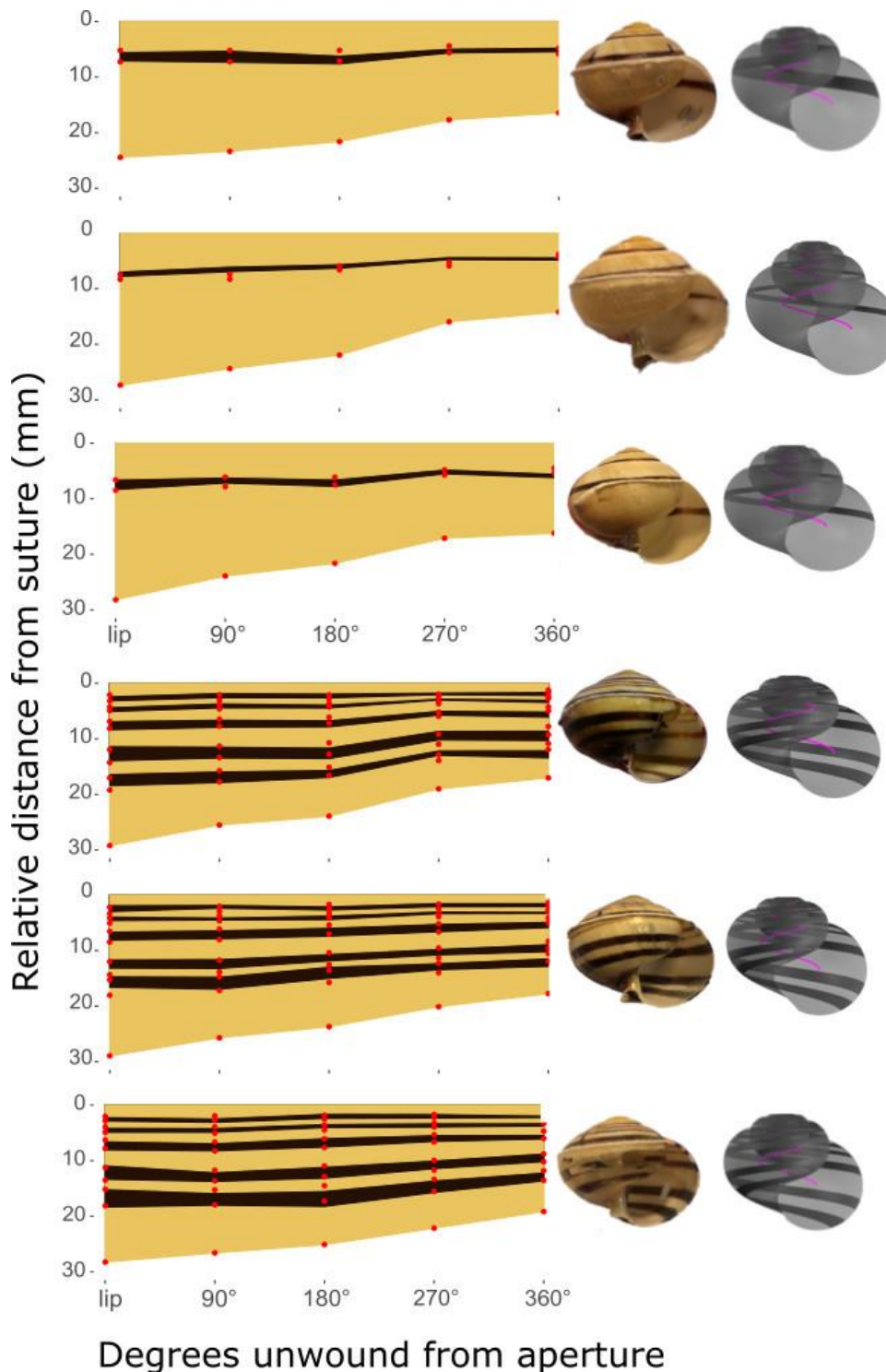
Figure 2.7: Projection of band position and width over last whorl of shell, using mid-banded (top three), and five-banded (bottom three) individuals. Manual (red points) and ShellShaper (dark shading) inferred measures show the same patterns. Also shown is a photo of each shell, and a 3D model generated by ShellShaper; photographs show individuals with the final variable 3cm of adult whorl removed to ensure established banding pattern is shown.

2.4.5 Allometric shell growth

In order to produce the convex spires seen in globose species such as *Cepaea,* allometric growth is necessary. The type of allometry needed for this requires an increase in height of a complete whorl being greater than the increase in width of the same whorl. To confirm the required type of allometry was present in growing shells, a basic allometry test was used to determine whether that the growth in width was smaller than the growth of the height in the shells measured with Shell Shaper. Wilcoxon Signed-rank tests indicate that the increase in whorl height is greater than the increase in whorl width ($V = 465$, $P = 0.00000009$), confirming the allometric growth parameters necessary to produce a convex spire.

2.5 Discussion

In the past, the banding phenotype of *Cepaea* snails has typically been scored as a qualitative character, even though shells with the same number of bands may have a quite different outward appearance. Here, we developed a method to describe quantitative variation in the banding patterns of both species, and then use these findings to test the interactions within and between bands and other shell characters. Broadly, we found that the precise position of bands depends upon the presence or absence of other bands, although the size of the effect is small. These findings give a first hint of the pathway that defines the positions and pigmentation of bands in the shell. By comparing the method with inferences from a 3D model, we show that the same quantitative measures may be applied to a 2D photo of a shell. Overall, the findings provide a starting point for exploration of how bands are placed in *Cepaea*, and the origins of fine variation in banding pattern.

2.5.1 Pigmentation of individual bands is independent

If the deposition of pigmentation in each band is independent of other bands, then one argument is that absence of individual bands in the adult shell should not impact upon the position or width of other bands. However, if there are fewer bands, then the absolute position of the remaining bands becomes of less importance, provided they do not overlap. Band position might then vary slightly, or the width might show greater variation in the absence of other bands. For example, a predator will tend to see a single mid-band, irrespective of the precise position on the shell. In comparison, in a five-banded snail, the mid-band must be distinct from the other bands (unless there is a genetically coded band fusion), which reduces the range of possible positions.

In comparisons between the position of the third band in mid-banded and five-banded shells, we found that the band positions were broadly the same. This was also true of comparisons between the positions of the first and third bands in individuals where the second band was present or absent. Bands occupied more or less the same shell space as the corresponding band in a fully banded snail and did not cross over into the space which the other bands normally occupy. Yet, there were some small but significant differences in position. For example, the second and third bands were typically found at 16.6% and 27.0% of the distance from the suture (**Figure 2.2 inset**); in mid-banded snails, the third band was slightly closer, 26.1%, to the suture. Similarly, the first and third bands were typically found 9.1% and 27.0% (as before) from the suture. When band 2 was missing, bands 1 and 3 were closer together, 10.2 % and 25.6% from the suture. Shells with a band 2 that was only present on the last part of the shell were intermediate for the position of bands 1 and 3. In comparison, we did not find any difference in the widths of any of the bands when other bands were absent, nor any evidence that the differences are influenced by shape or ground colour of the shell. These results therefore show that while the approximate position of the bands is the same, there is a very limited degree of lability in their placement that is contingent upon the presence or absence of other bands.

There are two main explanations for these findings. The first is that the position of all five bands is established and maintained early in shell development, even in the absence of individual bands. The spatial signal for the five bands is likely present in a molecular sense, but the pigmentation is lacking for individual bands. This would imply that the locus for band absence acts late in the pathway that establishes bands. An alternative explanation is that individual band positions are established independently of each other, such that if one band is not present, then this does not impact upon the position of others. In this case, individual band position would have to be defined relative to a fixed character, such as the suture. In our opinion this second explanation is

less credible because we found evidence that the bands do interact, at least to a small degree. Bands differed slightly in position when other bands are absent, including evidence that even late stage band expression can interfere with the position (**Figure 2.2**). More generally, if bands do not interact, it is difficult to understand why instances of mis-positioning of bands were not more common.

It should also be noted that an analysis of hyalozonate patterns similar to those displaying fully pigmented bands could shed light on the relationship between pattern establishment and pigmentation. If banding pattern establishment has two parameters - the determination of the track at a molecular level, and the subsequent pigmentation of said track, it would be beneficial to understand how a hyalozonate phenotype might fit into this. Whilst pigmentation is absent in hyalozonate individuals, the "bands" are still visible along the entirety of the shell, distinct from unbanded individuals in which the track is not visibly present, although it is plausible that it exists, at least in a molecular sense. Does ground colour pigmentation in band position show similar variations in position and widths as the fully pigmented bands? Or, is the position of hyalozonate banding more tightly controlled, serving as a template for pigment adhesion, allowing an amount of variation?

To further explore how bands are placed and interact with one another and shell edges, we investigated correlations between the band widths and the gaps between bands. This was also partly motivated by wanting to understand the reason that bands 3, 4 and 5 are consistently wider than bands 1 and 2. The temptation might be to put the differences down to natural selection, but the default explanation must be non-adaptive. For example, perhaps the top-most bands are narrow because they are constrained by the suture edge. Alternatively, the bottom-most bands might be wider because their expansion is correlated with growth of the

expanding whorl on the lower part of the shell, and band widening is simply an artefact of the deposition of new shell material.

Broadly speaking, the results showed that bands expand in width at the same rate. Where bands were wider in adult shells, the corresponding gap above and below each band was narrower (**Figure 2.3**). There were some unexpected slight negative correlations between the first gap (next to the suture) and the first band with other band-gaps, as well as negative correlations between the last gap (next to the umbilicus) and some other band-gaps. As the negative correlations mainly involved edges, then perhaps the band-gaps at the edges indirectly exert some effect to maintain a narrow gap between the band and the edge?

Moreover, the projections that were taken from manual measurements (**Figure 2.3**) and those inferred from 3D models (**Figure 2.7**) confirmed that all of the regions of the shell expand at the same rate, with the exception of the lowermost part of the shell, the final band-gap before the umbilicus (**Figure 2.7, Tables 2.3, 2.4**). The widths of the bands are significantly correlated for bands 3, 4 and 5 (R = -0.2, -0.3, -0.4, all P < 0.001; **Figure 2.4**) – as an individual band gets wider, then the last band-gap gets proportionately narrower – but there is no such relationship for bands 1 and 2 (R = -0.01, -0.1, neither significant). Overall, the relative difference between bands is unexpectedly small.

Although all bands and the gaps between them become progressively wider, the last gap (i.e. the gap between the end of the final band and the umbilicus) expands at a faster rate than the rest of the whorl. This implies that the lower bands are not simply wider as an artefact of shell material deposition during growth, but rather that the lower bands start wider, and so remain wider throughout growth. The consistency of growth rates across all bands, and therefore the gaps between them, suggests that the widths of all bands are under similar mechanisms of

control/constraint, irrelevant of their position on the shell. The increased growth rate of the lowermost part of the shell is perhaps simply due to the relative downward movement of the aperture in the allometric growth necessary to produce shells with a globose spire, such as *Cepaea*. It is perhaps also likely that the final band-gap becomes larger with shell growth due to a change in the generating curve in the final growth stages of the shell, where the angle of the aperture of an adult shell is further from vertical than in juveniles.

2.5.2 3D models to infer band position and shell shape parameters

The initial method used to measure bands used electrical tape and a dissecting microscope. This means that it was straightforward, but also laborious, difficult to scale, and limited in the data that was collected. These issues were resolved using ShellShaper software. By taking a 2D photo of a shell with the aperture facing upwards, ShellShaper was used to take the same band position measures, and also to make 3D reconstructions of the shell (**Figure 2.7**). Whilst the measurements were varied (95% limits of agreement of ~2% in either direction, there was very limited bias between the two methods, suggesting that neither method consistently under or overestimated the size of a shell segment. Whilst larger sections of the shell (i.e. those towards the umbilicus) appear to produce more variable results when comparing the two methods (**Figure 2.6**), this may simply be due to the very different nature of the two methods, and inevitable slight differences in exact measurement position or angle of an area which grows more rapidly than the rest of the shell. The overarching patterns remain constant between the two methods, despite small discrepancies in exact measurements of individual segments.

Using ShellShaper has the advantage that the method may be applied to species with smaller shells, and those with more bands than *Cepaea*. The method also generates a shell model that can be used for further analyses, including the extraction of growth parameters that will allow for

investigations of the similarities and differences within and between many different species of gastropods. Using Shell Shaper for such comparisons would allow high-throughput data collection, allowing the collection of much larger datasets in both comparative and species specific studies. Whilst Shell Shaper allows comparison of bands in a context similar to traditional geometric morphometrics, the version used here works on the assumption of circular apertures, limiting its use in understanding how band patterns might change in relation to the shape of the aperture or other shell characters. Continual development and increasing sophistication of 3D models produced by ShellShaper, means that such analysis with the use of varying aperture shapes is a possibility in the future. Complementary methods devised by others (e.g. Liew and Schilthuizen 2016) may also be used for the same function, and be more suitable, especially when there is great variability in shell form. Other methods require complex, time consuming, and expensive techniques, such as CT scanning. Shell Shaper has the advantage that a 3D structure can be generated from a single 2D photograph of the shell, which allows for relatively high throughput. Whilst other methods include options such as producing models with non-circular apertures and external shell ornamentation, the ease of inclusion of analysis of banding position and size in ShellShaper provides added advantages not present in other methods.

2.5.3 Inter-species variation

The banding patterns were broadly similar in the two species of *Cepaea*, albeit with some small differences. For example, bands 1 and 4 were narrower in *C. nemoralis*, and band 1 was closer to band 2, and band 5 closer to band 4. These results indicate that control of band deposition mechanisms are only subtly diverged in the two species. Such slight differences in phenotype are unlikely to be detectable to avian predators, although this requires experimental confirmation (Delhey et al. 2015, Davison et al. 2019). Understanding the variation, or lack thereof, present

in these banding patterns does however provide a starting point in establishing the underpinning genetic mechanism, including in relation to other species.

2.5.4 Reaction Diffusion Mechanism (RDM)

The underlying mechanisms behind both the formation, and the control of the position and widths of the bands, in *Cepaea* remain unexplored. Although the reaction-diffusion model has been hypothesised to be of importance in pattern formation in other organisms (Kondo 2002, Gravan and Lahoz-Beltra 2004), the interpretation of the models underlying shell pigmentation is limited to mathematical modelling of hypothetical signalling events (Budd et al. 2014). The models assume that pigmentation is caused by localised excitation and inhibition operating along a line of cells at the mantle edge during biomineralisation. It is not currently known whether the cells involved in pigment secretion are organised in this manner. The precise identity of the molecules involved in molluscan pigmentation also remains relatively uncertain (Budd et al. 2014). To date, there is no definitive evidence that the banding in *Cepaea* is under the control of the reaction-diffusion model.

In several land snail species, including *Cepaea*, the same pigmentation patterns can be observed on both the shell and the mantle (Emberton 1963). The presence of bands on the mantle suggests that the system controlling pigmentation may not be controlled by the simple "line of cells" as first assumed. It should be noted also that physical cues in marine gastropod shells possessing varices (thickened protrusions of shell) do not appear to be the main mechanism used to position new shell structures. Instead, it has been suggested that positional information of these structures is created by a Turing-like system, but with previous shell structures providing some fine-tuning feedback (Webster and Palmer 2019).

Whilst it may be hypothesised that Turing's reaction-diffusion model plays a role in the formation of shell patterns in molluscs, identification of the genes is a first step before testing whether the interacting substances are necessary in defining the patterns. We envisage two converging routes by which this may be made possible, either taking a gene mapping and pattern-led approach (Cossins et al. 2006, Harper et al. 2011, Peichel and Marques 2017), or else by comparing spatial gene expression (Landgrebe et al. 2002, Ståhl et al. 2016, Adamson et al. 2017).

It will certainly be interesting to investigate gene expression in relation to the wide diversity of shell phenotypes. For example, it is conceivable that unbanded *Cepaea* still contain the spatial molecular markers that correspond to bands, but that they are not pigmented – if that is the case then any subtractive method (comparing gene expression in banded versus unbanded snails) will not work. To date, proteomic and transcriptomic studies have begun to identify both novel and co-opted ancient genes involved in biomineralisation and shell deposition (Clark et al. 2010, Jackson et al. 2010, Joubert et al. 2010, Marie et al. 2013, Mann and Jackson 2014), which may ultimately assist in elucidating the formation and maintenance of variation within and between banding phenotypes in *Cepaea.*

Overall, by establishing a method for quantitatively measuring variation in an established banding pattern, and beginning to characterise pigments present in the bands, this work provides a baseline for further studies on the *Cepaea* banding polymorphism. This is true both from the perspective of understanding the presence and maintenance of variation in these banding patterns, and ultimately, the underpinning genetics involved. A next step must be to identify the component parts and evolutionary origins of the supergene in *Cepaea nemoralis* and *C.*

hortensis. A recent genome assembly is a first step towards achieving this aim (Saenko et al. 2021).

Author contributions

The published manuscript resulting from this chapter was the result of a collaborative effort, with the following contributions from listed authors:

Hannah Jackson and Angus Davison conceptualised the project, **Hannah Jackson** collected the data. Jenny Larsson created the 3D analysis software. **Hannah Jackson** performed the formal analysis and methodology, with input from Angus Davison and Jenny Larsson. **Hannah Jackson** produced the original draft, and Jenny Larsson and Angus Davison provided input on subsequent versions and reviewer comments.

Chapter 3: Shell colour variation in *Cepaea nemoralis* and *Cepaea hortensis*

3.1 Abstract

The shell colour of the land snails of the genus *Cepaea* have long been the focus of studies of colour polymorphisms and the inheritance of colour variation in natural populations. Traditionally, *Cepaea* have been scored as belonging to one of three discrete colour morphs – yellow, pink, or brown, which was sufficient for in-field studies. It has recently been established, however, that colour variation in *Cepaea nemoralis* is continuous, occurring around three peaks which roughly correspond to human-scored colour morphs. Here, this analysis is extended to establish whether the variation in *Cepaea hortensis* follows the same patterns. A combination of reflectance spectrophotometry and psychophysical models were used to establish the nature of colour variation in *Cepaea hortensis*, and to compare fine variation in colours between *Cepaea hortensis* and *Cepaea nemoralis*. It was revealed that colour variation in *Cepaea hortensis* is continuous, with no detectable effects of geographic location, except an association of the paleness of yellow shells with latitude. Differences between the colour of *Cepaea hortensis* and *Cepaea nemoralis*, both in terms of exact shade and overall colour are revealed; *Cepaea hortensis* are generally paler, and less pink-toned, but slightly more brown-toned. Precise shade variation of yellow individuals from genetically diverse lineages of *Cepaea nemoralis* are also revealed. The results presented have significance in furthering the understanding of the nuances of the colour polymorphism displayed in *Cepaea* spp., and the precise nature of the selection which acts upon it, as well as highlighting the importance of considering colour as a continuous trait, rather than binning it into discrete groups.

3.2 Introduction

Animal colouration and colour patterns serve a multitude of purposes throughout nature, including social and sexual signalling, thermoregulation, or predator avoidance strategies (Osorio and Vorobyev 2008, Stevens and Merilaita 2009, Cuthill et al. 2017b), and the study of animal colour has been critical in aiding understanding some of the key principles of evolution (Endler and Mappes 2017, San-Jose and Roulin 2017).

It is becoming increasingly apparent that in order to understand the ecological or evolutionary relevance of animal colour patterns that act as signals, it is important that a signal is considered "in the eye of the beholder" (Guilford and Dawkins 1991, Bennett et al. 1994, Endler and Mielke 2005). It is no longer necessary or appropriate to rely on subjective qualitative measures of colour, or methods which rely on human vision (Endler 1990, van den Berg et al. 2020). The way in which a colour is perceived is unique to a perceiver, and is impacted by both the physiological and cognitive perceptual abilities said perceiver, and the specific environmental context in which it occurs. Factors such as lighting conditions and levels of contrast against a given background also affect the way a colour is perceived in a given scenario (van den Berg et al. 2020). Due to the particular intricacies of the visual systems of any given perceiver, correctly and accurately measuring and recording colour, and the appropriateness of the subsequent modelling, are vital in the study of colour as a tool for visual signalling.

The way in which many species experience colour is wholly different to humans. For example, many insect pollinators and birds can see the ultraviolet (UV) end of the spectrum (Briscoe and Chittka 2001, Hart and Hunt 2007, Skorupski et al. 2007, Hirota et al. 2019); several species of diurnal bird have more than three retinal cone types, allowing them to

experience a far broader spectrum of colour than trichromats (Honkavaara et al. 2002, Holveck et al. 2017). The deep-sea dragon fish, *Malacosteus niger*, uses chlorophyll in far-red sensing (Douglas et al. 2016), and guppies (*Poecilia reticulata*) display visual plasticity, possessing the ability to change their perception of colour by adjusting the amount of carotenoid in their diets (Sandkam et al. 2016). The differences in visual sensitivities and cognitive processing abilities among species necessitates the development of specialised colour measurement technologies. These can be paired with psychophysical modelling techniques to provide non-arbitrary measurements of colour, which can be placed in an ecologically and evolutionarily relevant context (Delhey et al. 2015).

Reflectance spectrophotometry provides an objective method for accurately measuring colour and is becoming increasingly prevalent in animal colouration studies (Cassey et al. 2008, Taylor et al. 2016, Holveck et al. 2017, Dunning et al. 2018, Davison et al. 2019). When paired with psychophysical models of colour perception, reflectance spectrophotometry allows contextualisation of variation and how it may be perceived. The contextualisation of variation is useful in cases where the perceiver has a different number of cones to humans, and/or where variation cannot be directly observed or comprehended by a human observer. Reflectance spectrophotometry allows the collection of colour measurements spanning a wide range of wavelengths, from UV to near-infrared, catering for the modelling of colour in the context of visual systems of a wide range of perceivers (Delhey et al. 2015).

Historically, some of the most important species in the study of animal colouration have been snails of the genus *Cepaea, C. nemoralis* and *C. hortensis.* Alongside the peppered moth (Grant et al. 1996, Cook and Saccheri 2013), *Cepaea* spp. have formed the basis for much of the work which has shaped current understanding of the evolution and

maintenance of polymorphisms in natural populations (Ożgo 2011, Cameron and Cook 2012b, Cameron and Cook 2012a, Ożgo and Schilthuizen 2012, Cameron and Cook 2013, Ożgo et al. 2017). *Cepaea* presents a particularly useful study system for evolutionary biologists, not least due to the relative ease of their collection, and the abundance of historical information available regarding the colour of their shells. The distinctive phenotype and variation which is characteristic of *Cepaea* means that they lend themselves to citizen science projects such as The Evolution Megalab (Silvertown et al. 2011, Cameron and Cook 2012b, Worthington et al. 2012, Cook 2014). The Evolution Megalab in particular has played a vital role in the collection of large amounts of qualitative colour data, creating an invaluable resource which has formed the basis of many *Cepaea* colouration studies.

The polymorphism of *Cepaea* is characterised by variation across several shell traits, including ground colour, banding pattern, and lip pigmentation (Cain et al. 1968, Jones et al. 1977, Richards et al. 2013, Cook 2017). Approximately nine loci have been identified as having a role in the control of variation in *Cepaea* colour patterns, at least five of which are tightly linked and inherited together as a "supergene", with characteristically low recombination frequencies between them. Classically, *Cepaea* snails of either species have been scored as belonging to one of three discrete colour groups, yellow (Y), pink (P), or brown (B) (Cain and Sheppard 1954, Richards et al. 2013). Whilst this scoring system is useful due to its easy implementation both in the field and across citizen science led projects, it has some fundamental flaws. The ground colour of *Cepaea nemoralis* shells is now known to be continuously distributed in 3-dimensional colour space (Davison et al. 2019), albeit around three clusters which roughly correspond to human scored colour phenotypes. To ensure that *Cepaea* retains its status as a model system for the study of colour polymorphism, it is necessary to understand further the genetic basis of this variation, and how it appears in natural populations of both *Cepaea nemoralis* and *Cepaea hortensis.*

Whilst steps have been made to define both colour and banding phenotype accurately in *Cepaea nemoralis* (Davison et al. 2019, Jackson et al. 2021), it would be useful to extend these methods to consider the variation present in *Cepaea hortensis* in detail.

Previous attempts to quantify the colour variation of *Cepaea* shells have primarily relied on grouping individual snails into specific colour morphs, and considering these morphs as a whole (Cain and Sheppard 1950, Ortiz 1973, Cook et al. 1999, Ożgo and Schilthuizen 2012, Cameron et al. 2013b), rather than assessing the variation present within the individual morphs. Whilst 'binning' individuals into discrete groups may be useful on a small scale, as localised variation often falls into distinct categories (Davison et al. 2019), the distribution of colour morphs across the European population of *Cepaea nemoralis* is continuous. Collapsing observed variation into principal components, as per Delhey et al. (2015), provides insight beyond that gained by considering colours as discrete entities. For example, the banding pattern of *Cepaea nemoralis* shells is known to be associated with colour in various ways (Davison et al. 2019), but our understanding of this association has been restricted by the categorical approach to classifying shell colour. Breaking down phenotypic variation further, into its constituent components, may be beneficial to aid the understanding of how variation in banding and colour evolves and is maintained. Considering individual components of colour allows a more detailed understanding of the variation present in natural populations, how they interact with their environment, and ultimately how the genetic control mechanisms underpinning the variation may interact with one another.

In this chapter, I investigate the variation in colour across the European ranges of both *C. hortensis*, and *C. nemoralis*, in an ecologically and evolutionarily relevant context, with several aims. Firstly, I aim to determine whether variation in *C. hortensis* is continuous or discrete.

Secondly, I aim to determine whether colour variation in *C. hortensis* is associated with geographic location. I also aim to establish whether the same level of variation is present across both species. Next, I aim to determine whether yellow individuals of *C. nemoralis* form clusters in three-dimensional colour space, which correspond to discrete yellow phenotypes. Differences in yellow individuals might suggest the presence of multiple alleles controlling the yellow phenotype. Finally, I aim to determine whether banding phenotype interacts with the individual components of colour in yellow individuals of both species.

These aims were achieved by pairing reflectance spectrophotometry measurements with psychophysical modelling of colour and subsequent principal components analysis in tetrachromatic visual space, allowing the extraction of biologically relevant axes of variation. Determination of whether the same level of variation is present in *Cepaea hortensis* as is observed in *Cepaea nemoralis* allows speculation regarding divergence of the two species, and whether an avian predator might be able to distinguish between them. The idea that the colour variation of shells of *Cepaea nemoralis* occurs along a continuous spectrum of variation is built upon, to further consider how colour variation appears to an avian predator in *Cepaea*. The results have significance for understanding the *Cepaea* polymorphism, and the nature of the selection acting upon it, as well as providing a more complete picture of the variation by utilising samples across a broader and more complete distribution, encompassing the entirety of the *Cepaea* genus.

3.3 Materials and methods

3.3.1 Sample collection

Individual *C. nemoralis* and *C. hortensis* snails were collected opportunistically by volunteer-led collection and field trips across Europe. Snails were frozen at -80°C upon arrival at The University of Nottingham, subsequently thawed and bodies were extracted from shells and stored at -20°C. The ground colour of the shell was scored qualitatively as either yellow (Y), pink (P), or brown (B), and shell banding phenotype was scored as per Murray (1963a), with minor deviations where necessary (Davison et al. 2019) to allow for phenotypes such as fused and partial bands. Species were identified by phenotypic differences and known species distributions, and any available data regarding collection location was noted.

3.3.2 Spectrophotometry

Spectral readings were collected using an Ocean Optics spectrometer (model USB2000+UV-VIS-ES) and light source (DT-MINI-2-GS UB-VIS-NR) for individual shells, using a WS-1 diffuse white reflectance standard to set the baseline light spectrum (Teasdale et al. 2013, Taylor et al. 2016), and complete darkness to set the dark spectrum standard. All measurements were taken relative to these two standards, given as a relative percentage reading across wavelengths between 300-700nm, at intervals of 0.4nm. Reflectance measurements were taken on the underside of the shell (**Figure 3.1**), as it was usually area where the periostracum was fully intact, the area least exposed to sunlight so least susceptible to fading, and away from any colour boundaries created by bands; measurements taken from within 0.2mm of a colour boundary are inaccurate (Taylor et al. 2016). Before measurements were taken, all individuals were checked with the spectrophotometer for colour boundaries invisible to the human eye, such as UV patterning.

Figure 3.1: Underside of a yellow *Cepaea nemoralis* shell, showing approximate location of spectral measurements. Exact position varies between each shell to allow for damage to the periostracum, and between repeat measurements taken from individual shells to capture localised variation in ground colour.

The probe was held steady and targeted with a micro-manipulator (Prior, Cambridge, UK) during all measurements. A custom-made aluminium sheath ensured that point measurements were consistently taken at a 45° incident angle, 2mm away from the surface of the shell (Endler 1990, Taylor et al. 2016). Shell measurements were taken 3 times, non-consecutively, with software recalibrated against light and dark standards every 2-3 measurements to account for lamp drift. Non-consecutive repeat measurements were necessary to capture minor local variations in shell colour. Readings were collected using Ocean Optics SpectraSuite v.2.0.162 (software settings: integration time 750msec, boxcar width 5, scans to average 10), then repeats averaged, raw data smoothed with a loess smoothing parameter of 0.18, the lowest level of smoothing which both removed noise but maintained spectral shape. Smoothed data were then binned into 1nm groups using the package Pavo2 v.2.6.1 (Maia et al. 2019), in R version 4.04 (R Core Team 2021).

3.3.3 Spectral processing and psychophysical modelling

Reflectance spectra were analysed using a psychophysical model of colour vision to assess whether chromatic differences between reflectance spectra exceed a discrimination threshold, or a single 'Just noticeable difference' (JND) unit (Vorobyev and Osorio 1998, Vorobyev et al. 1998). A JND is the smallest unit of variation which can be perceived by a receiver, such as an avian predator (Delhey et al. 2015), and larger JND values represent more distinguishable perceived differences in colour signal (Maia and White 2018). A framework for psychophysical modelling analysis with tetrachromatic visual systems is set out in Delhey et al. (2015). The key to these models lies in the degree to which a particular combination of reflectance and illuminant spectra stimulates each of the four photoreceptors in the retina. In tetrachromats such as avian predators, these photoreceptors are four single cones used for colour vision, which are sensitive to long (L), medium (M), short (S), and very short (VS) wavelengths of light (Hart 2001b).

To analyse chromatic variation, the quantum catches for each cone type were converted into three chromatic coordinates (x, y and z) using the formulas of Cassey et al. (2008), where Euclidean distances between points in a 3-dimensional plot reflect differences in colour as perceived by a receiver. As there are no data available for the cone quantum catches of the song thrush, *Turdus philomelos*, which is the main avian predator of both *Cepaea nemoralis* and *C. hortensis* (Goodhart 1958, Cameron 1969, Cook 1998), inferences from the visual system of the closest available relative, the blackbird *Turdus merula,* were used (Hart et al. 2000, Hart 2001a), namely the relative abundance of each photoreceptor in the retina, or cone proportions of VS: 0.528, S: 0.904, M: 1.128, L: 1, and sensitivity functions of 373, 461, 543 and 603, respectively (**Table 3.1, Figure 3.2**). The analyses assumed that the L cone has a noise-to-signal ratio of 0.05 (Delhey et al. 2015), giving ratios for the other cones of VS: 0.0688, S: 0.0526 and M: 0.0471. There is

debate surrounding the appropriate noise-to-signal ratio for chromatic and achromatic vision, varying over a four-fold range from 0.05 to 0.1 or 0.2 (Olsson et al. 2018). Using a higher ratio would mean dividing all xyz values by 2 or 4, affecting the magnitude of the JNDs, but not the overall interpretation. The irradiance spectrum of "standard daylight" (d65), which is reflective of lighting conditions of open spaces, was used for the main analyses. Analyses were also run for "woodland shade" and "forest shade" in initial analyses on *Cepaea hortensis* colour to determine the influence of differing illuminant on avian perception of colour (Vorobyev et al. 1998).

Principal Components Analysis (PCA) was carried out on the chromatic coordinates (x, y, and z) to identify the three main axes of chromatic variation, referred to subsequently as PC_{xyz}. A covariance matrix rather than a correlation matrix was used to preserve the perceptual distances (JNDs) as which PC_{xyz} values are given (Delhey et al. 2015).

Table 3.1: Cone proportions, sensitivity functions, and noise:signal ratios for each of the four cone types present in the retina of *Turdus merula*. These parameters are central to the tetrachromatic psychophysical models used to convert reflectance spectra into xyz co-ordinates of colour. Cone proportion refers to the abundance of cone/photoreceptor type in the retina, relative to the number of L cones. The sensitivity functions refer to the differing sensitivities to wavelengths of light of the four cone types (also see **Figure 3.2**). The noise:signal ratio refers to the amount of signal captured by the photoreceptor, relative to the level of noise present in each receptor.

	Photoreceptor type			
	VS	**S**	**M**	**L**
Cone proportion	0.528	0.904	1.128	1
Sensitivity function (nm)	373	461	543	603
Noise:signal ratio	0.0688	0.0526	0.0471	0.05
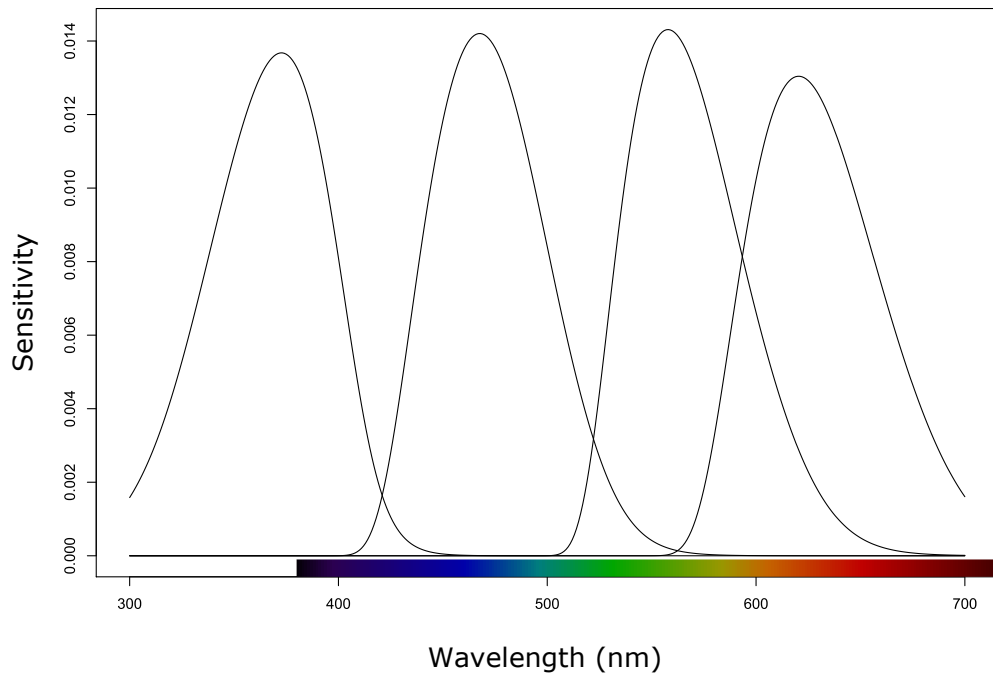
Figure 3.2: Cone sensitivities of *Turdus merula* for each of the four photoreceptor types (VS, S, M, L), displaying the range of wavelengths each cone is responsible for interpreting. Width of peak corresponds to the range of wavelengths processed. Stimulation of the S cone represents cone catch at the blue end of the spectrum, the M cone represents the yellow part of the visual spectrum, and the L cone represents red wavelengths of light being perceived.

3.3.4 *Cepaea hortensis* - discrete or continuous?
3.3.4.1 Gaussian finite mixture modelling

To explore whether the shell colour variation of *Cepaea hortensis* is discrete or continuous, a cluster analysis was performed on the processed spectral data. To identify potential clusters within the chromatic coordinate data, all cluster analysis by agglomerative Gaussian mixture modelling was carried out using Mclust 5.3 in R version 4.0.4 (Scrucca et al. 2016, R Core Team 2021). Agglomerative clustering involves a "bottom-up" approach, where each point constitutes a single-

element cluster (a leaf). At each step of the algorithm, the two most similar clusters are combined into a new, bigger cluster (a node); similarity is determined with the use of eigenvalues. This procedure iterates until all points are a member of a single cluster (the root). From this root, optimal nodes are determined by considering the Bayesian Information Criteria (BIC) of each fitted model. The inverse of this is "top-down", divisive clusters, where a single cluster containing all points is broken down iteratively. Bottom-up clustering is useful for detecting small clusters within a larger dataset, such as separating the small number of brown snails in populations of *Cepaea hortensis*.

Here, and in all subsequent cluster analyses both in **Chapter 3** and **Chapter 4**, 14 different model types were fitted to 3-dimensional data ten times, and each model type was fitted repeatedly assuming a different fixed number of clusters, between one and ten. In the multivariate setting, the volume, shape, and orientation of the cluster groupings, or covariances, can be constrained to be equal or variable. Thus, 14 possible models with different geometric characteristics can be specified. **Table 3.2** reports all such models with the corresponding data distribution structure, volume, shape, orientation, and associated model abbreviations used throughout **Chapter 3** and **Chapter 4**. In **Figure 3.3** the geometric characteristics of each of the models described in **Table 3.2** are shown graphically. A total of 140 model types were fitted to the data in each instance of Gaussian finite mixture modelling, and the best fitting model was determined as the one with the highest BIC, with significant differences determined using a bootstrap approach with 999 iterations. Resolved clusters were then compared to human-scored colours.

Table 3.2: Geometric distribution structures (these are related to the data distributions within each cluster, for example, an ellipsoidal data distribution structure assumes each of the three clusters have a gaussian distribution), volumes, shapes, and orientations of each of the 14 models and associated abbreviations fitted to cluster analysis. Each model has n ellipses fitted, according to number of clusters resolved, with the following characteristics.

Model name	Distribution	Volume	Shape	Orientation
EII	Spherical	Equal	Equal	-
VII	Spherical	Variable	Equal	-
EEI	Diagonal	Equal	Equal	xy
VEI	Diagonal	Variable	Equal	xy
EVI	Diagonal	Equal	Variable	xy
VVI	Diagonal	Variable	Variable	xy
EEE	Ellipsoidal	Equal	Equal	Equal
EVE	Ellipsoidal	Equal	Variable	Equal
VEE	Ellipsoidal	Variable	Equal	Equal
VVE	Ellipsoidal	Variable	Variable	Equal
EEV	Ellipsoidal	Equal	Equal	Variable
VEV	Ellipsoidal	Variable	Equal	Variable
EVV	Ellipsoidal	Equal	Variable	Variable
VVV	Ellipsoidal	Variable	Variable	Variable

Figure 3.3: Schematic of the 14 models (abbreviations defined in **Table 3.2**) fitted during cluster analysis, displayed in two dimensions. Ellipses represent clusters of different sizes, shapes and orientations, each panel represents a different model type, with differing geometric distributions, shapes, orientations, and volumes in individual clusters. Figure adapted from Scrucca et al., 2016.
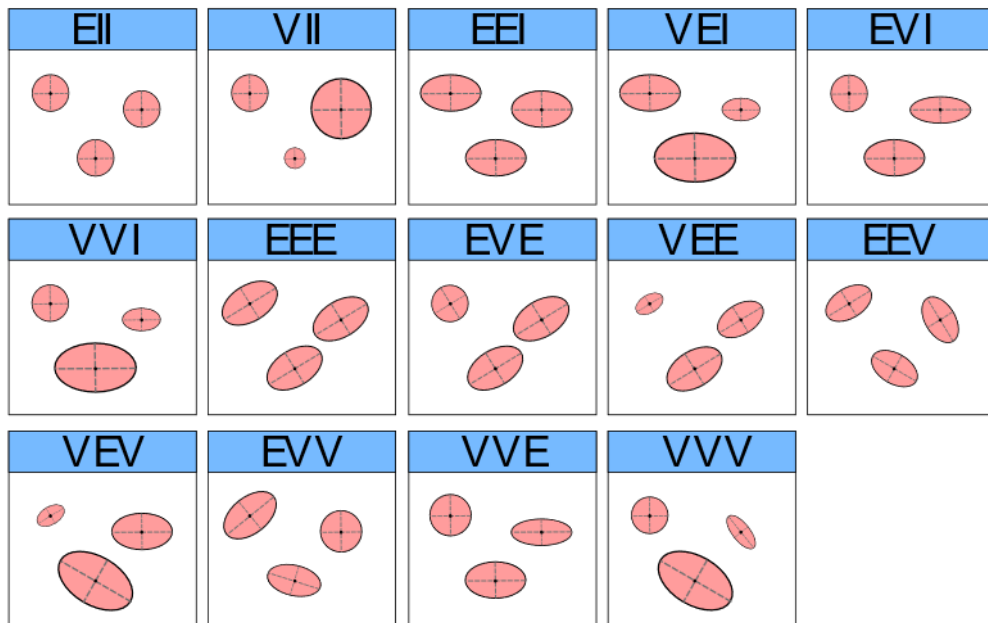
3.3.5 Cepaea geographical variation

To establish whether the continuous colour distribution of *Cepaea hortensis* shells, as defined by PC_{xyz} axes, varies across geographic space, generalised linear mixed effects models (GLMMs) were run, using the package lme4 in R version 4.04 (Bates et al. 2015, R Core Team 2021). Initially, three models were performed on measurement data from all three colour morphs, with all shells grouped together. To determine whether each PC_{xyz} axis varied with geographic location, a single model was run with each PC_{xyz} axis defined as the response variable. Models were initially fitted fully saturated, with fixed effects for latitude, longitude, and the quadratic of each of these to account for non-linear associations. A full set of two-way interactions were also included, apart from those between quadratic effects. Latitude and longitude are partially co-linear,

and this was reflected in the model fitting process. Random effects of country of collection were included in the model to control for possible effects of co-linearity or non-independence of populations from the same country for factors other than latitude and longitude. For model selection, a full set of models including every combination of fixed effect was generated. These models were ranked according to their Akaike Information Criterion (AIC). From a full model set, models with an AIC value within 2 of the best fitting model (value closest to zero) were considered to be equally supported, and so these were averaged. Full coefficients are quoted in the final averaged model, meaning that any terms not appearing in a given component model were assigned a coefficient of zero before averaging. Banding was not included as a fixed factor in models due to correlations present between banding and other fixed factors.

To determine whether the precise shade of yellow was affected by location, a second set of models was run on a subset of all individuals which had previously been categorised as falling into a "yellow" cluster with Gaussian mixed effects modelling. Models were again run on all three PC_{xyz} axes separately. Finally, to establish whether there was an effect of geographic location on the probability of an individual shell being classified as "yellow" by Gaussian finite mixture modelling, a similar model as those described above was run, but included a binomial error structure. Each of the seven models described above were repeated on colour measurements of *Cepaea nemoralis* shells.

3.3.6 *Cepaea hortensis vs Cepaea nemoralis* – is variation equal?

To determine whether there is a difference in colour phenotypes between *Cepaea nemoralis* and *Cepaea hortensis*, reflectance spectra from all individuals of *Cepaea hortensis*, and individuals of *Cepaea nemoralis* excluding those collected in the Pyrenees were collated. Pyrenean individuals were excluded from analysis due to a difference in clustering

between Pyrenean and European *C. nemoralis* shells (see **Sections 3.3.7** and **3.4.4)**. Tetrachromatic psychophysical colour modelling was performed, PC_{xyz} values extracted, and Gaussian finite mixture modelling carried out (**see section 3.3.4**).

A multidimensional extension of the Kolmogorov-Smirnov test, the Peacock's test (Fasano and Franceschini 1987) was run on xyz coordinates of each species to determine whether the shape of the distribution of points in three dimensions (xyz) was equal in *C. hortensis* and *C. nemoralis*. Kolmogorov-Smirnov tests are applicable to continuous one-dimensional data samples, and the Peacock's test extends this to allow comparison in of distributions of points in multidimensional space. Whilst computationally demanding, and so inappropriate for very large sample sizes, Peacock's tests are more stable than alternatives and do not have the problem of subjective variation in result according to user-defined parameters such as data binning, where sizes of bin can be manipulated manually (Lopes et al. 2008).

Three PC_{xyz} values were determined from xyz co-ordinates for each species, each of which provides an overview of the components of colour which comprise variation. These axes of variation were compared between species one at a time using pairwise Kolmogorov-Smirnov tests, first with raw data to establish if distributions of data along each PC_{xyz} axis were equal, and then with data where the mean of each PC_{xyz} axis of *Cepaea hortensis* individuals had been shifted to match the mean of *Cepaea nemoralis*. Comparison between the distributions shifted to centre around a single mean determined whether the spread of variation along a specific PC_{xyz} axis differed in one species over the other, irrespective of the mean. To establish whether the means of the three PC_{xyz} values differed among species, a GLMM was run on each principal component individually, with species as the sole fixed factor in all three

models, and random effects of banding and geographic location. To determine whether components of colour in individuals classified as particular colour morphs diverge between the two species, analysis was repeated on snails of a focal morph of yellow.

3.3.7 Are there different types of yellow?

To determine whether the variation within a single focal morph, in this case yellow, formed clusters which might represent different types of the focal morph of *Cepaea nemoralis,* Gaussian finite mixture modelling was carried out. Human scored yellow individuals were subset from the complete *Cepaea nemoralis* dataset, and psychophysical modelling and subsequent Gaussian finite mixture modelling were performed. The countries of origin of individuals were examined to determine whether clustering differences were associated with the country of origin. Human scores were used in this analysis as human scoring of colour is largely concordant with Gaussian finite mixture modelling scoring, particularly in yellow *Cepaea nemoralis* (Davison et al. 2019). Subsequent Peacock's, pairwise Kolmogorov-Smirnov tests, and GLMMs were also carried out on resolved groups of data, as described in **section 3.3.6.**

3.3.8 Interactions between colour and banding

To establish whether the presence of bands on a shell influences the ground colour of yellow *Cepaea* shells, the three most common banding types were extracted from the main dataset; these were non-banded (00000), mid-banded (00300), and five-banded (12345). To determine whether there was an effect of banding on the probability that a snail shell could be classified as yellow by Gaussian mixed effects modelling, a GLM with a binomial error structure and a fixed factor of banding was performed on data in which an individual was either scored as belonging to the focal morph (yellow), or not. The effect of banding pattern on the

precise shade of yellow as described individual PC_{xyz} axes was also established by running similar models, without a binomial error structure. These models were fit to all three PC_{xyz} values of yellow individuals separately. A single fixed factor of banding was included in the analyses, with a random factors of site, to alleviate any effects of co-linearity. Least-square means with Tukey adjustments for multiple comparisons were performed to allow direct comparison of banding phenotypes. Analysis was performed separately on *Cepaea nemoralis* and *Cepaea hortensis*.

3.4 Results

Reflectance spectra of 2415 individual shells were collected - 465 from *Cepaea hortensis*, 1950 from the European distribution of *Cepaea nemoralis*. Of these 1950, a high number (n = 813) were collected from several valleys in the Pyrenees. Individuals were from 204 populations, distributed throughout the UK and mainland Europe (**Figure 3.4**).
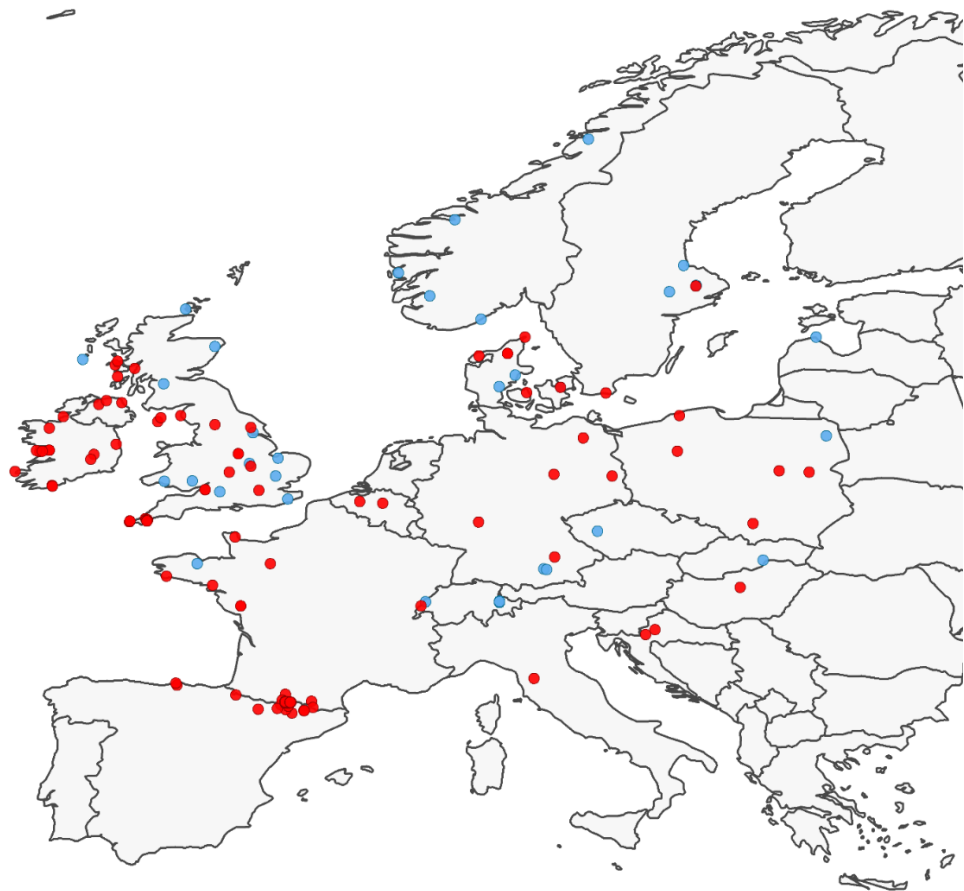
Figure 3.4: location of sampling locations of populations of *Cepaea nemoralis* and *Cepaea hortensis*. Populations of *Cepaea nemoralis* are shown in red, and blue dots indicate locations of populations of *Cepaea hortensis*.

3.4.1 *Cepaea hortensis* discrete or continuous

To determine whether colour morphs of *Cepaea hortensis* shells form clusters in three-dimensional chromatic space, and whether observed clusters correspond to human-observed qualitatively scored colour morphs, Gaussian finite mixture modelling was applied to the xyz visual space co-ordinates. The best model (model type = EEV; BIC = -5995.24; *P* < 0.001 when compared to the second best model) included three clusters, which roughly corresponded to human-scored yellow (n=360, 78.26%), pink (n=76, 16.52%), and brown (n=24, 5.22%), with the largest discrepancies present between modelled and human scoring of brown shells (**Table 3.3**), as is the case in *Cepaea nemoralis* (Davison et al. 2019). The second-best model also recovered three clusters (VEV; BIC = -6004.09; *P* < 0.001 compared with third best model), and the third recovered two clusters (VVV; BIC = -6009.63).

This analysis was repeated with both forest shade and woodland shade illuminance conditions to see if differentiation in lighting conditions affects the number of clusters identified, and how individual snail shells are classified by cluster analysis using Gaussian finite mixture modelling. In each of these analyses, the best fitting model identified three clusters from the data, although the numbers of individuals placed in each cluster differed slightly **(Table 3.3a)**.Within this classifications, banding impacted reclassifications differently **(Table 3.3b)**. The concordance of the results from the analysis using the three different illuminance spectra suggested that lighting conditions do not substantially alter perceptions of the shell morphs, and so standard daylight (d65) was used for all subsequent analysis.

Table 3.3a: Number of *Cepaea hortensis* individuals either human scored as belonging to a colour morph, or assigned to each colour category by Gaussian finite mixture modelling, when psychophysical modelling was performed under three illuminance conditions, standard daylight, forest shade, and woodland shade.

Colour/ category	Human scored	Standard daylight	Forest shade	Woodland shade
Yellow	420	360	370	372
Pink	32	76	64	60
Brown	8	24	26	28

Table 3.3b: Influence of banding pattern on reclassification of "colour category" by MClust algorithms

Human score	D65 category	Unbanded	Mid-banded	Five-banded	Other banding	Total
Yellow	Yellow	182	19	126	18	345
Yellow	Pink	26	0	39	2	67
Yellow	Brown	2	1	4	0	7
Pink	Yellow	9	0	1	0	10
Pink	Pink	9	0	0	0	9
Pink	Brown	8	3	2	0	13
Brown	Yellow	2	0	1	0	3
Brown	Pink	0	0	0	0	0
Brown	Brown	3	0	1	0	4

Within 3-dimensional colour space (defined by the xyz co-ordinates), and subsequent analyses in this chapter which refer to 3-dimensional colour space, variation along the z axis represents stimulation of the L cones relative to the other 3 cone types (M, S, and VS), variation along the y axis represents stimulation of the M cone relative to the S and VS cones, and the x axis represents variation in stimulation of VS relative to the S cone (Delhey et al. 2015, Davison et al. 2019).

Principal components analysis (PCA) on the three chromatic co-ordinates (x, y and z) derived from psychophysical modelling of reflectance spectra of *Cepaea hortensis* reveals that colour variation occurs along three main axes of variation, subsequently referred to as $PC_{xyz}1$, 2, and 3. After PCA has reframed variation to occur across meaningful axes, high values of $PC_{xyz}1$ represent differences in saturation between shells by high stimulation of L and M cones and lesser stimulation of S cones, with low $PC_{xyz}1$ values corresponding to low stimulation of L and M cones and high stimulation of S cones. High $PC_{xyz}1$ values represent shells which are more reflective relative to a white standard, so lighter in colour. High $PC_{xyz}2$ values represent relatively higher stimulation of S cones and lesser stimulation of L cones, low $PC_{xyz}2$ values represent the inverse of this. High $PC_{xyz}2$ values represent a shell which is more pink than yellow. High values of $PC_{xyz}3$ represents relatively high stimulation of the L cones compared to lesser stimulation of the M cones, and low $PC_{xyz}3$ values represent the inverse of this. High $PC_{xyz}3$ values represent a shell which is more brown than yellow. Dotted lines represent the peaks of quantum cone catch for each photoreceptor type (**Figure 3.5**).

$PC_{xyz}1$ explains 86.68% of variation, and has a strong positive loading for x (0.642), a strong negative loading for y (-0.634), and a slightly weaker negative loading for z (-0.431). In all subsequent analysis on *Cepaea hortensis* and *Cepaea nemoralis*, variation along the $PC_{xyz}1$ axis

does not separate cluster analysis scored yellow, pink and brown snails from one another (i.e. yellow individuals do not all have low $PC_{xyz}1$ values, pink shells do not all have middle-range $PC_{xyz}1$ values, and brown shells do not all have high $PC_{xyz}1$ values). In *C. hortensis*, $PC_{xyz}1$ slightly separates yellow snails from one another, but broadly represents saturation or intensity of colour. $PC_{xyz}2$ explains 11.36% of the total variation, and has strong or medium positive loadings for x (0.754), y (0.422), and z (0.503). $PC_{xyz}2$ separates pinks from browns and yellows, with a high $PC_{xyz}2$ value indicating a pink shell. $PC_{xyz}3$ explains only 1.95% of variation, and has a weak positive loading for x (0.137), a strong positive loading for y (0.648), and a strong negative loading for z (-0.749). $PC_{xyz}3$ broadly separates pink and brown from yellow shells, with a low $PC_{xyz}3$ value indicating a yellow shell. The range of observed variation in the data was large, at 36, 13, and 8 JNDs for PC_{xyz} 1, 2, and 3 respectively.

In *Cepaea hortensis*, there are three overlapping clusters resolved by Gaussian finite mixture modelling (**Figures 3.6, 3.7**). The overlap of these clusters suggests that the colour variation of *C. hortensis* shells is continuous, albeit occurring around three clusters which roughly correspond to human-scored definitions of colour phenotypes. Density plots in **Figure 3.7** show the distribution of individuals classified by colour category along the xyz axes of variation, although pink and brown individuals may appear overrepresented in these plots due to the small sample sizes of each of these colours.
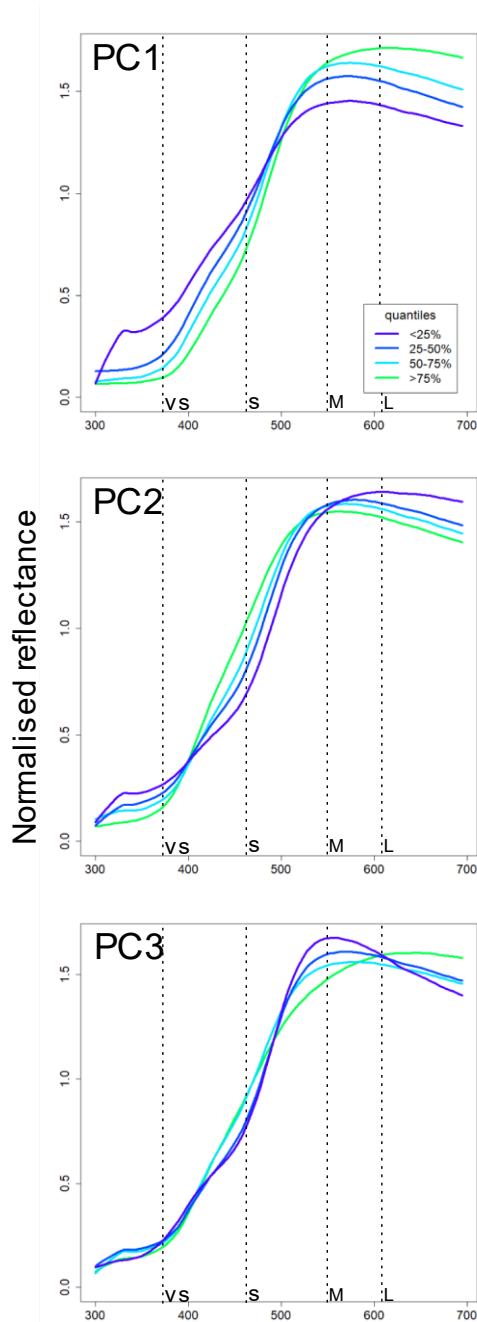
Figure 3.5: Interquartile ranges of the average normalised reflectance spectra of individual PC_{xyz} of *Cepaea hortensis*. Spectra are back calculated from psychophysical modelling equations, using the four quartiles of PC_{xyz} values at given wavelengths. These plots confirm that high values of $PC_{xyz}1$ represent differences in saturation between shells by high stimulation of L cones and lesser stimulation of S cones, relative to M cones; high $PC_{xyz}2$ values represent relatively higher stimulation of S cones and lesser stimulation of L cones; $PC_{xyz}3$ represents relatively high stimulation of the L cones compared to lesser stimulation of the M cones. Dotted lines represent the peaks of quantum cone catch for each photoreceptor type.
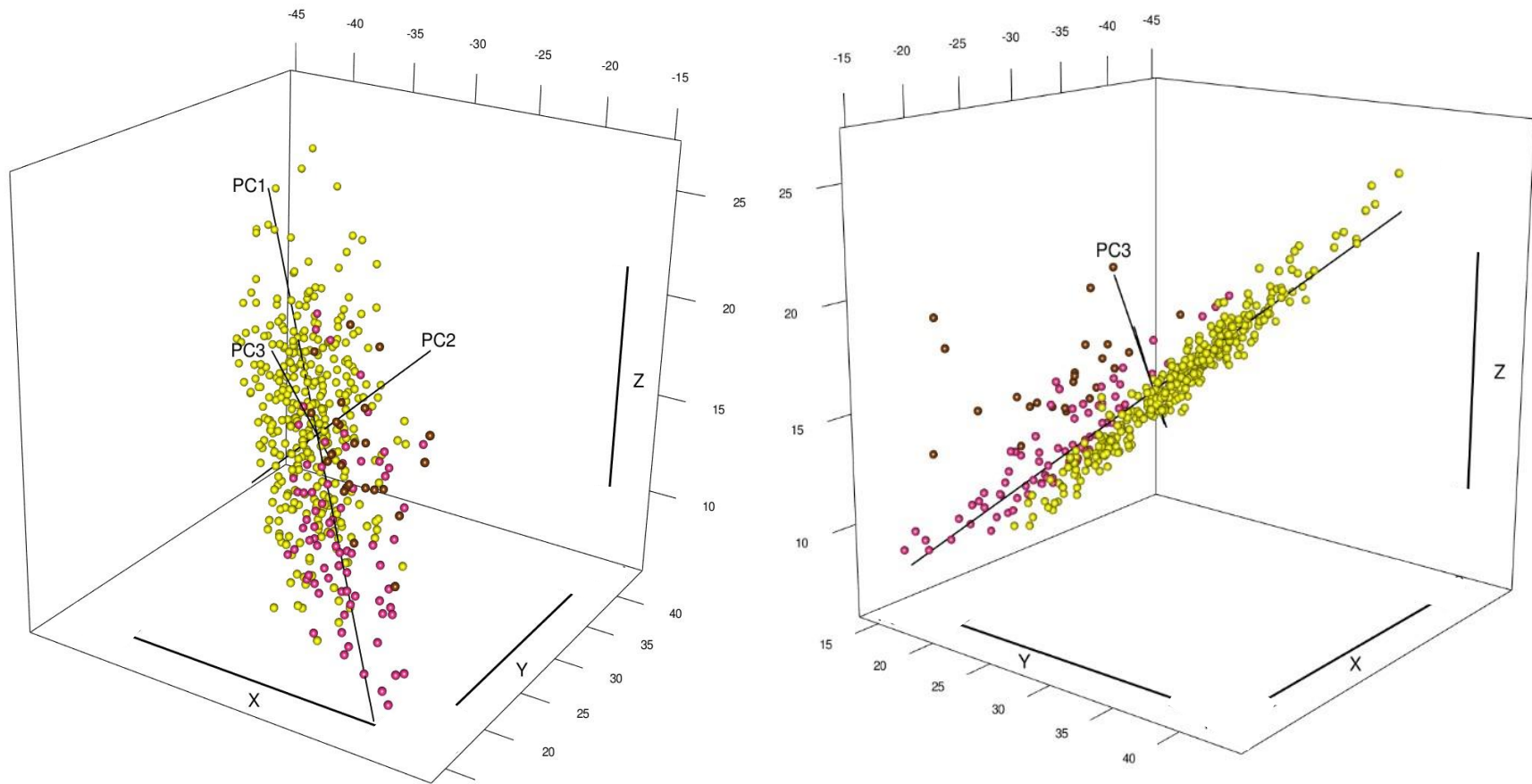
Figure 3.6: 3-dimensional xyz colour coordinates of *Cepaea hortensis* individuals. Data are coloured by Gaussian finite mixture modelling classification (yellow, pink, or brown), and PCs 1-3 are shown. Data are shown at 2 angles to allow best view of all 3 of the main axes of variation within the data. PC$_{xyz}$ axes are shown by solid black lines.
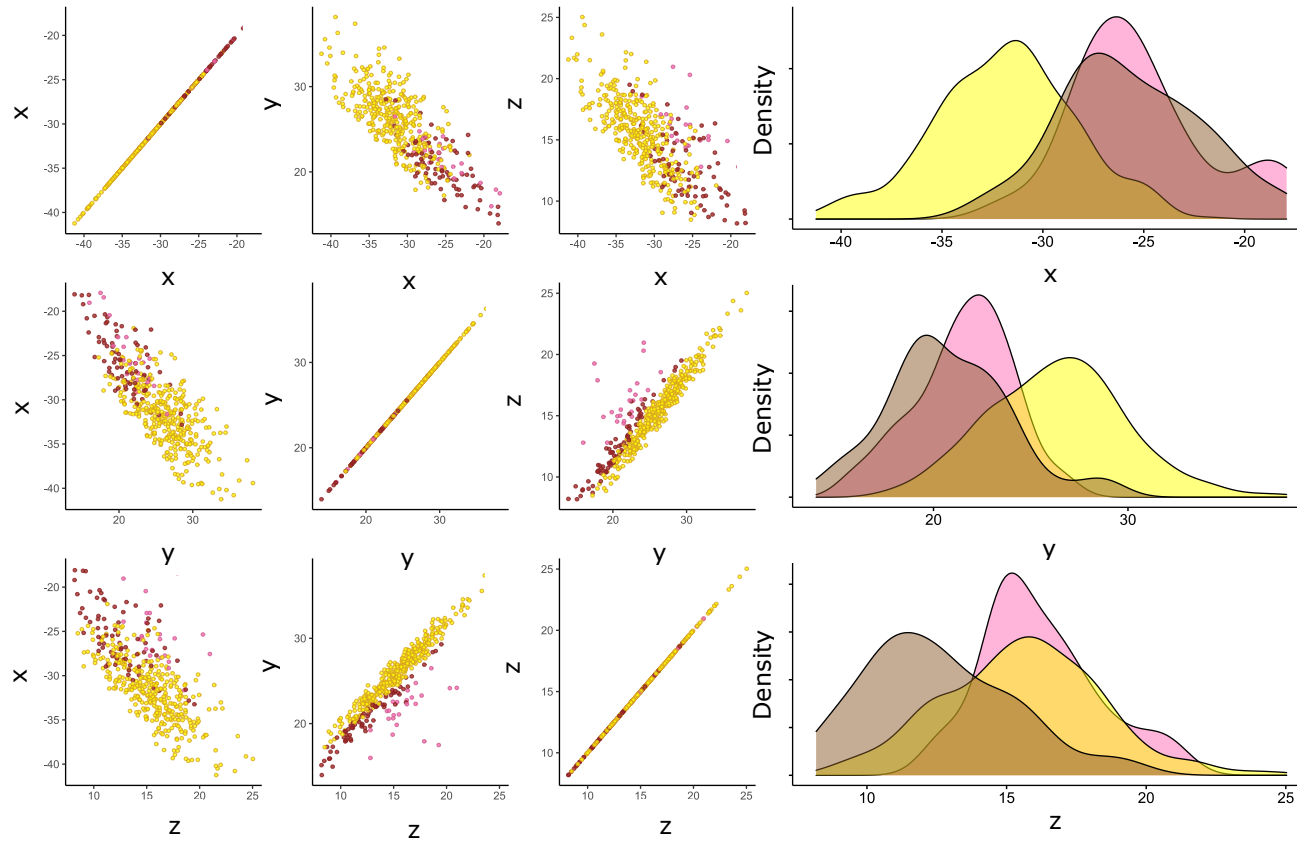
Figure 3.7: 2-dimensional representations of 3-dimensional distribution of colour measurements across xyz colour coordinates of *Cepaea hortensis* individuals. Each axis combination is plotted separately for clarity. Data are coloured by Gaussian finite mixture modelling cluster assignment, with clusters largely corresponding to human-scored yellow, pink, or brown colour morph categories. Density plots for each cluster grouping on each axis (xyz) also shown, although peak sizes are not representative of sample size, so brown and pink individuals may appear overrepresented.

3.4.2 Geographic variation in colour in *Cepaea hortensis* and *Cepaea nemoralis*

Latitude, longitude, and the quadratics of these were not significant predictors of shell colour variation in *Cepaea hortensis* along any of the three principal component axes in any of the averaged models (**Table 3.4a**), suggesting that geographic location does not influence individual components of colour variation in *Cepaea hortensis*. Latitude and longitude were not significant predictors of the probability of a snail being classified as yellow by Gaussian finite mixture modelling.

When data were subset to include only shells which had been classified as yellow by Gaussian finite mixture modelling, the first PC_{xyz} axis showed significant effects of both latitude and its quadratic, suggesting a non-linear relationship between latitude and "brightness" or intensity of colour in yellow shells of *Cepaea hortensis*, although it should be noted that the proportion of variance explained by these significant differences are small (**Table 3.4a**). No predictors were significant when considering $PC_{xyz}2$ and $PC_{xyz}3$ (**Figure 3.8**).

In individual PC_{xyz} axes of colour measurements of *Cepaea nemoralis* shells, irrespective of colour morph, no predictors are significant across any of the three PC_{xyz} values (**Table 3.4b**). As in *Cepaea hortensis*, when considering whether a shell belongs to a focal morph of "yellow" according to prior Gaussian finite mixture modelling analysis and models are run with a binomial error structure, no predictors are significant. When the PC_{xyz} of only yellow *Cepaea nemoralis* are considered, again, none of the predictors are significant across any of the three principal components **(Figure 3.9)**, which varies from the results of the same models run in *Cepaea hortensis*, where the first PC_{xyz} axes shows significant differences with latitude, in a non-linear fashion.

Table 3.4: Results of model averaging showing the effects of geographic predictors (latitude, longitude and interactions and quadratic terms thereof) on the colour of snail shells, as defined by three principal components (PC_{xyz}) of **a)** *Cepaea hortensis* and **b)** *Cepaea nemoralis* individuals. Generalised linear mixed effects models (GLMMs) were run for shells of all colours (denoted as All PC_{xyz}1-3), and repeated for all yellow shells separately (denoted as Yellow PC_{xyz}1-3). A single model with a binomial error structure was run on all shells, scored as either yellow or not yellow by Gaussian finite mixture modelling. From a full model subset, models with Akaike Information Criterion (AIC) values within two units of the best model were selected, and means of the coefficients were taken. All of the terms listed were included in all of the full models for each model, coefficients in bold indicate those for which the 95% confidence interval (CI) does not include zero (therefore the effect of the predictor is significant). Weight represents the sum of weights from models in which the variable in question appears in the final averaged model.

a) *Cepaea hortensis*

	Predictors	Coefficient	2.5% CI	97.5% CI	Weight
All PC_{xyz}1	*Latitude*	1.422	-2.752	5.596	0.72
	Longitude	-0.024	-1.283	0.079	0.31
	Latitude²	-0.010	-0.049	0.028	0.65
	Longitude ²	-0.001	-0.006	0.004	0.26
	Latitude:Longitude	-	-	-	-
All PC_{xyz}2	*Latitude*	-0.224	-1.501	1.053	0.58
	Longitude	-0.036	-0.125	0.052	0.63
	Latitude²	0.003	-0.009	0.015	0.64
	Longitude ²	0.001	-0.004	0.004	0.38
	Latitude:Longitude	-	-	-	-
All PC_{xyz}3	*Latitude*	0.026	-0.037	0.089	0.57
	Longitude	0.056	-0.177	0.290	0.53
	Latitude²	0.001	-0.001	0.001	0.37
	Longitude ²	-0.001	-0.002	0.001	0.30
	Latitude:Longitude	-0.001	-0.005	0.003	0.20

	Predictors	Coefficient	2.5% CI	97.5% CI	Weight
Yellow/Not Yellow	*Latitude*	-0.059	-0.402	0.283	0.37
	Longitude	0.023	-0.052	0.098	0.45
	Latitude²	0.0001	-0.003	0.003	0.36
	Longitude ²	- 0.0001	-0.004	0.003	0.32
	Latitude:Longitude	-	-	-	-
Yellow PC$_{xyz}$1	*Latitude*	**5.483**	**1.407**	**9.555**	**1.00**
	Longitude	0.010	-0.066	0.085	0.29
	Latitude²	**0.050**	**-0.088**	**-0.012**	**1.00**
	Longitude ²	-	-	-	-
	Latitude:Longitude	-	-	-	-
Yellow PC$_{xyz}$2	*Latitude*	-0.698	-2.682	1.286	0.69
	Longitude	-0.031	-0.128	0.067	0.50
	Latitude²	0.007	-0.011	0.026	0.80
	Longitude ²	0.001	-0.004	0.005	0.28
	Latitude:Longitude	-	-	-	-
Yellow PC$_{xyz}$3	*Latitude*	0.02547	-0.0254	0.076	0.52
	Longitude	0.00289	-0.0085	0.001	0.33
	Latitude²	0.00022	-0.0002	0.014	0.48
	Longitude ²	0.00007	-0.0004	0.001	0.22
	Latitude:Longitude	-	-	-	-

b)

b) *Cepaea nemoralis*

	Predictors	Coefficient	2.5% CI	97.5% CI	Weight
All PC$_{xyz}$1	*Latitude*	-0.094	-0.156	0.059	0.52
	Longitude	0.226	-0.475	0.928	1.00
	Latitude²	-0.002	-0.003	0.001	0.48
	Longitude ²	-0.002	-0.003	0.003	0.39
	Latitude:Longitude	-0.014	-0.016	0.011	0.18
All PC$_{xyz}$2	*Latitude*	-0.083	-0.221	0.055	0.71
	Longitude	-	-	-	-
	Latitude²	0.001	-0.001	0.004	0.71
	Longitude ²	0.00002	-0.0004	0.001	0.19
	Latitude:Longitude	-	-	-	-

All PC$_{xyz}$3	*Latitude*	0.005	-0.025	0.034	0.28
	Longitude	0.0002	-0.004	0.004	0.12
	Latitude^2	-0.0001	-0.001	0.0004	0.30
	Longitude ^{2}	0.00004	-0.0002	0.0002	0.12
	Latitude:Longitude	-	-	-	-
Yellow/Not Yellow	*Latitude*	0.113	-0.038	0.263	0.80
	Longitude	0.004	-0.015	0.023	0.80
	Latitude^2	-0.002	-0.004	0.001	0.29
	Longitude ^{2}	-	-	-	-
	Latitude:Longitude	-	-	-	-
Yellow PC$_{xyz}$1	*Latitude*	-0.022	-0.118	0.074	0.35
	Longitude	0.189	-0.409	0.787	1.00
	Latitude^2	-0.0002	-0.001	0.001	0.26
	Longitude ^{2}	-0.001	-0.004	0.002	0.45
	Latitude:Longitude	-0.002	-0.013	0.010	0.11
Yellow PC$_{xyz}$2	*Latitude*	-	-	-	-
	Longitude	-0.002	-0.018	0.013	0.249
	Latitude^2	0.00002	-0.0003	0.0003	0.208
	Longitude ^{2}	-	-	-	-
	Latitude:Longitude	-	-	-	-
Yellow PC$_{xyz}$3	*Latitude*	-	-	-	-
	Longitude	-0.001	-0.004	0.004	0.203
	Latitude^2	-	-	-	-
	Longitude ^{2}	-0.0001	-0.0002	0.0002	0.252
	Latitude:Longitude	-	-	-	-
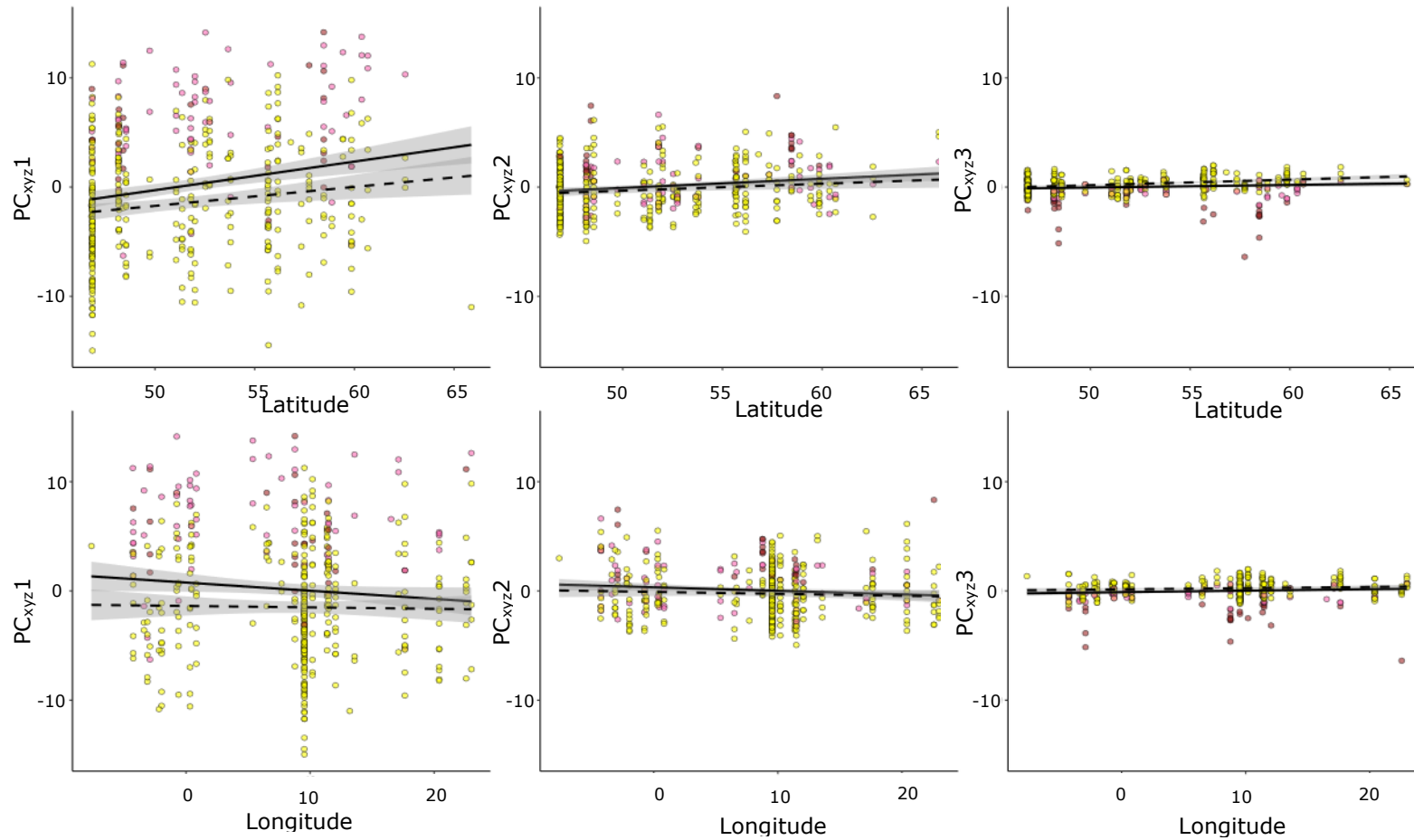
Figure 3.8: The relationship between colour (as indicated by PC_{xyz} scores) and latitude and longitude for shells of *Cepaea hortensis*. Points represent individual snail shells, coloured by the colour categories assigned by Gaussian finite mixture modelling. Solid line represents linear regression model fit for all shells, dashed line represents generalised linear regression model fitted for yellow shells only.
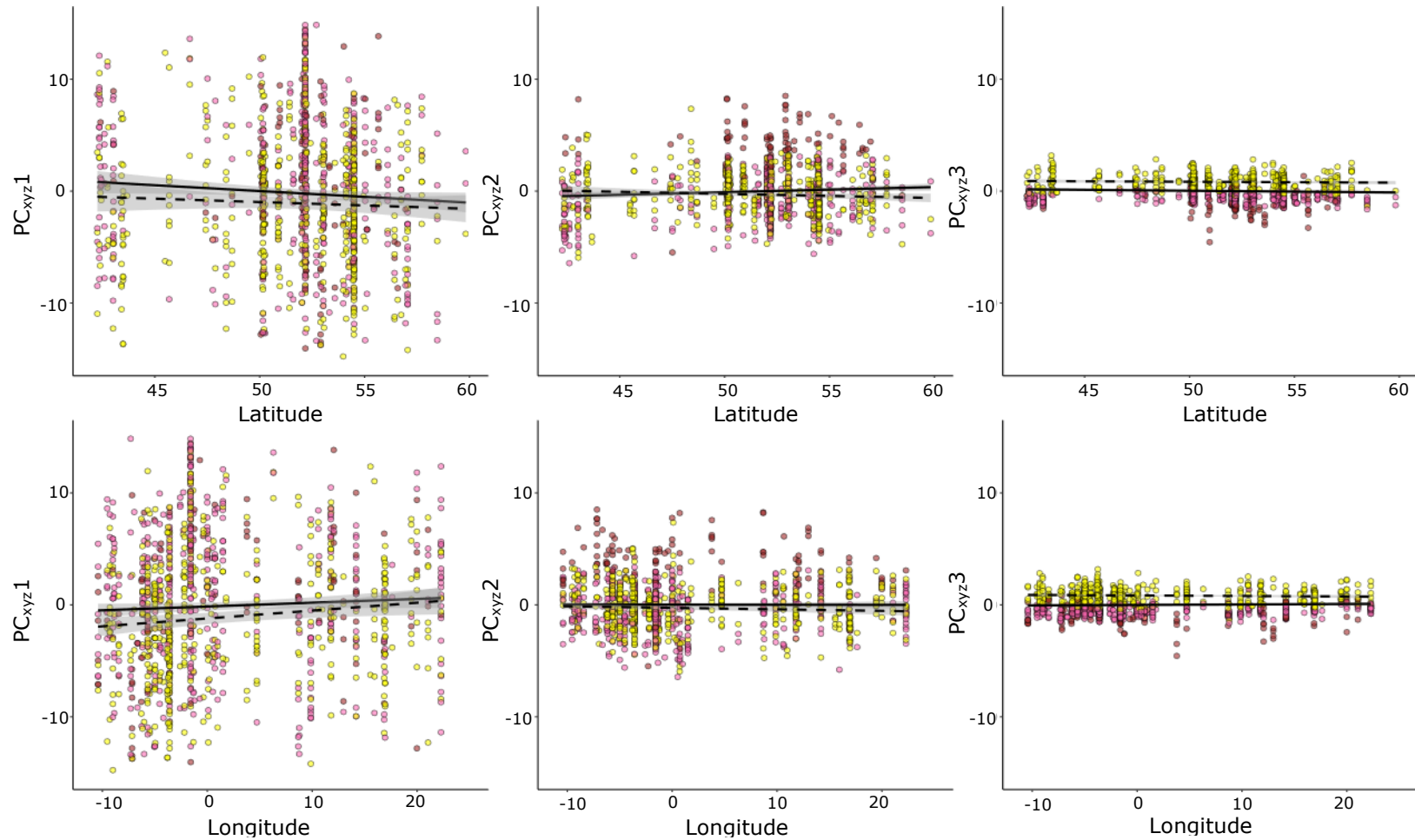
Figure 3.9: The relationship between colour (as indicated by PC_{xyz} scores) and latitude and longitude for shells of *Cepaea nemoralis*. Points represent individual snail shells, coloured by the colour categories assigned by Gaussian finite mixture modelling. Solid line represents linear regression model fit for all shells, dashed line represents generalised linear regression model fitted for yellow shells only.

3.4.3 *Cepaea hortensis* vs *Cepaea nemoralis* variation

3.4.3.1 All morphs

When all *Cepaea hortensis* and European *Cepaea nemoralis* data are collated, the best model includes three clusters (model type = VVV; BIC = -21795.74; $P < 0.001$ compared to the second-best model). The three clusters are of varying sizes (cluster 1 contains 548 individuals, cluster 2 contains 112, and cluster 3 contains 942). These clusters do not correspond to the three human defined colour groups, Chi-square tests indicate that there is a significant difference between human-scored colour groups and the clusters resolved by Gaussian finite mixture modelling ($\chi^2 = 41.383$, df = 2, $P = 1.03e\text{-}9$). The clusters also do not separate species from one another, although clusters do seem to broadly separate human scored yellow individuals from a combined grouping of pink and brown shells (**Table 3.5**).

The majority of *Cepaea hortensis* shells fall into cluster 3, although this is unsurprising as many of these shells were qualitatively scored as yellow. Whilst "yellow" shells fall mostly in cluster 3, and "pink" in cluster 1, the majority of human scored "brown" snails also fall into cluster 1 with the pink shells. Cluster 2 is the smallest and does not contain a majority of any of the human scored colours. The 2nd best model also resolved 3 clusters (VEV, BIC = -21831.85, P < 0.001 compared to the third best model), and the third best resolves 5 clusters (VEV, BIC = -21847.89).

Table 3.5: Distribution of human-scored colours and species across Gaussian finite mixture modelling resolved clusters in both *Cepaea hortensis* and *Cepaea nemoralis*.

Human scored colour

		Yellow	Pink	Brown	Total
Cluster 1	*C. nemoralis*	154	276	35	465
	C. hortensis	63	19	1	83
	Total	**217**	**295**	**36**	**548**
Cluster 2	*C. nemoralis*	27	51	9	87
	C. hortensis	15	6	4	25
	Total	**42**	**57**	**13**	**112**
Cluster 3	*C. nemoralis*	448	121	21	590
	C. hortensis	342	7	3	352
	Total	**790**	**128**	**24**	**942**
	Total	**1049**	**480**	**73**	

The three main axes of colour variation in both *C. nemoralis* and *C. hortensis* together are confirmed by principal components analysis (PCA) on the raw xyz co-ordinates of individual snails. $PC_{xyz}1$ explains 87.81% of variation, and has a strong positive loading for x (0.608), a strong negative loading for y (-0.642), and a slightly weaker negative loading for z (-0.468). $PC_{xyz}2$ explains 10.36% of the total variation, and has strong or medium positive loadings for x (0.761), y (0.302), and z (0.574). $PC_{xyz}3$

explains the remaining 1.81% of variation, and has a weak positive loading for x (0.227), a strong positive loading for y (0.705), and a strong negative loading for z (-0.672). These factor loadings are very similar to those described in *C. hortensis* alone, suggesting that the axes of variation present across the two species is very similar. The range of variation in *Cepaea nemoralis* is greater than that present in *Cepaea hortensis*, at 41, 22, and 8 JNDs for PC_{xyz} 1, 2, and 3 respectively, compared to 36, 13, and 8 JNDs along each axis of variation in *Cepaea hortensis*.

A 3-dimensional Peacock's test indicated that the points belonging to *Cepaea hortensis* and *Cepaea nemoralis* are not equally distributed in 3-dimensional colour space (xyz coordinates) (D = 0.390, *P* = 6.219e-38) (**Figures 3.10, 3.11**). The individual distributions of each of the three PC_{xyz} axes are significantly different between species (D = 0.302, *P* < 2.2e-16; D = 0.180, *P* = 1.213e-09; D = 0.209, *P* = 8.271e-13). When PC_{xyz} values of both species are centred around a single mean, Kolmogorov-Smirnov tests indicate that whilst the distributions of each of these axes is different, the specific shape of the distributions of PC_{xyz} 1 and 2 do not vary between species ($PC_{xz}1$: D = 0.037, *P* = 0.749; $PC_{xyz}2$: D = 0.035, *P* = 0.806). The specific shape of the distribution of points along $PC_{xyz}3$ is varied between species (D = 0.079, *P* = 0.032), with the distribution of points along $PC_{xyz}3$ having high levels of kurtosis in *Cepaea nemoralis* (**Figure 3.11**). The position in colour space of points along all three PC_{xyz} axes varies significantly, as demonstrated by GLMMs on each axis ($PC_{xyz}1$: $\chi^2 = 56.424$, df = 1, *P* = 5.841e-14; $PC_{xyz}2$: $\chi^2 = 4.15$, df = 1, *P* = 0.011; $PC_{xyz}3$: $\chi^2 = 11.993$, df = 1, *P* = 0.0005) (**Figure 3.12**). On average, *Cepaea hortensis* shells are more reflective and paler, indicated by a higher $PC_{xyz}1$ value. Shells of *C. hortensis* also tends to be less pink (lower $PC_{xyz}2$ value) and more brown (higher $PC_{xyz}3$ value) in all snails.
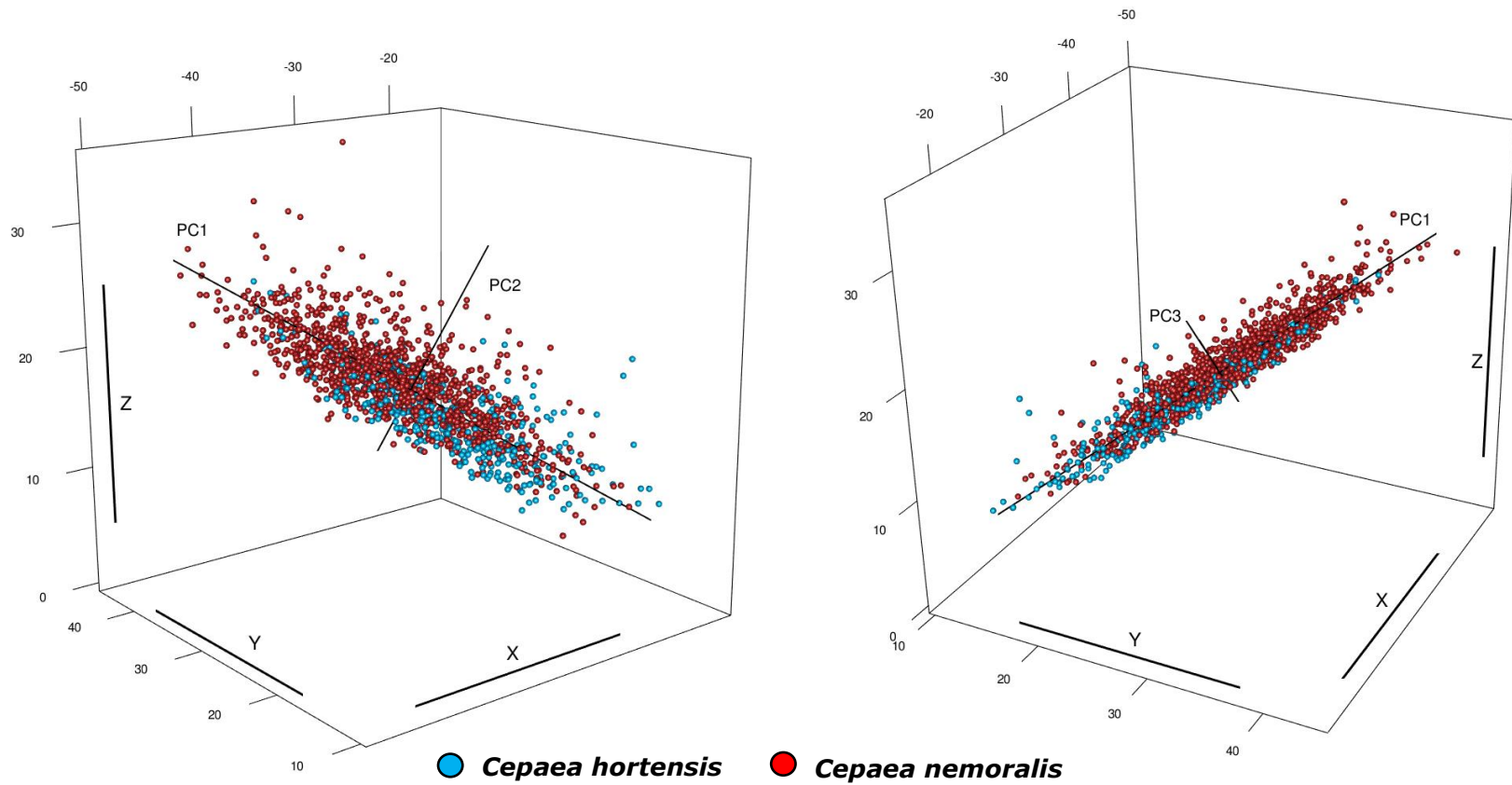
Figure 3.10: Colour of individual shells of both European *Cepaea nemoralis* (red) and all *Cepaea hortensis* (blue) individuals. Colour is represented in three-dimensional colour space, the location of which is determined by psychophysical modelling of reflectance spectra. Each point represents an individual measurement, displayed in 3-dimensional colour space. Data are shown in two orientations for clarity. Also displayed are the three PC_{xyz} values.
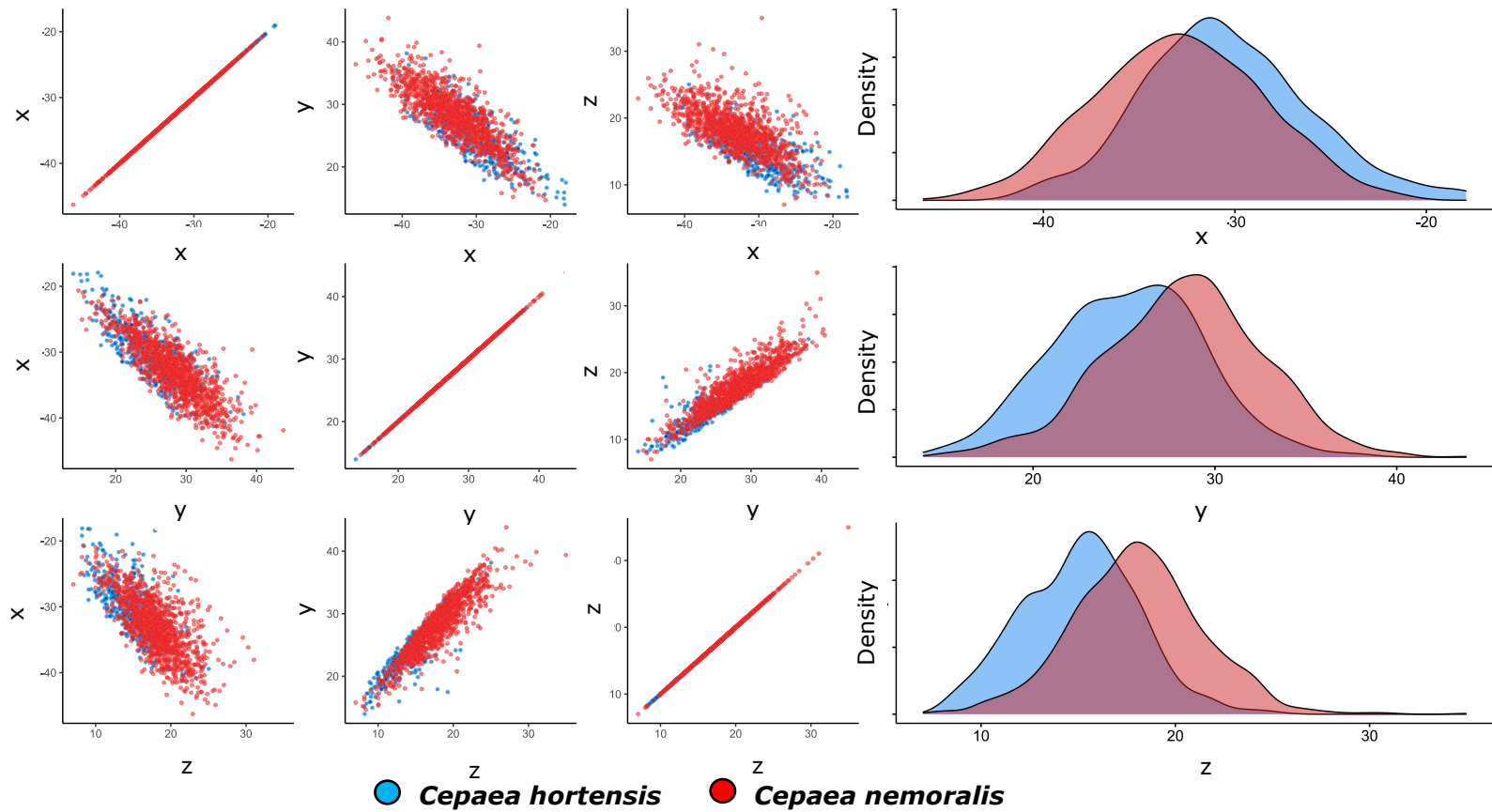
Figure 3.11: 2D representations of xyz colour coordinates of *Cepaea hortensis* and European *Cepaea nemoralis* individuals. Each axis combination is plotted separately to allow clear overview of groups. Data is coloured by species – *C. hortensis* is blue, and *C. nemoralis* is red. Density plots for each axis are also shown.
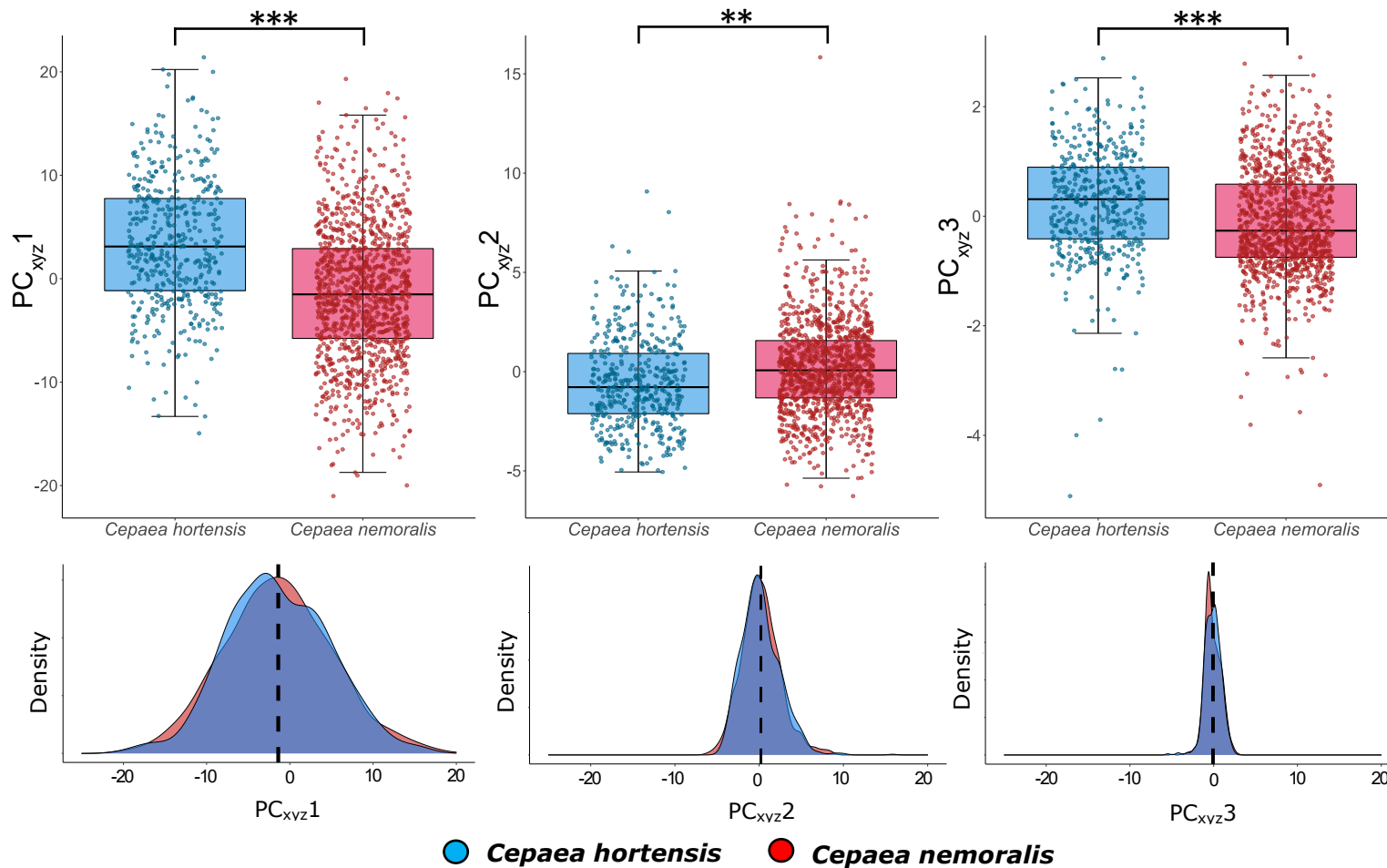
Figure 3.12: Box plots and associated density plots for each Principal component axis. *Cepaea hortensis* distributions have been shifted to centre around the same mean as *Cepaea nemoralis*. The dotted line in each case represents the mean. *Cepaea hortensis* is shown in blue, and *Cepaea nemoralis* in red. There is a significant difference between species along each of the PC_{xyz} axes. When distributions are shifted to centre around the same mean, there is no significant variation in the distribution of measurements along each of the three PC_{xyz} axes.

3.4.3.2 Yellow snails

To determine whether individual colour morphs diverge between the two species, analysis was carried out on snails of a focal morph. Yellow was chosen due to its large sample size. When only human-scored yellow individuals of both *Cepaea hortensis* and *Cepaea nemoralis* were considered, the best fitting model resolved 3 clusters (VVV, BIC = -13922.18; *P* < 0.001 when compared to the second-best model). The three clusters are of varying sizes (cluster 1 – 315; cluster 2 – 65; cluster 3 – 668). These clusters do not separate the two species from one another (**Table 3.6**). The 2nd and 3rd best fitting models both also resolve 3 clusters (EEV, BIC = -13937.85, *P* < 0.001 compared to third best model; EVV, BIC = -13942.51).

PCA on xyz co-ordinates of yellow *Cepaea nemoralis* and *Cepaea hortensis* confirm that the three main axes of variation remain largely consistent with the variation axes in individuals of all colours, with some slight differences. $PC_{xyz}1$ explains 89.21% of variation and has a strong positive loading for x (0.602), a strong negative loading for y (0.645), and a slightly weaker negative loading for z (-0.470). $PC_{xyz}2$ explains 9.46% of the total variation, and has strong or medium positive loadings for x (0.792), y (0.409), and z (0.453). $PC_{xyz}3$ explains only 1.33% of variation, and has a weak positive loading for x (0.100), a strong positive loading for y (0.645), and a strong negative loading for z (-0.758).

Table 3.6: Distribution of shells of human-scored yellow snails of both *Cepaea nemoralis* and *Cepaea hortensis* across the three colour clusters resolved by cluster analysis with Gaussian finite mixture modelling.

	Cepaea hortensis	*Cepaea nemoralis*	Total
Cluster 1	134	181	**315**
Cluster 2	16	49	**65**
Cluster 3	270	398	**668**
Total	**420**	**628**	

The positions in 3-dimensonal colour space as defined by the xyz coordinates of *Cepaea hortensis* and *Cepaea nemoralis* are not equally distributed, as demonstrated by 3-dimensional Peacock's tests (D = 0.368, *P* = 3.717e-25) (**Figure 3.13**). Two-sample Kolmogorov-Smirnov tests indicate that within these 3-dimensional distributions, none of the three individual PC_{xyz} axes share the same distributions of points along axes of colour variation ($PC_{xyz}1$: D = 0.323, P < 2.2e-16; $PC_{xyz}2$: D = 0.131, *P* = 0.0004; $PC_{xyz}3$: D = 0.126, *P* = 0.0007) (**Figure 3.14**). When data are shifted to centre around the same mean, the exact shapes of the distributions of PC_{xyz} 1 and 2 are equal (D = 0.0341, *P* = 0.932; D = 0.036, *P* = 0.898), and the distribution of points along $PC_{xyz}3$ are different (D = 0.087, *P* = 0.044), with *Cepaea nemoralis* having a slightly wider distribution (**Figure 3.14**). The average position in colour space of *Cepaea nemoralis* and *Cepaea hortensis* varies significantly between $PC_{xyz}1$ and $PC_{xyz}2$, according to GLMMs ($PC_{xyz}1$: χ^2 = 50.944, df = 1, *P*

= 9.504e-13; $PC_{xyz}2$: χ^2 = 12.262 , df = 1, P = 0.0005). $PC_{xyz}1$ is higher on average in *C. hortensis* indicating a paler less intense colour, and $PC_{xyz}2$ is lower in *C. hortensis*, suggesting that shells classified as yellow are less pink-toned. There was no significant difference in $PC_{xyz}3$ scores between species (χ^2 = 3.594, df = 1, P = 0.058) (**Figure 3.15**), suggesting no difference in how close to brown human-scored yellow shells are between the two species. As was the case where shells of all three colour morphs were compared between species (**Section 3.4.3.1**), *Cepaea hortensis* has, on average, a more reflective paler shell than *C. nemoralis*, indicated by a higher $PC_{xyz}1$ value. Yellow individuals of *C. hortensis* also tend to be a shade which is less pink (lower $PC_{xyz}2$ value), but more brown (higher $PC_{xyz}3$ value).
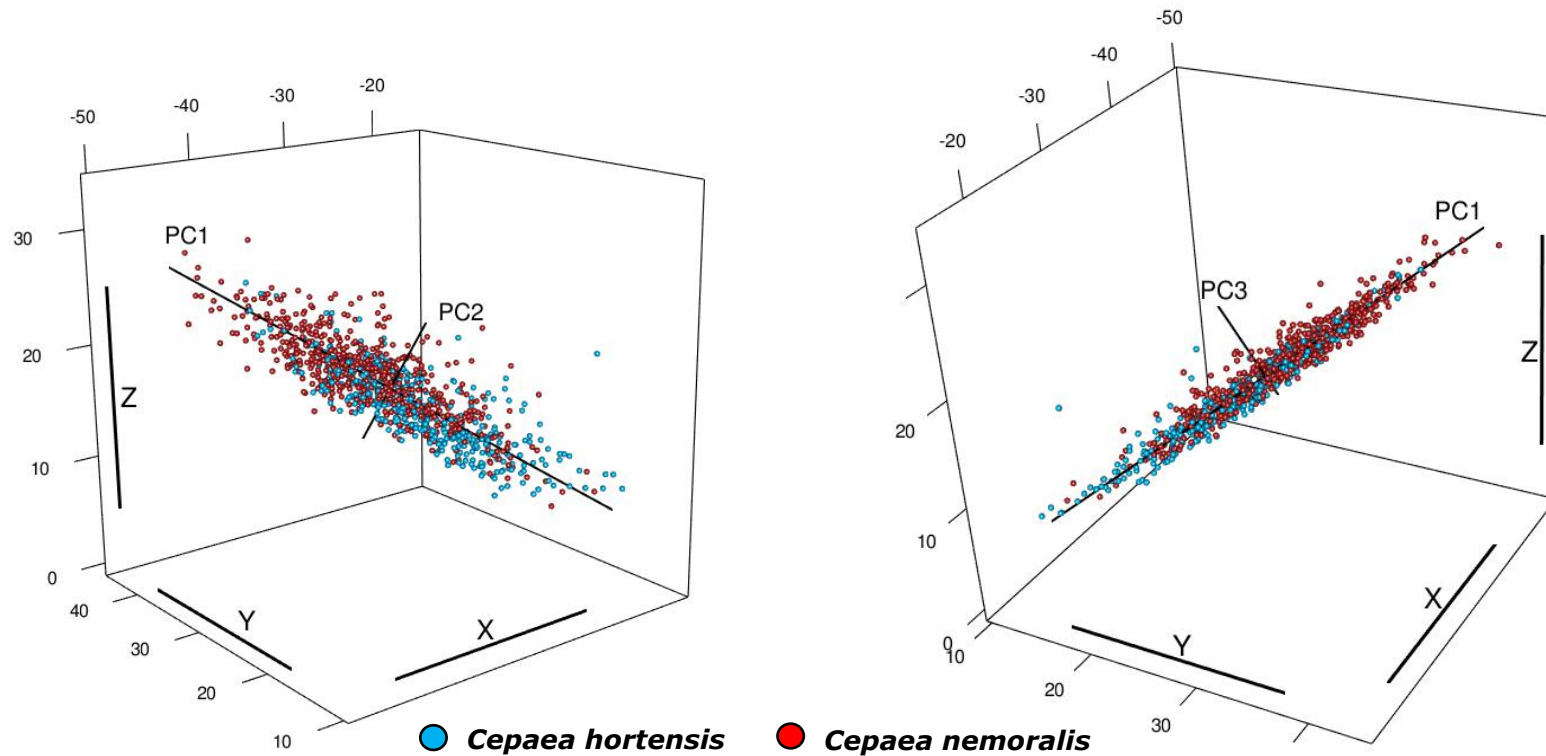
Figure 3.13: Exact shade of yellow colour of individual shells of both European *Cepaea nemoralis* (red) and all *Cepaea hortensis* (blue) individuals. Colour is represented in three-dimensional colour space, the location of which is determined by psychophysical modelling of reflectance spectra. Each point represents an individual measurement, displayed in 3-dimensional colour space. Data are shown in two orientations for clarity. Also displayed are the three PC_{xyz} values. All individual shells had previously been human-scored as belonging to the yellow phenotype.
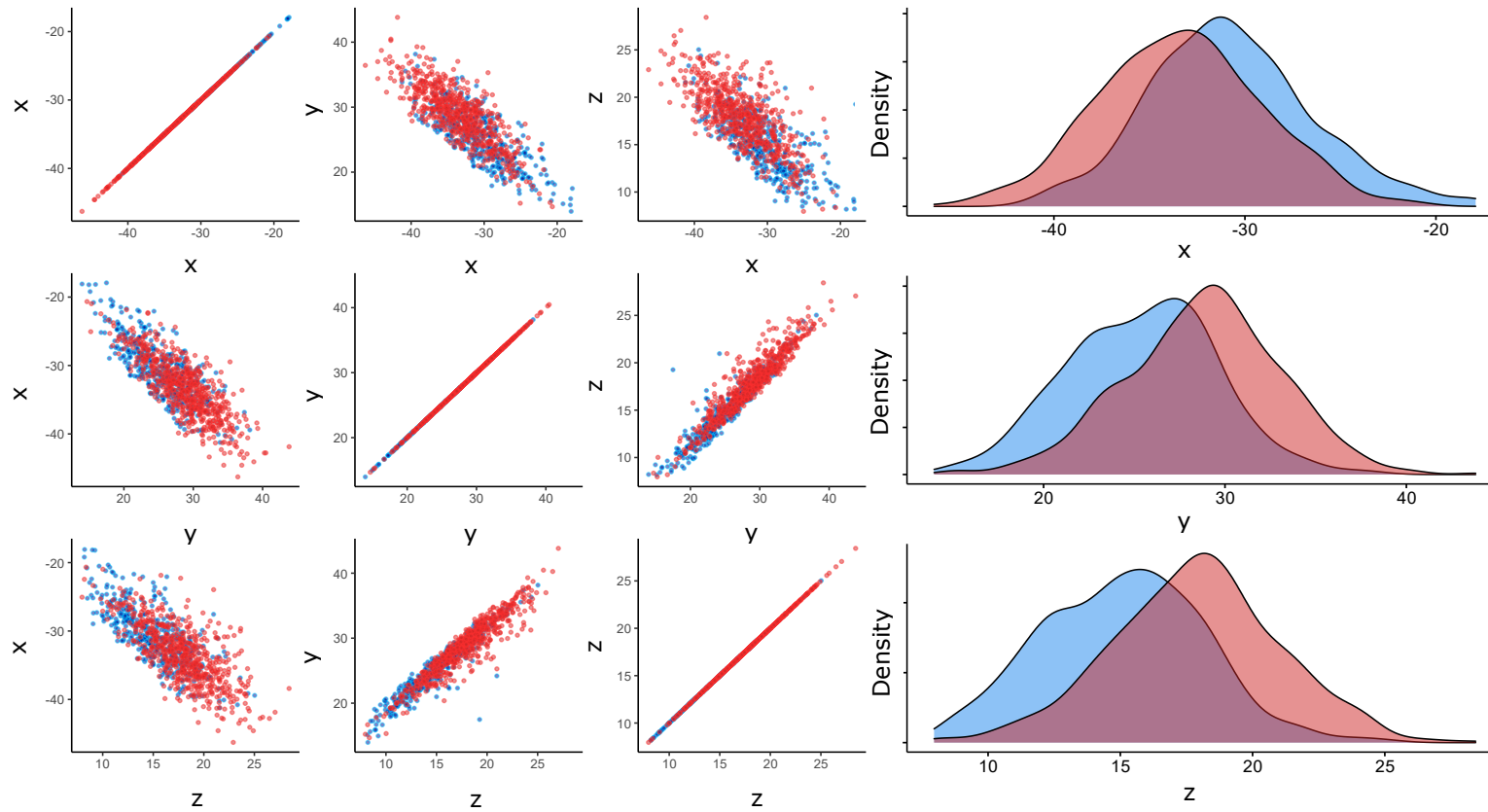
Figure 3.14: 2-dimensional representations of xyz colour coordinates of yellow *Cepaea hortensis* and *Cepaea nemoralis* individuals. Each axis combination is plotted separately to allow clear overview of groups. Data is coloured by species – *C. hortensis* is blue, and *C. nemoralis* is red. Density plots for each axis are also shown. Each individual had previously been human-scored as yellow prior to analysis.
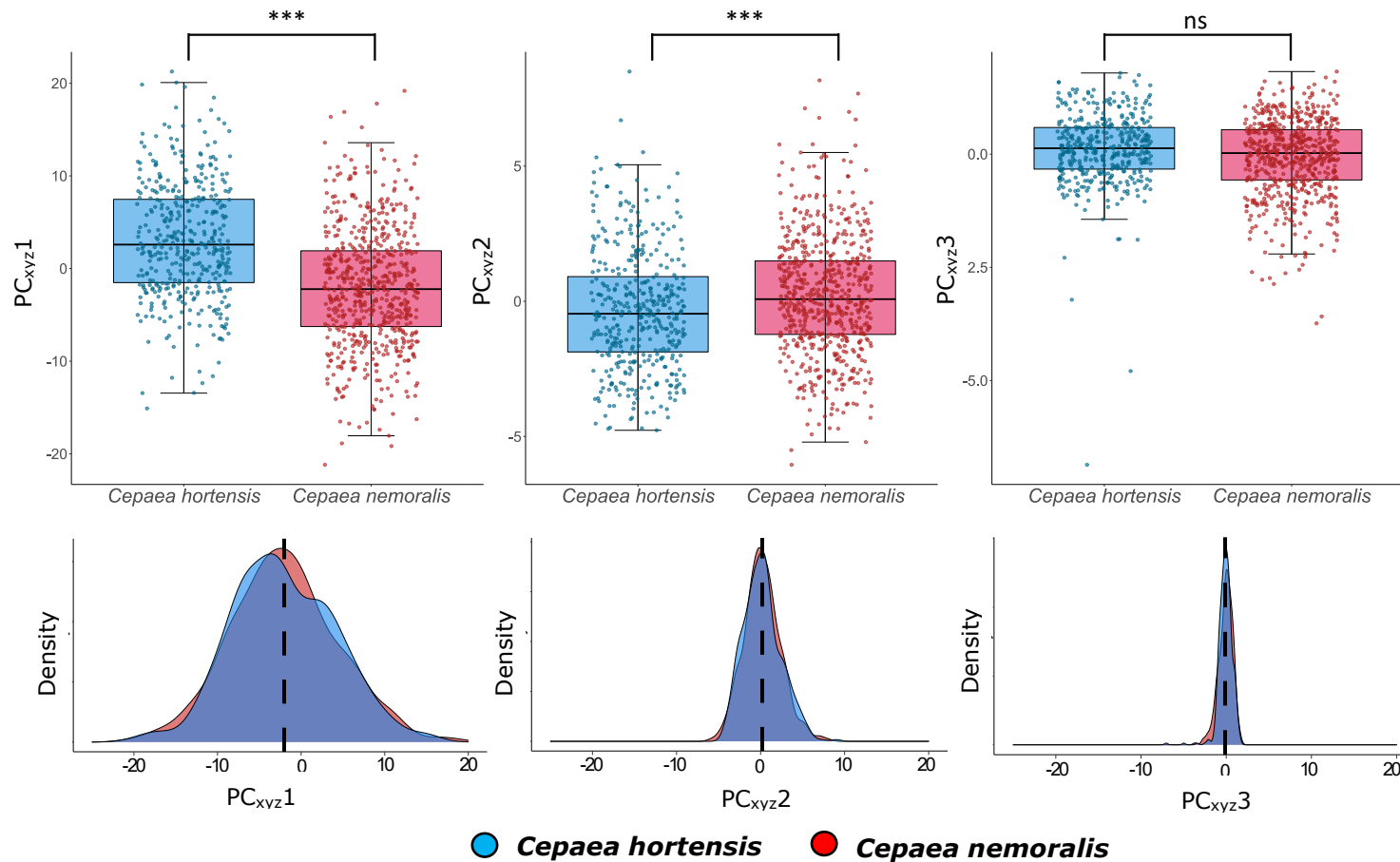
Figure 3.15: Box plots and associated density plots for each Principal component axis of yellow *Cepaea* shells. *Cepaea hortensis* distributions have been shifted to centre around the same mean as *Cepaea nemoralis*. The dotted line in each case represents the mean. *Cepaea hortensis* is shown in blue, and *Cepaea nemoralis* in red. There is a significant difference between species along each of the PC_{xyz} axes. When distributions are shifted to centre around the same mean, there is no significant variation in the distribution of measurements along each of the three PC_{xyz} axes.

3.4.4 Are there different types of yellow?

When cluster analysis was performed on all human scored yellow *Cepaea nemoralis* shells, the best fitting Gaussian finite mixture model resolves four clusters (VVV, BIC = -17073.81, $P < 0.001$ compared to the second-best model). The second-best model resolves 3 clusters (VVV, BIC = -17082.71, $P < 0.001$ compared to third best model), and the third-best fitting model resolves five clusters (VEV, BIC = -17099.77). The four clusters are not equally sized, with the first cluster containing 577 individuals, the second containing 361, and the third and fourth containing 272 and 86 respectively. The clusters largely split individuals into two groups, those from the main European distribution of *Cepaea nemoralis*, and a second group containing snails from populations originating from either the Pyrenees or Ireland. From the best fitting model, the first cluster contains 70% of the individuals from the European distribution of *Cepaea nemoralis* and only 27% of the individuals from the Pyrenees and Ireland (**Table 3.7**). The remaining clusters contain mostly individuals from the Pyrenees and Ireland, suggesting some separation in three-dimensional colour space between the two groups. Individuals from the European distribution are present in clusters two, three, and four, but these consist of only a few individuals, and with seemingly no pattern of locality. Pyrenean and Irish shells did not separate from one another within clusters, and were always both present in clusters, suggesting no difference between shells from the Pyrenees and those originating in Ireland.

There are three relevant axes of colour variation, as determined by PCA on the raw xyz co-ordinates in three-dimensional colour space. Of these axes, $PC_{xyz}1$ explains 87.15% of variation, and has a strong positive loading for x (0.608), a strong negative loading for y (-0.645), and a slightly weaker negative loading for z (-0.463). $PC_{xyz}2$ explains 11.53% of the total variation, and has strong or medium positive loadings for x (0.787), y (0.409), and z (0.463). $PC_{xyz}3$ explains 1.32% of variation, and

has a weak positive loading for x (0.109), a strong positive loading for y (0.645), and a strong negative loading for z (-0.756).

Table 3.7: Distribution of individual human-scored yellow snails of *Cepaea nemoralis* across the four Gaussian finite mixture modelling resolved clusters, according to whether they belong to the European or Pyrenean/Irish distribution

	Cluster 1	Cluster 2	Cluster 3	Cluster 4	Total
European	379	99	49	20	**547**
Pyrenean	198	262	223	66	**749**
Total	**577**	**361**	**272**	**86**	

A 3-dimensional Peacock's test indicates that the points belonging to Pyrenean/Irish and European distributions of *Cepaea nemoralis* are not equally distributed in 3D colour space (xyz coordinates) (D = 0.289, *P* = 1.226e-19) (**Figure 3.16**). Two-sample Kolmogorov-Smirnov tests suggest that within these 3-dimensional distributions, none of the three individual PC_{xyz} axes share the same distribution of points in 1-dimension (D = 0.181, *P* = 2.195e-9; D = 0.12188, *P* = 0.0002; D = 0.426, *P* < 2.2e-16) (**Figure 3.17**). When data are shifted to centre around the same mean, the exact shape of the distributions of points along $PC_{xyz}1$ is equal in each group of shells (D = 0.035, P = 0.823, and the shape of the distribution of points along $PC_{xyz}2$ and $PC_{xyz}3$ are different between groups (D = 0.117, *P* = 0.0004; D = 0.0779, P = 0.043) (**Figure 3.17**). Individual shells of the two groups of *Cepaea nemoralis* vary in three-dimensional colour space along all three PC_{xyz} axes, according to GLMMs ($PC_{xyz}1$: χ^2 = 5.991, df = 1, *P* = 0.014; $PC_{xyz}2$: χ^2 = 6.368, df = 1, *P* = 0.012; $PC_{xyz}3$: χ^2 = 37.917, df = 1, *P* = 7.383e-10) (**Figure 3.18**).
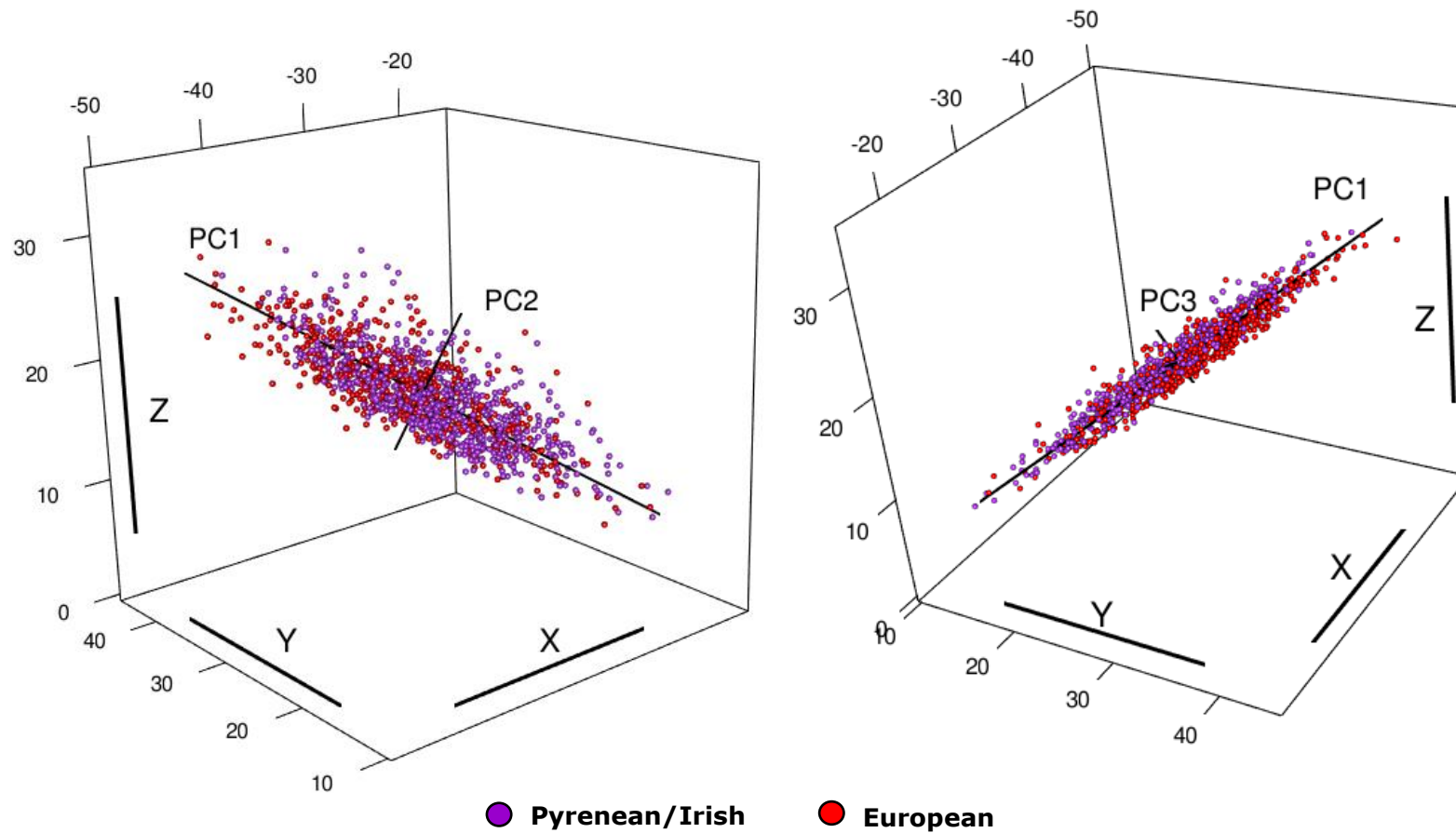
Figure 3.16: xyz co-ordinates of European *Cepaea nemoralis* (red) and Pyrenean/Irish *Cepaea hortensis* (purple) shells displayed in 3-dimensional colour space. Plots are shown in two angles for clarity. Solid black lines represent PC_{xyz} axes. All shells are human-scored yellow.
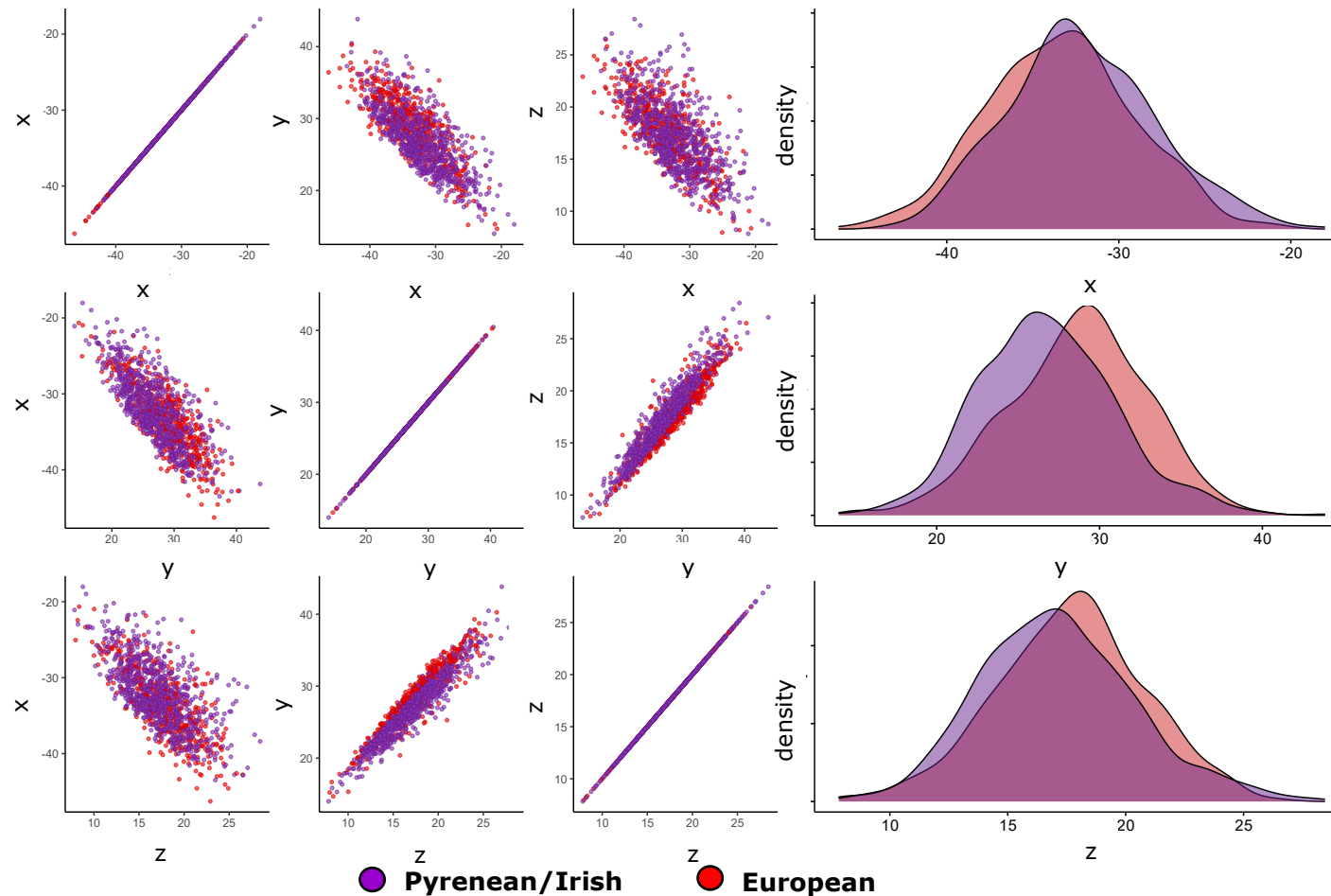
Figure 3.17: 2D representations of xyz colour coordinates of sub-setted yellow Pyrenean *Cepaea nemoralis* and European *Cepaea nemoralis* individuals. Each axis combination is plotted separately to allow clear overview of groups. Data is coloured by location of individual – Pyrenean *C. nemoralis* is purple, and European *C. nemoralis* is red. Density plots for each axis are also shown.
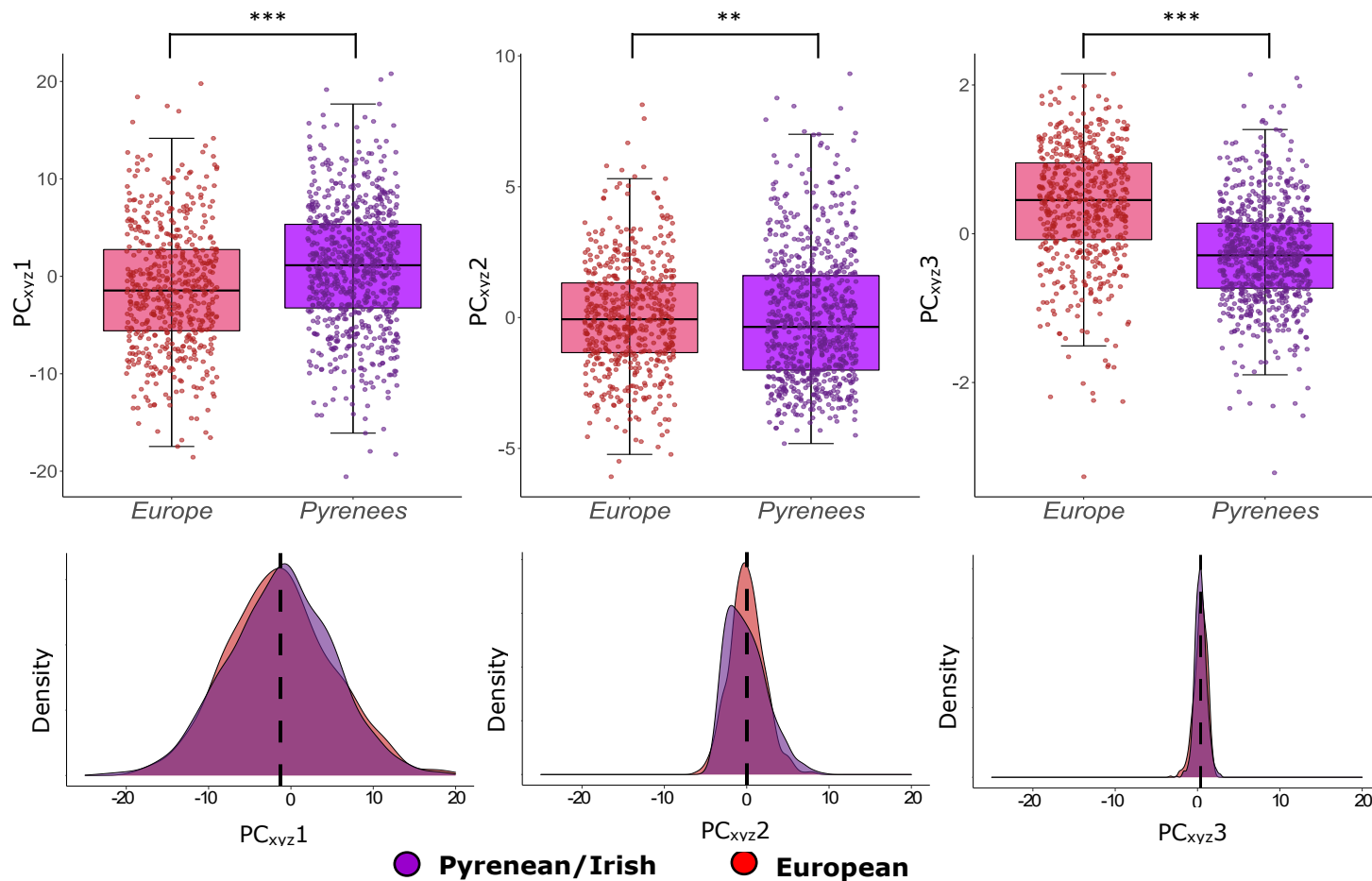
Figure 3.18: Box plots and associated density plots for each Principal component axis for yellow *Cepaea nemoralis* snails. Pyrenean distributions have been shifted to centre around the same mean as European *Cepaea nemoralis*. The dotted line in each case represents the mean. European *Cepaea nemoralis* are in red, and Pyrenean *Cepaea nemoralis* in purple.

3.4.5 Interactions between colour and banding

In *Cepaea hortensis*, the banding pattern of a shell did not affect the likelihood of the shell being classified as belonging to the "yellow" cluster by Gaussian finite mixture modelling - a banded shell is not more likely to be classed as yellow than an unbanded shell (χ^2 = 2.799, df = 2, *P* = 0.247). This is true of all pairwise comparisons between the three banding types considered (unbanded, mid-banded, five-banded) (**Table 3.8, Figure 3.19**).

Banding pattern is associated in various ways with the individual components of colour variation in 3-dimensional colour space (PC_{xyz} axes) within the Gaussian finite mixture modelling defined category of "yellow" (**Figure 3.19**). Banding pattern did not impact $PC_{xyz}1$ - the "brightness" component of shells (F = 0.563, df = 2,337, *P* = 0.569). Banding pattern is associated significantly with $PC_{xyz}2$, the "pinkness" component of colour variation (F = 50.560, df = 2,337, *P* = 0.004). There is no difference in $PC_{xyz}2$ between unbanded and mid-banded snails, or between mid-banded and five-banded snails. There is a significant difference in the $PC_{xyz}2$ value of unbanded and five banded snails, where unbanded snails tend to have a higher $PC_{xyz}2$ value on average than a five-banded shell. This higher $PC_{xyz}2$ value indicates a shell which is closer to the colour space occupied by pink shells when no bands are present. This difference occurs across 1.5 JND units, so is theoretically perceivable by an avian predator.

Banded snails also occupy a significantly different colour space along $PC_{xyz}3$ (the "brownness" of a shell) than unbanded individuals (F = 4.228, df = 2,337, *P* = 0.010). Within this, there is no difference between an unbanded and five-banded snail, or a mid-banded and five-banded snail,

but a significant difference between unbanded and mid-banded snails, where mid-banded snails have a lower $PC_{xyz}3$ value, corresponding to a less brown-toned phenotype. These pairwise comparisons indicate that the value of $PC_{xyz}3$ changes with banding pattern in a non-linear fashion (i.e. change in $PC_{xyz}3$ value is not directly proportional to the number of bands present on a shell), although it may be important to note that there was a smaller sample size of mid-banded snails.

In *Cepaea nemoralis,* similarly to in *Cepaea hortensis*, the banding pattern of an individual shell is not associated with whether a snail is classified as yellow or "not yellow" by a Gaussian finite mixture modelling ($\chi^2 = 3.146$, df = 2, $P = 0.207$; **Table 3.8**). However, the specific banding pattern of the snail interacts differently with each of the components of colour variation within yellow shells in *Cepaea nemoralis* (**Figure 3.19**)*.* Banding has a significant effect on the first and second PC_{xyz} axes of a yellow *Cepaea nemoralis* shell ($PC_{xyz}1$: F = 10.847, df = 2, 491, $P = 0.004$; $PC_{xyz}2$: F = 4.012, df = 2, 491, $P = 0.019$). In $PC_{xyz}1$ there is no difference between unbanded and five-banded shells, but a significant difference in the $PC_{xyz}1$ of unbanded and mid-banded and mid-banded and five-banded shells, where the $PC_{xyz}1$ value is significantly higher in both unbanded and five-banded shells than in mid-banded shells, suggesting a higher intensity of colour in both of these banding phenotypes relative to mid-banded individuals. In $PC_{xyz}2$ the difference between mid-banded and five-banded shells is significant; mid-banded shells have higher $PC_{xyz}2$ values on average than five-banded shells, corresponding to a shell which is more pink in mid-banded individuals. There are no differences between unbanded and mid-banded, and unbanded and five-banded shells along $PC_{xyz}2$. Unlike *Cepaea hortensis*, banding pattern does not influence $PC_{xyz}3$ in *C. nemoralis* (F = 0.856, df = 2, 491, $P = 0.426$), suggesting no difference in how brown individual shells are according to their banding phenotypes.

Table 3.8: Pairwise comparisons by Least-square means with Tukey adjustments for multiple comparisons of effects of banding pattern on the probability of a snail shell being classed as yellow, and on the three principal components describing shell colour in **a)** *Cepaea hortensis* and **b)** *Cepaea nemoralis*

	Comparison		*Estimate*	*SE*	*df*	*z-ratio*	*p-value*
Yellow/Not Yellow	**Unbanded**	**Mid banded**	-0.167	0.573	-	-0.291	0.955
	Unbanded	**Five banded**	0.368	0.236	-	1.562	0.262
	Mid banded	**Five banded**	0.535	0.576	-	0.928	0.623
PC$_{xyz}$1	**Unbanded**	**Mid banded**	1.250	1.271	337	0.984	0.588
	Unbanded	**Five banded**	0.348	0.602	337	0.577	0.832
	Mid banded	**Five banded**	-0.902	1.299	337	-0.695	0.767
PC$_{xyz}$2	**Unbanded**	**Mid banded**	0.799	0.506	337	1.580	0.256
	Unbanded	**Five banded**	0.775	0.240	337	3.234	0.004
	Mid banded	**Five banded**	-0.024	0.517	337	-0.046	0.999
PC$_{xyz}$3	**Unbanded**	**Mid banded**	0.465	0.162	337	2.871	0.012
	Unbanded	**Five banded**	0.120	0.077	337	1.564	0.263
	Mid banded	**Five banded**	-0.345	0.166	337	-2.083	0.095

B) *Cepaea nemoralis*

	Comparison		Estimate	SE	df	z-ratio	p-value
Yellow/Not Yellow	*Unbanded*	*Mid banded*	-0.28	0.512	-	-0.547	0.8480
	Unbanded	*Five banded*	-0.54	0.305	-	-1.773	0.1786
	Mid banded	*Five banded*	-0.26	0.503	-	-0.518	0.8627
$PC_{xyz}1$	*Unbanded*	*Mid banded*	**2.80**	**0.668**	**491**	**4.195**	**0.0001**
	Unbanded	*Five banded*	1.29	0.663	491	1.947	0.1267
	Mid banded	*Five banded*	**-1.51**	**0.653**	**491**	**-2.311**	**0.0552**
$PC_{xyz}2$	*Unbanded*	*Mid banded*	-0.155	0.200	491	-0.776	0.7179
	Unbanded	*Five banded*	0.383	0.199	491	1.929	0.1316
	Mid banded	*Five banded*	**0.539**	**0.196**	**491**	**2.750**	**0.0170**
$PC_{xyz}3$	*Unbanded*	*Mid banded*	-0.0225	0.076	491	-0.294	0.9535
	Unbanded	*Five banded*	0.0714	0.076	491	0.939	0.6162
	Mid banded	*Five banded*	0.0939	0.075	491	1.252	0.4230
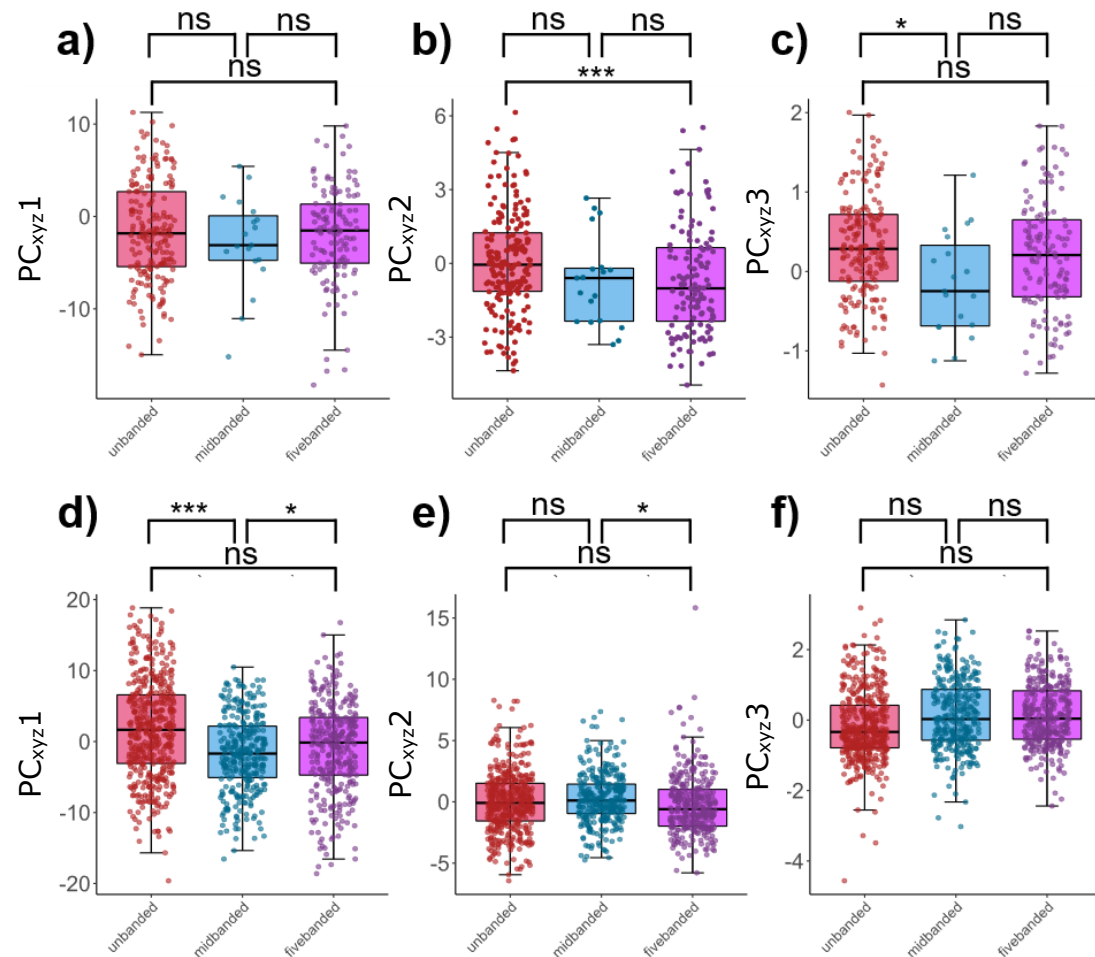
Figure 3.19: Differences in shell colour (as indicated by PC_{xyz} scores) among banding phenotypes for individuals of *Cepaea hortensis* (a, b, and c) and *Cepaea nemoralis* (d, e, and f). Scores for unbanded snails are in red, midbanded in blue, and fivebanded in purple. Statistical comparisons are pairwise comparisons by least-square means with Tukey adjustments for multiple comparisons.

3.5 Discussion

Measurements of the ground colour of *Cepaea hortensis* and *Cepaea nemoralis* across the entirety of their European distributions, combined with psychophysical models of avian colour vision, were used to understand how variation in colour, and specifically individual components of colour within individual morphs, might be perceived by drivers of selection. Broadly, it was established that, like *C. nemoralis*, the colour of *C. hortensis* shells varies continuously in three-dimensional colour space, around three clusters which roughly correspond to human scored yellow, pink, and brown. The colour of *Cepaea hortensis* does not vary with geographic location, although the saturation of the precise shade of yellow is associated with changes in latitude. The shell colours of *Cepaea hortensis* and *Cepaea nemoralis* occupy different locations in three-dimensional colour space, suggesting differences in both overall colour and precise shades of yellow. It was also found that precise shades of yellow vary within groups of *C. nemoralis*, and these differences are associated with the location of collection. Finally, it was established that there are various associations with banding and the exact shade of yellow of *C. hortensis* and *C. nemoralis* shells. The results presented have significance in furthering the understanding of the precise nature of the colour polymorphism displayed in *Cepaea* spp., and the nature of the selection which acts upon it, as well as highlighting the importance of considering colour as a continuous trait, rather than binning it into discrete groups.

3.5.1 *Cepaea hortensis* colour variation

Broadly, *Cepaea hortensis* displays continuous variation of colour across avian visual space. Perhaps unsurprisingly, like *Cepaea nemoralis* (Davison et al. 2019), colour variation in *Cepaea hortensis* is

continuously distributed in three-dimensional colour space, but this distribution is clustered around three points, which roughly correspond to human scored colour categories. These clusters are not wholly discrete, but instead overlap in 3-dimensional colour space. Chromatic variation is considerable, occurring over many units of perception (JNDs). It is likely, therefore, that this variation is perceivable by an avian predator. A predator is likely to be able to distinguish between clearly different coloured snails in an area where colour morphs are locally distinct, as is the case in some *Cepaea nemoralis* populations (Davison et al. 2019).

Cluster analysis in *Cepaea hortensis*, whilst still relatively concordant with human scoring of colour, was less so than in *Cepaea nemoralis.* It is unclear whether this is due to the small percentage of individuals which are not yellow in this instance. Sampling issues surrounding populations of *Cepaea hortensis* may be the root cause of the discrepancy between human scoring and colour categories assigned by cluster analysis, with the vast majority of *C. hortensis* shells collected being yellow. In the context of this chapter, this discrepancy is unfortunately unavoidable due to behavioural and habitat preferences; it is known that yellow morphs of *Cepaea hortensis* are more common in open spaces (Cain and Sheppard 1954), and because these open spaces are the most easily accessible for field collection, they are easily over represented in data collection. This bias may lead to a misrepresentation of natural populations, although this is mitigated as far as possible in analysis by implementing clustering algorithms which allow for the presence of smaller clusters in data distributions.

3.5.2 *Cepaea hortensis* geographical variation

The three principal component axes of individuals of all morphs of *C. hortensis* do not vary with latitude and longitude, suggesting that the variation in these individuals is not detectably associated with geographic location. The likelihood of a snail being classed as yellow (the focal

morph in this study), remains constant with geographic location in *Cepaea hortensis*, as do two of the three principal components describing the colour of yellow snails. The individual principal component explaining "brightness" or intensity of colour ($PC_{xyz}1$) varies significantly with latitude in yellow *Cepaea hortensis* snails (but not *C. nemoralis*) – snails tend to have a higher $PC_{xyz}1$ value at higher latitudes - which may have implications for thermoregulation. A higher $PC_{xyz}1$ value indicates high stimulation of M and L cones compared to VS, which when given as reflectance relative to a white standard, suggests a less saturated, lighter shell, with less intense colouration. This is perhaps surprising, as lighter shells are expected to be advantageous in hot conditions (Cain and Sheppard 1954, Cain and Currey 1963a), and average seasonal temperatures drop towards the North. $PC_{xyz}1$ remains constant across geographic space in yellow *Cepaea nemoralis*, but the range of *Cepaea hortensis* extends further north than that of *Cepaea hortensis*, and it has been hypothesised that this is reflective of their ability to better withstand colder temperatures (Cain and Currey 1963a); where the two species co-occur, *C. hortensis* tends to be found in cooler, damper environments, and are more active in a colder environment (Jones et al. 1977). It is perhaps the case that *C. hortensis* possess a trait which is beneficial to survival in colder temperatures, which is either more important than, or acts to counteract the theoretically disadvantageous light colour of shells in colder environments, such as providing camouflage in snowy environments where individuals hibernating just below the leaf litter or topsoil may become exposed. It is also possible that there is an association with banding and location in *C. hortensis* which is not present in *C. nemoralis* (Davison et al. 2019), where a heavily banded individual would gain thermoregulatory benefits from the presence of darker bands on the shell.

The results presented in **Section 3.4.2** differ from those in Davison et al. (2019), where yellow *Cepaea nemoralis* snails are shown to have a non-linear relationship with latitude, and were more common at mid-latitudes,

but relatively uncommon at high latitudes (~20% of all snails are yellow at 55° North). Here, there was no significant relationship between latitude and whether a snail was classified as yellow. This could be explained by the fact that in the 2019 paper banding was included as a fixed factor in generalised linear mixed effects models. Shell ground colour and banding are frequently in linkage disequilibrium (Cook 2017), so any effects of geographical location on colour linked to banding could be overlooked by the removal of banding from the model, particularly in cases where outputs of models are only marginally falling short of significance thresholds defined *a priori*. Here, banding was not included in the analysis due to issues with models failing to converge with its inclusion, possibly due to banding and colour patterns having some co-linearity across geographic space. It should also be noted that the nature of the data may impede the ability to look for spatial variance in colour pattern outside of colour classes, partly as a result of the interaction between banding and location, and in part due to differences among individual populations masking overall results, although this was mitigated as far as possible in the model fitting procedures. The analyses, therefore, considering only within colour class data (ie the analyses of exclusively yellow individuals) is perhaps more reliable.

3.5.3 *Cepaea hortensis* variation vs *Cepaea nemoralis* variation

In the same way as *Cepaea nemoralis*, the continuous colour variation in *C. hortensis* clusters around three points in three-dimensional colour space, which broadly correspond to human scored yellow, pink, and brown colour morphs. The variation present in *C. hortensis* does occur across a narrower scale, with less variation present. This is demonstrated clearly by the differences in JND ranges between the two species, where observed variation is smaller in *Cepaea hortensis* than in *Cepaea nemoralis*, occurring across fewer perceptual units.

Cepaea hortensis and *Cepaea nemoralis* are differently distributed in colour space, when plotted according to their raw xyz co-ordinates. This could be in part due to sampling bias causing a skewed distribution of colour in *Cepaea hortensis* samples, so to counteract this, the same analyses were run solely on the yellow individuals of each species. Cluster analysis does not distinguish between species in either a full analysis, or analysis of subset yellow individuals, but the distribution of points along $PC_{xyz}3$ differs between the species when all colour morphs are included in analysis. $PC_{xyz}3$ differentiates between how brown shells are in *Cepaea nemoralis* (Davison et al. 2019), so it is perhaps likely that this difference is due to a lack of brown individuals present in populations of *Cepaea hortensis* included in analyses. Cluster analysis on all individuals of both *C. hortensis* and *C. nemoralis* did not separate between the two species, or along any other axes of variation, apart from separating human scored yellow individuals from those scored as pink and brown. Pink and brown individuals tended to group together in a single cluster. There are two potential explanations for this. Firstly, whilst the agglomerative clustering algorithm used by the Mclust package was chosen as it does allow for the presence of smaller clusters, the lack of brown individuals of *C. hortensis*, and the disproportionately small number of brown individuals of both species relative to yellow may result in smaller clusters being grouped together, particularly where there is some overlap between human scored pink and brown and Gaussian finite mixture modelling determined pink and brown shells in *C. nemoralis* (Davison et al. 2019). Alternatively, other explanations for the occurrence of this clustering could be true, in which there is a parameter aside from the PC_{xyz} axes or species which causes individuals to form clusters, such as habitat preference, or propensity of the shell to bleaching.

The distribution of points along the "brightness" ($PC_{xyz}1$) and "pinkness" ($PC_{xyz}2$) axes does not differ between species in solely yellow individuals, but the distribution along the "brownness" axis ($PC_{xyz}3$) does. The distribution of $PC_{xyz}3$ is marginally wider in *Cepaea nemoralis*,

suggesting more variation in the "brownness" of yellow snails in *C. nemoralis*, as $PC_{xyz}3$ broadly separates brown from yellow. Mean values of $PC_{xyz}3$, or "brownness" are significantly different between species in all individuals, but not when yellow snails are considered separately. This is likely because $PC_{xyz}3$ separates brown shells from pink and yellow shells; whilst the *range* of "brownness" is larger in yellow snails of *Cepaea nemoralis*, the *mean position* in 3-dimensional colour space does not differ, so there is a broader range of colours, centred around a mean colour which does not vary. On average, how brown a yellow snail shell is remains generally consistent between the two species, but is more variable in *C. nemoralis*. There are several explanations for this difference in distribution around an equal mean - perhaps alleles for yellow individuals are not particularly well separated or diverged between *C. hortensis* and *C. nemoralis*, suggesting that species share the same yellow alleles, with divergences being only slight. There is a slight divergence between the two species in terms of range of available shell colour, which is also reflected in the slight differences in banding patterns (**Chapter 2**) (Jackson et al. 2021).

Historical comparisons between the two species suggests that there is some resource competition in lab-based settings (Cowie and Jones 1987), but that the species differ in habitat preference in unmixed populations (Cameron and Carter 1979, Cameron et al. 1980). The two species often diverge in heritable shell patterns in areas where the two species co-occur (Clarke 1962). Hybrids have been produced in laboratory settings with some difficulty, but their presence in natural populations is thought to be rare (Cain and Sheppard 1954), and in cases in which co-occurrence occurs, the phenotypes between the species tend to be markedly different, and *C. hortensis* individuals are often smaller . The geographic distributions of *C. hortensis* and *C. nemoralis* are different; the known distribution of *Cepaea hortensis* extends further north than that of *C. nemoralis*. These differences in habitat preference and heritable shell characteristics such as colour seem at odds to the

observation that the polymorphism displayed in *Cepaea hortensis* tends to be less diverse, with a higher proportion of shells being yellow, and the amount of variation within the colour of yellow shells being smaller. Where the two species co-occur, *C. hortensis* are more often found in hedgerows, where it would potentially be beneficial in terms of crypsis and thermoregulation for shells to be darker. If visual predation were the singular driving factor behind the proportions of phenotypes, the two species would show parallel variation (Lamotte, 1959), this however is not the case. Despite this, it could be reasoned that visual predation may be influenced by the non-visual selective values of phenotypes, such as thermoregulation properties of darker or more heavily banded shells.

It could be the case that the difference in colouration between species is not the result of finely tuned adaption, but a property of genetic divergence between species. It is also difficult to rule out that the observed differences in colour between species are not an artefact of field collections favouring easily accessible open areas, and the potential for differences in microhabitat preferences between morphs, as observed in *Theba pisana,* where individuals with heavily pigmented banded shells select shadier habitats (Hazel and Johnson 1990, Johnson 2011).

3.5.4 Are there different types of yellow?

Cluster analysis on all yellow *Cepaea nemoralis* shells broadly separated individuals from the Pyrenees and Ireland from the rest of the European distribution of the species. The differences present in clustering groups suggests that there is possible genetic divergence within these two groups, which corresponds to a slight difference in colour in yellow snails. Individuals from the Pyrenees and Ireland and individuals from across the remainder of the European distribution of *C. nemoralis* show significant differences along all three axes of variation between the two groups. This, alongside the difference in cluster analysis groupings, hints

at the presence of genetic divergence between the two groups. So far, the divergence of colour has only been considered in *Cepaea nemoralis*, and only between these two groups of individuals. $PC_{xyz}1$ values vary with location in *Cepaea hortensis*, so it is perhaps worthwhile to carefully consider location and origin of populations when observing colour variation in natural populations of *Cepaea hortensis*. Previous evidence from mitochondrial DNA has shown that *Cepaea* in Ireland, and particularly populations from the West of Ireland, are at least partly derived from snails from the Pyrenees, and are divergent from UK populations (Grindon and Davison 2013), so it is unsurprising that these individuals fall into the same clusters. The most likely origin of this is thought to be the movement of Mesolithic humans.

It could also be the case that differences in colour between yellow shells belonging to *Cepaea nemoralis* is the result of environmental factors, such as bleaching related to climate or habitat type. Snails in the Pyrenean distribution may well have been exposed to more intense UV, which is known to increase in intensity with altitude (Blumthaler et al. 1997), causing bleaching of the shell. In two species of land snail, *Theba pisana,* and *Xeropicta derbentina*, hot summer conditions resulted in fewer banded individuals, it is unclear whether this is due to selection against banded phenotypes, or due to shell bleaching (Johnson 2011, 2012, Dieterich et al. 2013), so it is certainly possible that bleaching is responsible for colour differences in *C. nemoralis*. Despite this, the inclusion of Irish snails with the Pyrenean distribution makes it unlikely that environmental conditions causing shell bleaching is the sole reason for the colour divergence between groups, however it is possible that a combination of genetic divergence and other factors interact to cause differences.

3.5.5 Colour and banding interactions

The banding pattern of shells interacts with both overall colour and the various principal components within the yellow morphs in various ways across both *Cepaea nemoralis* and *Cepaea hortensis.* In both species, the presence of any band, irrespective of overall pattern phenotype, does not change the likelihood of being classified as yellow in Gaussian finite mixture modelling. Within yellow individuals, however, the banding pattern of individuals interacts with the components of yellow in several ways. These interactions with PC_{xyz} axes and colour differ between species in all three analyses, which is concordant with the conclusion that the banding patterns of *C. hortensis* and *C. nemoralis* are subtly different (Jackson et al. 2021)(**Chapter 2**), suggesting some divergence between the two species.

In *Cepaea nemoralis*, mid-banded snails are less saturated than their unbanded and five-banded counterparts. A possible adaptive explanation for this could be that snails with a single band are more visible to predators, so it may be disadvantageous to highlight this band with the presence of a lighter contrasting colour around it. The same is not true of *Cepaea hortensis*, although *C. hortensis* tend to be lighter, implied by having a higher $PC_{xyz}1$ value on average than *C. nemoralis*. It would certainly be interesting to extend analysis to compare ground colour in fully pigmented banded snails to hyalozonate snails – i.e. those with structural bands which remain unpigmented. It would also be particularly useful to determine whether the areas of ground colour on the underside of the snail and between the bands are the same. Repeating the above methods focussing solely on measuring the colour of the areas between the bands in both *Cepaea nemoralis* and *Cepaea hortensis* would also be beneficial as it would allow the quantitative determination of whether any variation in colour between the underside of the shell and areas between bands is present, and whether this apparent lightening of the area between the bands would be theoretically detectable to an avian predator.

In *Cepaea nemoralis*, the greatest interactions between colour and banding are seen in pink snails (Davison et al. 2019), but unfortunately there was not a large enough sample size in *Cepaea hortensis* to verify if this was true across both species. This presents a potential future avenue of investigation to determine whether the differences between species in yellow snails were also present in pink morphs.

3.5.6 "In the eye of the beholder"

Whilst it is important to consider colour in the manner which it is perceived by a receiver, there is speculation present concerning whether the use of a single JND unit is a realistic determination of difference threshold in a natural context; instead several studies chose to adopt higher thresholds of 2-4 JNDs (Siddiqi et al. 2004, Taylor et al. 2016). Whilst there is no behavioural evidence to support a threshold other than 1 JND (Olsson et al. 2015), there are several factors which may make discrimination of colours more difficult *in situ*. For example, a predator may not have the opportunity to view two prey items next to one another before making a selection. Thrushes use anvils to break open shells and are often observed carrying whole snails or shell segments to these anvils (Goodhart 1958, Cameron 1969, Kwiecinski et al. 2019), so it is perhaps likely that a close view of the shell is possible before selection and attack, so a lower selection threshold is theoretically appropriate in this case. It is also likely that, in this case, a thrush is attempting to detect items of prey against a background, as well as distinguishing individual snails from one another. Individual differences may be less important for prey selection than ease of detection against a background, or similarity in colour to the pre-established prey search image of the thrush.

Whilst this chapter describes how an avian predator might perceive variation in *Cepaea hortensis* and *C. nemoralis*, this is not necessarily reflective of how a predator might react to a stimulus. If a bird can perceive differences between stimuli, it is not a guarantee that there will be a reaction to it; other stimuli might be more important. Ultimately, behavioural experiments with live birds selecting from a variety of shells which vary along each PC_{xyz} axis would be necessary to confirm what variation is important in prey selection, and how levels of variation affect behavioural reactions. Similar studies using artificial models of wood tiger moths, *Arctica plamtaginis*, have been utilised to determine whether avian predators react to differing hindwing patch colours (Rönkä et al. 2018). These colour patches vary continuously between red and yellow in female moths (Lindstedt et al. 2010), but males are categorised as distinctly red, white or yellow (Rönkä et al. 2018). Blue tits, *Cyanistes caeruleus*, were allowed to attack models of various discrete morphs for food rewards in a series of behavioural experiments to determine preference or learned morph avoidance behaviour to further understand the nature of the aposematic polymorphism of the moth. Extending the scope of studies such as these to focus on continuous variation rather than individual morphs would be useful, and particularly applicable to *Cepaea*.

3.5.8 Continuous colour variation

Whilst several studies use reflectance spectrophotometry to categorise colour, or to determine whether variation is continuous or discrete (Cassey et al. 2008, Taylor et al. 2016, Holveck et al. 2017, Dunning et al. 2018, Davison et al. 2019), few of these focus on the presence of continuous colour variation within individual colour morphs. This is particularly relevant when colour is a continuous trait, as separating colour into its constituent morphs may no longer be appropriate. Using the PC_{xyz} axes generated by the methods of Delhey et al. (2015) provides a more definitive understanding of colour variation at a fine scale and

allows a clearer picture of variation to be built. Generally, collapsing colour into a few meaningful variables is difficult. There are several other widely utilised methods of achieving this, which use indices of colour such as hue and chromacy, but these can be problematic in their own right (Delhey et al. 2015). Indices can be computed by a variety of methods, and preferred indices vary between different spectral shapes (i.e. colours). This means that index choice is subjective, and influenced by factors other than real patterns of chromatic variation (Stevens and Cuthill 2007). PC_{xyz} axes and the specific values along these are preferable for considering colour variation because of their objectivity, but these values alone are tricky to interpret out of context. This difficulty can be largely mitigated with the use of psychophysical modelling, but this requires a detailed knowledge of the perceiver's visual system, or at least the visual system of a close taxonomic relative of the perceiver.

The above analysis of individual principal components as well as colour in its entirety highlights the importance of understanding the smaller details of variation within a population. African cuckoo finch eggs, *Anomalospiza imberbis*, display continuous variation when modelled using avian visual systems, although this variation falls broadly into four categories to a human perceiver (Spottiswoode and Stevens 2010). Whilst some work focusses on what areas of cuckoo finch egg colour and patterning are likely to cause rejection by a host, these tend to use colour as a single trait. Some studies are beginning to use similar methods as those above to analyse continuous variation within colour morphs along more than one axis of variation (Spottiswoode and Stevens 2011), but would be useful to be able to create models which vary continuously along single axes of variation to determine what is important in egg rejection decisions by host birds. Unfortunately, this has not been possible thus far due to the sophisticated nature of the host bird's ability to spot and reject brood parasite eggs (Spottiswoode and Stevens 2010).

Reflectance spectrophotometry is revealing that variation of colour in several species of lizard is continuous, rather than discrete as previously

assumed (Cote et al. 2008, Vercken et al. 2008, Paterson and Blouin-Demers 2017). However, even within populations which do possess wholly discrete colour morphs, it is likely that there is some variation within these discrete categories. This is true of the tawny dragon lizard (*Ctenophorus decresii*) in which the colour variation is discrete, but there are large amounts of variation within these morphs (Teasdale et al. 2013). Whilst understanding that the variation may appear discrete to the perceiver is potentially ecologically or evolutionarily meaningful, it is worthwhile attempting to further understand the nature of the variation within these morphs. Differences within morphs may influence predation/crypsis/life history strategy, but these intricacies are at risk of being overlooked in favour of the more apparent large-scale variation present in these populations. This may also be applicable to polymorphisms which are classically considered as presence/absence of a trait, or dimorphisms. Any importance of slight variations present in these contexts may be overlooked in favour of a tendency to recognise easily scorable and interpretable discrete differences, which may lead to oversimplification of the underlying genetic mechanisms which cause variation and behavioural traits which may be responsible for its maintenance, masking any impact which the intricacies of specific components of variation may have.

The use of reflectance spectrophotometry and psychophysical modelling to determine how an avian predator might perceive the colour signal of an individual is, of course, not without flaws. For example, it is possible that different sources of noise could cause clusters to overlap. It is likely that measurement error introduces noise to the data, although this was mitigated as far as possible with the use of a micromanipulator and custom-made aluminium sheath probe to ensure measurement position remained as consistent as possible to reduce noise. It is also likely that there will be environmental effects which introduce noise such as sun bleaching or erosion of the shell periostracum, which varies among individuals, which may also cause differentiation of clustering patterns of

shells, however, environmental induced noise is likely to be perceived by an avian predator, so may play a role in prey selection.

3.5.7 The Evolution Megalab

The Evolution Megalab, whilst focussing primarily on *Ceapea nemoralis*, provides an invaluable resource for the study of phenotypic associations with climate and habitat across Europe. This, when paired with the decades of focussed research on the *Cepaea* polymorphism between the 1930s and the 1980s, gives an overall picture of the phenotypic variation present in the *Cepaea* genus throughout its natural population range. With sample information collected mainly in 2009, Silverton *et al* (2011) concur with Jones (1940) in suggesting that there is a significant increase in the proportion of yellow shells in the hottest part of the range (ie in southern regions). Here, the same trend is not described, and no significance is found when examining the associations of latitude and colour. This is not the case in *Cepaea hortensis*, however - Jones 1940 describes a distribution of *Cepaea hortensis* which is similar to that described above. Whilst there is no overall trend in frequency of yellow individuals with latitude and longitude in either case, this chapter does describe a change in the saturation of colour in yellow individuals with latitude. The data collected by the Evolution Megalab project also allows the examination of relationships between habitat and shell polymorphism (Worthington et al. 2012); unfortunately, habitat data is not easily accessible for several populations analysed above, although accounting for this may reveal some interesting insights into associations with *Ceapea* and habitat over time.

The Evolution Megalab acquired several records of variation for *Cepaea hortensis*, although the nature of the project and its reliance on amateur naturalists meant that much of this data was rendered unreliable for assessing temporal change relative to data collected about *Cepaea nemoralis* (Worthington et al. 2012, Cameron 2013).

Despite this potential unreliability, it was possible to look at local level geographic variation at a single timepoint, and the pre-existing hypothesis that the polymorphism present in *C. hortensis* was less varied than that in its sister species was validated (Cameron 2013), an observation which is matched by the spectral data analysed in this chapter.

3.5.8 Colour in a wider context

Reflectance spectrophotometry provides a useful starting point for categorising and understanding colour variation in natural populations - several studies have begun to pair this with other techniques to further understand how colour polymorphisms may evolve in various contexts. For example, reflectance spectra have been utilised alongside mtDNA sequence data, and single nucleotide polymorphisms (SNPs) to establish taxonomic relationships between colour morphs across geographic space in the Amazonian poison frog (Rojas et al. 2020). Reflectance spectra have also been paired with liquid chromatography mass spectrometry and scanning electron microscopy to analyse colour alongside pigmentation and microstructure in the plumage of various tanagers to further understand the presence and evolution of brightly coloured signals in birds (McCoy et al. 2021). Applying some of these techniques to *Cepaea* would present a useful next step in aiding the understanding the context of how the polymorphism might have evolved particularly in light of the recent genome assembly in *Cepaea nemoralis* (Saenko et al. 2021). It would also be useful to collect colour information regarding the substrate or background on which individual snails were located, and determine colour differences both among individuals of a population, and between said individuals and these backgrounds.

Overall, by further analysing the ground colour polymorphism of *Cepaea nemoralis*, and expanding this analysis to include *Cepaea hortensis*,

allowing comparison between the two species, this chapter provides further insight into how this variation presents itself in natural populations, utilising principal components of colour to understand variation in a more precise manner. Placing the variation into an ecologically relevant context gives a clearer idea of what selective pressures might be acting upon the polymorphism to maintain its presence in natural populations. Ultimately, the next step in understanding the variation present across the *Cepaea* genus is to identify the component parts of the supergene which underpin this variation, and attempt to further understand how variation is maintained in populations.

Author Contributions

Hannah Jackson and Angus Davison conceptualised the project, with discussion with Tom Reader. **Hannah Jackson** collected the data, with some input from Daniel Ramos Gonzalez. **Hannah Jackson** performed the analysis, and wrote the original draft. Angus Davison and Tom Reader provided input on subsequent versions.

Chapter 4: Phenotypic variation in the Hawaiian land snail genus *Auriculella*

4.1 Abstract

Oceanic islands are often hotspots for diversity and speciation; the Pacific Islands house the greatest diversity of land snails in the world, with over 6000 species, most of which are endemic to single islands. Unfortunately, land snails are also the taxa with the most recorded extinctions since the 1600s, and Pacific Island land snails make up most of those extinctions - despite this, there are large gaps in understanding in some taxa of conservation concern. Species of the Hawaiian genus *Auriculella* are variable in both colour and chirality, but there are only thought to be 14 of the 32 described species remaining extant across the Hawaiian archipelago. This chapter combines objective reflectance measurements and psychophysical modelling across four species of *Auriculella* to describe differences in variation at several scales, ranging from colour variation within individual shells, to variation across islands. It demonstrates that there are differences in colour within a single shell, similar to variation displayed by other Pacific Island snails. The chapter also describes significant variation between isolated populations of the same species, then demonstrates that there are no differences present in colour between species, except for a single difference in shell lightness between *Auriculella pulchra* and *Auriculella crassula*. The chapter also demonstrates a lack of variation between individuals found on the islands of Oahu and Maui, highlighting the differences between populations of a single species. The similarities of species found across Oahu and Maui are also discussed, resulting in speculation regarding similar selection pressures on islands. Finally, the chapter demonstrates that there is no difference in colour between dextral and sinistral individuals, suggesting that interchiral mating is not uncommon, and that the loci responsible for

colour variation and chirality are not closely linked. By describing the variation present in *Auriculella* in an ecologically and evolutionarily relevant context, inference regarding genetic mechanisms of variation becomes possible in a taxa of conservation concern. The importance of museum collections is highlighted, as is the application of technology to enhance information which can be gleaned from historical collections. In the future, it would be beneficial to extend this analysis of colour to other species of the genus, and other taxa at risk of extinction.

4.2 Introduction

Oceanic islands are widely considered to be useful systems for studying fundamental questions in evolutionary ecology, and the study of islands has inspired the formation of a wide variety of ecological and evolutionary paradigms (MacArthur and Wilson 1967, Warren et al. 2015, Grant and Grant 2016), the most pivotal of these being Darwin's theory of evolution through natural selection (Darwin 1859). The ecology of oceanic islands is unique due to their relative isolation and high availability of empty niche spaces allowing an increased rate of speciation and diversification (Paulay 1994). The diversity of species on islands is uniquely susceptible to anthropogenic interference, such as deforestation and the introduction of non-native species (Cincotta et al. 2000, Myers et al. 2000, Agoramoorthy and Hsu 2007, Szabo et al. 2012); one group of islands where this is particularly prevalent is the Hawaiian archipelago (Sakai et al. 2001, Doherty et al. 2016, Pejchar et al. 2020). The Hawaiian Islands support some of the world's most impressive diversity and are part of a collection of Pacific Island biodiversity hotspots, an area with characteristically high levels of endemism and a large number of species per km^2 (Donachie et al. 2004, Carlos et al. 2008, Vetter et al. 2010).

The level of diversity present across the entirety of the Pacific Islands is exemplified by the diversity of land snails which, relative to land area, remains unrivalled by anywhere else on the planet (Cowie 2001b). The 25,000 islands in the Pacific are home to more than 6000 land snail species (Cowie 2000), many of which are endemic to a single island. Of particular note, the Hawaiian Islands support one of the most spectacular land snail radiations in the world, containing species belonging to 10 families (Cowie et al. 1995). According to estimates, these families include between 750-1460 species (Solem 1990, Cowie et al. 1995), all but three of which are endemic to the archipelago, most to a single island (Yeung and Hayes 2018), and many to a particular mountain range (Pilsbry 1895).

Despite their diversity, Pacific land snails are among the most threatened taxa in the world, with more recorded extinctions since 1600 than any other group of fauna (Regnier et al. 2009). Estimates of extinction rates in Hawaii range from 50%-75% (Solem 1990), although the true rate is likely to be at the higher end of the scale; according to Solem, the lower bound of this estimate is "wildly optimistic". These extinctions have been driven primarily by anthropogenic activity, including the introduction of invasive species both as pets and biological control agents (Yeung et al. 2019). Oceanic island ecosystems such as those of the Hawaiian archipelago are typically sensitive to introduction of non-native species due to low functional redundancy whereby functional traits are rapidly lost from a system as diversity declines (O'Dowd et al. 2003, McConkey and Drake 2015). They are also sensitive to introductions of non-native species due to the relative simplicity of predator-prey relationships and associated food webs (Pimm 1991), and the characteristic disharmonic biota with an unevenly distributed representation of the taxa which is found on the mainland (Wallace 1965, Taylor et al. 2019). Land snails in particular may be susceptible to extinction through the introduction of alien predators due to their restricted geographic ranges and low vagility (Lydeard et al. 2004, Chiba and Cowie 2016, Gerlach et al. 2021).

Roughly 50% of all organisms on the Hawaiian Islands are non-native (Asner et al. 2008), with at least 5300 alien species established (Eldredge 2006), and up to 500 of these species are classified has having caused significant environmental or economic damage (Loope and Kraus 2009). Several of these non-native species have been introduced as biological control agents, including the rosy wolf snail *Euglandina rosea* and *Platydemus manokwari* flatworms (Hadfield et al. 1993, Gerlach et al. 2021). The carnivorous *Euglandina rosea*, now known to be a complex of species, at least two of which have been widely introduced to Hawaii (Meyer et al. 2017), were introduced as a biological control mechanism of the giant African snail *Achatina fulica* but have instead been implicated in the mass extinction of native Hawaiian

molluscan fauna. *Euglandina* were introduced to Hawaii from Florida in 1955 (Gerlach et al. 2021), and their distribution has been found to extend to altitudes where many of the remaining extant native land snails persist (Meyer 2006, Meyer and Cowie 2011, Gerlach et al. 2021). *E. rosea* follow slime trails to track prey, and in selection experiments show preference for native Hawaiian *Achatinella* snails over their intended biocontrol target, *A. fulica* (Holland et al. 2012). Their introduction has been associated with decline not only in Hawaii, but across the Pacific islands (Hadfield and Mountain 1980, Clarke et al. 1984, Coote and Loève 2003), whilst not affecting populations of their intended biocontrol target *A. fulica* (Civeyrel and Simberloff 1996, Cowie 2001a, Meyer et al. 2017).

Other non-native organisms also pose a threat to Hawaii's land snail populations - introduced rat species such as the black rat, *Rattus rattus*, are particularly devastating to snail populations, and are common in areas of native snail habitat. Rats are known to predate on snails, causing extreme impact upon populations (Hadfield and Mountain 1980). Once a rat has identified a snail as an item of prey, it can quickly navigate the tree canopy and decimate a population (Whisson et al. 2007, Hadfield and Saufler 2009, Foster et al. 2011), although recovery of susceptible snail populations from rat predation is theoretically more easily possible due to a rat's preference for larger shells (Hadfield et al. 1993). *R. rattus* also effectively predate on both *E. rosea* and *A. fulica*, so may be considered useful in the removal of introduced molluscan pests, although the extent of this is not well documented (Meyer and Shiels 2009). Jackson's chameleons, *Chamaeleo jacksonii*, are also important predators of snails in Hawaii, where they were introduced as part of the pet trade in the 1970s (Holland et al. 2010). The inter-island trade in chameleons as pets remained unrestricted until 1997, despite multiple self-sustaining populations becoming established across the islands of Oahu, Lanai, and Kauai by the mid-1990s (Kraus et al. 2012, Chiaverano and Holland 2014). Now, there are established populations in these

areas as well as on Maui and the island of Hawaii. Due to their large size and ability to easily navigate a canopy, the presence of Jackson's chameleons in Hawaii leaves native species susceptible to predation (Kraus et al. 2012). In dissections of chameleons, shells of native snail species including *Auriculella* and *Achatinella* spp. have been found in the gut (Holland et al. 2010).

One of the taxonomic groups most threatened by non-native predators is the Achatinellidae (Holland and Hadfield 2002). It is one of the most diverse families of land snails in the Hawaiian Islands, with 210 species in five subfamilies (Holland et al. 2017). Interest and study within these subfamilies is not evenly distributed across species, with favour being given to the larger, more colourful and charismatic individuals. Within the Achatinellidae, the genus *Achatinella* is the focal point of both literature and conservation effort (Yeung and Hayes 2018, Hadfield and Haraway 2019, Meyer et al. 2021). To date, there is much less known about the smaller, less colourful *Auriculella* spp., a genus which whilst less dramatic than *Achatinella*, presents a wide range of variation in shell colour, pattern, and chirality (Hartman 1888, Asami et al. 1998, Schilthuizen and Davison 2005, Holland et al. 2018). The genetic mechanisms which underpin the variation in both colour and chirality in *Auriculella* remain elusive, with the genus receiving little attention relative to other Pacific Island land snails.

Much of the variation present in *Auriculella* spp. is likely to be related to stochastic events (Cowie 1992), including founder effects and genetic drift, as small propagules became isolated in the numerous steep-sided valleys of the Hawaiian islands, rather than variation being attributed to finely tuned adaptation. *Auriculella* are unique amongst the Hawaiian land snails in that they appear to be able to persist on non-native flora in areas where native vegetation is no longer found (Holland et al. 2017). Despite this, only 14 of the 32 described species of *Auriculella* remain

extant (Yeung, pers. comm.), and the conservation statuses of these are poorly described (Holland et al. 2017). Whilst biologically endangered, this status is not yet officially recognised by the IUCN (Holland et al. 2010, Kraus et al. 2012).

It is important to characterise the variation observed in these species before it is lost completely. Whilst museum specimens are useful for this, the use of these specimens comes with inherent difficulties attached; extant species are in rapid decline; and little is known about the *Auriculella* genus. As far as it is possible to tell, no consistent qualitative phenotype description is in place for *Auriculella*. The presence of a large quantity of specimens of both extinct and extant species of the genus in the Bernice Pauahi Bishop Museum malacology collection (Oahu, Hawaii) provides an ideal resource for the quantification of some of the variation present in *Auriculella* species, both in terms of variation within single shells, and within and between four *Auriculella* species. Regnier et al. (2009) state that "effective conservation strategies require knowledge about extinction-prone groups", therefore, whilst *Auriculella* species are not presently defined by variation in colour patterning of shells, understanding the variation in an ecologically relevant context (i.e. that of a potential predator and disperser), may provide a framework for understanding how variation within and between species might have evolved, and how it might be maintained naturally, as well as with conservation efforts. The results have significance in furthering the understanding of a relatively sparsely studied genus, in terms of both conservation and evolutionary ecology.

In this chapter, I aim to define the difference in colour present in *Auriculella* shells across several parameters. Firstly, I aim to define differences in variation present in individual shells with measurements of apical and apertural areas of shell. Secondly, I aim to establish phenotypic overlap in shell colour across historical populations of the

same species. Thirdly, I aim to determine whether phenotypic variation is present between different species, and extend this to consider variation present between islands. Finally, I aim to establish whether there is a relationship between colour and chirality in *Auriculella* shells.

By achieving each of these aims in turn, variation in *Auriculella* can be understood at a variety of scales, from small scale variation within individuals, up to whole island scale variation. At a small scale, defining the difference in colour which is present across individual shells allows some inference to be made regarding the likely genetic mechanisms controlling this variation, which is similar to that displayed in other Pacific land snails, namely members of the genus *Partula*. Secondly, the establishment of phenotypic overlap in shell colour across historical populations of the same species, and between different species suggests that of using the colour of dried shells as a tool for identification may be of low accuracy, and indicates that the possibility of cryptic species within museum collections of dried shells might benefit from further consideration. Thirdly, determining whether the colour of individuals varies between islands in the Hawaiian archipelago furthers understanding regarding selective environments – if species vary across islands it may be indicative of differential selection pressures between islands. Finally, understanding whether colour varies with chirality aims to determine whether there is assortative mating between the two phenotypes, and whether the gene determining chirality is closely linked to the genetic mechanisms which underpin colour variation in *Auriculella*.

4.3 Materials and methods

4.3.1 Snails

Samples of four species (*Auriculella auricula, Auriculella crassula, Auriculella pulchra*, and *Auriculella uniplicata*) were selected from the 135,000 lots of *Auriculella* species housed within the Bernice Pauahi Bishop Museum malacology collection. Populations of each species were selected from the collection, and available data on collection location, collection date, and chirality of individuals were noted. Samples were collected by various museum volunteers throughout the 1900s, with some populations being donated to the museum's collection as early as 1901.

Species were selected based on criteria required for collection of spectral measurements using methodology described below (**Section 4.3.2**), including ensuring individuals were of a suitable size, and did not display notable colour boundaries on individual whorls of the shell in the form of banding patterns etc. Within species, lots were selected at random, and those which had been separated by chirality were combined into a single lot. Within lots, all individuals were measured in both locations, provided they were of an appropriate size and the condition of the shell was acceptable to provide accurate measurements from both locations, and ensuring the shell displayed no immediately noticeable signs of fading.

4.3.2 Spectrophotometry

Spectral readings were collected using an Ocean Optics spectrometer (model USB2000+UV-VIS-ES) and light source (DT-MINI-2-GS UB-VIS-NR) as per **Section 3.3.2**, with minor deviations. Reflectance measurements were collected at two places on each shell to capture variation within individual shells. A point measurement was taken on the bottom-most whorl of the shell (apertural measurement), and a second on the third whorl from the top (apical measurement) (**Figure 4.1**). Each

of these measurements was repeated three times to capture local variation within shell areas. Before measurements were taken for each location on each individual, the spectrophotometer was used to check
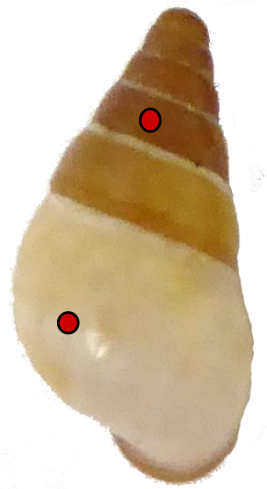
Figure 4.1: *Auriculella uniplicata* shell, showing approximate location of the two spectral measurements taken on each shell. Exact position varies between each shell to allow for damage, and between repeat measurements taken from individual shells to capture localised variation in ground colour.

individuals for colour boundaries which were not visible to the human eye. Shells of all four species did not show any reflectance in the UV, so reflectance measurements were restricted to 400-700nm. Readings were collected using Ocean Optics SpectraSuite v.2.0.162 (software settings: integration time 750msec, boxcar width 5, scans to average 10), then repeats averaged, raw data smoothed with a loess smoothing parameter of 0.18, the lowest level of smoothing which both removed noise but maintained spectral shape. Smoothed data was then binned into 1nm groups using Pavo2 v2.6.1 (Maia et al. 2019).

4.3.2 Psychophysical modelling

To give colour measurements an appropriate ecological context, measurements were analysed according to the visual system of a

tetrachromatic passerine avian observer, as per **Section 3.3.3**, with some deviations. The visual system of the American goldfinch (*Spinus tristis*) was used as it is the closest relative available to the Po'ouli (*Melamprosops phaeosoma*), an extinct Hawaiian honeycreeper. The Po'o-uli is the only member of its genus, but belongs to the Fringilidae, the true finches, the same family as the American goldfinch. The Po'ouli was endemic to Maui, so it is unlikely that predation by this species of bird is the sole driver behind inter-individual and inter-species variation observed in the *Auriculella*, but there is limited information available regarding natural predators of *Auriculella* outside of the primary focus of non-native species. Po'ouli have been recorded as having land snails as a part of their diet (Baldwin and Casey 1983), and in Japanese feeding trials, it has been noted that small snails can survive transit through the digestive system of some birds (Wada et al. 2012). Survival of transit through the gut of a predator facilitating dispersal has also been recorded in pond snails (Brown 2007), so it seems likely that bird predation has played a role in dispersal of snails across the Hawaiian islands. The American goldfinch, like the Po'o-uli, is a tetrachromat, with cone proportions of VS: 0.514, S: 1.119, M: 1.213, L: 1, and sensitivity functions of 399, 442, 512 and 580 respectively (**Table 4.1, Figure 4.2**) (Baumhardt et al. 2014). As per **Section 3.3.3**, the analyses assumed that the L cone has a noise-to-signal ratio of 0.05 (Delhey et al. 2015), giving ratios for the other cones of VS: 0.0688, S: 0.0526 and M: 0.0471. Values of variation are given in JND units (Just Noticeable Differences), a single JND unit represents the minimum Euclidean distance between points in 3-dimensional colour space which would be perceptible by a predator (Delhey et al. 2015). Psychophysical modelling was performed in the R package Pavo2 v2.6.1 (Maia et al. 2019), in R version 4.04 (R Core Team 2021).

Table 4.1: Cone proportions, sensitivity functions (nm) and noise:signal ratios for the four cones (VS, S, M, and L) of the American goldfinch (*Spinis tristis*), the visual system used in tetrachromatic psychophysical modelling.

	Cone			
	VS	**S**	**M**	**L**
Cone proportion	0.514	1.119	1.213	1
Sensitivity function (nm)	399	442	512	580
Noise:signal ratio	0.0688	0.0526	0.0471	0.05
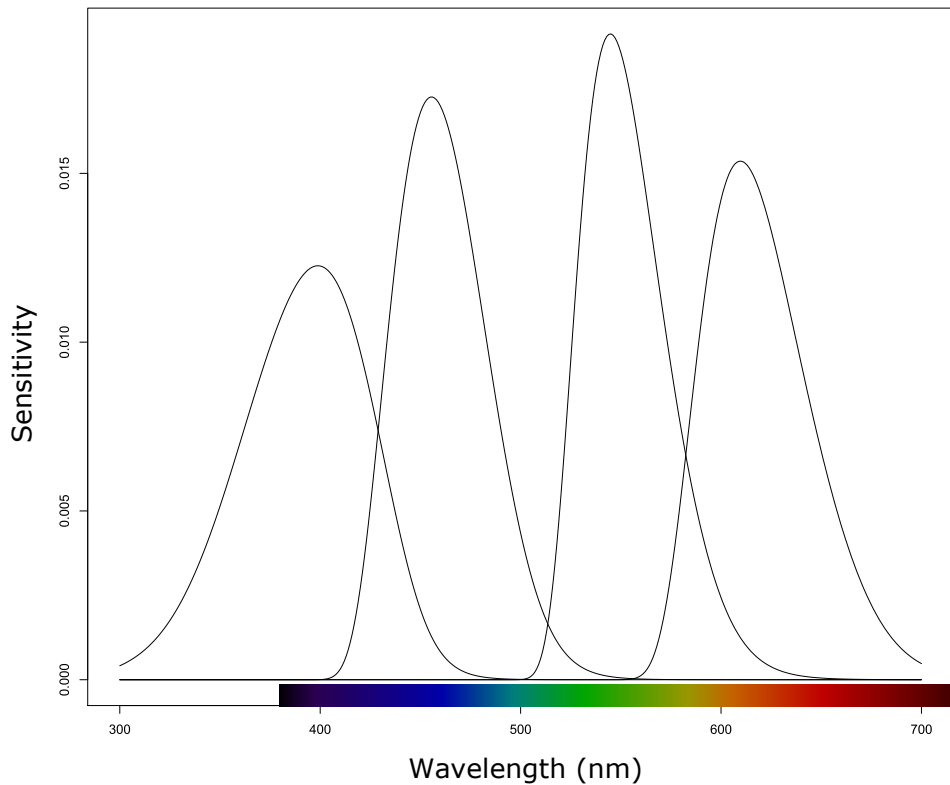
Figure 4.2: Cone sensitivities (nm) for the four cones (VS, S, M, and L) of the American goldfinch (*Spinis tristis*), the visual system used in tetrachromatic psychophysical modelling, demonstrating the range of wavelengths responsible for stimulation of each of the four cones.

4.3.4 Statistical analysis

All analyses were carried out in R version 4.04 (R Core Team 2021). Principal Components Analysis (PCA) was carried out on the chromatic coordinates (x, y, and z) to identify the three main axes of chromatic variation present in three-dimensional colour space, referred to subsequently as PC_{xyz}. A covariance matrix rather than a correlation matrix was used to preserve the perceptual distances, given in units of Just Noticeable Differences (JNDs) (Delhey et al. 2015). All difference in three-dimensional space, and distance along PC_{xyz} axes are given in JNDs.

4.3.4.1 Within species colour variation

The difference between spectra of individuals of all species was analysed by cluster analysis performed in Mclust, as described in **3.3.4**. Within this, the individuals were deemed as being either the same or different dependent on cluster assignment of their apical or apertural colour measurements.

Whilst cluster analysis alone is informative for determining overall pattern of colour in a species, it does not directly compare the two point measurements taken in each individual. To determine whether the differences in colour between the shells of *Auriculella* would be observable by an avian predator, Euclidean distances between points belonging to the same individual (ie the apical and apertural measurements) in 3 dimensional colour space were calculated using a standard 3D distance formula:

$$d = \sqrt{((x_2 - x_1)^2 + (y_2 - y_1)^2 + (z_2 - z_1)^2)}$$

These distances were calculated in four directions - overall distance in 3-dimensional colour space, and distance apart along each of the three PC_{xyz} axes. Peacock's tests were used to determine whether the distribution of datapoints in 3-dimensional space was equal between the apical and apertural measurements of individuals of each species, Kolmogorov-Smirnov tests were used to determine whether the distribution of these points was equal when distributions were shifted to centre around a single mean, determining whether there was a difference in variability of the groups of paired measurements along each of the three PC_{xyz} axes. Finally, GLMMs determined whether groups of measurements from shell sections differed significantly from one another. Each species was treated and analysed independently.

4.3.4.2 Between population variation

GLMMs with fixed effects of population, and random effect of chirality were fit for both apertural and apical measurements of shells of a single species, each with a response variable of one of the three PC_{xyz} axes. Paired apical and apertural measurements are non-independent, so treated separately throughout analyses.

4.3.4.3 Between species variation

GLMMs with a fixed factor species, and a response variable of each PC_{xyz} axis for apical and apertural measurements (treated independently) were fitted to establish whether there is a difference in these between species. To determine whether points are distributed differently along the PC_{xyz} axes, both generally and between combinations of individual species, k-samples Anderson darling tests followed by Bonferroni corrected Anderson-Darling all pairs comparison tests were performed.

4.3.4.4 Between island variation

GLMMs with a fixed factor of island and random factors of species, population, and chirality were fitted to colour data of individuals from each of the two islands sampled, with response variables of PC_{xyz} axis. Population is inherently nested in species, as each population consists of a single species, and this was reflected in the model fitting procedure. A total of six models were fitted, one for each response PC_{xyz} axis in both the apical and apertural measurement positions.

4.3.4.5 Variation with chirality

GLMMs with a fixed factor of chirality and random factors of species, population, and island were fitted to colour data of individuals from across all four species, again with response variables of each PC_{xyz} axis. The nesting of random effects was reflected in the model fitting procedure. Six models were fitted, one for each response PC_{xyz} axis in each group of measurements according to the position on the shell from which they were taken, either apical or apertural.

4.4 Results

Reflectance spectra of 548 individual shells were collected, with measurements taken from two locations per shell. These shells belonged to four species, 71 *Auriculella auricula,* 118 *A. crassula,* 106 *A. pulchra,* and 117 *A. uniplicata.* The individuals were from 30 populations, historically collected from various locations across the islands of Oahu and Maui.

4.4.1 Principal components

The analysis carried out below (**Sections 4.4.2 – 4.4.5**) relies heavily on the collapsing of initial raw spectral reflectance wavelength data into 3-dimensional co-ordinates in tetrachromatic colour space with the use of psychophysical modelling (as described in **Section 3.3.3**). The subsequent implementation of principal components analysis allows the framing of these co-ordinates along three meaningful primary axes of variation, the PC_{xyz} axes. Each of these three axes represents a different parameter of variation within the colour differences observed across the four species (**Figures 4.3, 4.4, 4.5**). $PC_{xyz}1$ represents the reflectiveness of the shell surface, rather than differences in colour – a high $PC_{xyz}1$ value relates to a high amount of light being reflected from the shell into the probe, this high level of reflectance could be either due to variation in saturation levels, as in *Cepaea* (Section **3.4.1**), or, due to differences in the reflectivity of the periostracum. A low $PC_{xyz}1$ score corresponds either to a heavily pigmented shell with strong colouration, or to a shell with a matte surface, with minimal reflection of light back into the spectrophotometer probe. $PC_{xyz}2$ represents the darkness of shell pigmentation, ranging from a low $PC_{xyz}2$ value being a light-coloured pigment, irrespective of colour, to a high PC_{xyz} value being representative of a dark shell. Changes in $PC_{xyz}3$ correspond to changes in "yellowness" of the shell, a low $PC_{xyz}3$ value represents a clearly yellow shell, and a high $PC_{xyz}3$ value is representative of an obviously brown shell.

Within *Auriculella* shells, $PC_{xyz}1$, explains 86.36% of variation, with a very weak positive loading for x (0.058), a medium positive loading for y (0.556), and a strong positive loading for z (0.829). $PC_{xyz}2$, explains 12.92% of variation, and has a strong positive loading for x (0.866), a medium negative loading for y (-0.441), and a weaker positive loading for z (0.235). $PC_{xyz}3$ explains the remaining 0.07% of the variation, and has medium and strong positive loadings for x (0.496) and y (0.705), and a medium negative loading for z (-0.507).
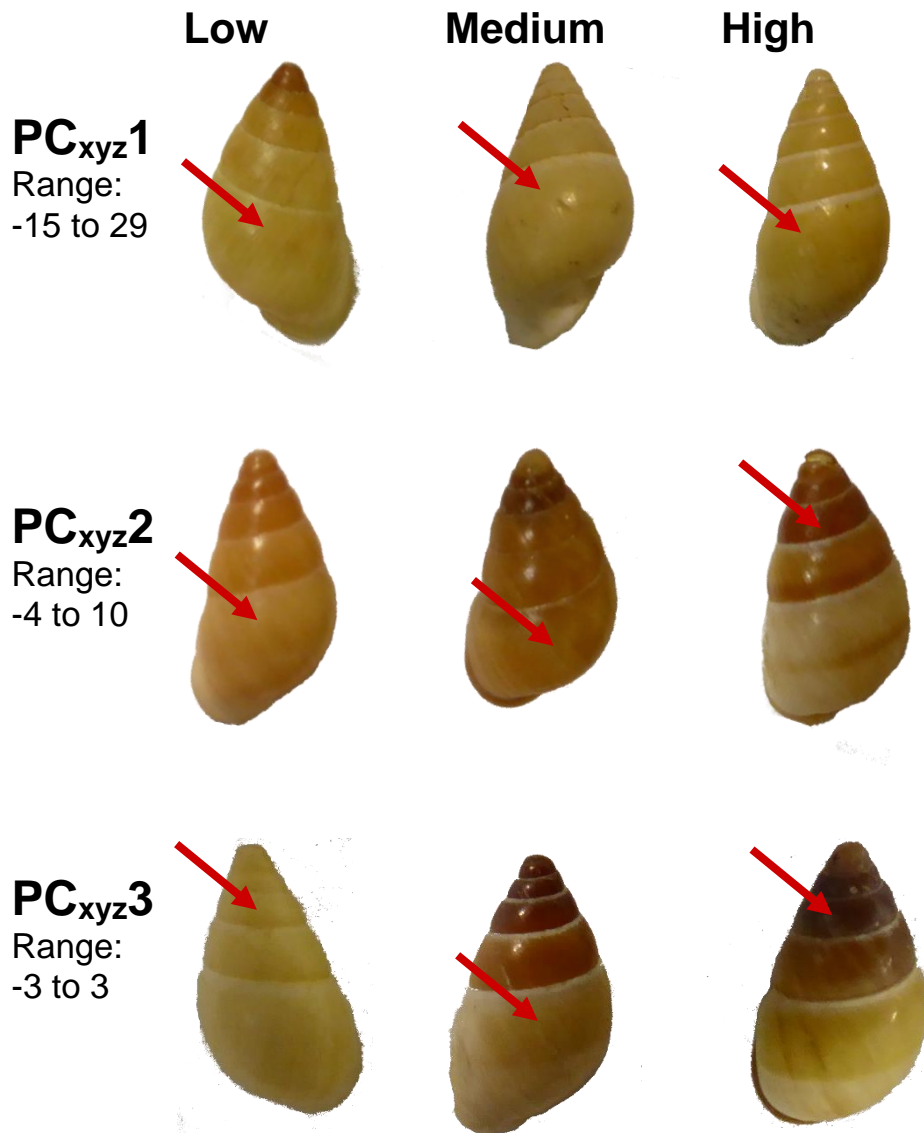
Figure 4.3: Representation of a high, medium, and low PC_{xyz} value for each axis, with measurements of remaining two axes as consistent as possible. Measurement location indicated by red arrows, and is either taken from the bottommost whorl, or the third whorl from the apex. PC_{xyz} ranges for each axis are included, units of these ranges are given in JNDs. Low measurements consisted of readings in the bottom 25th percentile of the range, medium consisted of readings within the 12.5^{th} percentile either side of the median measurement, and high within the 75th percentile for each axis. The position along the two non-focal PC_{xyz} axes was kept as constant as samples allowed.
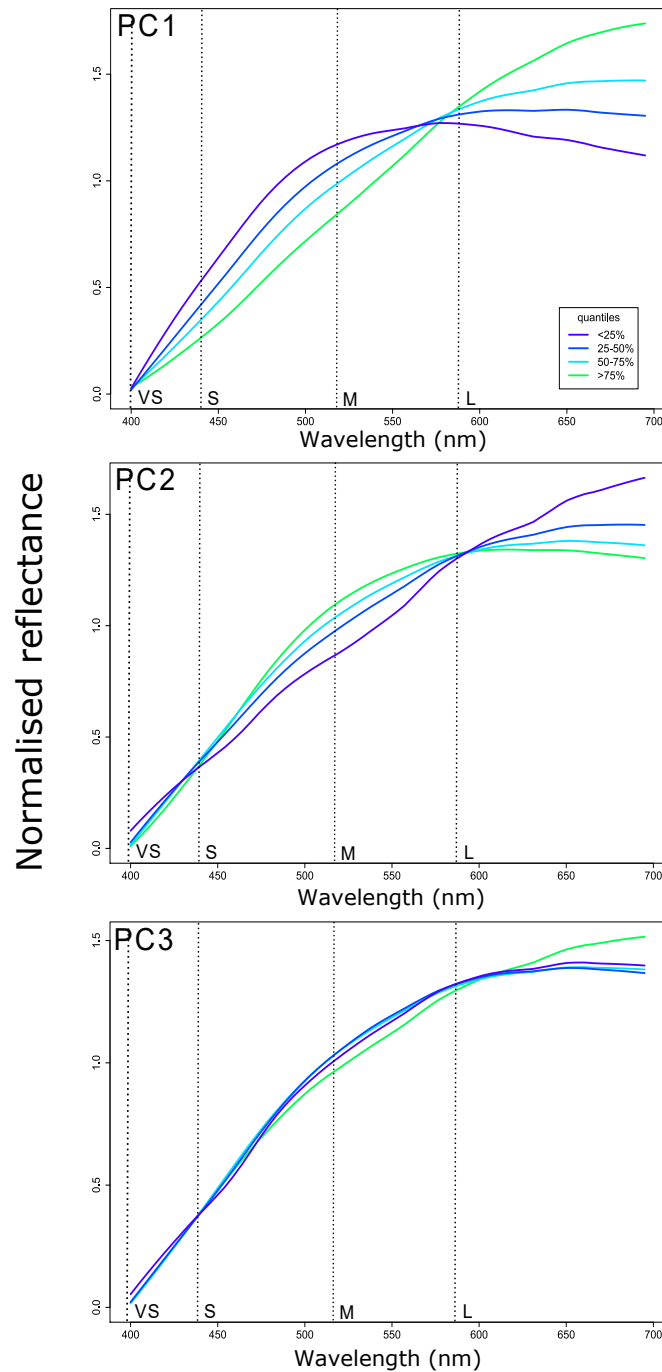
Figure 4.4: Interquartile ranges of the average normalised reflectance spectra of individual PC_{xyz} of all four *Auriculella* species. Variation along $PC_{xyz}1$ mainly represents a decrease in S and M cone stimulation, and an increase in L cone stimulation. Differences along $PC_{xyz}2$ represent the opposite of $PC_{xyz}1$, with a decreased L cone stimulation, and differences along $PC_{xyz}3$ are mostly concentrated at the yellow – red end of the spectrum, where L cone stimulation is focussed, with high $PC_{xyz}3$ values representing higher stimulation towards red wavelengths. Dotted lines represent the peaks of quantum cone catch for each photoreceptor type.
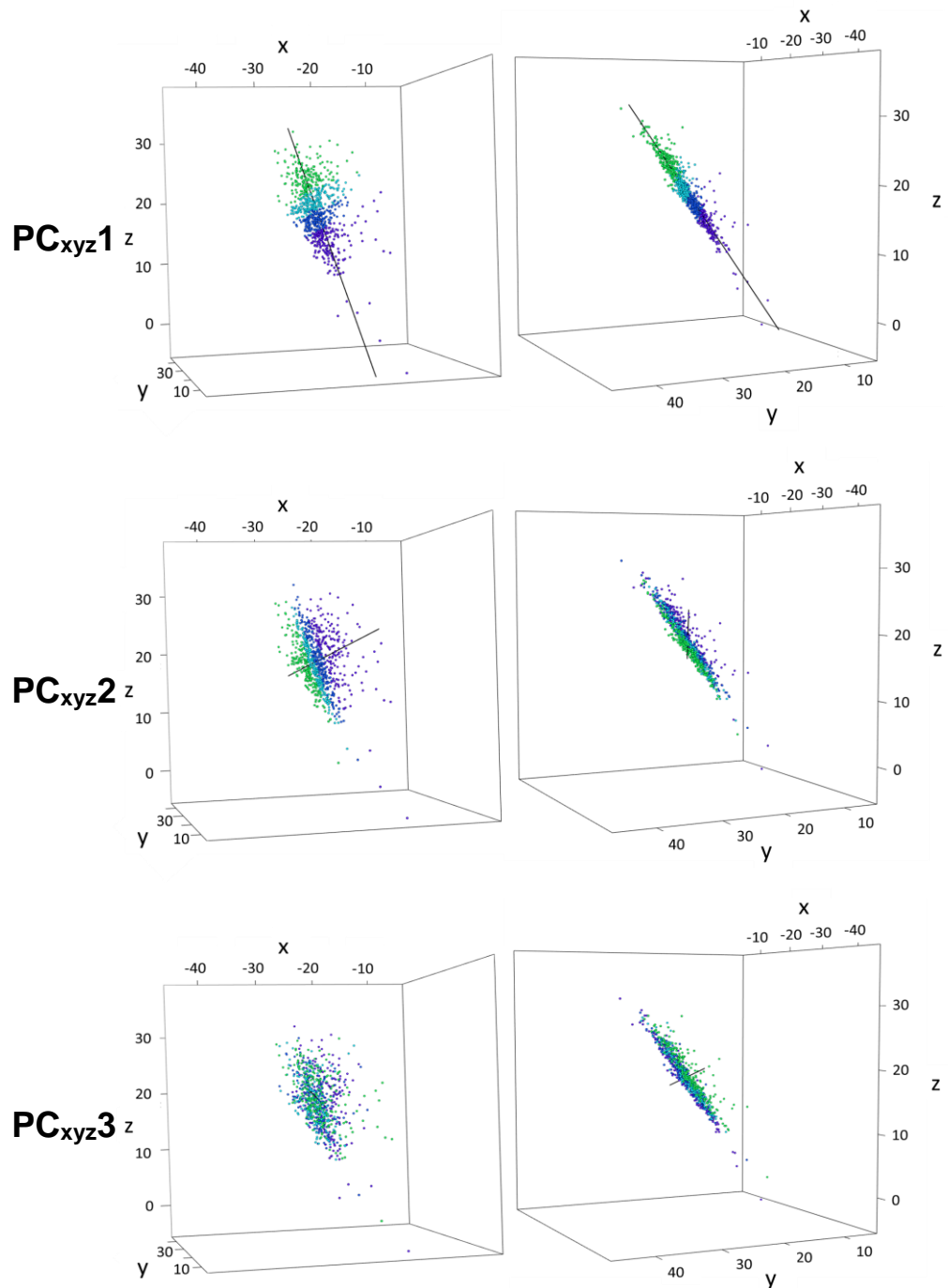
Figure 4.5: 3-dimensional representation of interquartile ranges of spectra of individual PC_{xyz} of all four species of *Auriculella*. Plots are shown in two orientations for clarity. These plots demonstrate how variation along each of the three PC_{xyz} axes of variation translates into position (defined by xyz co-ordinates) in 3-dimensional tetrachromatic colour space. Each point represents a single measurement (two points per individual), and colour of points represents PC_{xyz} quantile, with colour scheme the same as **Figure 4.4**. Black lines are reflective of PC_{xyz} axes.

4.4.2 Within individual variation
4.4.2.1 *Auriculella auricula*

Earlier principal components analysis (PCA) (**Section 4.4.1**) confirmed that the variation present in all *Auriculella* shells occurs along 3 main axes of variation $PC_{xyz}1$, 2, and 3. *Auriculella auricula* displays a wide range of variation between and within shells according to each of these principal components, with a $PC_{xyz}1$ range of 24 JNDs, $PC_{xyz}2$ range of 11 JNDs, and a $PC_{xyz}3$ range of 4 JNDs. Variation in apertural shell measurements was present across all 3 PC_{xyz} values at a slightly lesser extent than variation in 3-dimensional space at 22, 8, and 2 JNDs respectively. Variation in apical shell measurements was greater than that present in the apertural measurement across the 3 PC_{xyz} axes, at 23, 10, and 4 JNDs respectively.

When cluster analysis is performed on both the apical and apertural measurements of *Auriculella auricula,* the best fitting model resolves two clusters (EVV, ellipsoidal, equal volume and variable shape, BIC -1668.072, $P < 0.001$ compared to 2nd best model). The two clusters are not equal in size, with cluster 1 containing 28 of the measurements, and cluster 2 containing the remaining 114 (**Table 4.2**). The second and third best fitting models both resolved 3 clusters (EEV, BIC -1669.794, $P <$ 0.05 compared to 3rd best and VVV, BIC -1670.052 respectively). The cluster analysis suggests that most but not all individuals of *A. auricula* have similar coloured areas of shell - all individuals whose apertural measurement falls into cluster 1 also have an apical measurement which falls into cluster 1. All individuals with an apical measurement which falls into cluster 2, also have a apertural measurement which is grouped with cluster 2, suggesting similarity in shell colour in 3-dimensional space. There are 12 indivuals with an apertural measurement in cluster 2, and an apical measurement in cluster 1, suggesting a potential difference in colour between these areas.

Table 4.2 – *Auriculella auricula* individuals placed in one of two clusters resolved by Mclust algorithms, grouped according to location of shell measurement (either apical or apertural). Numbers in italics represent individuals with two shell measurements (ie top and bottom) which fall into the same cluster.

		Apical		
		Cluster 1	**Cluster 2**	**Total**
Apertural	**Cluster 1**	*8*	0	**8**
	Cluster 2	12	*51*	**63**
	Total	**20**	**51**	

A conservative threshold of 3 JNDs was used as a lower limit for distinguishability between shell sections, based on the small size of the shells, and the small scale in which the variation occurs (Siddiqi et al. 2004, Taylor et al. 2016). Of the 71 individuals of *A. auricula* measured, 38 of these had a difference of 3 or greater JNDs between measurement points in 3-dimensional colour space (**Appendix 4.1**), a proportion of 53.5% of all individuals. 26 individuals differ by more than 3 JNDs in $PC_{xyz}1$, 12 in $PC_{xyz}2$, and no individuals have a difference in points of 3 or more JNDs in $PC_{xyz}3$. Of the 26 which differ in $PC_{xyz}1$, only three individuals also differ along $PC_{xyz}2$.

A 3-dimensional Peacock's test indicated that the measurements from the top and bottom of shells of *Auriculella auricula* are not equally distributed in 3D colour space (xyz coordinates) ($D = 0.479$, $P = 0.00001$)

(**Figures 4.6, 4.7**). When PC_{xyz} values are shifted to centre around the same mean to assess differences in precise shape of distributions, Kolmogorov-Smirnov tests indicate that the distributions of all PC_{xyz} vales do not vary between measurement locations (D =0.141, P = 0.487; D = 0.113, P = 0.762; D = 0.211, P = 0.084), suggesting that distributions of points are not more variable between shell measurement locations along the three axes (**Figure 4.8**). When means are not shifted, assessing the distribution itself, distributions are the same for both measurement types along $PC_{xyz}1$ (D = 0.155, P = 0.364), but significantly different for $PC_{xyz}2$ and 3 (D = 0.423, P = 0.000004; D = 0.239, P = 0.034). GLMMs indicate that of all three PC_{xyz} axes, only $PC_{xyz}2$ contains significantly different measurements from shell locations (χ^2 = 0.509, df = 1, P = 0.475; χ^2 = 32.787, df = 1, P = 0.000001; χ^2 = 0.212, df = 1, P = 0.645), where $PC_{xyz}2$ is higher on average in the apical measurements, suggesting a darker shell apex.

The average distance in JNDs within a single area of shell measurement is greater on average in both the apical and apertural measurements of the shell than the average difference between paired measurements of an individual shell in *Auriculella auricula* (**Appendix 4.1**). The average distance in between two parts of the same shell is 3.573 JNDs, the average distance between apical measurements of all shells is 6.606, and the average distance between apertural measurements of the shells is 6.957, suggesting more variation in colour within the apertural section of shells than the apical, and indicating that differences in individual shells are not greater than those observed between the two shell sections. The same is true of $PC_{xyz}1$ where the average difference between the apical and apertural measurements of a single shell is 2.611 JNDs, and the average distance between all of the apical measurements is 5.617, and the average apertural measurement distance is 6.398. In $PC_{xyz}2$ and 3, the average distance of the apical measurements is greater than the average distance between parts of an individual shell, but the average difference in the apertural measurements is not,

although these differences do not extend beyond the threshold of 3 JND units, so are theoretically imperceptible to a predator ($PC_{xyz}2$: difference between individual shell parts = 1.891 JNDs, average difference between all apical measurements = 2.308, average difference between all apertural measurements = 1.783; $PC_{xyz}3$: difference between shell parts = 0.375 JNDs, average difference between apical measurements = 0.637, average difference between apertural measurements = 0.357).
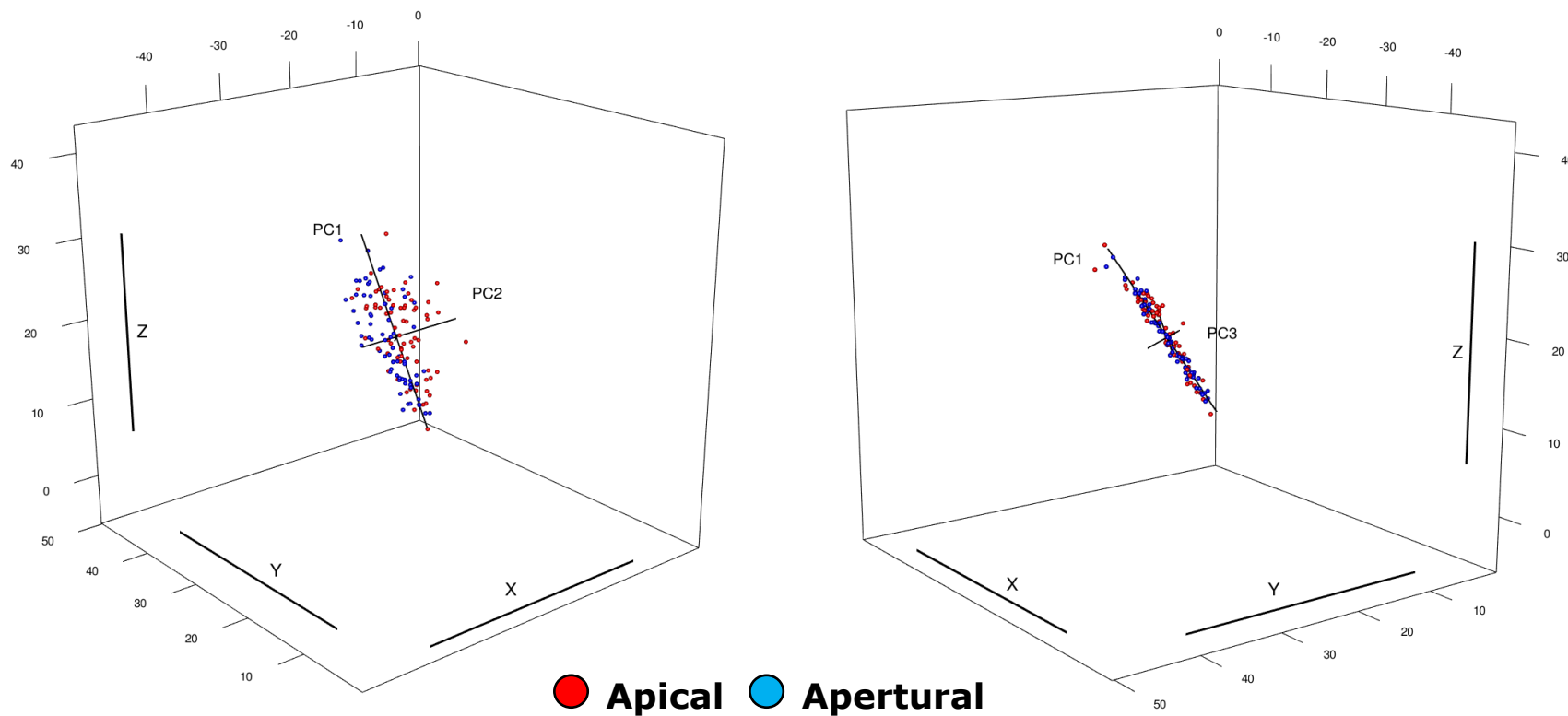
Figure 4.6 – 3D representation of location of all measurements of *Auriculella auricula* in tetrachromatic colour space. Red points represent measurements from the top section of the shell, and blue points show measurements from the bottom of the shell. PC$_{xyz}$ axes are shown. Figure in two orientations for clarity.
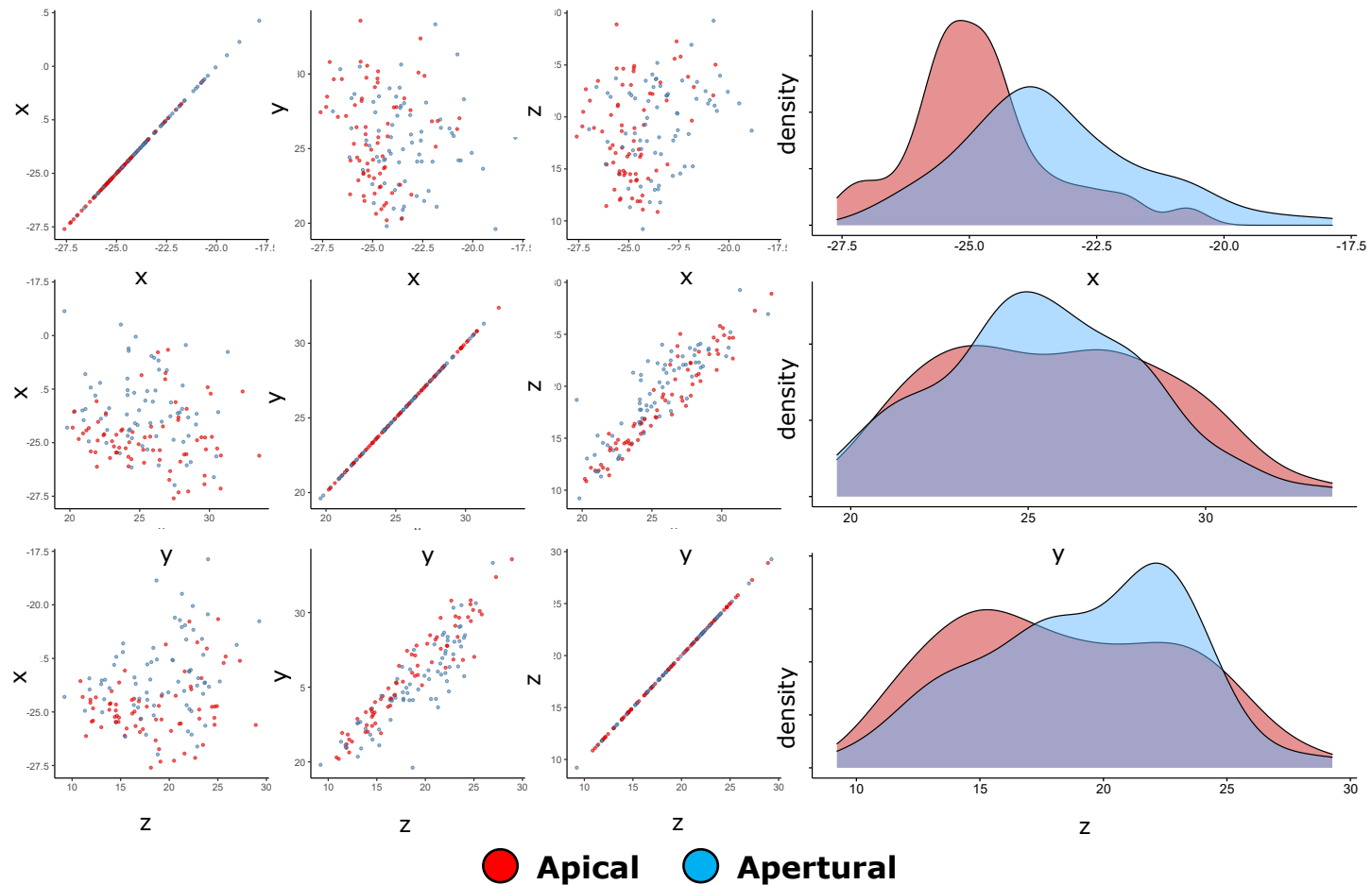
Figure 4.7 – 2D representation of location of all measurements of *Auriculella auricula* in tetrachromatic colour space, and associated density plots along each axis (xyz). Red points/plots represent measurements from the top section of the shell, and blue points/plots show measurements from the bottom of the shell.
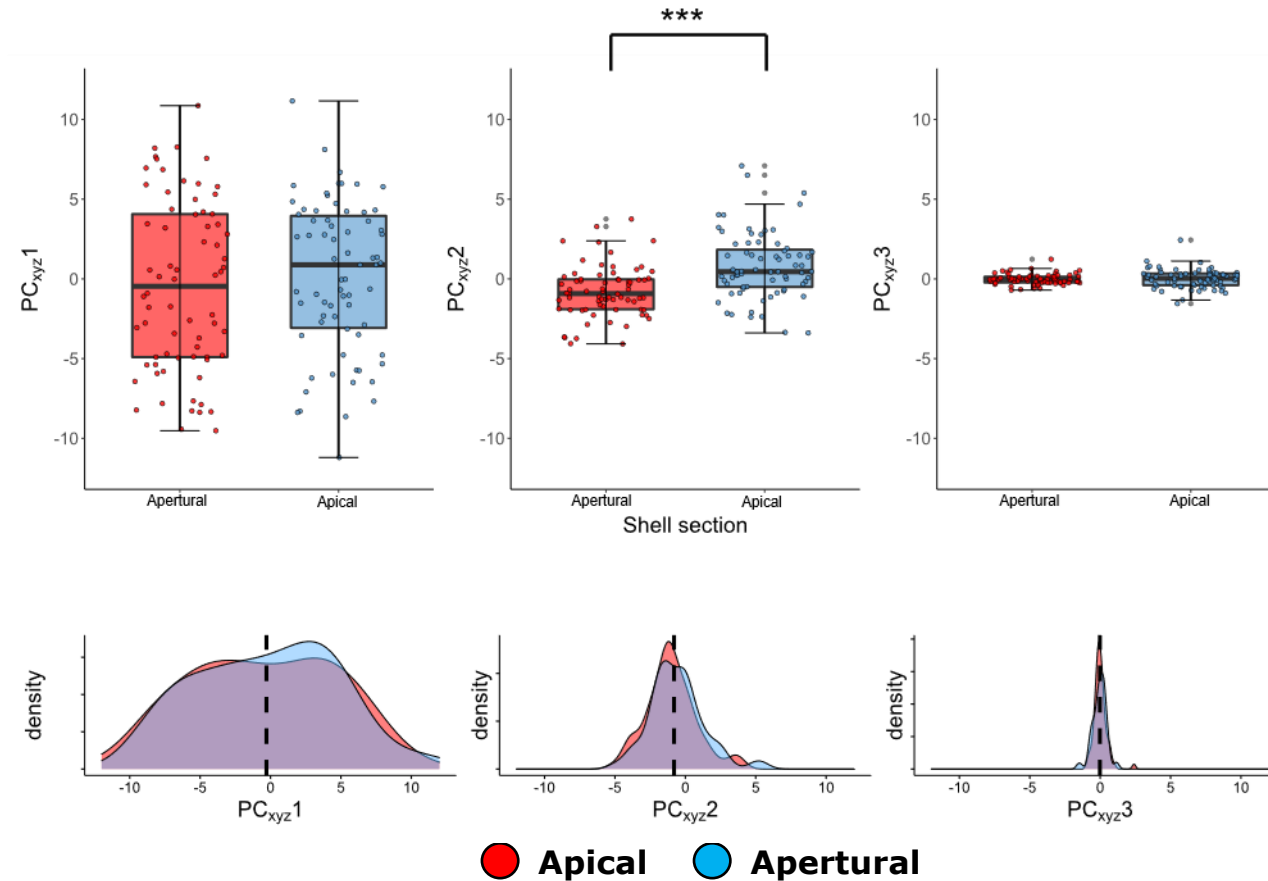
Figure 4.8 – differences in PC_{xyz} values between top and bottom measurements of *Auriculella auricula.* Apical and apertural measurements of shells differ significantly along $PC_{xyz}2$, where the apertural section of the shell has a lower $PC_{xyz}2$ value, so is lighter in colour than the apical section of the shell. None of the other axes differ significantly. Distributions shifted to centre around the same mean are also shown to display distribution of points along PC_{xyz} axes, none of which differ significantly between shell areas, suggesting that there is no difference in amount of variability of data.

4.4.2.2 *Auriculella crassula*

In *Auriculella crassula*, the range of variation present along the three main axes of variation is larger than that of *A. auricula*, with a $PC_{xyz}1$ variability of 31 JNDs, $PC_{xyz}2$ range of 12 JNDs, and $PC_{xyz}3$ range of 4 JNDs. The apertural measurement of *A. crassula* are slightly less variable than the combination of both apertural and apical measurements, with a $PC_{xyz}1$ range of 25 JNDs, and $PC_{xyz}2$ and 3 ranges of 8 and 2 JNDs. The apical measurements suggest variability in this section of the shell is slightly different to that in the apertural part of the shell, with a $PC_{xyz}1$ range of 31 JNDs, $PC_{xyz}2$ range of 8 JNDs, and a $PC_{xyz}3$ range of 4 JNDs.

Cluster analysis indicates that best fitting model when applied to data from the measurements of both shell sections, resolves three clusters (VEE, ellipsoidal, variable volume and equal shape, BIC -2700.874, $P <$ 0.001 compared to 2nd best model). The three clusters are not equal in size, with cluster 1 containing 103 of the measurements, cluster 2 containing 111, and cluster 3 containing the remaining 22. The second and third best fitting models resolved 4 and 3 clusters (VEE, BIC -2718.674, $P <$ 0.001 compared to 3rd best and VVE, BIC -2719.689 respectively). Neither apical nor apertural measurements were equally distributed between clusters (**Table 4.3**), and individuals with a apical shell measurement in cluster 1 always also had an associated apertural measurement which also fell into the first cluster. Only three of the apertural measurements fell into the third cluster, with the majority of the apertural measurements falling into cluster 1, and the majority of the apical measurements in the second cluster, suggesting that those individuals with apical measurements in cluster 1 have at least relatively unchanging colouration throughout the entire shell.

Table 4.3: *Auriculella crassula* individuals placed in one of three clusters resolved by Mclust algorithms, grouped according to location of shell measurement (either apical or apertural). Numbers in italics represent individuals where both apertural and apical measurements are assigned to the same cluster.

		Apical			
		Cluster 1	**Cluster 2**	**Cluster 3**	**Total**
Apertural	**Cluster 1**	*24*	43	12	**79**
	Cluster 2	0	*31*	5	**36**
	Cluster 3	0	1	*2*	**3**
	Total	**24**	**75**	**19**	

Of the 118 individuals of *A. crassula*, 80 had a difference of 3 or more JNDs between measurement points in 3-dimensional colour space; thus 67.7% of all individuals had shells with a variation in colour between the top and bottom measurements different enough to be perceived by an avian predator (**Appendix 4.1**). 66 individuals differed by more than 3 JNDs in $PC_{xyz}1$, 18 in $PC_{xyz}2$, and 1 individual had a difference in points of 3 or more JNDs in $PC_{xyz}3$. Of the 66 individuals which differed along $PC_{xyz}1$, 13 of these also differed by more than 3 JND units along $PC_{xyz}2$, and one individual differed by more than 3 JND units along all three axes.

A 3-dimensional peacock's test showed that apertural and apical measurements of *Auriculella crassula* are not equally distributed in 3D

colour space (xyz coordinates) (D = 0.5, P = 4.056e-10) (**Figures 4.9, 4.10**). When PC_{xyz} values are standardised to the same mean to assess precise shape of distributions, Kolmogorov-Smirnov tests indicate that none of the distributions of points along all PC_{xyz} axes vary between parts of *Auriculella crassula* shells (D = 0.144, P = 0.173; D = 0.153, P = 0.128; D = 0.119, P = 0.377) (**Figure 4.11**), suggesting that none of the three PC_{xyz} axes are more variable between measurement areas. When means are not shifted, distributions are significantly different for all three PC_{xyz} axes (D = 0.339, P = 0.000003; D = 0.466, P = 1.471e-11; D = 0.220, P = 0.007), indicating differences in distribution in three-dimensional colour space. GLMMs indicate that $PC_{xyz}1$ and 2 each have measurements of shell areas which occupy different 3-dimensional colour space (χ^2 = 15.466, df = 1, P = 0.00008; χ^2 = 63.602, df = 1, P = 1.523e-15), $PC_{xyz}1$ is higher on average in apertural measurements, and $PC_{xyz}2$ is lower in apertural measurements, indicating that apertural measurements are both less reflective and lighter than apical measurements. $PC_{xyz}3$ does not differ between shell measurement locations (χ^2 = 3.494, df = 1, P = 0.062).

As in *A. auricula*, the average distance (JNDs) between all individuals is greater in both groups of apical and apertural measurements than the average distance between parts of an individual shell in *Auriculella crassula.* The average distance in JNDs between two parts of the same shell is 4.991, the average distance between apical measurements is 6.617, and the average distance between measurements of the apertural measurements is 5.982. The same is true of $PC_{xyz}1$ where the average difference between the apical and apertural measurement of a single shell is 4.263 JNDs, and the difference between all the apical measurements is 5.789, and apertural measurement distance is 5.545. In $PC_{xyz}2$ and 3, the average of the apical measurements is greater than the average distance between parts of an individual shell, but the average difference in the apertural measurements of all shells is not, although this difference does not extend beyond 3 JNDs, so is

theoretically imperceptible to a predator ($PC_{xyz}2$: difference between shell parts = 1.864 JNDs, average difference between apical measurements = 2.085, average difference between apertural measurements = 1.388; $PC_{xyz}3$: difference between shell parts = 0.446 JNDs, average difference between apical measurements = 0.637, average difference between apertural measurements = 0.426). These trends are directionally the same as those observed in *A. auricula* but are of a slightly higher magnitude.
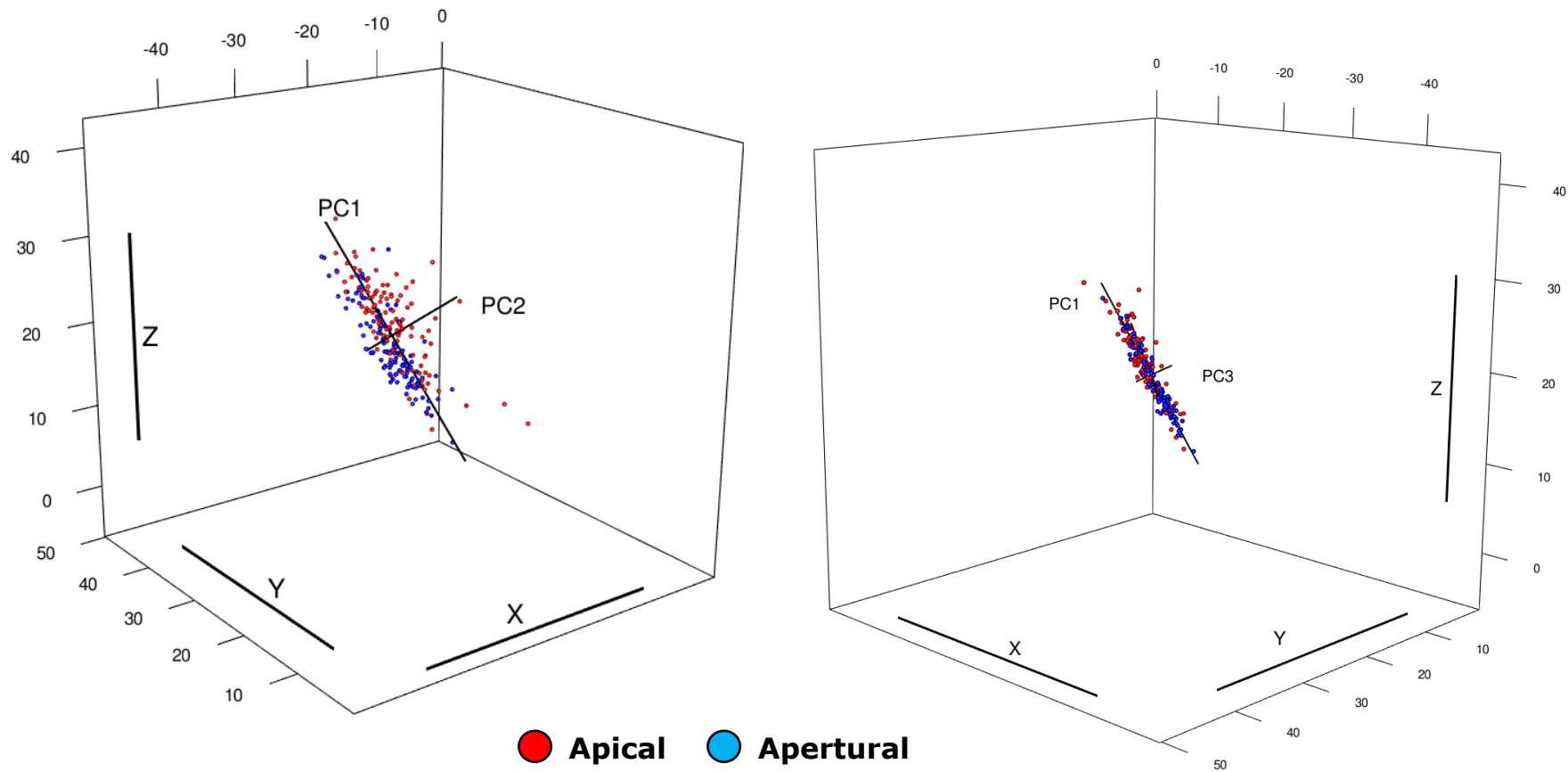
Figure 4.9 – 3D representation of location of all measurements of *Auriculella crassula* in tetrachromatic colour space. Red points represent measurements from the apical section of the shell, and blue points show measurements from the apertural section of the shell. PC$_{xyz}$ axes are shown. Figure in two orientations for clarity.
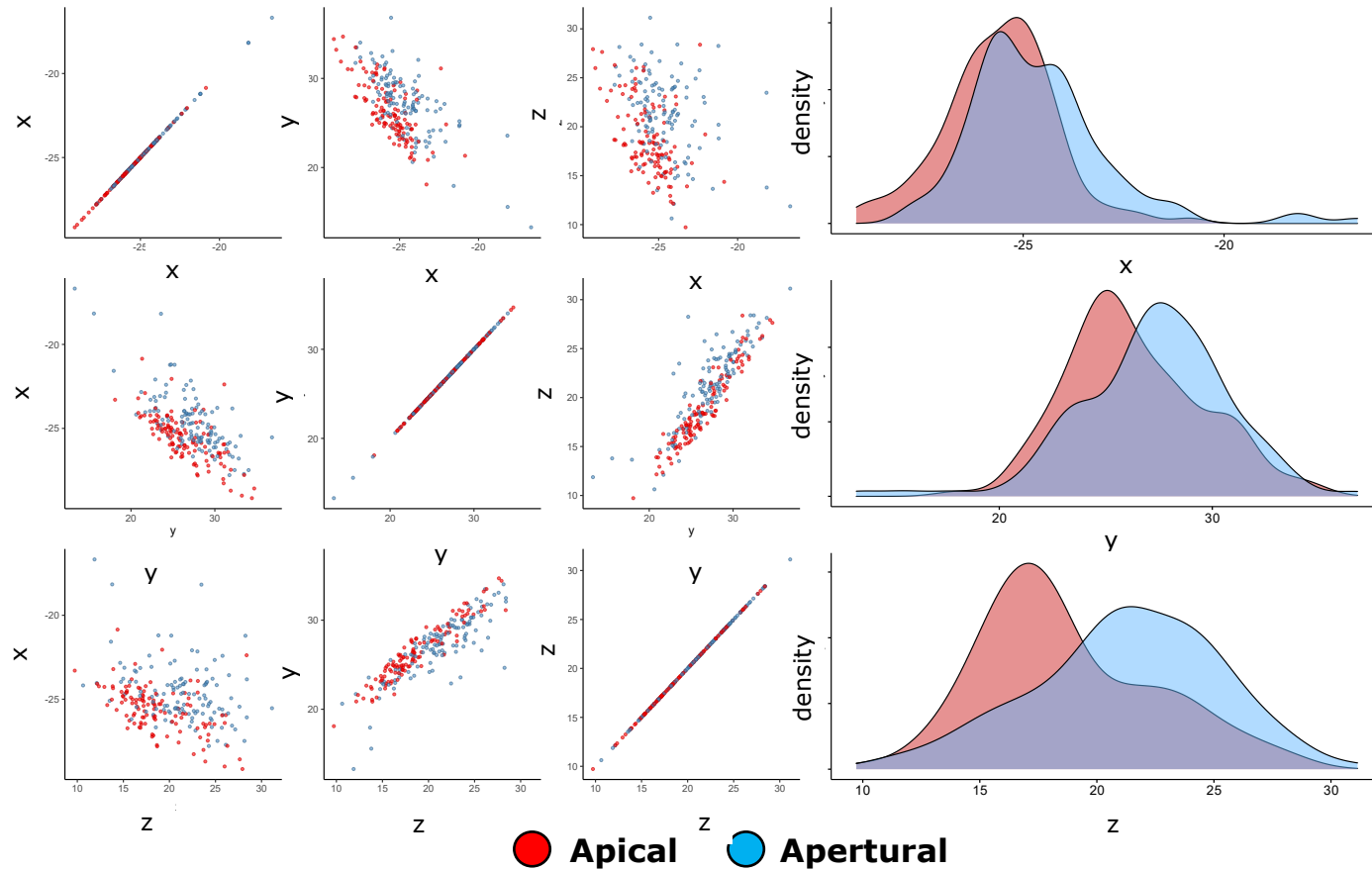
Figure 4.10 – 2D representation of location of all measurements of *Auriculella crassula* in tetrachromatic colour space, and associated density plots along each axis (xyz). Red points/plots represent measurements from the apical section of the shell, and blue points/plots show measurements from the apertural section of the shell.
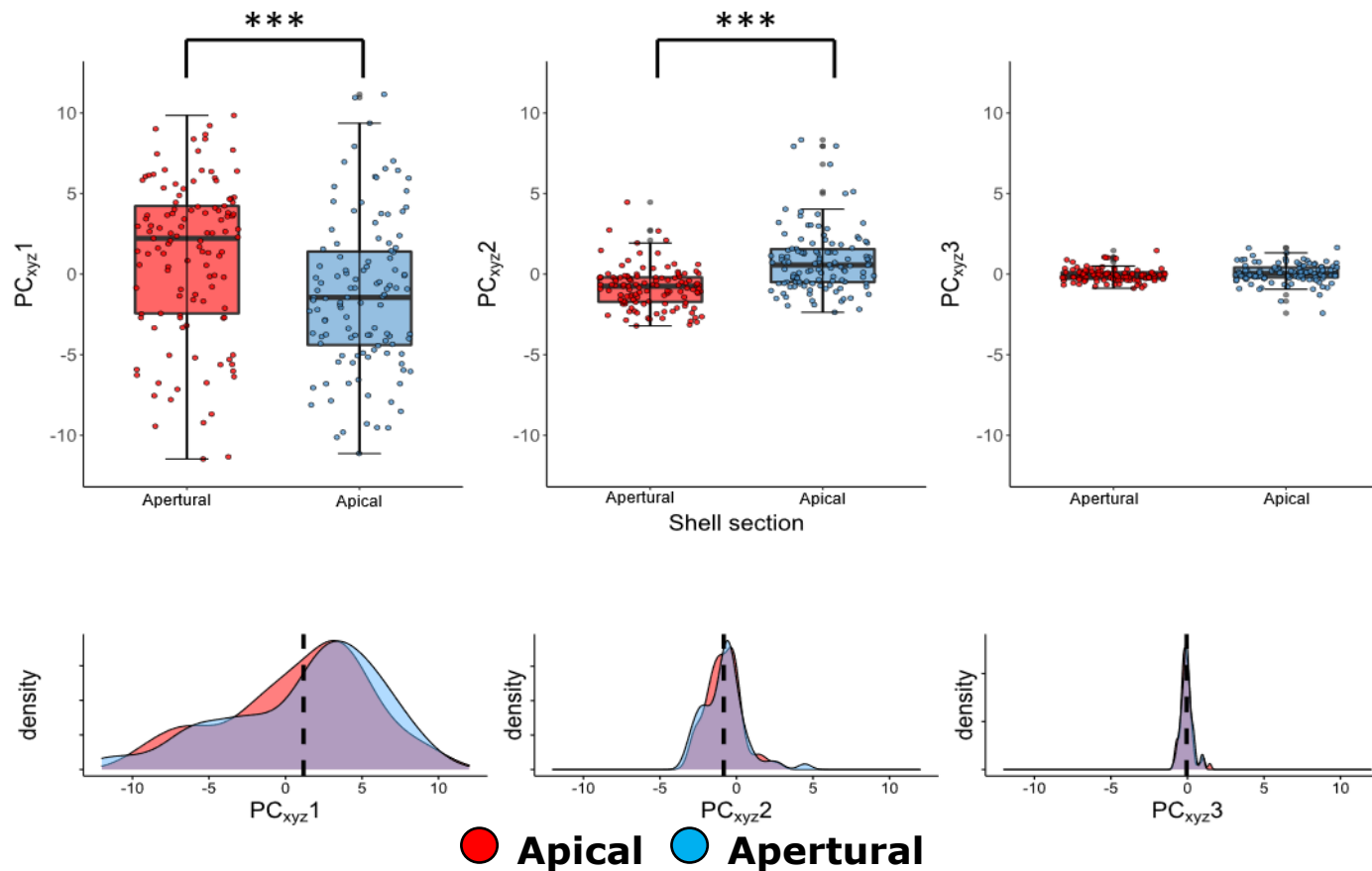
Figure 4.11 – differences in PC_{xyz} values between apical and apertural measurements of *Auriculella crassula.* Measurements of the shell sections differ significantly along $PC_{xyz}2$, where the apertural section of the shell has a lower $PC_{xyz}2$ value, so is lighter in colour than the apical section of the shell. None of the other axes differ significantly. Distributions shifted to centre around the same mean are also shown to display distribution of points along PC_{xyz} axes, none of which differ significantly between shell areas, suggesting that there is no difference in amount of variability of data.

176

4.4.2.3 *Auriculella pulchra*

Along the three PC_{xyz} axes, in *A. pulchra,* the range of variation is large, with a $PC_{xyz}1$ variability of 37 JNDs, $PC_{xyz}2$ range of 11 JNDs, and $PC_{xyz}3$ range of 4 JNDs. The apertural measurement of *A. pulchra* is slightly less variable than the variation in both apertural and apical measurements combined, with a $PC_{xyz}1$ range of 29 JNDs, and $PC_{xyz}2$ and 3 ranges of 9 and 2 JNDs. The apical measurement has similar variation along all axes apart from $PC_{xyz}1$, with a $PC_{xyz}1$ range of 32 JNDs, $PC_{xyz}2$ range of 9 JNDs, and a $PC_{xyz}3$ range of 2 JNDs.

Cluster analysis performed by Mclust on both the apical and apertural shell measurements resolved two clusters (VEE, ellipsoidal, equal volume and variable shape, BIC -2431.495, *P* < 0.001 compared to second best fitting model). The two clusters are unequal in size, with 61 measurements in the first cluster, and 151 in the second (**Table 4.4**). The second and third best fitting models were not significantly different from one another, and resolved 3 and 2 clusters (VEV, BIC -2433.382, *P* = 0.383 compared to third best model, and VEV, BIC -2436.849).

Table 4.4: *Auriculella pulchra* individuals placed in one of two clusters resolved by Mclust algorithms, grouped according to location of shell measurement (either apical or apertural section of shell). Numbers in italics represent individuals with two shell measurements which fall into the same cluster.

		Apical		
		Cluster 1	**Cluster 2**	**Total**
Apertural	**Cluster 1**	*16*	3	**19**
	Cluster 2	26	*61*	**87**
	Total	**42**	**64**	

Of the 106 individuals of *A. pulchra* measured, 71 had a difference of 3 or more JNDs between measurement points in 3-dimensional colour space, a proportion of 66.98% of all individuals (**Appendix 4.1**). 58 individuals differ by more than 3 JNDs along $PC_{xyz}1$, 15 along $PC_{xyz}2$, and 0 individuals had a difference between points of 3 or more JNDs along $PC_{xyz}3$. Of the 58 individuals which differed by 3 JND units along $PC_{xyz}1$, 9 of these also differed along $PC_{xyz}2$.

A 3-dimensional peacock's test indicated that the measurements from the apex and aperture of shells of *Auriculella pulchra* are not equally distributed in 3D colour space (xyz coordinates) ($D = 0.359$, $P = 0.00008$) (**Figures 4.12, 4.13**). When PC_{xyz} values are shifted to centre around the

same mean, Kolmogorov-Smirnov tests indicate that the distributions of all three PC_{xyz} axes do not vary between species (D = 0.066, P = 0.975; D = 0.169, P = 0.094; D = 0.179, P = 0.066) (**Figure 4.14**), suggesting no difference in the variability of points along any of the three axes. When means are not shifted, distributions are significantly different for all PC_{xyz} axes (D = 0.245, P = 0.003; D = 0.274, P = 0.0007; D = 0.255, P = 0.002). GLMMs indicate that $PC_{xyz}1$ and 2 are significantly different from one another between species (χ^2 = 13.244, df = 1, P = 0.0003; χ^2 = 43.456, df = 1, P = 4.336e-11), but $PC_{xyz}3$ is not (χ^2 = 1.856, df = 1, P = 0.173). $PC_{xyz}1$ and 2 are both higher on average in apical shell measurements, indicating that the apical area of shells of *A. pulchra* are both more reflective and darker than the apertural measurements of the same shell.

The average distance between all individuals is greater in both the apical and apertural areas of the shell than the average distance between two parts of an individual shell in *Auriculella pulchra* (**Appendix 4.1**)*.* The average distance in JNDs between two parts of the same shell is 4.419, the average distance between points of the apical measurements is 6.617, and the average distance between measurements of the apertural measurements is 5.982. The same is true of $PC_{xyz}1$ and $PC_{xyz}2$; along $PC_{xyz}1$, the average difference between the apical and apertural measurements of a single shell is 3.761 JNDs, between apical measurements is 5.536, and between apertural measurements is 5.332. Along $PC_{xyz}2$ the average distance between paired shell measurements is 1.611 JNDs, the average distance between all apical measurements is 2.462, and the average distance between apertural measurements is 1.677. The distance between points along $PC_{xyz}3$ is greater in the apical section of the shell (0.627) than the average distance between pairwise measurements (0.441), but slightly lower in the apertural section of the shell (0.404)
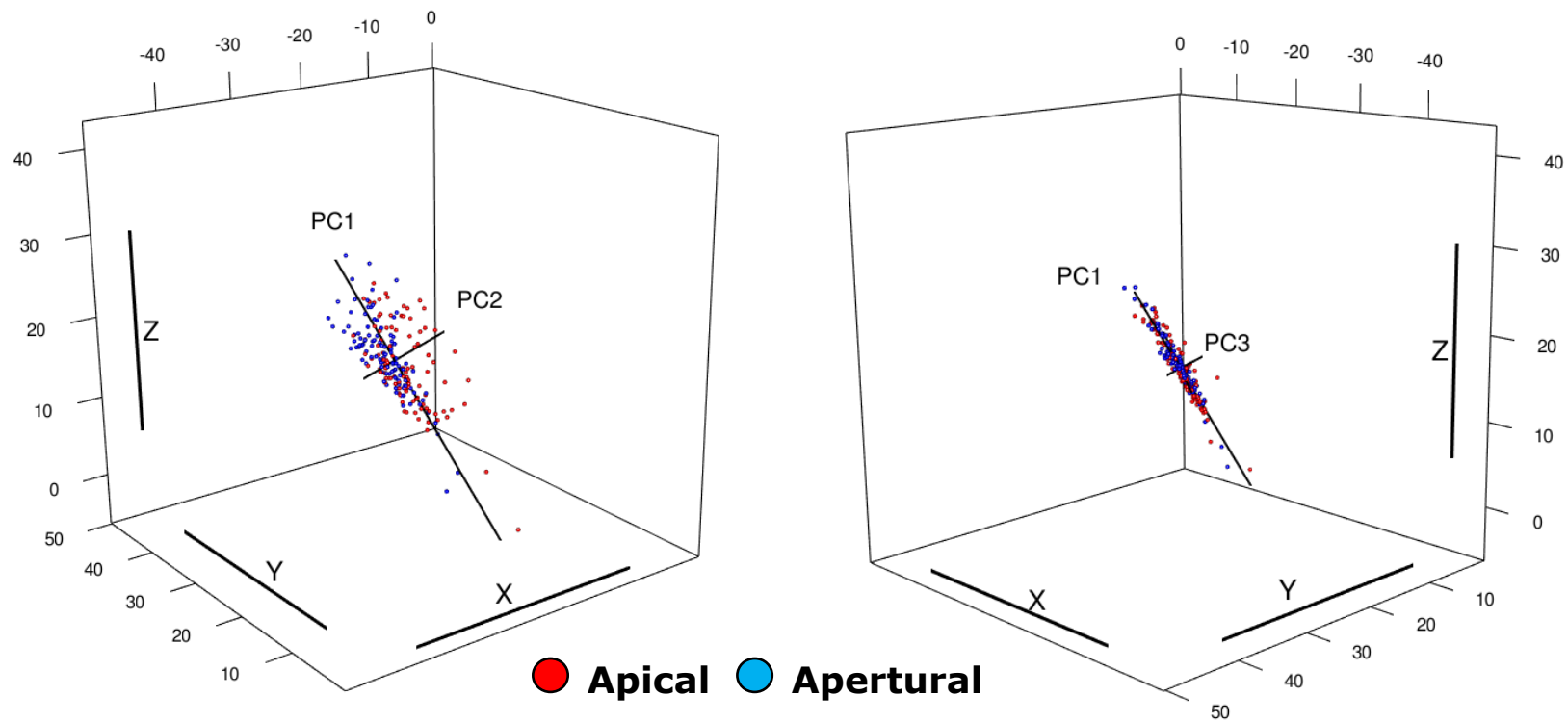
Figure 4.12 – 3D representation of location of all measurements of *Auriculella pulchra* in tetrachromatic colour space. Red points represent measurements from the apical section of the shell, and blue points show measurements from the apertural section of the shell. PC_{xyz} axes are shown. Figure in two orientations for clarity.
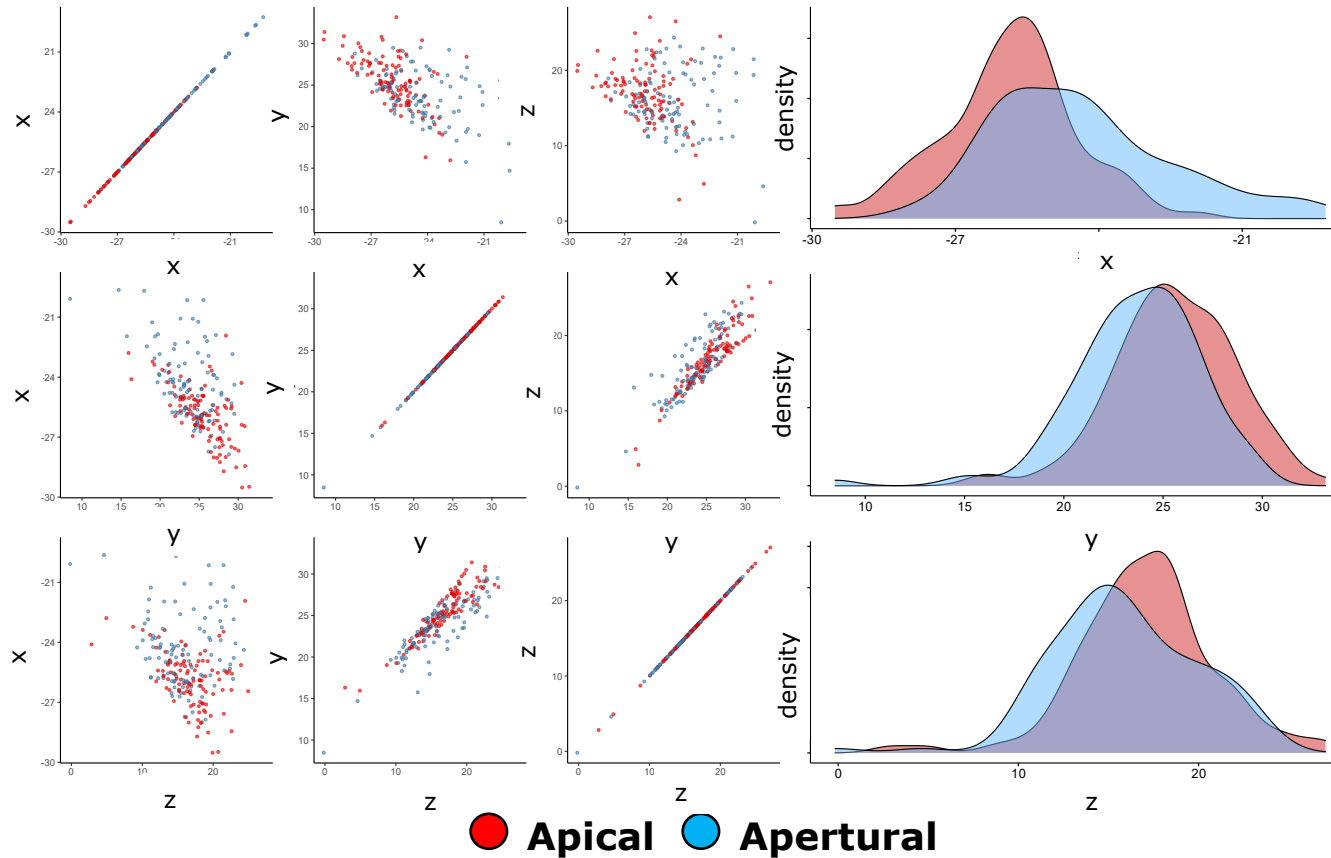
Figure 4.13 – 2D representation of location of all measurements of *Auriculella pulchra* in tetrachromatic colour space, and associated density plots along each axis (xyz). Red points/plots represent measurements from the apical section of the shell, and blue points/plots show measurements from the apertural section of the shell.
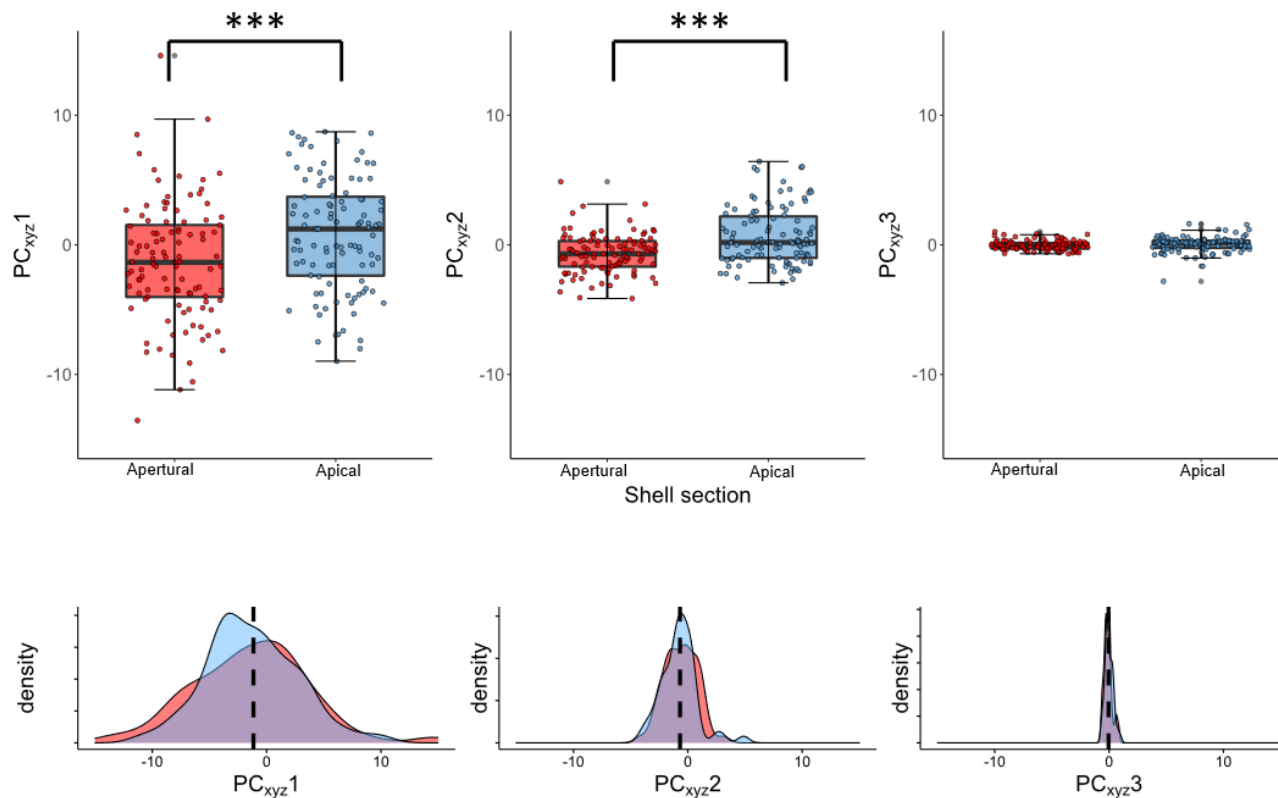
Figure 4.14 – differences in PC_{xyz} vales between apical and apertural measurements of *Auriculella pulchra.* Measurements of the shell sections differ significantly along $PC_{xyz}1$ and 2, where the apertural section of the shell has a lower $PC_{xyz}2$ value, so is both less reflective and lighter in colour than the apical section of the shell. $PX_{xyz}3$ does not differ significantly between shell sections. Distributions shifted to centre around the same mean are also shown to display distribution of points along PC_{xyz} axes, none of which differ significantly between shell areas, suggesting that there is no difference in amount of variability of data.

4.4.2.4 *Auriculella uniplicata*

The range of variation present along each axis of variation in *Auriculella uniplicata*, like the other three species, is large with a $PC_{xyz}1$ variability of 41 JNDs, $PC_{xyz}2$ range of 13 JNDs, and $PC_{xyz}3$ range of 6 JNDs. The apertural measurement of *A. uniplicata* is slightly less variable than the overall variability, with a $PC_{xyz}1$ range of 28 JNDs, and $PC_{xyz}2$ and 3 ranges of 8 and 2 JNDs. The apical measurement has a larger range of variation along all axes, with a $PC_{xyz}1$ range of 41 JNDs, $PC_{xyz}2$ range of 13 JNDs, and a $PC_{xyz}3$ range of 6 JNDs.

Cluster analysis on the apical and apertural shell measurements combined revealed that the best fitting model resolved four clusters (VEE, ellipsoidal, equal shape and orientation, BIC -2696.256, $P < 0.001$ compared to second best fitting model). Three of the four clusters are roughly equal in size, with a smaller second cluster (**Table 4.5**). The first cluster contains 79 measurements, the second contains 14, and the third and fourth clusters contain 68 and 73 measurements. The second and third best fitting models both resolved 3 clusters (VEE, BIC -2696.370, $P < 0.001$ compared to third best model, and VEV, BIC -2700.589).

Table 4.5: *Auriculella uniplicata* individuals placed in one of four clusters resolved by Mclust algorithms, grouped according to location of shell measurement (either apical or apertural). Numbers in italics represent individuals with two shell measurements which fall into the same cluster.

Apical

		Cluster 1	Cluster 2	Cluster 3	Cluster 4	Total
Aperutral	**Cluster 1**	*17*	3	7	21	**48**
	Cluster 2	0	*1*	1	0	**2**
	Cluster 3	12	6	*15*	11	**44**
	Cluster 4	2	2	1	*18*	**23**
	Total	**31**	**12**	**24**	**50**	

Of the 117 individuals of *A. uniplicata* measured, 73 had a difference of 3 or greater JNDs between measurement points in 3-dimensional colour space, a proportion of 62.39% of all individuals (**Appendix 4.1**). 58 individuals differ by more than 3 JNDs in $PC_{xyz}1$, 22 in $PC_{xyz}2$, and 1 individual had a difference in points of 3 or more JNDs in $PC_{xyz}3$. Of those individuals which differed along $PC_{xyz}1$, 13 of these also differed along $PC_{xyz}2$, and a single individual differed along both $PC_{xyz}1$ and $PC_{xyz}3$. No individuals differed by more than 3 JND units along all three axes of variation.

The average distance between all individuals is greater in both the apical and apertural areas of the shell than the average distance between two measurements of an individual shell in *Auriculella uniplicata.* The average distance in JNDs between two parts of the same shell is 4.521, the average distance between apical measurement points is 6.796, and the average distance between apertural measurements is 5.962. The same is true of $PC_{xyz}1$, along which the average difference between the apical and apertural measurements of a single shell is 3.701 JNDs, between apical measurements is 5.644, and between all measurements of the apertural section of the shell is 5.446. Along $PC_{xyz}2$ the average distance between paired shell measurements is 1.851 JNDs, the average distance between all apical measurements of the shell is larger than this at 2.615, and the average distance between apertural measurements is smaller than the average distance between paired measurements, at 1.465 JNDs. The same is true of points along $PC_{xyz}3$, where the average distance between paired measurements belonging to the same snail is 0.506 JNDs, the average distance between all apical measurements is 0.699, and the average position along $PC_{xyz}3$ differs by 0.391 JNDs between all apertural measurements.

A 3-dimensional peacock's test indicated that apical and apertural measurements of shells of *Auriculella uniplicata* are not equally distributed in 3D colour space (xyz coordinates) (D = 0.479, P = 0.00001) (**Figures 4.15, 4.16**). When PC_{xyz} values are shifted to centre around the same mean, Kolmogorov-Smirnov tests indicate that the distributions of $PC_{xyz}1$ and 3 do not vary between species (D = 0.085, P = 0.786; D = 0.171, P = 0.066), but the distribution of points along $PC_{xyz}2$ is different (D = 0.239, P = 0.002) (**Figure 4.17**). When means are not shifted, distributions are equal between top and bottom measurements in $PC_{xyz}1$ (D = 0.068, *P* = 0.947), but significantly different for $PC_{xyz}2$ and 3 (D = 0.333, P = 0.000004; D = 0.325, P = 0.000008). GLMMs indicate that the mean of $PC_{xyz}1$ does not differ between top and bottom measurements, but $PC_{xyz}2$ and 3 are significantly different from one another between

parts of the shell ($PC_{xyz}1$ $\chi^2 = 0.155$, df = 1, P = 0.694; $PC_{xyz}2$ $\chi^2 = 38.9$, df = 1, P = 4.46e-10; $PC_{xyz}3$ $\chi^2 = 12.379$, df = 1, P = 0.0004). Both $PC_{xyz}2$ and 3 are higher on average in apical measurements of shells, indicating that the apex of an *A. uniplicata* shell is both darker and more brown than the apertural measurement, although the difference in average $PC_{xyz}3$ position occurs over a single JND unit, so is unlikely to be perceptible by a predator.
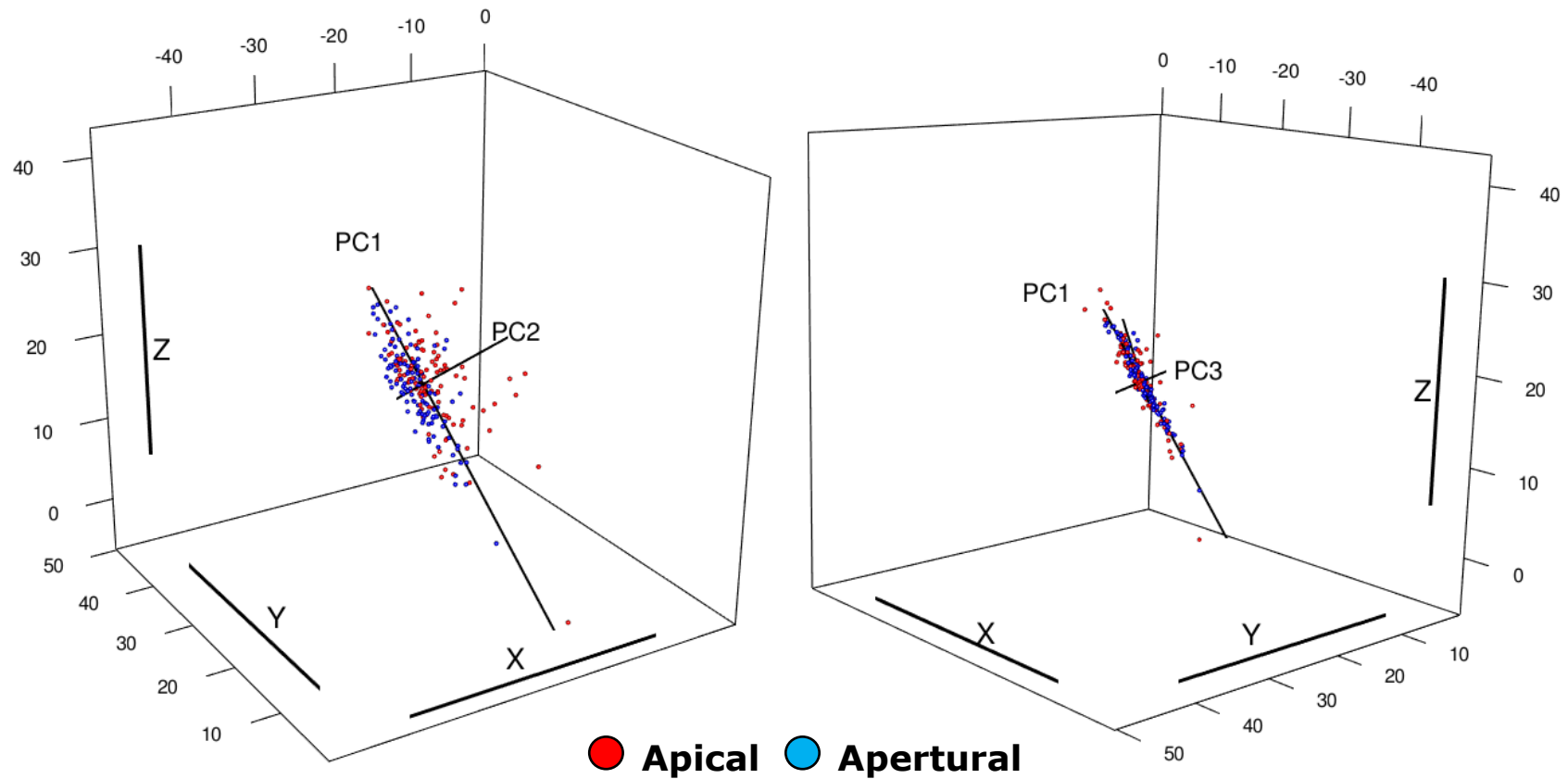
Figure 4.15 – 3D representation of location of all measurements of *Auriculella uniplicata* in tetrachromatic colour space. Red points represent measurements from the apical section of the shell, and blue points show apertural measurements. PC$_{xyz}$ axes are shown. Figure in two orientations for clarity.
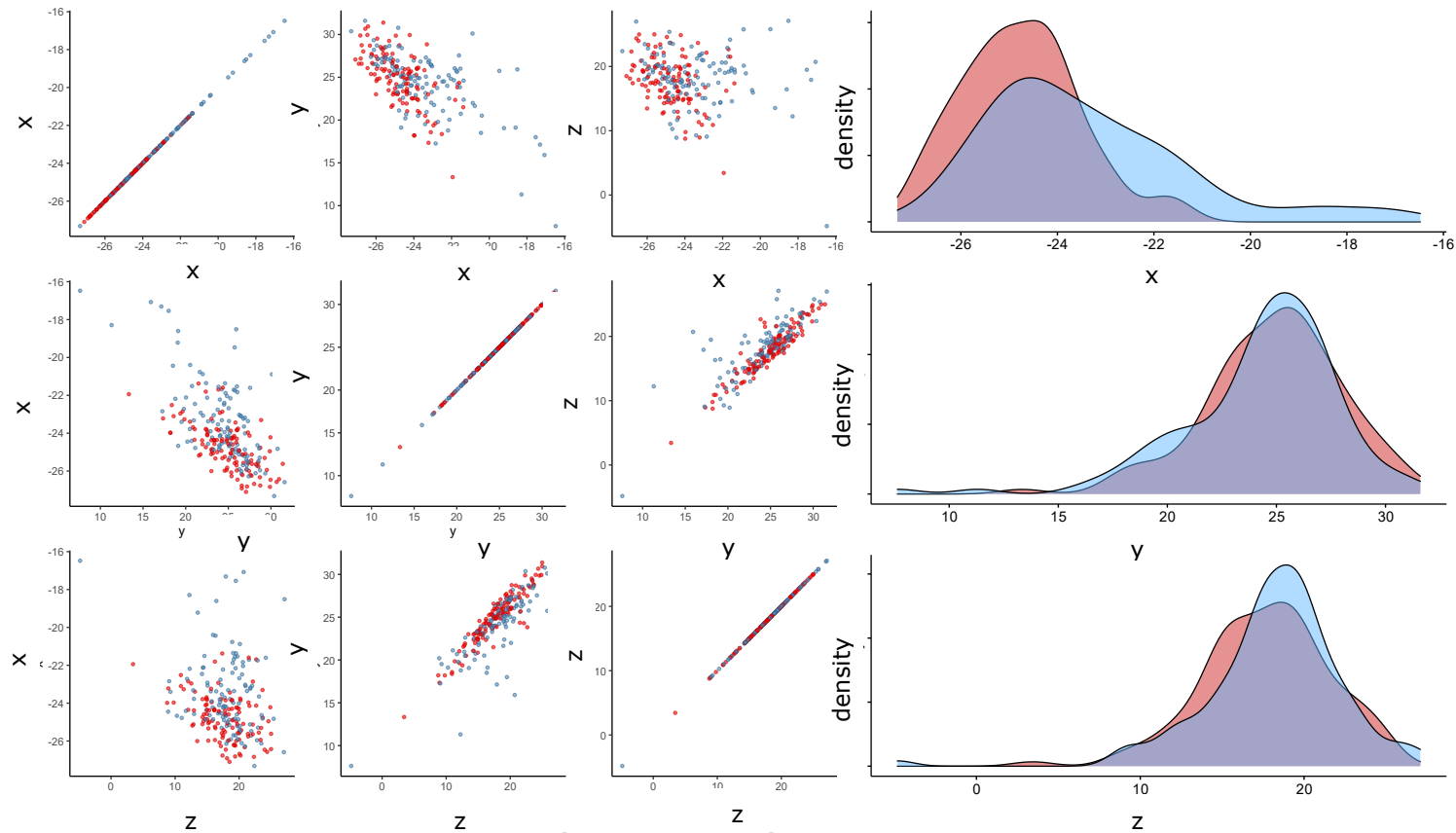
Figure 4.16 – 2D representation of location of all measurements of *Auriculella uniplicata* in tetrachromatic colour space, and associated density plots along each axis (xyz). Red points/plots represent measurements from the apical section of the shell, and blue points/plots show measurements from the apertural section of the shell.

188
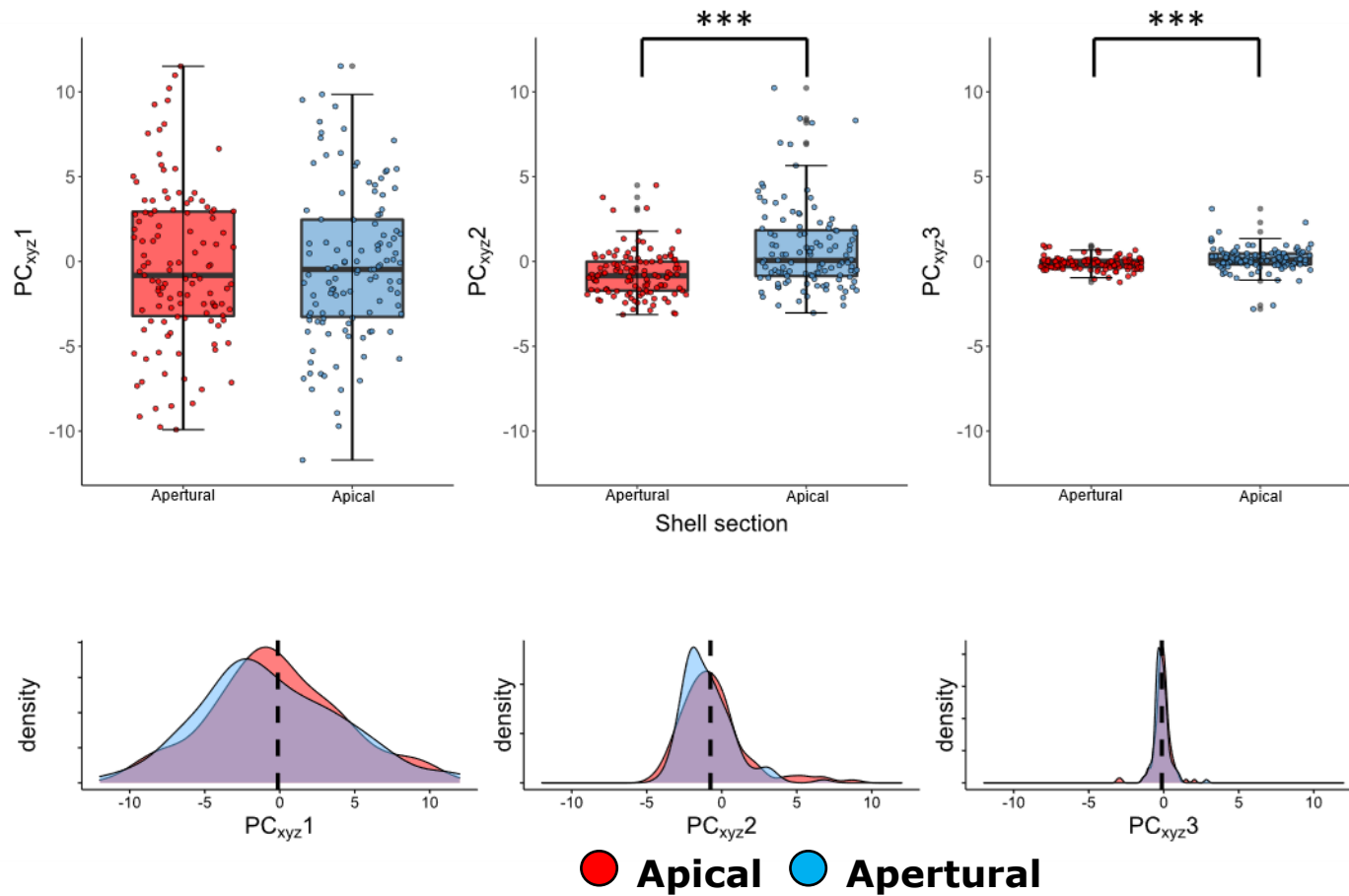
Figure 4.17 – differences in PC$_{xyz}$ vales between apical and apertural measurements of *Auriculella uniplicata.* Measurements of the apical and apertural sections of shells differ significantly along PC$_{xyz}$2 and 3, where the aperutral section of the shell has lower PC$_{xyz}$2 and 3 values, so is both lighter in colour and more yellow toned than the apical section of the shell. PC$_{xyz}$1 does not differ significantly between shell sections. Distributions shifted to centre around the same mean are also shown to display distribution of points along PC$_{xyz}$ axes, none of which differ significantly between shell areas, suggesting that there is no difference in amount of variability of data.

4.4.3 Between species variation

The variation present between the analyses of the different species is presented in Table **4.6**. There are varying numbers of clusters resolved by the Gaussian finite mixture modelling performed with Mclust, and perhaps unsurprisingly, the number of individuals with both measurements in the same cluster is associated with this. Where there are small numbers of clusters there seem to also be a high percentage of individuals with both measurements assigned to the same cluster. The proportion of individuals with both shell measurements in the same cluster is not necessarily reflected in the proportion of individuals with apical and apertural shell segments which are indistinguishable to an avian predator, where with the exception of *A. auricula*, there is no large discrepancy between species. The PC_{xyz} axes ranges are different between species along $PC_{xyz}1$, which ranges from 24 JNDs in *A. auricula* to 41 JNDs in *A. uniplicata*, suggesting a greater variation in shell reflectivity in *A. uniplicata*. This range of differences is not seen in $PC_{xyz}2$ and 3, which are similar in magnitude across all four species, although $PC_{xyz}3$ has a range in *A. uniplicata* of 6, double that seen in *A. auricula*, so whilst the magnitude is not vastly different, it is a relatively large change.

All four species have a significantly different distribution of points between apical and apertural measurements in 3D colour space according to Peacock's tests, and all four species vary significantly in colour space occupied along $PC_{xyz}2$ between shell measurements. *A. crassula* and *A. pulchra* vary significantly between apical and apertural measurements along $PC_{xyz}1$, and only *A. uniplicata* varies along $PC_{xyz}3$. When distributions along each PC_{xyz} axis is considered independently of the rest of the variation, none of the species display differences in the distribution of apical and apertural measurements, with the exception of *A. uniplicata*, where $PC_{xyz}2$ has a wider distribution in apical measurements than apertural.

Table 4.6: Summary of results from **Section 4.4.2** detailing differences between species in the size of variation present along each of the three PC_{xyz} axes, number of clusters resolved in Mclust analysis, and percentage of individuals with apical and apertural shell measurements in the same cluster, the percentage of individuals from each species with apical and apertural shell colour measurements which are indistinguishable from one another by an avian predator (with a conservative discrimination threshold of 3 JNDs), and results of Peacocks tests, GLMMs, and Kolmogorov-smirnov tests along each of the three PC_{xyz} axes of variation. A tick (✓) symbol indicates a significant difference, where a cross (x) indicates no significant difference in each statistical analysis.

Species	n	Nº clusters	% same cluster	% same JNDs	Range $PC_{xyz}1$	Range $PC_{xyz}2$	Range $PC_{xyz}3$	Peacocks 3D distribution	GLMM per PC_{xyz} axis			K-S per PC_{xyz} axis		
A. auricula	71	2	83.09	53.54	24	11	3	✓	x	✓	x	x	x	x
A. crassula	118	3	48.31	67.72	31	12	4	✓	✓	✓	x	x	x	x
A. pulchra	106	2	72.64	66.98	37	11	4	✓	✓	✓	x	x	x	x
A. uniplicata	117	4	43.59	62.39	41	13	6	✓	x	✓	✓	x	✓	x

4.4.3.1 Apical measurements

GLMMs indicate that there are no differences between species in any of the three PC_{xyz} axes (χ^2 = 2.991, df = 3, *P* = 0.393; χ^2 = 0.454, df = 3, *P* = 0.929; χ^2 =1.308, df = 3, *P* = 0.727) (**Figure 4.18**). Generally, this is also reflected in pairwise comparisons between species for all three principal components (**Table 4.7**) – there is no difference between any species in PC_{xyz} axes in the apical measurement of shells. K-sample Anderson-Darling tests show that distributions between species are not all equal along $PC_{xyz}1$ (AD = 12.34, *P* = 0.00007), but are equal along $PC_{xyz}2$ and 3 (AD = 2.214, *P* = 0.691; AD = 2.540, *P* = 0.567). Subsequent pairwise Anderson-Darling all pairs comparison testing between all possible species pairs (**Table 4.8**) suggests that along $PC_{xyz}1$, *A. auricula* and *A. crassula* have significantly different distributions of points, as do *A. crassula* and *A. pulchra*, and *A. crassula* and *A. uniplicata*. The distribution of *A. crassula* along $PC_{xyz}1$ is significantly different from all three other species, however these do not differ from one another. The distributions of all species do not differ along either of the two other PC_{xyz} axes.
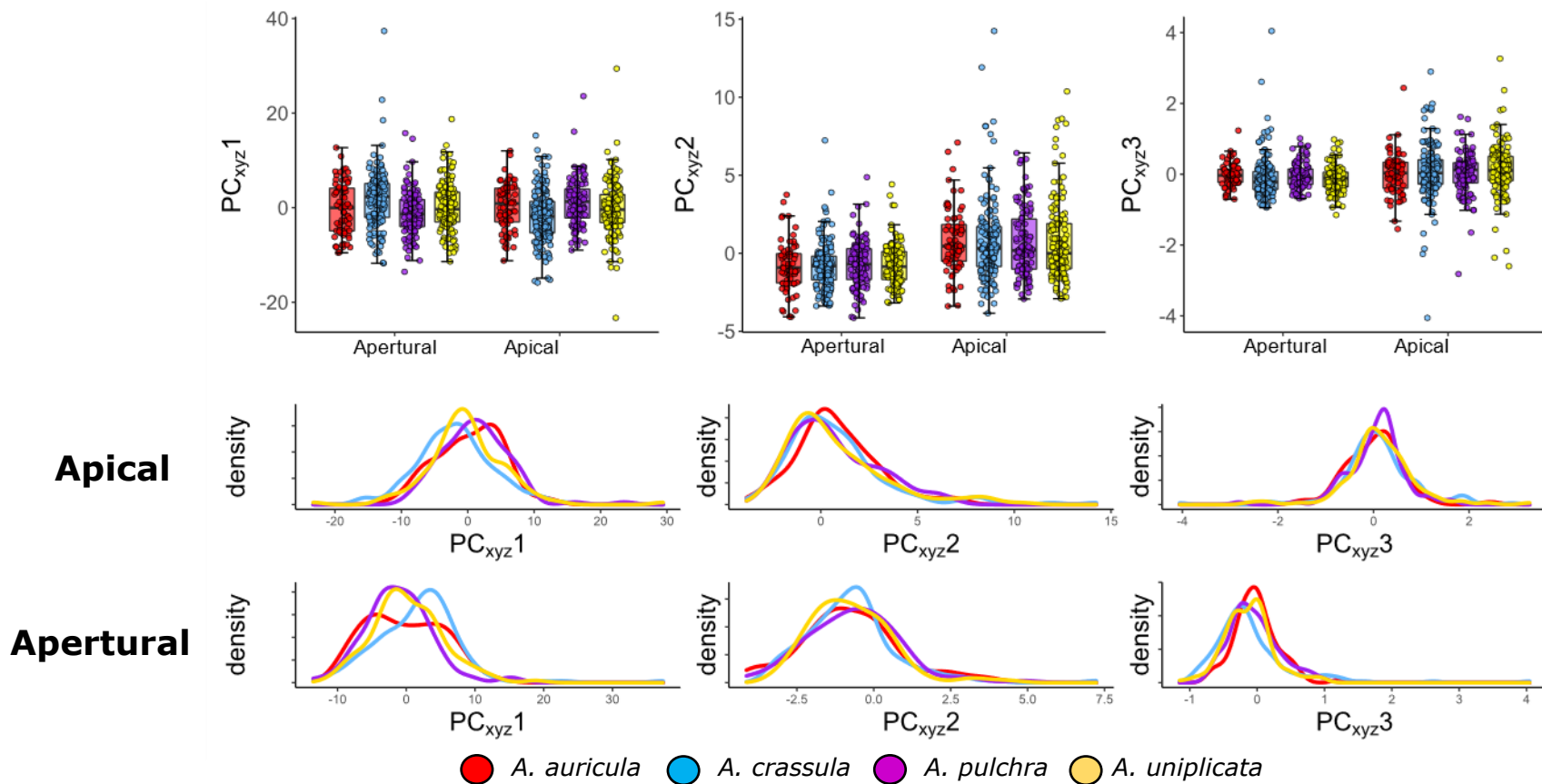
Figure 4.18 – differences in PC$_{xyz}$ vales between apical and apertural measurements of all species of *Auriculella.* No pairwise comparisons suggest significant differences between species along any of the three PC$_{xyz}$ axes in either the apical or apertural sections of the shell, except for comparison between *A. crassula* and *A. pulchra* along PC$_{xyz}$2, where *A. crassula* has a significantly lower value, suggesting a lighter shell. Distributions of points along PC$_{xyz}$ axes are also shown, several of which differ significantly from one another in pairwise Anderson-Darling tests. *A. auricula* is represented in red, *A. crassula* in blue, *A. pulchra* in purple, and *A. uniplicata* in yellow.

Table 4.7 – Results of pairwise least-square means with Tukey adjustments for multiple comparisons performed between the apical measurements of pairs of species to elucidate pairwise differences in colour along the three PC_{xyz} axes between species. There were no significant differences in occupied colour space between any of the possible combinations of species pairs along any of the three PC_{xyz} axes.

	Comparison		*Estimate*	*SE*	*df*	*z-ratio*	*p-value*
$PC_{xyz}1$	*auricula*	*crassula*	1.096	1.46	38.0	0.753	0.8749
	auricula	*pulchra*	-0.811	1.49	35.1	-0.543	0.9477
	auricula	*uniplicata*	0.918	1.42	38.1	0.646	0.9164
	crassula	*pulchra*	-1.907	1.29	37.9	-1.478	0.4605
	crassula	*uniplicata*	-0.179	1.07	83.7	-0.168	0.9983
	pulchra	*uniplicata*	1.728	1.25	38.1	1.382	0.5180
$PC_{xyz}2$	*auricula*	*crassula*	0.0371	0.688	38.1	0.054	0.9999
	auricula	*pulchra*	0.3535	0.707	34.7	0.500	0.9585
	auricula	*uniplicata*	0.2046	0.672	37.8	0.304	0.9900
	crassula	*pulchra*	0.3163	0.610	38.0	0.519	0.9541
	crassula	*uniplicata*	0.1674	0.492	92.8	0.340	0.9864
	pulchra	*uniplicata*	-0.1489	0.591	37.7	-0.252	0.9943
$PC_{xyz}3$	*auricula*	*crassula*	-0.0791	0.1150	33.9	-0.688	0.9009
	auricula	*pulchra*	-0.0278	0.1194	41.2	-0.233	0.9955
	auricula	*uniplicata*	-0.1062	0.1150	40.6	-0.924	0.7925
	crassula	*pulchra*	0.0514	0.1017	33.2	0.505	0.9573
	crassula	*uniplicata*	-0.0271	0.0949	41.8	-0.285	0.9918
	pulchra	*uniplicata*	-0.0784	0.1017	42.0	-0.772	0.8668

Table 4.8 – Results of pairwise Anderson-Darling all pairs comparison tests performed between the apical measurements of pairs of species to determine pairwise differences in distributions of data in all possible combinations of the four species of *Auriculella*. There were no significant differences in distributions between any of the possible combinations of species pairs along any of the three PC_{xyz} axes.

	Comparison		T2N Value	p-value
$PC_{xyz}1$	*auricula*	*crassula*	4.777	0.022
	auricula	*pulchra*	-0.181	0.650
	auricula	*uniplicata*	0.084	0.650
	crassula	*pulchra*	12.107	0.00004
	crassula	*uniplicata*	3.597	0.047
	pulchra	*uniplicata*	1.958	0.151
$PC_{xyz}2$	*auricula*	*crassula*	-0.179	0.437
	auricula	*pulchra*	0.070	0.330
	auricula	*uniplicata*	0.721	0.165
	crassula	*pulchra*	-0.678	0.762
	crassula	*uniplicata*	-0.806	0.861
	pulchra	*uniplicata*	-0.760	0.826
$PC_{xyz}3$	*auricula*	*crassula*	-0.071	0.387
	auricula	*pulchra*	-0.765	0.830
	auricula	*uniplicata*	0.278	0.263
	crassula	*pulchra*	0.061	0.333
	crassula	*uniplicata*	-0.576	0.684
	pulchra	*uniplicata*	-0.186	0.440

4.4.3.2 Apertural measurements

There is a difference in colour space occupied between species along $PC_{xyz}1$ (χ^2 = 11.011, df = 3, P = 0.012), but there are no differences between species in $PC_{xyz}2$ or 3 (χ^2 = 0.581, df = 3, P = 0.901; χ^2 = 0.214, df = 3, P = 0.239) (**Figure 4.18**). Pairwise comparisons between species are non-significant, except for $PC_{xyz}1$ comparisons between *A. crassula* and *A. pulchra*, where *A. crassula* has a lower $PC_{xyz}1$ value than *A. pulchra*, suggesting a difference in reflectiveness of the shell (**Table 4.9**). K-sample Anderson-Darling tests show that distributions between species are not all equal along $PC_{xyz}1$ or 3 (AD = 13.160, P = 0.00003; AD = 9.288, P = 0.002), but are equal along $PC_{xyz}2$ (AD = 2.037, P = 0.759). Pairwise Anderson-Darling all pairs comparison testing between all possible species pairs (**Table 4.10**) suggests that along $PC_{xyz}1$, the distribution of *A. crassula* is significantly different from all three other species, as are the distributions of *A. pulchra* and *A. uniplicata*. Distributions of all species do not differ along $PC_{xyz}2$. Distributions along $PC_{xyz}3$ show differences between all species combinations except *A. pulchra* and *A. auricula*, and *A. pulchra* and *A. uniplicata*, and *A. crassula* and *A. uniplicata*.

Table 4.9 – Results of pairwise least-square means with Tukey adjustments for multiple comparisons performed between the apertural measurements of pairs of species to elucidate pairwise differences in colour along the three PC_{xyz} axes between species. significant differences in occupied colour space are highlighted in bold.

	Comparison		Estimate	SE	df	z-ratio	p-value
$PC_{xyz}1$	*auricula*	*crassula*	-2.326	1.38	36.9	-1.684	0.347
	auricula	*pulchra*	1.078	1.41	34.7	0.763	0.870
	auricula	*uniplicata*	0.219	1.35	37.5	0.163	0.998
	crassula	*pulchra*	3.404	1.22	36.9	2.781	**0.041**
	crassula	*uniplicata*	2.546	1.03	75.2	2.469	0.073
	pulchra	*uniplicata*	-0.859	1.19	37.5	-0.724	0.887
$PC_{xyz}2$	*auricula*	*crassula*	-0.113	0.414	38.1	-0.273	0.993
	auricula	*pulchra*	-0.028	0.426	34.6	-0.065	0.999
	auricula	*uniplicata*	0.096	0.404	37.8	0.238	0.995
	crassula	*pulchra*	0.086	0.367	38.1	0.233	0.996
	crassula	*uniplicata*	0.209	0.294	95.8	0.712	0.892
	pulchra	*uniplicata*	0.124	0.356	37.6	0.348	0.985
$PC_{xyz}3$	*auricula*	*crassula*	0.055	0.091	35.6	0.609	0.929
	auricula	*pulchra*	0.026	0.093	37.6	0.275	0.993
	auricula	*uniplicata*	0.144	0.089	38.9	1.616	0.382
	crassula	*pulchra*	-0.029	0.080	35.3	-0.370	0.982
	crassula	*uniplicata*	0.089	0.073	51.8	1.223	0.615
	pulchra	*uniplicata*	0.119	0.079	39.6	1.509	0.442

Table 4.10 – Results of pairwise Anderson-Darling all pairs comparison tests performed between the apertural measurements of pairs of species to determine pairwise differences in distributions of data in all possible combinations of the four species of *Auriculella*. Significant differences are highlighted in bold.

	Comparison		T2N Value	p-value
$PC_{xyz}1$	auricula	crassula	3.163	**0.0171**
	auricula	pulchra	1.386	0.086
	auricula	uniplicata	0.542	0.199
	crassula	pulchra	13.713	**0.00001**
	crassula	uniplicata	4.205	**0.007**
	pulchra	uniplicata	2.066	**0.046**
$PC_{xyz}2$	auricula	crassula	-0.423	0.577
	auricula	pulchra	-0.749	0.818
	auricula	uniplicata	-0.489	0.622
	crassula	pulchra	-0.179	0.437
	crassula	uniplicata	-0.580	0.687
	pulchra	uniplicata	-0.176	0.436
$PC_{xyz}3$	auricula	crassula	7.013	**0.0006**
	auricula	pulchra	-0.127	0.412
	auricula	uniplicata	2.534	**0.029**
	crassula	pulchra	4.036	**0.008**
	crassula	uniplicata	1.599	0.070
	pulchra	uniplicata	0.881	0.140

Perhaps unsurprisingly, species with more clusters tend to have fewer individuals with both measurements belonging to a single cluster. This is not reflected in the percentage of individuals whose top and bottom measurements are outside of the distance threshold of 3 JNDs, suggesting that measurements belonging to different clusters is not an indication of colour differences within individuals, but it does give an idea of what variation might look like within three-dimensional colour space, and which parts of a shell occupy what colour space.

4.4.4 Between population variation

Each of the four species display differing levels of variation between populations, often also differing in significance between comparisons of the top and the bottom of shells. In the 6 populations of *Auriculella auricula*, the first PC_{xyz} axis differed significantly between populations in both the apical and apertural measurements of the shell ($\chi^2 = 22.169$, df $= 5$, $P = 0.0005$; $\chi^2 = 14.066$, df $= 5$, $P = 0.015$), meaning that the saturation or dullness of the shell varies between populations. $PC_{xyz}2$ differs significantly between populations of *A. auricula* in the apical part of the shell, but not the apertural ($\chi^2 = 39.303$, df $= 5$, $P = 0.000002$; $\chi^2 = 8.764$, df $= 5$, $P = 0.119$), suggesting a difference in colour darkness unique to the apical part of the shell, and $PC_{xyz}3$ does not differ between populations in either part of the shells ($\chi^2 = 7.982$, df $= 5$, $P = 0.157$; $\chi^2 = 4.387$, df $= 5$, $P = 0.495$), suggesting no difference in how yellow toned either part of the shell is between populations.

The variation between populations in *Auriculella crassula* is somewhat different to that in *A. auricula* with all possible combinations of shell section and PC_{xyz} axes differing between populations. Across the 6 populations, the first PC_{xyz} axis differs in both the apical and apertural areas of the shell ($\chi^2 = 41.837$, df $= 5$, $P < 0.001$, 6.355e-8; $\chi^2 = 28,6$, df $= 5$, $P < 0.001$, 2.778e-5), suggesting a difference in the saturation or

shininess of the shell in both parts of the shell. The same was true of PC$_{xyz}$2 for both sections of shell (χ^2 = 14.528, df = 5, P = 0.013; χ^2 = 31.657, df = 5, P = 0.000007), suggesting a difference in darkness of shell colour between populations. Again, both parts of the shell occupied significantly different colour space between populations along PC$_{xyz}$3 (χ^2 = 20.136, df = 5, P = 0.001; χ^2 = 18.777, df = 5, P = 0.002), meaning that there is a difference in "yellowness" between populations of *A. crassula*.

Again, the variation between the 8 populations of *Auriculella pulchra* is different to the variation between populations of *A. auricula* and *A. crassula*. There is significant difference between populations both in the apical and apertural sections of the shell along PC$_{xyz}$1 (χ^2 = 15.299, df = 7, P = 0.032; χ^2 = 36.804, df = 7, P = 0.00005). The same is true of both parts of the shell along PC$_{xyz}$2 (χ^2 = 95.906, df = 7, P <2.2e-16; χ^2 = 48.835, df = 7, P = 2.445e-8). PC$_{xyz}$3 does not vary between populations of *A. pulchra* in either section of shells (χ^2 = 5.205, df = 7, P = 0.635; χ^2 = 26.720, df = 7, P = 0.0004).

In the 8 populations of *Auriculella uniplicata*, as in *A. pulchra*, there was a difference between populations in both the apical and apertural measurement of shells along PC$_{xyz}$1 (χ^2 = 28.135, df = 7, P = 0.0002; χ^2 = 17.844, df = 7, P = 0.013). The same was true of PC$_{xyz}$2 (χ^2 = 24.845, df = 7, P = 0.0008; χ^2 = 36.919, df = 7, P = 4.859e-9). There are no differences between populations of *A. uniplicata* in either section of the shell in PC$_{xyz}$3 (χ^2 = 7.603, df = 7, P = 0.369; χ^2 = 9.192, df = 7, P = 0.239).

4.4.5 Between island variation

Individual species were grouped according to their island localities, *Auriculella auricula* and *A. pulchra* are both endemic to Oahu, and *A. crassula* and *A. uniplicata* to Maui. In total, there are 177 individuals from

Oahu, and 235 from Maui. GLMMs on each PC_{xyz} axis along the apical measurement of shells suggest that there are no differences in any of the three PC_{xyz} axes between individuals on Oahu and Maui ($\chi^2 = 1.761$, df $= 1$, $P = 0.185$; $\chi^2 = 0.070$, df $= 1$, $P = 0.791$; $\chi^2 = 0.716$, df $= 1$, $P = 0.261$) (**Figure 4.19**). Kolmogorov-Smirnov tests also indicate that when data from both islands are shifted to centre around a single mean, there is no difference in the precise shape of distribution of points along any of the three PC_{xyz} axes, indicating no differences in variability of colour between islands (D = 0.099, $P = 0.276$; D = 0.077, $P = 0.592$; D = 0.100, $P = 0.426$). The same is true of all relationships between measurements taken from the apertural section of the shells, both in GLMMs ($\chi^2 = 1.634$, df $= 1$, $P = 0.201$; $\chi^2 = 0.0004$, df $= 1$, $P = 0.985$; $\chi^2 = 3.387$, df $= 1$, $P = 0.066$) and Kolmogorov-Smirnov tests (D = 0.074, $P = 0.643$; D = 0.081, $P = 0.524$; D = 0.048, $P = 0.97$), indicating that there is no difference in either distribution or mean of colour measurements along any PC_{xyz} axis between islands, in either the apical or apertural measurement location of shells.
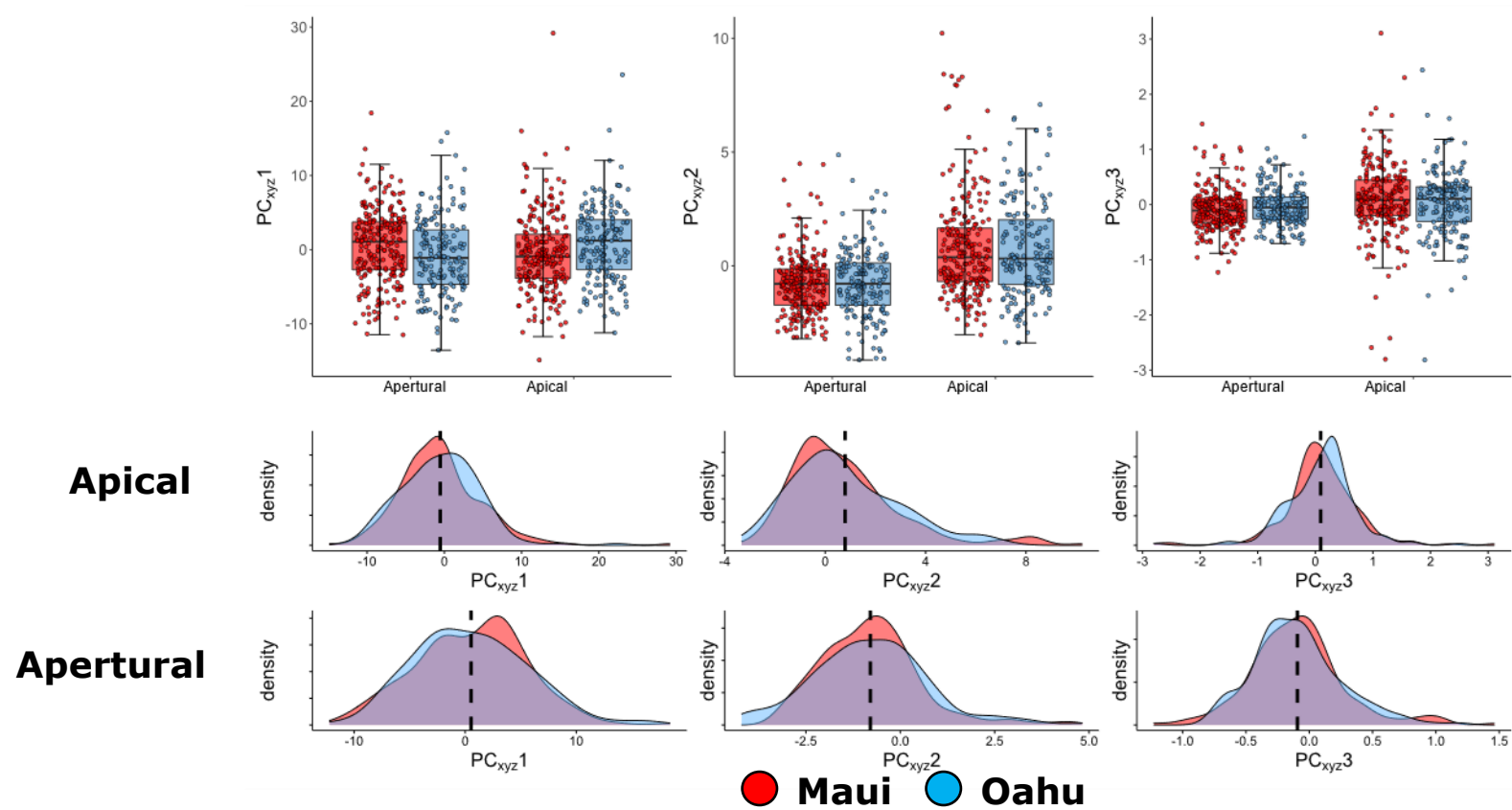
Figure 4.19 – differences in PC_{xyz} vales between both apical and apertural measurements of snail species according to endemic island. Snails from Maui (*A. crassula* and *A. uniplicata*) are represented in red, and species from Oahu (*A. auricula* and *A. pulchra*) in blue. There are no significant differences in colour space occupied between islands in measurements from the apical or apertural colour measurements of the shell along any of the three PC_{xyz} axes, and there is no difference in distributions of points along any of these axes in either shell section, suggesting that neither island has more variable phenotypes than the other.

4.4.6 Variation with chirality

GLMMs show that the apical section of the shell does not occupy different colour space along each of the three PC_{xyz} axes according to chirality (χ^2 = 0.024, df = 1, P = 0.877; χ^2 = 0.076, df = 1, P = 0.728; χ^2 = 0.387, df = 1, P = 0.534) (**Figure 4.20**). Despite the apical measurement of both sinistral and dextral individuals existing in the same colour space, a Peacock's test indicates that the points are not equally distributed in space according to their 3-dimensional xyz co-ordinates (D = 0.268, P = 0.003). Kolmogorov-Smirnov tests show that the distribution of points along the main axes of variation differs between chirality phenotypes along $PC_{xyz}1$ (D = 0.193, P = 0.008), but not PC_{xyz} 2 or 3 (D = 0.076, P = 0.788; D = 0.097, P = 0.501).

The same is true for the apertural section of the shell – sinistral and dextral individuals occupy the same colour space along each of the three axes of variation (χ^2 = 0.149, df = 1, P = 0.699; χ^2 = 0.125, df = 1, P = 0.723; χ^2 = 0.232, df = 1, P = 0.629) (**Figure 4.20**). Peacock's test indicates that as with the apical section of the shell, points are not equally distributed in xyz colour space (D = 0.223, P = 0.037). Despite this variation in 3-dimensional space, the distributions of points of individuals of different chiralities do not differ along each PC_{xyz} axis (D = 0.092, P = 0.562; D = 0.125, P = 0.204; D = 0.066, P = 0.907).
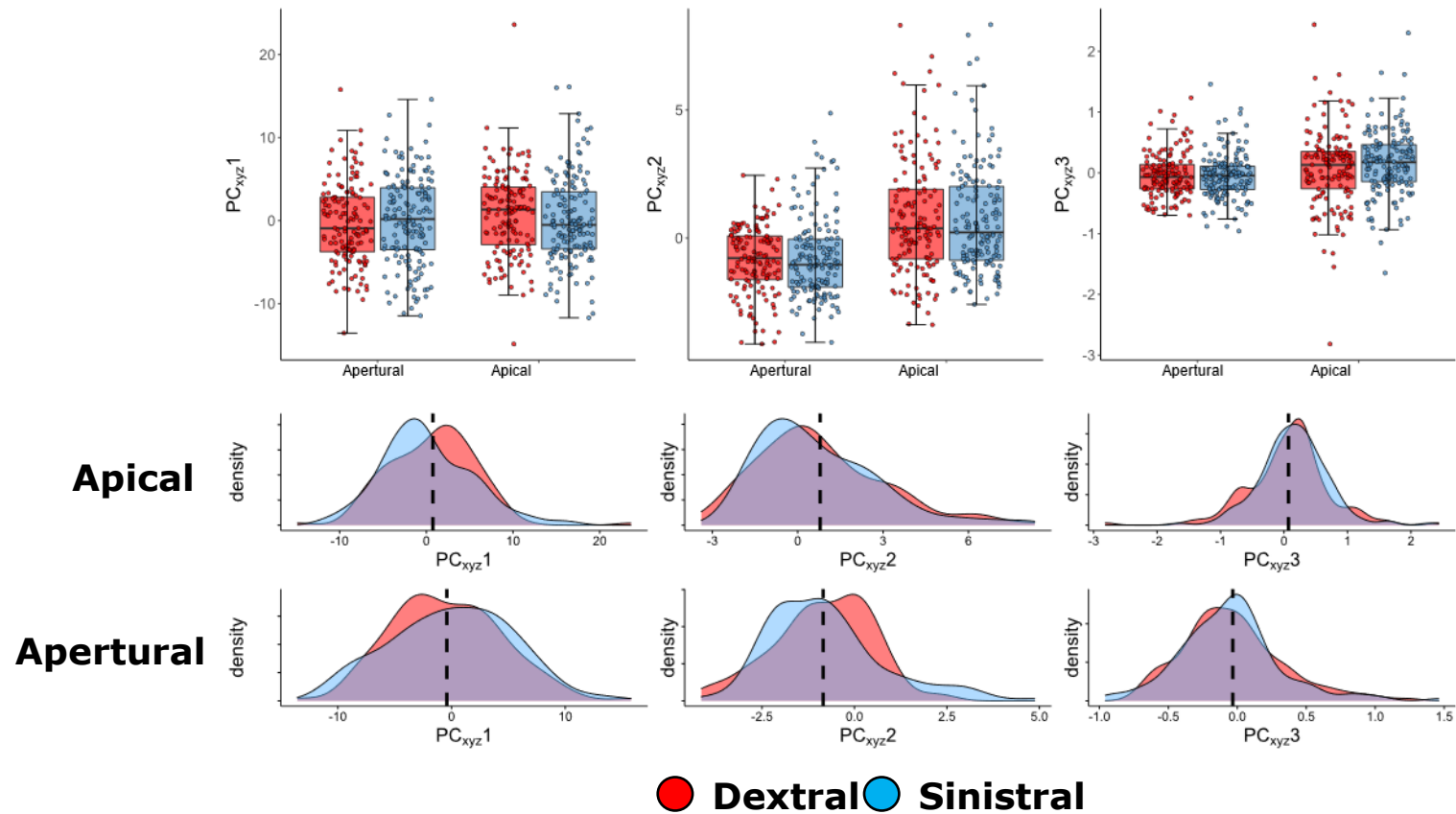
Figure 4.20 – differences in PC_{xyz} vales between both the apical and apertural measurements of *Auriculella* according to chirality. Dextral individuals are represented in red, and sinistral in blue. There are no significant differences in colour space occupied between islands in measurements from the apical or apertural section of the shell along any of the three PC_{xyz} axes, and there is no difference in distributions of points along any of these axes in either section of the shell, except for a significant difference in data distributions between sinistral and dextral shells along $PC_{xyz}1$ in the apical measurements of the shell. The shell measurements occupy the same colour space, but points are distributed differently within this space.

4.5 Discussion

4.5.1 Colour variation within individual shells:

Variation within individual shells is present in all four species considered. Differences between the apical and apertural sections of shells are highlighted by individuals falling into different clusters in 3-dimensional colour space, and by the Euclidean distances in JNDs both in colour space as a whole, and along each of the three axes of variation (**Table 4.6**). The magnitude of the variation decreases along all axes in all four species, although this is unsurprising as the amount of variation present in the data also declines with PC_{xyz} axis.

Differing numbers of clusters resolved and significant results of Peacock's tests in each species highlight the difference in data distributions in 3-dimensional colour space between species. GLMMs showed that apical area of shell is always darker on average than the apertural section of shell in all species (**Table 4.6, Figure 4.18**). It is possible that there is an adaptive reason for this darkening, such as habitat migration with age, and an inability to change embryonic phenotype. *Auriculella* snails resemble galls on the underside of leaves; the galls also darken towards their tip (**Figure 4.21**), and the divergence in colour down the shell may well be a form of mimicry or crypsis employed as an anti-predation strategy. Gall mimicry is also thought to occur in a species of orb weaving spider *Poltys stygius*, though there have been limited studies investigating this (Smith 2005).
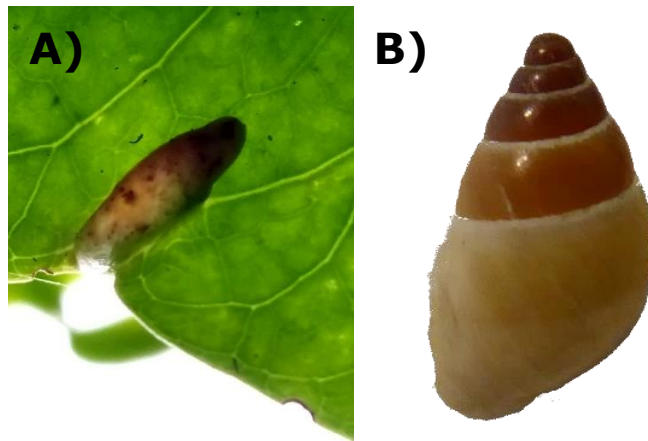
Figure 4.21 – **A)** a gall on the underside of a leaf in the Waianae mountains, and **B)** an individual shell of *Auriculella auricula*, also from the Waianae range. Both the gall and the shell show similar gradients of colour darkening from bottom to top.

The differences in darkness between the top and bottom sections of shell seem to occur along a gradient of colour, which may well vary among individuals, but this is difficult to capture with point reflectance spectrophotometry methods. This is also true of the reflectiveness of the shell surface in *Auriculella crassula* and *A. pulchra*, which, according to $PC_{xyz}1$ measurements, is higher in the apertural measurements of *A. crassula* than the apical, with the reverse being true of *A. pulchra*. *Auriculella uniplicata* also has a significant difference in how brown the shell is, unlike any of the other three species, where the apertural section of the shell tends to have a lower $PC_{xyz}3$ value than the apical, translating to a shell which is more yellow on the lowermost whorl. The lack of significance in Kolmogorov-Smirnov suggests that whilst the sections of shell may occupy different space along PC_{xyz} axes, the distribution of points along these axes is not more variable in either shell section, except for a significant result in $PC_{xyz}2$ measurements of *Auriculella uniplicata*, in which the apical section of the shell has a larger range of variation in darkness than the bottom section.

A similar pattern of non-uniformly coloured shells is present in *Partula taeniata*, where a significant proportion of shells have a darkened spire, with the earliest whorls being markedly darker than the rest of the shell (Murray and Clarke 1966, Barker 2001). Shell background colour, lip colour, spire colour, and banding morphs in *P. taeniata* are controlled by a supergene consisting of at least six tightly-linked loci (Murray and Clarke 1976). The colour of the spire is determined by the locus *S* with a dark colouration dominant to a light spire. An intermediate spire colour shows the same pattern of dominance but determining whether the phenotype is present due to a separate allele remains problematic. Whilst little is known about the genetic mechanisms underpinning the colour variation in *Auriculella*, or the more prominently studied *Achatinella*, *Achatinella* in particular are very similar to *Partula*, in their morphology, geographic distribution, and life history strategies (Hickman 2002), so it is perhaps possible that the phenotypic variation in *Achatinella* and *Auriculella* might be controlled by similar means. It would be beneficial to apply reflectance spectroscopy methods to shells of *Achatinella, Partula,* and other land snail radiations within the Pacific Islands to understand whether variation is similar across each of these taxonomic groups. This understanding of the genetic mechanisms underpinning the spire colour variation in *Partula* could be paired with similar analysis to that detailed above, allowing comparisons to be drawn between taxa, which may ultimately aid in elucidating the cause of spire variation in *Auriculella*.

Measurements of variation within individuals are however potentially problematic due to methodological constraints – if the colour variation is present at a higher point in the spire than the points measured, it would not be captured. One of the limits with spectrophotometry is that measurements within 0.2mm of a colour boundary are inaccurate (Taylor et al. 2016), highlighting some of the issues faced when working with small specimens such as *Auriculella*. It is possible to alleviate the problems arising from samples with small colour patches by employing

alternative techniques, such as those involving microscopic or collimating lenses which narrow beams of light to become more aligned in a specific direction (Fleishman et al. 2006, Badiane et al. 2017). Spectrophotometers may also be fitted with a sighting optic which, similarly to the viewfinder of a camera, allows visualisation of the patch being measured, a method which has been utilised in quantifying the colours of small patches on Hawaiian coral reef fish (Marshall et al. 2003). It is also important to note that whilst paired point measurements serve to capture the variation within individual shells to a certain extent, a greater number of point measurements would enable establishment of the gradient of colour change, which would potentially give clues regarding the generalities of the genetic control of shell colouration.

A further constraint which is worth noting in determining differences in colour between sections in individual shells, and one which is inherent in the use of museum specimens, is the relationship between specimen age and the fading of colour over time. If the two areas of shell are pigmented differently, it is a possibility that these pigments will fade at different rates over time, and either exacerbate, or detract from any differences in the colour of an individual shell detected by spectrophotometry (Cameron et al. 2014, Gheoca et al. 2019).

4.5.2 Colour variation between populations

Populations of each species of *Auriculella* vary significantly in different ways. In all four species, there was a significant difference in the reflectivity of the shells ($PC_{xyz}1$) between populations in both the apical and apertural measurements. The same is true of the apical measurements of all species along the darkness axes, $PC_{xyz}2$, which differed significantly between populations of the same species, the apertural shell section also differed significantly between populations in all species except *A. auricula*. *Auriculella crassula* was the only species

in which PC$_{xyz}$3, the "brownness" index, differed significantly between populations, where a difference was present in both shell sections.

The differences in shell measurements across populations is perhaps related to the dispersal methods of shells, and relative isolation of populations. Unfortunately, it is difficult to determine levels of isolation between populations at present due to a lack of precise locality data, which is stored in fieldwork notebooks from historic museum collectors. The Bishop Museum are currently in the process of digitising these records (Yeung and Hayes, pers. comms.), so the accessibility of location information beyond island level will be available in the future. This will potentially allow the determination of clines of phenotypic variation within and between species along geographical parameters of single islands – ie does chirality or colour vary between mountain ranges in reproductively isolated populations. This will allow more detailed studies to be performed and utilise the resources of natural history museums to their full potential. It should be noted however that populations of *Auriculella* were collected from as early as 1901, so location data is perhaps unlikely to be particularly precise, but it will at least be possible to identify population locations to the level of the valley from which they originate.

As individuals of *Auriculella* spp. vary seemingly continuously in colour both between and within separate measurements of individual shells, referring to the four species described above as "polymorphic" with respect to shell colour may be inappropriate. Whilst other species may be polymorphic with respect to banding patterns and other shell characters such as chirality, the seemingly continuous colour variation described in this chapter could feasibly be present as individuals are subjected to various pressures other than visual selection, such as thermoregulation. This is particularly relevant when the differences in apertural and apical shell darkness are considered.

4.5.3 Between species variation

There is little variation present in colour between the four species, with no significant differences along any of the three axes of variation in pairwise comparisons between species, with the exception of a difference in $PC_{xyz}1$, the reflectivity axis, between *A. crassula* and *A. pulchra*. *Auriculella crassula* has a lower $PC_{xyz}1$ value than *A. pulchra*, suggesting a difference in shell surface reflectance. Differences between species are perhaps masked by the large inter-population differences in colour within each species. If populations of a single species are reproductively isolated from one another, persisting as small propagules in isolated patches of remaining suitable habitat, creating a large range of phenotypic diversity *within* species, it is unsurprising that the range of variation *between* species may not be large, relative to this. Analysis would, ultimately, benefit from the inclusion of more species of *Auriculella*. Understanding any potential historical hybridisation events between species, and disentangling taxonomic relationships between species would also aid in understanding why a lack of variation between these species is present. The adaptive hypothesis of similar selective environments may help to explain why variation is maintained, but not in understanding how it was established in the first instance.

4.5.4 Between island variation

The colour of individual shells does not vary between the islands of Maui and Oahu, either in terms of the 3-dimensional colour space occupied by the shells, or the distribution of points within this space, suggesting that neither island gives rise to a more variable phenotype of shell. This could imply a lack of differential selection pressures across islands, allowing the evolution of similar phenotypes across the land snail radiation between the islands of Oahu and Maui, although these are only two of the multiple islands of the Hawaiian archipelago. This is concurrent with

the presence of established populations of the non-native predators such as *Euglandina rosea*, *Rattus rattus*, and *Chamaeleo jacksonii* across all of the Hawaiian islands (Hadfield et al. 1993, Meyer 2006, Meyer and Cowie 2011, Kraus et al. 2012, Chiaverano and Holland 2014, Gerlach et al. 2021).

It would be beneficial to obtain data for species endemic to other islands to determine whether the lack of variation between islands is present across the entirety of the archipelago. Oahu and Maui are geographically in relatively close proximity, with only two islands between them (Molokai and Lanai), so it would be interesting to establish whether variation on the two most geographically distant islands, Kauai and Hawaii are also equal, or whether there is a trend towards a certain direction of variation across the islands, as transportation or dispersal of individuals occurred throughout the islands. If initial colonisation and distribution of individuals across the Hawaiian archipelago occurred via a sequential process of "island hopping", it is likely that there will be a continuous gradient of genetic variation across the islands, according to geographical proximity, where the islands furthest from one another will possess individuals or species which are the most phenotypically distinct from one another. In this case, islands which are in close proximity to one another are likely to host morphologically and genetically similar species, which get progressively more disparate from one another as geographic proximity decreases. Progressive colonisation of volcanic islands according to geographic age is referred to as the 'progression rule', and was coined in reference to the Hawaiian islands (Wagner and Funk 1995). Examples of this can be seen in several taxonomic groups with island distributions, including differences in the mitochondrial genome of a species of crab spider, *Misumenops rapaensis*, in the Austral islands (Garb and Gillespie 2006). Crab spiders are thought to employ a strategy of ariel distribution known as "ballooning", whereby a spiderling will produce silk strands which catch air currents to facilitate dispersal (Cho et al. 2018). Whilst *M. rapaensis* remains classified as a single species, the genetic diversity

observed is consistent with the sequential colonisation of islands, and subsequent divergence due to reproductive isolation. Individuals from islands further apart from one another are more genetically distinct, and individuals from the same island form monophyletic groups, consistent with the idea that populations further apart from one another show greater genetic disparity.

4.5.5 Variation with chirality

The lack of variation in colour associated with chirality is perhaps unsurprising, as *Auriculella* spp. have been observed mating interchirally in the field (Davison, unpublished data). This seems to be a relatively uncommon phenomenon across chirally variable snail species, where usually a single population is restricted to a fixed chirality by frequency dependent selection (Johnson 1982, Davison et al. 2005). Interchiral mating can be dependent on shell morphology (Asami et al. 1998), as well as reproductive behavioural plasticity – low spired individuals have difficulty engaging genitalia between sinistral and dextral individuals in their typical face-to-face reciprocal mating behaviours, where genitalia exposed on the left side of the head of a sinistral individual are incompatible with the genitalia exposed on the right side of a dextral snail's head. High spired individuals such as *Partula* spp. are able to overcome this (Lipton and Murray 1979, Asami 1993), due to their non-reciprocal mating behaviour in which the "male" copulates by mounting the shell of the "female", in a position whereby both snails are aligned in the same direction. This difference in mating behaviour allows for interchiral mating, albeit with some necessary adjustments in reproductive behaviour. Individuals of opposite chiralities showing no difference in shell colour suggests that the genes responsible for colour and chirality are not tightly linked, so unlikely to be in close physical proximity to one another.

4.5.6 Museum specimens

Natural history collections, such as the malacology collection at the BPBM, house specimens representing many endangered and extinct species. Advances in molecular techniques have permitted genetic analysis of ancient specimens, allowing more accurate quantification of loss of diversity in extinct species (Suarez and Tsutsui 2004) The loss of genetic diversity in the great prairie chicken *Tympanus cupido* has been precisely estimated by genetic studies comparing current populations with prairie chickens collected and stored 65 years ago at the Illinois Natural History Survey. The loss of genetic diversity has been tied to a lack of fitness in lost individuals; conservation efforts can thereby be focussed on effective recovery. Methods are being developed for extracting historic DNA from the shells of molluscs; with specialised DNA extraction and sequencing approaches (Geist et al. 2008, Hawk and Geller 2019). Previously, the only way to distinguish between several more cryptic species of Hawaiian snails required additional molecular or morphological data, such as DNA sequences, radula examination, or reproductive tissue dissections (Yeung et al. 2020), which are an impossibility in dry-preserved museum specimens. The development of ancient DNA extraction methods from molluscan shells will allow the unambiguous classification of phenotypically similar shells. Accessing historic genetic data will allow better quantification of diversity and identification of historic species, providing a genetic basis for understanding historical population variation, which may prove crucial for conservation efforts (Yeung and Hobbs, pers. comms.).

4.5.7 Conservation of Hawaiian land snails – fighting a losing battle?

The recent rediscovery of *Auriculella pulchra* in 2015, a species previously thought to be extinct, provides some hope that conservation efforts of these snails are not merely fighting a losing battle (Yeung et al. 2015). The discovery of a new species, *Auriculella gagneorum*, discovered in 2020 in the Waianae mountains, Oahu, also gives some hope for conservation efforts (Yeung et al. 2020). Despite occasional discovery/rediscovery, continued habitat destruction and introduction of non-native predators necessitate the development and deployment of effective conservation strategies to save the remainder of the *Auriculella* genus before it is lost entirely (Solem 1990, Regnier et al. 2009, Yeung and Hayes 2018).

In an attempt to alleviate some of the predation threat posed by non-native organisms, some of the most precious species of Hawaiian snail are housed in semi-wild exclosures (Price et al. 2015), with a variety of obstacles to keep non-native pests out (Gerlach et al. 2021). These barriers include a rolled cap on the top of the fence, electric wires, a copper mesh, and an angle barrier (Rohrer et al. 2016). The exclosure fences are tall, surviving the unpredictable weather of the Hawaiian mountains with concrete footed steel posts buried deep in the ground, and a mesh skirt with ground pins holding the fence in place. The exclosure sites are monitored regularly, and any errant predators which may pose a danger to the snails are removed.

With the addition of spectral measurements from a broader selection of species distributed more widely across the islands, including both extinct and extant species, it would be possible to determine whether there is a phenotypic distinction between these groups, or whether there is a directionally selective process occurring in extinction of *Auriculella*

species. This is a potentially interesting area of study, as it has implications for the conservation of a genus which is at risk of extinction. If extinct species share a trait or set of traits, extant snails possessing those traits are potentially at a higher extinction risk, so conservation efforts can be directed at these species.

Overall, by presenting the first quantitative analysis of colour variation within and between four species of *Auriculella* in an ecologically relevant light by using the visual system of a potential disperser, some light has been shed on the intricacies of colour variation present in a genus of conservation interest in the Hawaiian Islands. Understanding precisely how colour varies in *Auriculella* species allows the deduction of some of the underlying genetic control, such as the colour and chirality polymorphisms being unlinked to one another. Quantifying the presence of variation within individual shells along components of colour variation also allows inference of possible genetic control mechanisms for this difference, by comparison to known loci in *Partula*. Analysis of colour variation between species shows that shell colour alone is not a sufficient identification tool, and further highlights the importance of ancient DNA extraction techniques in the sorting of morphologically cryptic specimens of historical collections. The collection of colour data from *Auriculella* has demonstrated the use of spectrophotometry as a colour phenotype quantification tool in smaller shells and has highlighted the importance of gastropod museum specimens in conservation efforts.

Ultimately, it would be beneficial to expand this analysis to cover more of the genus, to further understand the variation present, and include other taxonomic groups of Pacific Island land snails in order to understand the treasure trove of molluscan variation present across the Pacific islansds before it is lost entirely.

Author Contributions

Hannah Jackson and Angus Davison conceptualised the project in conversation with Ken Hayes and Norine Yeung. Samples were sourced from the BPBM collection by Norine Yeung and Chris Hobbs. **Hannah Jackson** collected the data, with some input on chirality counts from Angus Davison. **Hannah Jackson** performed the analysis and wrote the original draft. Angus Davison and Andrew MacColl advised on subsequent versions.

Chapter 5: Discussion

5.1 Summary of results

By developing and implementing quantitative methods for defining variation in phenotypes of polymorphic molluscan genera, this thesis has sought to establish the usefulness of such methods in elucidating potential genetic mechanisms underpinning variation in natural populations. By quantitatively defining phenotypic variation in species of both *Cepaea* and *Auriculella*, I present several key findings, outlined below.

In **Chapter 2**, I use two methods of quantitatively defining fine variation in banding position of *Cepaea* spp. to establish that absence of individual bands has minor but significant impact on the position of other bands, suggesting that the locus which is responsible for controlling band presence or absence acts mainly after band position has been established. Small differences in banding pattern are highlighted between *Cepaea nemoralis* and *Cepaea hortensis*, implying slight divergence of the genetic mechanisms controlling fine-scale variation. I also establish that all sections of a shell grow equally with the deposition of new material, with the exception of the lowermost dorsal section, close to the umbilicus, indicating that differences in banding position between banding patterns and species are not artefacts of shell growth. The results have significance in understanding the genetic control of the polymorphism in *Cepaea* by establishing a method to quantitatively define variation within and between banding pattern phenotypes, although these could ultimately be extended to include hyalozonate and fused band phenotypes to create a more complete picture of variation.

In **Chapter 3**, I use reflectance spectrophotometry and psychophysical modelling techniques to accurately define colour variation in both

Cepaea hortensis and *Cepaea nemoralis*. I establish that the distribution of colour in *C. hortensis* is continuous in 3-dimensional space, and that the precise degree of paleness of *C. hortensis* shells is associated with latitude. Differences in exact shade of *Cepaea hortensis* and *Cepaea nemoralis* are highlighted, suggesting that alleles which control fine-scale colour variation may be somewhat diverged from one another between the two species. I also detect some slight differences in shade between two genetic lineages of *Cepaea nemoralis*. Overall, this chapter has significance for understanding the shell colour variation present in the *Cepaea* genus, and the nature of selective processes which may be acting upon it, as well as highlighting the importance of considering within-morph variation in polymorphic species.

In **Chapter 4**, I again use a combination of reflectance spectrophotometry and psychophysical models to define the variation present in four species of the *Auriculella* genus. Variation is explored at a number of scales, ranging from colour variation within individual shells, to variation across islands of the Hawaiian archipelago. I demonstrate that there are often large differences in colour within a single shell, similar to a phenotypic trait displayed in *Partula*. The magnitude of this colour difference is variable across individuals, but is present in all four species. I also establish that there are differences in colour in both apical and apertural measurements of reproductively isolated populations of single species, but this difference is not reflected between species, which do not vary in overall colour. These results have significance in understanding the phenotypic variation in an understudied system, which is of conservation concern. Understanding the variation allows inferences to be made regarding the genetic mechanisms which control the variation.

5.2 The Cepaea polymorphism

In both **Chapter 2** and **Chapter 3** of this thesis, I demonstrate some of the differences between *Cepaea nemoralis* and *Cepaea hortensis*, both in terms of banding pattern and shell colour. Slight differences between species are present in the fine variation of both shell colour and banding. Whilst, broadly speaking, banding patterns were similar between species, there are some differences present, albeit at a small scale; this small magnitude was also reflected in slight colour differences between species, where the variation in shell colour of *Cepaea hortensis* occurs over a smaller number of perceptual units than variation in *C. nemoralis.* The presence of these differences between species, although slight, suggest subtle divergence of underlying genetic control mechanisms of both banding and colour variation between the two species. These differences occur within identically scored phenotypes; for example, a snail of either species could have five bands, and be scored as having a banding phenotype of 12345, but there are subtle differences in the precise placement of these bands. The slight nature of these differences suggest that they are perhaps not important in prey selection, or even perceptible to predators., although they may be useful in detecting differences in the genetic architecture of the supergene between *Cepaea nemoralis* and *Cepaea hortensis.*

The *Cepaea* supergene is thought to have pre-dated the speciation event separating *C. hortensis* and *C. nemoralis* (Cook 1998), so slight differences in structure between these species have likely come about as a result of lack of gene flow. Some hybridisation between *C. nemoralis* and *C. hortensis* is theoretically possible in areas of co-occurrence, hybridisation events are thought to be rare in natural populations (Cain and Sheppard 1954). Genome sequencing of both species, and subsequent comparison of variances (in the form of SNPs, for example) between species, could aid in the determination of the location of genes responsible for the slight banding and colour differences. If, when sequences are aligned, differences occur in regions known to be involved in pigmentation of the periostracum (giving the ground colour of a shell),

or the banding pattern, it may be inferred that these are potential candidate genes for controlling the variation in precise colour shade and banding pattern in *Cepaea*.

Defining phenotypic variation differences in *Cepaea* outside of the context of "binning" a trait into a discrete may provide an effective "springboard" from which to proceed in furthering understanding of the evolution and maintenance of the supergene controlling variation. With the advent of affordable technology for defining phenotypes accurately, it is now possible to look within individual morphs for variation. It would certainly be beneficial to further understand the fine-scale variation present in many polymorphic species so as to ensure that important variation within morphs is not overlooked. For example, there are large amounts of variation present in the discrete morphs of the tawny dragon lizard (*Ctenophorus decresii*) (Teasdale *et al.* 2013), understanding the levels of variation in these morphs may help to elucidate the reason for their presence, and determine how and why the variation is maintained in natural populations.

5.2.1 Future direction of work on the *Cepaea* supergene

It is certainly an exciting time to be researching the polymorphism in *Cepaea* in particular. With the recent assembly of the *Cepaea nemoralis* genome (Saenko et al. 2021), several avenues for future research have opened. Firstly, a clear next step in understanding the evolution and maintenance of the supergene controlling phenotypic variation in *Cepaea nemoralis* is to use the newly assembled genome and next generation sequencing methods to perform fine-scale mapping of the supergene. Methods such as genome-wide association studies (GWAS) could be used to genotype several individuals with

variable phenotypic traits, and search for genetic variations which may be responsible for influencing phenotype traits (Husby et al. 2015, Saenko and Schilthuizen 2021). GWAS has successfully been utilised to identify a genomic region associated with the carotenoid-based orange colour variant in the Yesso scallop (Zhao et al. 2017); three candidate genes known to have carotenoid metabolism function were found in the identified region.

In *Cepaea nemoralis* specifically, having good coverage and good quality illumina sequencing reads that can be aligned against a reference genome (Saenko et al. 2021) will allow the calling of SNPs (single nucleotide polymorphisms) against said reference genome to search for markers that are in association with the colour phenotype. If known crosses are used, recombination frequencies can be estimated, and linkage mapping can be performed. As the supergene exists in tight linkage, any area of the linkage map which is in "complete linkage" provides candidates for the location of the supergene. When good quality high coverage reads are paired with the presence of known markers flanking the supergene (Richards et al. 2013), it becomes possible to determine the contents inside of two recombination break points. The combination of sequencing methods with linkage and trait mapping will allow differences between genotypes linked to specific phenotypes to be searched for. Once differences are detected, it is possible to look within these differences for genes which may be homologous to those in other taxa. This is particularly useful in pigmentation genes, as it is likely that these, or genes similar to these, will be present in other species.

Three classes of pigments have been identified in molluscan shells to date, melanins, tetrapyrroles, and carotenoids (Comfort 1951, Saenko and Schilthuizen 2021). If a gene implicated in the biosynthesis of these pigments in a different species is found in *Cepaea*, it is likely to be involved. Identification of the pigments involved in both the ground colour

and banding pattern of *Cepaea* could also be a useful step in further elucidating the genetic structure of the supergene. If the pigments are known, this information can be usefully paired with genomic data to elucidate candidate genes from variable phenotypes. Methods such as Raman spectroscopy and high-performance liquid chromatography (HPLC) could be used on isolated areas of shell pigmentation to establish the nature of the pigments responsible for variation. Whilst melanin has long been thought to be the pigment responsible for the dark colouration of the banding pattern in *Cepaea*, there is a lack of unequivocal evidence to prove this (Williams 2017). Affenzeller et al. (2020) suggest that eumelanin is not the responsible pigment, although the HPLC analysis that they carry out does not reveal any further information about the nature of the molecules responsible for the pigmentation of bands, so further analysis is required. Performing these analyses may also aide in understanding the hyalozonate phenotype, where bands are present but unpigmented. A combination of the above analyses, compared with spectral methods and analyses of banding patterns would allow a complete picture of variation to be built and understood in *Cepeaa*. This would progress elucidating the remaining questions surrounding the supergene further – understanding the function of a gene allows more straightforward identification of putative candidates within the supergene.

More specifically to the data presented in this thesis, ideas and methodologies from **Chapter 2** and **Chapter 3** could be combined, to allow analysis of colour patterns within individuals. In mid-banded individuals of *Cepaea nemoralis*, the band often appears to be highlighted by an area of lighter pigmentation; the use of reflectance spectrophotometry and psychophysical modelling could establish whether this variation is visible to a predator. It is thought that predators use achromatic signals to recognise variation of elements within the same pattern; using the framework for achromatic variation set out in (Delhey et al. 2015) would mean that this analysis is possible. Doing this would allow further understanding of the interaction between colour and

banding pattern in *Cepaea*. Similar processes have been used in determination of the necessary precision of mimetic accuracy in Hymenoptera, specifically in *Apis* and *Vespula* mimics (Taylor et al. 2016). A combination of spectral measurements and a pattern determination algorithm were used, albeit separately, to determine the impact of mimetic accuracy of abdomen patterns in hoverfly mimics (Taylor et al. 2013). These techniques were paired to artificially manipulate mimetic patterning, which could be utilised to determine the appropriateness of the selected thresholds of difference to perceivers, and understand the importance of the slight differences in signals to a potential predator.

Whilst quantitative methods allow theoretical establishment of perception of signals by non-human observers, a signal being perceived does not necessarily mean that it is important, or will be acted upon. Whilst **Chapter 3** and **Chapter 4**, and the theoretical future work outlined above use methods of determining potential signal perception by a driver of selection, it is ultimately necessary to carry out behavioural experiments with predators in natural settings to establish whether variation in these signals is important (Thomas et al. 2004). In **Chapter 3**, individual elements of colour signal are highlighted as being visible to an avian predator; a potential avenue for confirming that this variation is important to predators is to select individual snail shells which vary in colour along a single axis of variation, whilst the other components remain approximately equal, and implement prey selection experiments with avian predators, namely the song thrush *Turdus philomelos*.

5.3 Quantitative definition of phenotypes and genetic inferences

In **Chapter 3** and **Chapter 4**, I highlight the usefulness of the implementation of reflectance spectrophotometry and psychophysical modelling in tandem to understand colour variation of gastropod shells in an ecologically relevant context. **Chapter 3** and **Chapter 4** utilise the techniques of reflectance spectrophotometry and psychophysical modelling in subtly different ways. **Chapter 3** considers the colour variation of *Cepaea*, a species in which the shell polymorphism is well defined and understood, with pre-established and recognised colour morphs present across populations, where reflectance spectra can be compared to human-scored colours. **Chapter 4** uses reflectance spectrophotometry with a somewhat different approach. Very little is known about *Auriculella*, the colour variation is poorly defined. Instead, reflectance spectra and associated xyz coordinates in 3-dimensional colour space are used to determine whether colours differ, focussing on potential implications for conservation, and understanding how variation is present across a series of levels of increasing magnitude. This subtle difference highlights the usefulness of quantitative definitions of phenotypic variation for inference of genetic information, both for understanding fine-scale mapping of genetic architecture in species where the genetics are largely understood, and as a first attempt at understanding how variation might be controlled in species where little is known about the genetics.

The application of quantitative methods for defining phenotypic variation both within and between recognised morphs in **Chapter 2, Chapter 3, and Chapter 4** has allowed the inference of potential genetic mechanisms which might be controlling variation across multiple taxa. Inferences can be from **Chapter 2** regarding the locus which controls band presence/absence acting mainly after the position of bands has been established. It is perhaps likely that the band is "present", at least in a molecular sense, before pigmentation is added. From the results presented in **Chapter 3**, it can be inferred that there is some divergence between the genetic mechanisms controlling variation in *Cepaea*

hortensis and *Cepaea nemoralis*. The shell colour of the two species varies slightly, with variation occurring across a smaller number of perceptual differences in *Cepaea hortensis*. In **Chapter 4**, colour variation between apical and apertural measurements of the same shell is present to varying degrees across all four species of *Auriculella*.

5.4 Gastropods as study systems

Examining phenotypic variation with methods which allow quantitative definition has proved extremely applicable in the Gastropoda, not least due to the nature of the gastropod shell. Whilst preserving gastropod tissue requires storage solutions which rely on tissue and genetic information to be preserved, shells are easily stored. Due to the ease of their preservation, both the molluscan fossil record, and the number of shells stored in collections is impressive. Once ancient DNA removal techniques are perfected (Ferreira et al. 2020, Martin et al. 2021), the pairing of these with quantitative methods of phenotype description will allow access to datasets, the potential of which thus far have not been recognised. Specifically, further implementation of these non-destructive methodologies would be beneficial to further understand the phenotypic variation in this broadly diverse taxa, particularly in species such as *Polymita*, where the causes of the impressive variation are not known.

These methodologies, paired with DNA extraction from shells, may also aid in the conservation of endangered species, such as the Hawaiian genera *Achatinella* and *Auriculella*. In order to direct conservation efforts effectively, it is useful to understand the genetics underlying variation present within a species. For example, if populations of extinct species all share a gene or trait which may cause them to be more susceptible to extinction through predation, it may be possible to redirect conservation efforts to extant species sharing this trait. This could also be applied more

widely to land snails, both those from the Pacific Islands, and from across the rest of the world, to further understand the variation present in, therefore assist in understanding the best methods of conservation of imperilled species.

Hopefully, in a more broad sense, access to these museum collections for genetic and genomic studies, paired with quantitative methods of analysing phenotypic variation will unlock the potential for future study of gastropods in a way which has not previously been possible. In doing this, an invaluable resource will be accessible, which will open many avenues for future study on the variation of gastropods, and allow the use of currently underutilised resources around the world. The use of DNA extraction techniques from museum specimens will also allow the extraction of genetic material from extinct species, perhaps allowing further information to be gleaned with regards to how and why species go extinct, thus having potential implications for conservation of related and/or endangered mollusc species. Ultimately, accessing these resources will aid in the goal of understanding how phenotypic variation is established and maintained in natural populations, in both gastropod species, and more broadly throughout the natural world.

5.4 Concluding Remarks

Broadly, I have quantitatively defined variation in several phenotypic traits of two molluscan genera, and in doing so, the outcomes of this thesis have been fourfold. Firstly, I have demonstrated the usefulness of terrestrial molluscs in studies of evolution and ecology, as the nature of shell growth preserves an entire life history for each individual. Secondly, I have highlighted the diversity of phenotypic variation of shells in individual species and taxonomic groups of terrestrial gastropod, and have illustrated how understanding this variation in a quantitative manner allows inferences to be made regarding the mechanisms underpinning this variation. Thirdly, I have demonstrated the variation present within historically defined morphs, and highlighted the importance of this variation in an ecological and evolutionary context. Finally, I have established that both new and pre-existing methods of quantitatively describing phenotypic variation are broadly applicable across gastropod taxa, and provide a more accurate method of quantification of phenotype without the need to "bin" traits into groups, whilst overlooking variation present within these groups.

Several key questions still remain, particularly with regards to the evolution and maintenance of the supergene responsible for controlling phenotypic variation in *Cepaea*. What is the nature of the pigments responsible for colouration in ground shell colour and banding? What is the precise location of the supergene, and how does its architecture reflect in the variation present in natural populations? Some key next steps in understanding the evolution and maintenance of the *Cepaea* polymorphism can be undertaken by answering these remaining questions. Ultimately, by providing frameworks for analysing variation, and pointing out the usefulness of gastropods as study species, I hope that these methods will be utilised in the future to answer these

questions, and more broadly to elucidate further the incredible phenotypic variation which is observed across the Gastropoda.

References

Adamson, K. J., T. Wang, B. A. Rotgans, T. Kruangkum, A. V. Kuballa, K. B. Storey, and S. F. Cummins. 2017. Genes and associated peptides involved with aestivation in a land snail. General and Comparative Endocrinology **246**:88-98.

Affenzeller, S., K. Wolkenstein, H. Frauendorf, and D. J. Jackson. 2020. Challenging the concept that eumelanin is the polymorphic brown banded pigment in Cepaea nemoralis. Scientific Reports **10**:2442.

Agoramoorthy, G., and M. J. Hsu. 2007. Ritual releasing of wild animals threatens island ecology. Human Ecology **35**:251-254.

Aguilera, F., C. McDougall, and B. M. Degnan. 2017. Co-Option and De Novo Gene Evolution Underlie Molluscan Shell Diversity. Molecular Biology and Evolution **34**:779-792.

Allen, C. E., B. J. Zwaan, and P. M. Brakefield. 2011. Evolution of sexual dimorphism in the Lepidoptera. Annu Rev Entomol **56**:445-464.

Amar, A., A. Koeslag, G. Malan, M. Brown, and E. Wreford. 2014. Clinal variation in the morph ratio of Black Sparrowhawks Accipiter melanoleucus in South Africa and its correlation with environmental variables. Ibis **156**:627-638.

Andersson, M. 1982. Sexual selection, natural selection and quality advertisement. Biological Journal of the Linnean Society **17**:375-393.

Arthur, W., D. Phillips, and P. Mitchell. 1993. Long-term stability of morph frequency and species distribution in a sand-dune colony of *Cepaea*. Proceedings of the Royal Society B: Biological Sciences **251**:159-163.

Asami, T. 1993. Genetic variation and evolution of coiling chirality in snails. Forma **8**:263-276.

Asami, T., R. H. Cowie, and K. Ohbayashi. 1998. Evolution of mirror images by sexually asymmetric mating behavior in hermaphroditic snails. American Naturalist **152**:225-236.

Asner, G. P., D. E. Knapp, T. Kennedy-Bowdoin, M. O. Jones, R. E. Martin, J. Boardman, and R. F. Hughes. 2008. Invasive species detection in Hawaiian rainforests using airborne imaging spectroscopy and LiDAR. Remote Sensing of Environment **112**:1942-1955.

Aubertin, D. 1927. On the anatomy of the land snails (Helicidae) Cepaea hortensis Müller and Cepaea nemoralis L. Proceedings of the Zoological Society of London **97**:553-582.

Badiane, A., G. P. I. de Lanuza, M. D. Garcia-Custodio, P. Carazo, and E. Font. 2017. Colour patch size and measurement error using reflectance spectrophotometry. Methods in Ecology and Evolution **8**:1585-1593.

Baldwin, P., and T. Casey. 1983. A preliminary list of foods of the Po'o-uli'. Elepaio **43**:53-56.

Ball, P. 2015. Forging patterns and making waves from biology to geology: A commentary on Turing (1952) 'The chemical basis of morphogenesis'. Philosophical Transactions of the Royal Society B: Biological Sciences:370.

Barker, G. M. 2001. The biology of terrestrial molluscs. CABI.

Bates, D., M. Mächler, B. Bolker, and S. Walker. 2015. Fitting linear mixed-effects models using lme4. Journal of Statistical Software **67**.

Baumhardt, P. E., B. A. Moore, M. Doppler, and E. Fernandez-Juricic. 2014. Do American goldfinches see their world like passive prey foragers? A study on visual fields, retinal topography, and sensitivity of photoreceptors. Brain Behavior and Evolution **83**:181-198.

Beasley, C. R., C. Fernandes, C. P. Gomes, B. A. Brito, S. M. Lima, and C. H. Tagliaro. 2005. Molluscan diversity and abundance among coastal habitats of northern Brazil.

Bennett, A. T. D., I. C. Cuthill, and K. J. Norris. 1994. Sexual selection and the mismeasure of color. The American Naturalist **144**:848–860.

Blumthaler, M., W. Ambach, and R. Ellinger. 1997. Increase in solar UV radiation with altitude. Journal of Photochemistry and Photobiology B: Biology **39**:130-134.

Bouchet, P. 1997. Inventorying the molluscan diversity of the world: What is our rate of progress? Veliger **40**:1-11.

Briscoe, A. D., and L. Chittka. 2001. The evolution of color vision in insects. Annual Review of Entomology **46**:471-510.

Brisson, D. 2018. Negative Frequency-Dependent Selection Is Frequently Confounding. Front Ecol Evol **6**.

Brown, K. M., C. Lydeard, J. H. Thorp, and A. P. Covich. 2010. Chapter 10 - Mollusca: Gastropoda. Pages 277-306 Ecology and

Classification of North American Freshwater Invertebrates (Third Edition). Academic Press, San Diego.

Brown, R. J. 2007. Freshwater mollusks survive fish gut passage. Arctic **60**:124-128.

Budd, A., C. McDougall, K. Green, and B. M. Degnan. 2014. Control of shell pigmentation by secretory tubules in the abalone mantle. Frontiers in Zoology **11**.

Cain, A. J. 1988. The scoring of polymorphic colour and pattern variation and its genetic basis in molluscan shells. Malacologia **28**:1-15.

Cain, A. J., and J. D. Currey. 1963a. Area Effects in *Cepaea*. Philosophical Transactions of the Royal Society of London Series B-Biological Sciences **246**:1-81.

Cain, A. J., and J. D. Currey. 1963b. The causes of area effects. Heredity **18**:467-471.

Cain, A. J., J. M. B. King, and P. M. Sheppard. 1960. New data on the genetics of polymorphism in the snail *Cepaea nemoralis* L. Genetics **45**:393-411.

Cain, A. J., and P. M. Sheppard. 1950. Selection in the polymorphic land snail *Cepaea nemoralis*. Heredity **4**:275-294.

Cain, A. J., and P. M. Sheppard. 1952. The effects of natural selection on body colour in the land snail *Cepaea nemoralis*. Heredity **6**:217-231.

Cain, A. J., and P. M. Sheppard. 1954. Natural Selection in *Cepaea*. Genetics **39**:89-116.

Cain, A. J., P. M. Sheppard, and J. King. 1968. Studies on *Cepaea* I. The genetics of some morphs and varieties of *Cepaea nemoralis* (L.). Philosophical Transactions of the Royal Society of London. Series B, Biological Sciences **253**:383-396.

Cameron, R. A. D. 1969. Predation by song thrushes *Turdus ericetorum* (Turton) on the snails *Cepaea hortensis* (Mull.) and *Arianta arbustorum* (L.) near Rickmansworth. Journal of Animal Ecology **38**:547-553.

Cameron, R. A. D. 1992. Change and stability in *Cepaea* populations over 25 years: A case of climatic selection. Proceedings of the Royal Society B: Biological Sciences **248**:181-187.

Cameron, R. A. D. 2013. The poor relation? Polymorphism in Cepaea hortensis (O. F. Müller) and the Evolution Megalab. Journal of Molluscan Studies **79**:112-117.

Cameron, R. A. D., and M. A. Carter. 1979. Intraspecific and interspecific effects of population-density on growth and activity in some helicid land snails (Gastropoda, Pulmonata). Journal of Animal Ecology **48**:237-246.

Cameron, R. A. D., M. A. Carter, and M. A. Pallesclark. 1980. *Cepaea* on Salisbury plain - patterns of variation, landscape history and habitat stability. Biological Journal of the Linnean Society **14**:335-358.

Cameron, R. A. D., and L. M. Cook. 2012a. Correlated phenotypic responses to habitat difference in *Cepaea nemoralis* (L.). Folia Malacologica **20**:255-263.

Cameron, R. A. D., and L. M. Cook. 2012b. Habitat and the shell polymorphism of *Cepaea nemoralis* (L.): Interrogating the Evolution Megalab database. Journal of Molluscan Studies **78**:179-184.

Cameron, R. A. D., and L. M. Cook. 2013. Temporal morph frequency changes in sand-dune populations of Cepaea nemoralis (L.). Biological Journal of the Linnean Society **108**:315-322.

Cameron, R. A. D., L. M. Cook, and J. J. D. Greenwood. 2013a. Change and stability in a steep morph-frequency cline in the snail *Cepaea nemoralis* (L.) over 43 years. Biological Journal of the Linnean Society **108**:473-483.

Cameron, R. A. D., L. M. Cook, and J. J. D. Greenwood. 2013b. Change and stability in a steep morph-frequency cline in the snail *Cepaea nemoralis* (L.) over 43 years. Biological Journal of the Linnean Society **108**:473-483.

Cameron, R. A. D., R. J. Cox, T. Von Proschwitz, and M. Horsák. 2014. *Cepaea nemoralis* (L.) in Göteborg, S.W. Sweden: variation in a recent urban invader. Folia Malacologica **22**:169-182.

Cameron, R. A. D., B. M. Pokryszko, and M. Horsak. 2009. Contrasting patterns of variation in urban populations of Cepaea (Gastropoda: Pulmonata): a tale of two cities. Biological Journal of the Linnean Society **97**:27-39.

Cameron, R. A. D., and T. von Proschwitz. 2020. *Cepaea nemoralis* (L.) on Öland, Sweden: recent invasion and unexpected variation. Folia Malacologica **28**:303-310.

Carlos, G., A. Velmurugan, B. A. Jerard, R. Karthick, and I. Jaisankar. 2008. Biodiversity of Polynesian islands: Distribution and threat from climate change. Pages 105-125 *in* C. Sivaperuman, A. Velmurugan, A. K. Singh, and I. Jaisankar, editors. Biodiversity

and climate change adaptation in tropical islands. Academic Press.

Carter, M. A., R. C. V. Jeffery, and P. Williamson. 1979. Food overlap in co-existing populations of the land snails *Cepaea nemoralis* (L) and *Cepaea hortensis* (Mull). Biological Journal of the Linnean Society **11**:169-176.

Cassey, P., M. Honza, T. Grim, and M. E. Hauber. 2008. The modelling of avian visual perception predicts behavioural rejection responses to foreign egg colours. Biology Letters **4**:515-517.

Checa, A. G., C. Salas, E. M. Harper, and D. Bueno-Perez Jde. 2014. Early stage biomineralization in the periostracum of the 'living fossil' bivalve Neotrigonia. Plos One **9**:e90033.

Chiaverano, L. M., and B. S. Holland. 2014. Impact of an invasive predatory lizard on the endangered Hawaiian tree snail *Achatinella mustelina*: a threat assessment. Endangered Species Research **24**:115-123.

Chiba, S. 1997. Novel colour polymorphisms in a hybrid zone of Mandarina (Gastropoda: Pulmonata). Biological Journal of the Linnean Society **61**:369-384.

Chiba, S. 1999. Character displacement, frequency-dependent selection, and divergence of shell colour in land snails Mandarina (Pulmonata). Biological Journal of the Linnean Society **66**:465-479.

Chiba, S., and R. H. Cowie. 2016. Evolution and extinction of land snails on oceanic islands. Annual Review of Ecology, Evolution, and Systematics **47**:123-141.

Cho, M., P. Neubauer, C. Fahrenson, and I. Rechenberg. 2018. An observational study of ballooning in large spiders: Nanoscale multifibers enable large spiders' soaring flight. PloS Biology **16**.

Cincotta, R. P., J. Wisnewski, and R. Engelman. 2000. Human population in the biodiversity hotspots. Nature **404**:990-992.

Civeyrel, L., and D. Simberloff. 1996. A tale of two snails: is the cure worse than the disease? Biodiversity & Conservation **5**:1231-1252.

Clark, M. S., M. A. S. Thorne, F. A. Vieira, J. C. R. Cardoso, D. M. Power, and L. S. Peck. 2010. Insights into shell deposition in the Antarctic bivalve *Laternula elliptica*: Gene discovery in the mantle transcriptome using 454 pyrosequencing. BMC Genomics **11**:362.

Clarke, B. 1962. Natural selection in mixed populations of 2 polymorphic snails. Heredity **17**:319-345.

Clarke, B. 1966. The Evolution of Morph-Ratio Clines. The American Naturalist **100**:389-402.

Clarke, B., and D. Kirby. 1966. Maintenance of histocompatibility polymorphisms. Nature **211**:999-1000.

Clarke, B., and J. Murray. 1962. Changes of Gene-Frequency in Cepaea Nemoralis (L). Heredity **17**:445-&.

Clarke, B., J. Murray, and M. S. Johnson. 1984. The extinction of endemic species by a program of biological control. Pacific Science **38**:97-104.

Clarke, B. C. 1979. The evolution of genetic diversity. Proceedings of the Royal Society B: Biological Sciences **205**:453-474.

Clutton-Brock, T. 2007. Sexual selection in males and females. Science **318**:1882-1885.

Comfort, A. 1951. The Pigmentation of Molluscan Shells. Biological Reviews **26**:285-301.

Cook, L. M. 1967. The genetics of *Cepaea nemoralis*. Heredity **22**:397-410.

Cook, L. M. 1998. A two-stage model for *Cepaea* polymorphism. Philosophical Transactions of the Royal Society of London. Series B: Biological Sciences **353**:1577-1593.

Cook, L. M. 2005. Disequilibrium in some *Cepaea* populations. Heredity **94**:497-500.

Cook, L. M. 2008. Variation with habitat in *Cepaea nemoralis*: The Cain & Sheppard diagram. Journal of Molluscan Studies **74**:239-243.

Cook, L. M. 2014. Morph frequency in British *Cepaea nemoralis*: What has changed in half a century? Journal of Molluscan Studies **80**:43-46.

Cook, L. M. 2017. Reflections on molluscan shell polymorphisms. Biological Journal of the Linnean Society **121**:717-730.

Cook, L. M., R. H. Cowie, and J. S. Jones. 1999. Change in morph frequency in the snail *Cepaea nemoralis* on the Marlborough downs. Heredity **82**:336-1999.

Cook, L. M., and P. M. Freeman. 1986. Heating properties of morphs of the mangrove snail *Littoraria pallescens*. Biological Journal of the Linnean Society **29**:295-300.

Cook, L. M., and I. J. Saccheri. 2013. The peppered moth and industrial melanism: Evolution of a natural selection case study. Heredity **110**:207-212.

Coote, T., and É. Loève. 2003. From 61 species to five: endemic tree snails of the Society Islands fall prey to an ill-judged biological control programme. Oryx **37**:91-96.

Cossins, A., J. Fraser, M. Hughes, and A. Gracey. 2006. Post-genomic approaches to understanding the mechanisms of environmentally induced phenotypic plasticity. Journal of Experimental Biology **209**:2328-2336.

Cote, J., J. F. Le Galliard, J. M. Rossi, and P. S. Fitze. 2008. Environmentally induced changes in carotenoid-based coloration of female lizards: a comment on Vercken et al. Journal of Evolutionary Biology **21**:1165-1172.

Cowie, R. H. 1992. Evolution and extinction of Partulidae, endemic Pacific island land snails. Philosophical Transactions of the Royal Society of London. Series B: Biological Sciences **335**:167-191.

Cowie, R. H. 2000. New records of alien land snails and slugs in the Hawaiian Islands. Bishop Museum Occasional Papers **64**:51-53.

Cowie, R. H. 2001a. Can snails ever be effective and safe biocontrol agents? International Journal of Pest Management **47**:23 - 40.

Cowie, R. H. 2001b. Invertebrate invasions on pacific islands and the replacement of unique native faunas: A synthesis of the land and freshwater snails: contribution no. 2001-001 of Bishop Museum's pacific biological survey. Biological Invasions **3**:119-136.

Cowie, R. H., N. L. Evenhuis, and C. C. Christensen. 1995. Catalog of the native land and freshwater molluscs of the Hawaiian Islands. Backhuys Publishers.

Cowie, R. H., and J. S. Jones. 1987. Ecological interactions between *Cepaea nemoralis* and *Cepaea hortensis*: competition, invasion but no niche displacement. Functional Ecology **1**:91-97.

Cuthill, I. C., W. L. Allen, K. Arbuckle, B. Caspers, G. Chaplin, M. E. Hauber, G. E. Hill, N. G. Jablonski, C. D. Jiggins, A. Kelber, J. Mappes, J. Marshall, R. Merrill, D. Osorio, R. Prum, N. W. Roberts, A. Roulin, H. M. Rowland, T. N. Sherratt, J. Skelhorn, M. P. Speed, M. Stevens, M. C. Stoddard, D. Stuart-Fox, L. Talas, E. Tibbetts, and T. Caro. 2017a. The biology of color. Science **357**:eaan0221.

Cuthill, I. C., W. L. Allen, K. Arbuckle, B. Caspers, G. Chaplin, M. E. Hauber, G. E. Hill, N. G. Jablonski, C. D. Jiggins, A. Kelber, J.

Mappes, J. Marshall, R. Merrill, D. Osorio, R. Prum, N. W. Roberts, A. Roulin, H. M. Rowland, T. N. Sherratt, J. Skelhorn, M. P. Speed, M. Stevens, M. C. Stoddard, D. Stuart-Fox, L. Talas, E. Tibbetts, and T. Caro. 2017b. The biology of color. Science **357**:1-7.

Darwin, C. 1859. On the origin of species by means of natural selection, or preservation of favoured races in the struggle for life. London : J Murray, 1859.

Davison, A. 2002. Land snails as a model to understand the role of history and selection in the origins of biodiversity. Population Ecology **44**:0129-0136.

Davison, A. 2020. Flipping shells! Unwinding LR asymmetry in mirror-image molluscs. Trends in Genetics **36**:189-202.

Davison, A., S. Chiba, N. H. Barton, and B. Clarke. 2005. Speciation and gene flow between snails of opposite chirality. PloS Biology **3**:1559-1571.

Davison, A., H. J. Jackson, E. W. Murphy, and T. Reader. 2019. Discrete or indiscrete? Redefining the colour polymorphism of the land snail *Cepaea nemoralis*. Heredity **123**:162-175.

Davison, A., G. S. McDowell, J. M. Holden, H. F. Johnson, C. M. Wade, S. Chiba, D. J. Jackson, M. Levin, and M. L. Blaxter. 2020a. Formin, an opinion. Development **147**.

Davison, A., P. Thomas, and J. t. s. c. scientists. 2020b. Internet 'shellebrity' reflects on origin of rare mirror-image snails. Biology Letters **16**:20200110.

de Carvalho, G. P., P. R. Cavalcante, A. C. de Castro, and M. O. Rojas. 2000. Preliminary assessment of heavy metal levels in *Mytella falcata* (Bivalvia, Mytilidae) from Bacanga River estuary, Sao Luis, state of Maranhao, northeastern Brazil. Revista Brasileira de Biologia **60**:11-16.

Delhey, K., V. Delhey, B. Kempenaers, and A. Peters. 2015. A practical framework to analyze variation in animal colors using visual models. Behavioral Ecology **26**:367-375.

Delima-Baron, E. M., R. Ureta, E. K. Fancobila, C. M. Badua, C. L. Ynot, C. J. Macad, and A. B. M. Mohaga. 2017. Band pattern of land snail shells from Lake Sebu, South Cotabato, Philippines. Imperial journal of interdisciplinary research **3**:614-616.

Dieterich, A., U. Fischbach, M. Ludwig, M. A. Di Lellis, S. Troschinski, U. Gartner, R. Triebskorn, and H. R. Kohler. 2013. Daily and seasonal changes in heat exposure and the Hsp70 level of individuals from a field population of *Xeropicta derbentina*

(Krynicki 1836) (Pulmonata, Hygromiidae) in Southern France. Cell Stress Chaperones **18**:405-414.

Doherty, T. S., A. S. Glen, D. G. Nimmo, E. G. Ritchie, and C. R. Dickman. 2016. Invasive predators and global biodiversity loss. Proceedings of the National Academy of Sciences of the United States of America **113**:11261-11265.

Donachie, S. P., S. Hou, K. S. Lee, C. W. Riley, A. Pikina, C. Belisle, S. Kempe, T. S. Gregory, A. Bossuyt, J. Boerema, J. Liu, T. A. Freitas, A. Malahoff, and M. Alam. 2004. The Hawaiian Archipelago: A microbial diversity hotspot. Microbial Ecology **48**:509-520.

Douglas, R. H., M. J. Genner, A. G. Hudson, J. C. Partridge, and H. J. Wagner. 2016. Localisation and origin of the bacteriochlorophyll-derived photosensitizer in the retina of the deep-sea dragon fish *Malacosteus niger*. Scientific Reports **6**:1-12.

Dunning, J., A. W. Diamond, S. E. Christmas, E. L. Cole, R. L. Holberton, H. J. Jackson, K. G. Kelly, D. Brown, I. R. Rivera, and D. Hanley. 2018. Photoluminescence in the bill of the Atlantic Puffin *Fratercula arctica*. Bird Study **65**:570-573.

Ebert, D., and P. D. Fields. 2020. Host-parasite co-evolution and its genomic signature. Nature Reviews Genetics **21**:754-768.

Egorov, R. 2018. On the distribution of introduced species of the genus *Cepaea*, 1838 (Gastropoda: Pulmonata: Helicidae) in European Russia. Nachrichtenblatt der Ersten Vorarlberger Malakologischen Gesellschaft **25**:79-102.

El-Gendy, K. S., A. F. Gad, and M. A. Radwan. 2021. Physiological and behavioral responses of land molluscs as biomarkers for pollution impact assessment: A review. Environmental Research **193**.

Eldredge, L. G. 2006. Numbers of Hawaiian species for 2003–2005. Bishop Museum Occasional Papers **88**:62-79.

Emberton, L. R. B. 1963. Relationships between pigmentation of shell and of mantle in the snails *Cepaea nemoralis* (L.) and *Cepaea hortensis* (Mull.). Proceedings of the Zoological Society of London **140**:273-293.

Endler, J. A. 1980. Natural Selection on Color Patterns in Poecilia Reticulata. Evolution **34**:76-91.

Endler, J. A. 1990. On the Measurement and Classification of Color in Studies of Animal Color Patterns. Biological Journal of the Linnean Society **41**:315-352.

Endler, J. A., and J. Mappes. 2017. The current and future state of animal coloration research. Philosophical Transactions of the Royal Society B: Biological Sciences **372**.

Endler, J. A., and P. W. Mielke, JR. 2005. Comparing entire colour patterns as birds see them. Biological Journal of the Linnean Society **86**:405-431.

Fasano, G., and A. Franceschini. 1987. A multidimensional version of the Kolmogorov–Smirnov test. Monthly Notices of the Royal Astronomical Society **225**:155-170.

Ferreira, S., R. Ashby, G. J. Jeunen, K. Rutherford, C. Collins, E. V. Todd, and N. J. Gemmell. 2020. DNA from mollusc shell: a valuable and underutilised substrate for genetic analyses. PeerJ **8**.

Fisher, R. A., and C. Diver. 1934. Crossing-over in the land snail *Cepaea nemoralis*, L. Nature **133**:834-835.

Fleishman, L. J., M. Leal, and J. Sheehan. 2006. Illumination geometry, detector position and the objective determination of animal signal colours in natural light. Animal Behaviour **71**:463-474.

Ford, E. B. 1945. Polymorphism. Biological Reviews of the Cambridge Philosophical Society **20**:73-88.

Ford, E. B. 1975. Ecological Genetics. Chapman and Hall.

Forsman, A. 2016. Is colour polymorphism advantageous to populations and species? Molecular Ecology **25**:2693-2698.

Forsman, A., and M. Hagman. 2009. Association of coloration mode with population declines and endangerment in Australian frogs. Conservation Biology **23**:1535-1543.

Foster, S., C. King, B. Patty, and S. Miller. 2011. Tree-climbing capabilities of Norway and ship rats. New Zealand Journal of Zoology **38**:285-296.

Fronhofer, E. A., A. Kubisch, T. Hovestadt, and H. J. Poethke. 2011. Assortative mating counteracts the evolution of dispersal polymorphisms. Evolution **65**:2461-2469.

Garb, J. E., and R. G. Gillespie. 2006. Island hopping across the central Pacific: mitochondrial DNA detects sequential colonization of the Austral Islands by crab spiders (Araneae : Thomisidae). Journal of Biogeography **33**:201-220.

Geist, J., H. Wunderlich, and R. Kuehn. 2008. Use of mollusc shells for DNA-based molecular analyses. Journal of Molluscan Studies **74**:337-343.

Gerlach, J., G. M. Barker, C. S. Bick, P. Bouchet, G. Brodie, C. C. Christensen, T. Collins, T. Coote, R. H. Cowie, G. C. Fiedler, O. L. Griffiths, F. B. V. Florens, K. A. Hayes, J. Kim, J. Y. Meyer, W. M. Meyer, I. Richling, J. D. Slapcinsky, L. Winsor, and N. O. W. Yeung. 2021. Negative impacts of invasive predators used as biological control agents against the pest snail *Lissachatina fulica*: the snail *Euglandina 'rosea'* and the flatworm *Platydemus manokwari*. Biological Invasions **23**:997-1031.

Gheoca, V. 2018. The First Record of Cepaea nemoralis (Linnaeus, 1758) (Stylommatophora: Helicidae) from Romania. Acta Zoologica Bulgarica **70**:129-132.

Gheoca, V., A. M. Benedek, R. A. D. Cameron, and R. C. Stroia. 2019. A century after introduction: variability in Cepaea hortensis (Muller, 1774) in Sibiu, central Romania. Journal of Molluscan Studies **85**:197-203.

Gillespie, R. G., and G. S. Oxford. 1998. Selection on the color polymorphism in Hawaiian happy-face spiders: Evidence from genetic structure and temporal fluctuations. Evolution **52**:775-783.

Glaser, M. 2003. Interrelations between mangrove ecosystem, local economy and social sustainability in Caete Estuary, North Brazil. Wetlands Ecology and Management **11**:265-272.

Gonzalez, D. R., A. C. Aramendia, and A. Davison. 2019. Recombination within the Cepaea nemoralis supergene is confounded by incomplete penetrance and epistasis. Heredity **123**:153-161.

Goodhart, C. B. 1958. Thrush predation on the snail *Cepaea hortensis*. Journal of Animal Ecology **27**:47-57.

Goodhart, C. B. 1963. Area Effect and Non-Adaptive Variation between Populations of Cepaea (Mollusca). Heredity **18**:459-&.

Grant, B. S., D. F. Owen, and C. A. Clarke. 1996. Parallel rise and fall of melanic peppered moths in America and Britain. Journal of Heredity **87**:351-357.

Grant, P. R., and B. R. Grant. 2016. Introgressive hybridization and natural selection in Darwin's finches. Biological Journal of the Linnean Society **117**:812-822.

Gravan, C., and R. Lahoz-Beltra. 2004. Evolving morphogenetic fields in the zebra skin pattern based on Turing's morphogen hypothesis. International Journal of Applied Mathematics and Computer Science **14**:351-361.

Gray, S. M., and J. S. McKinnon. 2007. Linking color polymorphism maintenance and speciation. Trends in Ecology and Evolution **22**:71-79.

Grindon, A. J., and A. Davison. 2013. Irish *Cepaea nemoralis* land snails have a cryptic Franco-Iberian origin that is most easily explained by the movements of Mesolithic humans. Plos One **8**:e65792.

Guilford, T., and M. S. Dawkins. 1991. Receiver psychology and the evolution of animal signals. Animal Behaviour **42**:1-14.

Gupta, S. K., and J. Singh. 2011. Evaluation of molluscs as sensitive indicatior of heavy metal pollution in aquatic system: A review. Institute of Integrative Omics and Applied Biotechnology **2**:49-57.

Gural-Sverlova, N. V., and R. I. Gural. 2021. Shell banding and colour polymorphism of introduced snail Cepaea hortensis (Gastropoda, Pulmonata, Helicidae) from some parts of Eastern Europe. Ruthenica **31**:59-76.

Hadfield, M., and B. S. Mountain. 1980. A field study of a vanishing species, *Achatinella mustelina* (gastropoda, pulmonata), in the Waianae mountains of Oahu. Pacific Science **34**:345-358.

Hadfield, M. G., and D. J. Haraway. 2019. The tree snail manifesto. Current Anthropology **60**:209-235.

Hadfield, M. G., S. E. Miller, and A. H. Carwile. 1993. The decimation of endemic Hawai'ian tree snails by alien predators. American Zoologist **33**:610-622.

Hadfield, M. G., and J. E. Saufler. 2009. The demographics of destruction: isolated populations of arboreal snails and sustained predation by rats on the island of Moloka'i 1982-2006. Biological Invasions **11**:1595-1609.

Harosi, F. I. 1996. Visual pigment types and quantum-catch ratios: implications from three marine teleosts. The Biological Bulletin **190**:203-212.

Harper, M. A., Z. Chen, T. Toy, I. M. P. Machado, S. F. Nelson, J. C. Liao, and C. J. Lee. 2011. Phenotype sequencing: Identifying the genes that cause a phenotype directly from pooled sequencing of independent mutants. Plos One **6**:e16517.

Hart, N. S. 2001a. Variations in cone photoreceptor abundance and the visual ecology of birds. Journal of Comparative Physiology A: Neuroethology Sensory Neural and Behavioral Physiology **187**:685-697.

Hart, N. S. 2001b. The visual ecology of avian photoreceptors. Progress in Retinal and Eye Research **20**:675-703.

Hart, N. S., and D. M. Hunt. 2007. Avian visual pigments: Characteristics, spectral tuning, and evolution. American Naturalist **169**:7-26.

Hart, N. S., J. C. Partridge, I. C. Cuthill, and A. T. D. Bennett. 2000. Visual pigments, oil droplets, ocular media and cone photoreceptor distribution in two species of passerine bird: the blue tit (*Parus caeruleus* L.) and the blackbird (*Turdus merula* L.). Journal of Comparative Physiology A: Sensory Neural and Behavioral Physiology **186**:375-387.

Hartman, W. D. 1888. A bibliographic and synonymic catalogue of the genus *Achatinella*. Proceedings of the Academy of Natural Sciences of Philadelphia **40**:16-56.

Hawk, H. L., and J. B. Geller. 2019. DNA entombed in archival seashells reveals low historical mitochondrial genetic diversity of endangered white abalone *Haliotis sorenseni*. Marine and Freshwater Research **70**:359-370.

Hazel, W. N., and M. S. Johnson. 1990. Microhabitat choice and polymorphism in the land snail *Theba pisana* (Muller). Heredity **65**:449-454.

Heath, D. J. 1975. Color, Sunlight and Internal Temperatures in Land-Snail Cepaea-Nemoralis (L). Oecologia **19**:29-38.

Hegna, R. H., R. A. Saporito, and M. A. Donnelly. 2013. Not all colors are equal: predation and color polytypism in the aposematic poison frog Oophaga pumilio. Evolutionary Ecology **27**:831-845.

Heller, J. 1981. Visual versus climatic selection of shell banding in the landsnail *Theba pisana* in Israel. Journal of Zoology **194**:85-101.

Hickman, C. S. 2002. Origination, evolutionary radiation, and extinction in the modern world: The story of partulid tree snails. The Paleontological Society Special Publications **11**:211-226.

Hirota, S. K., N. Miki, A. A. Yasumoto, and T. Yahara. 2019. UV bullseye contrast of *Hemerocallis* flowers attracts hawkmoths but not swallowtail butterflies. Ecology and Evolution **9**:52-64.

Hoagland, K. E. 1977. Gastropod Color Polymorphism - One Adaptive Strategy of Phenotypic Variation. Biological Bulletin **152**:360-372.

Hodge, J. R., F. Santini, and P. C. Wainwright. 2020. Colour dimorphism in labrid fishes as an adaptation to life on coral reefs.

Proceedings of the Royal Society B: Biological Sciences **287**:20200167.

Hohagen, J., and D. J. Jackson. 2013. An ancient process in a modern mollusc: early development of the shell in Lymnaea stagnalis. Bmc Developmental Biology **13**.

Holland, B. S., L. M. Chiaverano, and C. K. Howard. 2017. Diminished fitness in an endemic Hawaiian snail in nonnative host plants. Ethology Ecology & Evolution **29**:229-240.

Holland, B. S., T. Chock, A. Lee, and S. Sugiura. 2012. Tracking behavior in the snail *Euglandina rosea*: First evidence of preference for endemic vs. biocontrol target pest species in Hawaii. American Malacological Bulletin **30**:153-157.

Holland, B. S., M. Gousy-Leblanc, and J. Y. Yew. 2018. Strangers in the dark: behavioral and biochemical evidence for trail pheromones in Hawaiian tree snails. Invertebrate Biology **137**:124-132.

Holland, B. S., and M. G. Hadfield. 2002. Islands within an island: phylogeography and conservation genetics of the endangered Hawaiian tree snail *Achatinella mustelina*. Molecular Ecology **11**:365-375.

Holland, B. S., S. L. Montgomery, and V. Costello. 2010. A reptilian smoking gun: first record of invasive Jackson's chameleon (*Chamaeleo jacksonii*) predation on native Hawaiian species. Biodiversity and Conservation **19**:1437-1441.

Holmes, I. A., M. R. Grundler, and A. R. Davis Rabosky. 2017. Predator perspective drives geographic variation in frequency-dependent polymorphism. The American Naturalist **190**:78-93.

Holveck, M. J., A. Gregoire, R. Guerreiro, V. Staszewski, T. Boulinier, D. Gomez, and C. Doutrelant. 2017. Kittiwake eggs viewed by conspecifics and predators: implications for colour signal evolution. Biological Journal of the Linnean Society **122**:301-312.

Honkavaara, J., M. Koivula, E. Korpimaki, H. Siitari, and J. Viitala. 2002. Ultraviolet vision and foraging in terrestrial vertebrates. Oikos **98**:505-511.

Hughes, J. M., and P. B. Mather. 1986. Evidence for Predation as a Factor in Determining Shell Color Frequencies in a Mangrove Snail Littorina Sp (Prosobranchia, Littorinidae). Evolution **40**:68-77.

Hurst, C. C. 1906. On the inheritance of coat colour in horses. Proceedings of the Royal Society of London. Series B, Containing Papers of a Biological Character **77**:388-394.

Husby, A., T. Kawakami, L. Ronnegard, L. Smeds, H. Ellegren, and A. Qvarnstrom. 2015. Genome-wide association mapping in a wild avian population identifies a link between genetic and phenotypic variation in a life-history trait. Proceedings of the Royal Society B-Biological Sciences **282**.

Hutchinson, J. M. C. 1989. Control of Gastropod Shell Shape - the Role of the Preceding Whorl. Journal of Theoretical Biology **140**:431-444.

Huxley, J. 1955. Morphism in birds. Acta: International Congress of Ornithology **11**:309-328.

Jackson, D. J., C. McDougall, K. Green, F. Simpson, G. Worheide, and B. M. Degnan. 2006. A rapidly evolving secretome builds and patterns a sea shell. BMC Biol **4**:40.

Jackson, D. J., C. McDougall, B. Woodcroft, P. Moase, R. A. Rose, M. Kube, R. Reinhardt, D. S. Rokhsar, C. Montagnani, C. Joubert, D. Piquemal, and B. M. Degnan. 2010. Parallel Evolution of Nacre Building Gene Sets in Molluscs. Molecular Biology and Evolution **27**:591-608.

Jackson, D. J., G. Worheide, and B. M. Degnan. 2007. Dynamic expression of ancient and novel molluscan shell genes during ecological transitions. Bmc Evolutionary Biology **7**:160.

Jackson, H. J., J. Larsson, and A. Davison. 2021. Quantitative measures and 3D shell models reveal interactions between bands and their position on growing snail shells. Ecology and Evolution **11**:6634-6648.

Jacobs, G. H. 2009. Evolution of colour vision in mammals. Philosophical Transactions of the Royal Society B: Biological Sciences **364**:2957-2967.

Jacobs, G. H. 2012. The Evolution of Vertebrate Color Vision. Sensing in Nature **739**:156-172.

Jamie, G. A., and J. I. Meier. 2020. The persistence of polymorphisms across species radiations. Trends in Ecology and Evolution **35**:795-808.

Jiang, Y., D. I. Bolnick, and M. Kirkpatrick. 2013. Assortative mating in animals. The American Naturalist **181**:E125-138.

Johannesson, K., and R. K. Butlin. 2017. What explains rare and conspicuous colours in a snail? A test of time-series data against models of drift, migration or selection. Heredity **118**:21-30.

Johnson, A. B., N. S. Fogel, and J. D. Lambert. 2019. Growth and morphogenesis of the gastropod shell. Proceedings of the National Academy of Sciences **116**:6878-6883.

Johnson, M. S. 1982. Polymorphism for direction of coil in *Partula suturalis* - behavioral isolation and positive frequency-dependent selection. Heredity **49**:145-151.

Johnson, M. S. 2011. Thirty-four years of climatic selection in the land snail *Theba pisana*. Heredity **106**:741-748.

Johnson, M. S. 2012. Epistasis, phenotypic disequilibrium and contrasting associations with climate in the land snail *Theba pisana*. Heredity **108**:229-235.

Jones, J. S., B. H. Leith, and P. Rawlings. 1977. Polymorphism in *Cepaea*: A problem with too many solutions? Annual Review of Ecology and Systematics **8**:109-143.

Joubert, C., D. Piquemal, B. Marie, L. Manchon, F. Pierrat, I. Zanella-Cléon, N. Cochennec-Laureau, Y. Gueguen, and C. Montagnani. 2010. Transcriptome and proteome analysis of *Pinctada margaritifera* calcifying mantle and shell: Focus on biomineralization. BMC Genomics **11**:613.

Kelber, A. 2019. Bird colour vision - from cones to perception. Current Opinion in Behavioral Sciences **30**:34-40.

Kelber, A., and D. Osorio. 2010. From spectral information to animal colour vision: experiments and concepts. Proceedings of the Royal Society B: Biological Sciences **277**:1617-1625.

Kemp, D. J. 2007. Female mating biases for bright ultraviolet iridescence in the butterfly Eurema hecabe (Pieridae). Behavioral Ecology **19**:1-8.

Kerkvliet, J., T. de Boer, M. Schilthuizen, and K. Kraaijeveld. 2017. Candidate genes for shell colour polymorphism in *Cepaea nemoralis*. PeerJ **5**:e3715.

Kniprath, E. 1981. Ontogeny of the molluscan shell field: A review. Zoologica Scripta **10**:61-79.

Kocot, K. M., F. Aguilera, C. McDougall, D. J. Jackson, and B. M. Degnan. 2016. Sea shell diversity and rapidly evolving secretomes: insights into the evolution of biomineralization. Frontiers in Zoology **13**:23.

Kondo, S. 2002. The reaction-diffusion system: A mechanism for autonomous pattern formation in the animal skin. Genes to Cells **7**:535-541.

Kondo, S., and T. Miura. 2010. Reaction-diffusion model as a framework for understanding biological pattern formation. Science **329**:1616-1620.

Kottler, M. J. 1980a. Darwin, Wallace, and the origin of sexual dimorphism. Proceedings of the American Philosophical Society **124**:203-226.

Kottler, M. J. 1980b. Darwin, Wallace, and the origin of sexual dimorphism. Proc Am Philos Soc **124**:203-226.

Kouchinsky, A. 2000. Shell microstructures in Early Cambrian molluscs. Acta Palaeontologica Polonica **45**:119-150.

Kraus, F., A. Medeiros, D. Preston, C. S. Jarnevich, and G. H. Rodda. 2012. Diet and conservation implications of an invasive chameleon, *Chamaeleo jacksonii* (Squamata: Chamaeleonidae) in Hawaii. Biological Invasions **14**:579-593.

Kunte, K. 2009. The diversity and evolution of batesian mimicry in Papilio swallowtail butterflies. Evolution **63**:2707-2716.

Kuroda, R., and M. Abe. 2020a. The pond snail Lymnaea stagnalis. Evodevo **11**.

Kuroda, R., and M. Abe. 2020b. Response to 'Formin, an opinion'. Development **147**.

Kwiecinski, Z., Z. M. Rosin, L. Jankowiak, T. H. Sparks, and P. Tryjanowski. 2019. Thrush anvils are calcium source hotspots for many bird species. Biological Journal of the Linnean Society **128**:603-610.

Lamotte, M. 1959. Polymorphism of natural populations of *Cepaea nemoralis*. Cold Spring Harbor Symposia on Quantitative Biology **24**:65-86.

Landgrebe, J., G. Welzl, T. Metz, M. M. Van Gaalen, H. Ropers, W. Wurst, and F. Holsboer. 2002. Molecular characterisation of antidepressant effects in the mouse brain using gene expression profiling. Journal of Psychiatric Research **36**:119-129.

Larsson, J., A. M. Westram, S. Bengmark, T. Lundh, and R. K. Butlin. 2020. A developmentally descriptive method for quantifying shape in gastropod shells. Journal of the Royal Society Interface **17**:20190721.

Layton, K. K. S., C. P. K. Warne, A. Nicolai, A. Ansart, and J. R. deWaard. 2019. Molecular evidence for multiple introductions of the banded grove snail (Cepaea nemoralis) in North America. Canadian Journal of Zoology **97**:392-398.

Liew, T.-S., and M. Schilthuizen. 2016. A method for quantifying, visualising, and analysing gastropod shell form. Plos One **11**:e0157069.

Limerick, S. 1980. Courtship behavior and oviposition of the poison-arrow frog *Dendrobates pumilio*. Herpetologica **36**:69-71.

Lindberg, W. F. P. D. R. 2008. Phylogeny and Evolution of the Mollusca. Univ of California Press.

Lindstedt, C., J. H. R. Talsma, E. Ihalainen, L. Lindström, and J. Mappes. 2010. Diet quality affects warning coloration indirectly: Excretion costs in a generalist herbivore. Evolution **64**:68-78.

Lipton, C. S., and J. Murray. 1979. Courtship of land snails of the genus *Partula*. Malacologia **19**:129-146.

Loope, L., and F. Kraus. 2009. Preventing establishment and spread of invasive species: Current status and needs. Yale University Press.

Lopes, R. H. C., P. R. Hobson, and I. D. Reid. 2008. Computationally efficient algorithms for the two-dimensional Kolmogorov–Smirnov test. Journal of Physics: Conference Series **119**:042019.

Lydeard, C., R. H. Cowie, W. F. Ponder, A. E. Bogan, P. Bouchet, S. A. Clark, K. S. Cummings, T. J. Frest, O. Gargominy, D. G. Herbert, R. Hershler, K. E. Perez, B. Roth, M. Seddon, E. E. Strong, and F. G. Thompson. 2004. The global decline of nonmarine mollusks. Bioscience **54**:321-330.

MacArthur, R. H., and E. O. Wilson. 1967. The theory of island biogeography. Princeton University Press, Princeton, N.J.

Maia, R., H. Gruson, J. A. Endler, and T. E. White. 2019. pavo 2: New tools for the spectral and spatial analysis of colour in R. Methods in Ecology and Evolution **10**:1097-1107.

Maia, R., and T. E. White. 2018. Comparing colors using visual models. Behavioral Ecology **29**:649-659.

Majerus, M. E. N., C. F. A. Brunton, and J. Stalker. 2000. A bird's eye view of the peppered moth. Journal of Evolutionary Biology **13**:155-159.

Mann, K., and D. J. Jackson. 2014. Characterization of the pigmented shell-forming proteome of the common grove snail *Cepaea nemoralis*. BMC Genomics **15**:249.

Marie, B., D. J. Jackson, P. Ramos-Silva, I. Zanella-Cleon, N. Guichard, and F. Marin. 2013. The shell-forming proteome of *Lottia*

gigantea reveals both deep conservations and lineage-specific novelties. FEBS J **280**:214-232.

Marie, B., C. Joubert, A. Tayale, I. Zanella-Cleon, C. Belliard, D. Piquemal, N. Cochennec-Laureau, F. Marin, Y. Gueguen, and C. Montagnani. 2012. Different secretory repertoires control the biomineralization processes of prism and nacre deposition of the pearl oyster shell. Proceedings of the National Academy of Sciences of the United States of America **109**:20986-20991.

Marshall, N. J., K. Jennings, W. N. McFarland, E. R. Loew, and G. S. Losey. 2003. Visual biology of Hawaiian coral reef fishes. III. Environmental light and an integrated approach to the ecology of reef fish vision. Copeia **3**:467-480.

Martin, K. R., L. P. Waits, and C. E. Parent. 2021. Teaching an Old Shell New Tricks: Extracting DNA from Current, Historical, and Ancient Mollusk Shells. Bioscience **71**:235-248.

McConkey, K., and D. Drake. 2015. Low redundancy in seed dispersal within an island frugivore community. Annals of Botany: Plants **7**.

McCoy, D. E., A. J. Shultz, C. Vidoudez, E. van der Heide, J. E. Dall, S. A. Trauger, and D. Haig. 2021. Microstructures amplify carotenoid plumage signals in tanagers. Scientific Reports **11**:8582.

McLean, C. A., and D. Stuart-Fox. 2014. Geographic variation in animal colour polymorphisms and its role in speciation. Biological Reviews **89**:860-873.

Medina, M., S. Lal, Y. Valles, T. L. Takaoka, B. A. Dayrat, J. L. Boore, and T. Gosliner. 2011. Crawling through time: Transition of snails to slugs dating back to the Paleozoic, based on mitochondrial phylogenomics. Marine Genomics **4**:51-59.

Meinhardt, H., and M. Klingler. 1987. A model for pattern formation on the shells of molluscs. Journal of Theoretical Biology **126**:63-89.

Meyer, W. M. 2006. Records of rare ground-dwelling land snails on Oahu. Bishop Museum Occasional Papers **88**:57-58.

Meyer, W. M., and R. H. Cowie. 2011. Distribution, movement, and microhabitat use of the introduced predatory snail *Euglandina rosea* in Hawaii: implications for management. Invertebrate Biology **130**:325-333.

Meyer, W. M., L. M. Evans, C. J. K. Kalahiki, J. Slapcinsky, T. C. Goulding, D. G. Robinson, D. P. Kaniaupo-Crozier, J. R. Kim, K. A. Hayes, and N. W. Yeung. 2021. Plants critical for Hawaiian land snail conservation: arboreal snail plant preferences in Puʻu Kukui Watershed, Maui. Oryx:1-6.

Meyer, W. M., and A. B. Shiels. 2009. Black rat (*Rattus rattus*) predation on nonindigenous snails in Hawai'i: Complex management implications. Pacific Science **63**:339-347.

Meyer, W. M., N. W. Yeung, J. Slapcinsky, and K. A. Hayes. 2017. Two for one: inadvertent introduction of *Euglandina* species during failed bio-control efforts in Hawaii. Biological Invasions **19**:1399-1405.

Muller, P., K. W. Rogers, B. M. Jordan, J. S. Lee, D. Robson, S. Ramanathan, and A. F. Schier. 2012. Differential Diffusivity of Nodal and Lefty Underlies a Reaction-Diffusion Patterning System. Science **336**:721-724.

Murray, J. 1963a. Inheritance of some characters in *Cepaea hortensis* and *Cepaea nemoralis* (Gastropoda). Genetics **48**:605-615.

Murray, J. 1963b. The inheritance of some characters in *Cepaea hortensis* and *Cepaea nemoralis* (Gastropoda). Genetics **48**:605-615.

Murray, J., and B. Clarke. 1966. The inheritance of polymorphic shell characters in *Partula* (gastropoda). Genetics **54**:1261-1277.

Murray, J., and B. Clarke. 1976. Supergenes in polymorphic land snails. I. *Partula taeniata*. Heredity **37**:253-269.

Myers, N., R. A. Mittermeier, C. G. Mittermeier, G. A. B. da Fonseca, and J. Kent. 2000. Biodiversity hotspots for conservation priorities. Nature **403**:853-858.

Nakamasu, A., G. Takahashi, A. Kanbe, and S. Kondo. 2009. Interactions between zebrafish pigment cells responsible for the generation of Turing patterns. Proceedings of the National Academy of Sciences of the United States of America **106**:8429-8434.

Neiber, M. T., and B. Hausdorf. 2015. Molecular phylogeny reveals the polyphyly of the snail genus *Cepaea* (Gastropoda: Helicidae). Molecular Phylogenetics and Evolution **93**:143-149.

Neiber, M. T., C. Sagorny, and B. Hausdorf. 2016. Increasing the number of molecular markers resolves the phylogenetic relationship of *'Cepaea' vindobonensis* (Pfeiffer 1828) with *Caucasotachea Boettger* 1909 (Gastropoda: Pulmonata: Helicidae). Journal of Zoological Systematics and Evolutionary Research **54**:40-45.

Noda, T., N. Satoh, and T. Asami. 2019. Heterochirality results from reduction of maternal diaph expression in a terrestrial pulmonate snail. Zoological Letters **5**.

O'Dowd, D. J., P. T. Green, and P. S. Lake. 2003. Invasional 'meltdown' on an oceanic island. Ecology Letters **6**:812-817.

Olsson, P., O. Lind, and A. Kelber. 2015. Bird colour vision: behavioural thresholds reveal receptor noise. Journal of Experimental Biology **218**:184-193.

Olsson, P., O. Lind, and A. Kelber. 2018. Chromatic and achromatic vision: parameter choice and limitations for reliable model predictions. Behavioral Ecology **29**:273-282.

Örstan, A. 2010. Gastropoda, Pulmonata, Helicidae, Cepaea nemoralis (Linnaeus, 1758): New records for Montreal, Canada. Check List **6**:054-055.

Ortiz, E. 1973. Genetic polymorphism and natural-selection in Spanish populations of the snail *Cepaea nemoralis*. Genetics **74**:205-205.

Osorio, D., and M. Vorobyev. 2008. A review of the evolution of animal colour vision and visual communication signals. Vision Research **48**:2042-2051.

Osterauer, R., L. Marschner, O. Betz, M. Gerberding, B. Sawasdee, P. Cloetens, N. Haus, B. Sures, R. Triebskorn, and H. R. Kohler. 2010. Turning snails into slugs: induced body plan changes and formation of an internal shell. Evolution & Development **12**:474-483.

Ożgo, M. 2005. *Cepaea nemoralis* (L.) in southeastern Poland: Association of morph frequencies with habitat. Journal of Molluscan Studies **71**:93-103.

Ożgo, M. 2011. Rapid evolution in unstable habitats: A success story of the polymorphic land snail *Cepaea nemoralis* (Gastropoda: Pulmonata). Biological Journal of the Linnean Society **102**:251-262.

Ożgo, M. 2012. Shell polymorphism in the land-snail *Cepaea nemoralis* (L.) along a west-east transect in continental Europe. Folia Malacologica **20**:181-253.

Ożgo, M., and A. Komorowska. 2009. Shell banding polymorphism in *Cepaea vindobonensis* in relation to habitat in southeastern Poland. Malacologia **51**:81-88.

Ożgo, M., T. S. Liew, N. B. Webster, and M. Schilthuizen. 2017. Inferring microevolution from museum collections and resampling: Lessons learned from *Cepaea*. PeerJ **5**:e3938.

Ożgo, M., and M. Schilthuizen. 2012. Evolutionary change in *Cepaea nemoralis* shell colour over 43 years. Global Change Biology **18**:74-81.

Parkhaev, P. Y. 2017. Origin and the Early Evolution of the Phylum Mollusca. Paleontological Journal **51**:663-686.

Paterson, J. E., and G. Blouin-Demers. 2017. Distinguishing discrete polymorphism from continuous variation in throat colour of tree lizards, *Urosaurus ornatus*. Biological Journal of the Linnean Society **121**:72-81.

Paulay, G. 1994. Biodiversity on oceanic islands - its origin and extinction. American Zoologist **34**:134-144.

Peichel, C. L., and D. A. Marques. 2017. The genetic and molecular architecture of phenotypic diversity in sticklebacks. Philosophical Transactions of the Royal Society B: Biological Sciences **372**:20150486.

Pejchar, L., C. A. Lepczyk, J. E. Fantle-Lepczyk, S. C. Hess, M. T. Johnson, C. R. Leopold, M. Marchetti, K. M. Mcclure, and A. B. Shiels. 2020. Hawaii as a microcosm: Advancing the science and practice of managing introduced and invasive species. Bioscience **70**:184-193.

Pérez i de Lanuza, G., E. Font, and P. Carazo. 2012. Color-assortative mating in a color-polymorphic lacertid lizard. Behavioral Ecology **24**:273-279.

Pilsbry, H. A. 1895. Manual of conchology. Index to Helices (2) **9**:1-126.

Pimm, S. L. 1991. The balance of nature: ecological issues in the conservation of species and communities. University of Chicago Press.

Price, M. R., D. Sischo, M. A. Pascua, and M. G. Hadfield. 2015. Demographic and genetic factors in the recovery or demise of ex situ populations following a severe bottleneck in fifteen species of Hawaiian tree snails. PeerJ **3**:e1406.

Punzalan, D., F. H. Rodd, and K. A. Hughes. 2005. Perceptual Processes and the Maintenance of Polymorphism Through Frequency-dependent Predation. Evolutionary Ecology **19**:303-320.

R Core Team. 2021. R: A language and environment for statistical computing. R Foundation for Statistical Computing, Vienna, Austria. URL https://www.R-project.org/.

Raffaelli, D. 1982. Recent Ecological Research on Some European Species of Littorina. Journal of Molluscan Studies **48**:342-354.

Rankin, K. J., C. A. McLean, D. J. Kemp, and D. Stuart-Fox. 2016. The genetic basis of discrete and quantitative colour variation in the

polymorphic lizard, Ctenophorus decresii. Bmc Evolutionary Biology **16**.

Reed, C. F. 1964. *Cepaea nemoralis* (Linn.) in eastern North America. Sterkiana **16**:11-18.

Regnier, C., B. Fontaine, and P. Bouchet. 2009. Not knowing, not recording, not listing: Numerous unnoticed mollusk extinctions. Conservation Biology **23**:1214-1221.

Reid, D. G. 1987. Natural selection for apostasy and crypsis acting on the shell color polymorphism of a mangrove snail, *Littoraria filosa* (Sowerby) (Gastropoda, Littorinidae). Biological Journal of the Linnean Society **30**:1-24.

Richards, P. M., M. M. Liu, N. Lowe, J. W. Davey, M. L. Blaxter, and A. Davison. 2013. RAD-Seq derived markers flank the shell colour and banding loci of the *Cepaea nemoralis* supergene. Molecular Ecology **22**:3077-3089.

Rohrer, J., V. Costello, J. Tanino, L. Bialic-Murphy, M. Akamine, J. Sprague, S. Joe, and C. Smith. 2016. Development of tree snail protection enclosures: from design to implementation. Pacific Cooperative Studies Unit Technical Report:194.

Rojas, D., A. P. Lima, P. Momigliano, P. I. Simoes, R. Y. Dudaniec, T. C. S. de Avila-Pires, M. S. Hoogmoed, Y. O. da Cunha Bitar, I. L. Kaefer, A. Amezquita, and A. Stow. 2020. The evolution of polymorphism in the warning coloration of the Amazonian poison frog *Adelphobates galactonotus*. Heredity **124**:439-456.

Rönkä, K., C. De Pasqual, J. Mappes, S. Gordon, and B. Rojas. 2018. Colour alone matters: no predator generalization among morphs of an aposematic moth. Animal Behaviour **135**:153-163.

Rosenberg, G. 2014. A new critical estimate of named species-level diversity of the recent Mollusca. American Malacological Bulletin **32**:308-322.

Rosin, Z. M., J. Kobak, A. Lesicki, and P. Tryjanowski. 2013. Differential shell strength of *Cepaea nemoralis* colour morphs - Implications for their anti-predator defence. Naturwissenschaften **100**:843-851.

Rotarides, M. 1926. Uber die Bandervariation von *Cepaea vindobonensis* Fer. Zoologischer Anzeiger **67**:28-44.

Roulin, A. 2004. The evolution, maintenance and adaptive function of genetic colour polymorphism in birds. Biological Reviews of the Cambridge Philosophical Society **79**:815-848.

Saenko, S. V., D. S. J. Groenenberg, A. Davison, and M. Schilthuizen. 2021. The draft genome sequence of the grove snail *Cepaea nemoralis*. G3: Genes, Genomes, Genetics **11**:jkaa071.

Saenko, S. V., and M. Schilthuizen. 2021. Evo-devo of shell colour in gastropods and bivalves. Current Opinion in Genetics & Development **69**:1-5.

Sakai, A. K., F. W. Allendorf, J. S. Holt, D. M. Lodge, J. Molofsky, K. A. With, S. Baughman, R. J. Cabin, J. E. Cohen, N. C. Ellstrand, D. E. McCauley, P. O'Neil, I. M. Parker, J. N. Thompson, and S. G. Weller. 2001. The population biology of invasive species. Annual Review of Ecology and Systematics **32**:305-332.

San-Jose, L. M., and A. Roulin. 2017. Genomics of coloration in natural animal populations. Philosophical Transactions of the Royal Society B-Biological Sciences **372**:20160337.

Sandkam, B. A., K. A. Deere-Machemer, A. M. Johnson, G. F. Grether, F. H. Rodd, and R. C. Fuller. 2016. Exploring visual plasticity: dietary carotenoids can change color vision in guppies (*Poecilia reticulata*). Journal of Comparative Physiology A: Neuroethology Sensory Neural and Behavioral Physiology **202**:527-534.

Schilthuizen, M., P. G. Craze, A. S. Cabanban, A. Davison, J. Stone, E. Gittenberger, and B. J. Scott. 2007. Sexual selection maintains whole-body chiral dimorphism in snails. Journal of Evolutionary Biology **20**:1941-1949.

Schilthuizen, M., and A. Davison. 2005. The convoluted evolution of snail chirality. Naturwissenschaften **92**:504-515.

Schwander, T., R. Libbrecht, and L. Keller. 2014. Supergenes and complex phenotypes. Current Biology **24**:288-294.

Scrucca, L., M. Fop, T. B. Murphy, and A. E. Raftery. 2016. Mclust 5: Clustering, classification and density estimation using gaussian finite mixture models. R Journal **8**:289-317.

Shine, R. 1989. Ecological causes for the evolution of sexual dimorphism: a review of the evidence. The Quarterly Review of Biology **64**:419-461.

Siddiqi, A., T. W. Cronin, E. R. Loew, M. Vorobyev, and K. Summers. 2004. Interspecific and intraspecific views of color signals in the strawberry poison frog *Dendrobates pumilio*. Journal of Experimental Biology **207**:2471-2485.

Silvertown, J., L. Cook, R. Cameron, M. Dodd, K. McConway, J. Worthington, P. Skelton, C. Anton, O. Bossdorf, B. Baur, M. Schilthuizen, B. Fontaine, H. Sattmann, G. Bertorelle, M. Correia, C. Oliveira, B. Pokryszko, M. Ożgo, A. Stalažs, E. Gill,

Ü. Rammul, P. Sólymos, Z. Féher, and X. Juan. 2011. Citizen science reveals unexpected continental-scale evolutionary change in a model organism. Plos One **6**:e18927.

Skorupski, P., T. Doring, and L. Chittka. 2007. Photoreceptor spectral sensitivity in island and mainland populations of the bumblebee, *Bombus terrestris*. Journal of Comparative Physiology A: Sensory Neural and Behavioral Physiology **193**:485-494.

Smith, H. M. 2005. A preliminary study of the relationships of taxa included in the tribe Poltyini (Araneae, Araneidae). The Journal of Arachnology **33**:468-481.

Solem, A. 1990. How many Hawaiian land snail species are left? And what we can do for them. Bishop Museum Occasional Papers **30**:27-40.

Spottiswoode, C. N., and M. Stevens. 2010. Visual modeling shows that avian host parents use multiple visual cues in rejecting parasitic eggs. Proceedings of the National Academy of Sciences of the United States of America **107**:8672-8676.

Spottiswoode, C. N., and M. Stevens. 2011. How to evade a coevolving brood parasite: egg discrimination versus egg variability as host defences. Proceedings of the Royal Society B: Biological Sciences **278**:3566-3573.

Ståhl, P. L., F. Salmén, S. Vickovic, A. Lundmark, J. F. Navarro, J. Magnusson, S. Giacomello, M. Asp, J. O. Westholm, M. Huss, A. Mollbrink, S. Linnarsson, S. Codeluppi, Å. Borg, F. Pontén, P. I. Costea, P. Sahlén, J. Mulder, O. Bergmann, J. Lundeberg, and J. Frisén. 2016. Visualization and analysis of gene expression in tissue sections by spatial transcriptomics. Science **353**:78-82.

Staikou, A. E. 1999. Shell temperature, activity and resistance to desiccation in the polymorphic land snail *Cepaea vindobonensis*. Journal of Molluscan Studies **65**:171–184.

Stavenga, D. G., and B. D. Wilts. 2014. Oil droplets of bird eyes: microlenses acting as spectral filters. Philosophical Transactions of the Royal Society B: Biological Sciences **369**.

Stevens, M., and I. C. Cuthill. 2007. Hidden Messages: Are Ultraviolet Signals a Special Channel in Avian Communication? Bioscience **57**:501-507.

Stevens, M., and S. Merilaita. 2009. Animal camouflage: current issues and new perspectives. Philosophical Transactions of the Royal Society B: Biological Sciences **364**:423-427.

Suarez, A. V., and N. D. Tsutsui. 2004. The value of museum collections for research and society. Bioscience **54**:66-74.

Summers, K., R. Symula, M. Clough, and T. Cronin. 1999. Visual mate choice in poison frogs. Proceedings of the Royal Society B: Biological Sciences **266**:2141-2145.

Surmacki, A., A. Ożarowska-Nowicka, and Z. M. Rosin. 2013. Color polymorphism in a land snail *Cepaea nemoralis* (Pulmonata: Helicidae) as viewed by potential avian predators. Naturwissenschaften **100**:533-540.

Svensson, E. I. 2017. Back to basics: using colour polymorphisms to study evolutionary processes. Molecular Ecology **26**:2204-2211.

Szabo, J. K., N. Khwaja, S. T. Garnett, and S. H. M. Butchart. 2012. Global patterns and drivers of avian extinctions at the species and subspecies level. Plos One **7**:e47080.

Takahashi, Y., S. Morita, J. Yoshimura, and M. Watanabe. 2011. A geographic cline induced by negative frequency-dependent selection. Bmc Evolutionary Biology **11**.

Takahashi, Y., J. Yoshimura, S. Morita, and M. Watanabe. 2010. Negative frequency-dependent selection in female color polymorphism of a damselfly. Evolution **64**:3620-3628.

Taylor, A., P. Weigelt, C. Konig, G. Zotz, and H. Kreft. 2019. Island disharmony revisited using orchids as a model group. New Phytologist **223**:597-606.

Taylor, C. H., F. Gilbert, and T. Reader. 2013. Distance transform: a tool for the study of animal colour patterns. Methods in Ecology and Evolution **4**:771-781.

Taylor, C. H., T. Reader, and F. Gilbert. 2016. Hoverflies are imperfect mimics of wasp colouration. Evolutionary Ecology **30**:567-581.

Teasdale, L. C., M. Stevens, and D. Stuart-Fox. 2013. Discrete colour polymorphism in the tawny dragon lizard (*Ctenophorus decresii*) and differences in signal conspicuousness among morphs. Journal of Evolutionary Biology **26**:1035-1046.

Thomas, R. J., L. A. Bartlett, N. M. Marples, D. J. Kelly, and I. C. Cuthill. 2004. Prey selection by wild birds can allow novel and conspicuous colour morphs to spread in prey populations. Oikos **106**:285-294.

Thompson, M. J., and C. D. Jiggins. 2014. Supergenes and their role in evolution. Heredity **113**:1-8.

Tillier, S. 1989. Comparative morphology, phylogeny and classification of land snails and slugs (Gastropoda: Pulmonata: Stylommatophora). Malacologia **30**:1-303.

Tinbergen, L. 1960. The Natural Control of Insects in Pinewoods. Archives Néerlandaises de Zoologie **13**:265-343.

Torii, K. U. 2012. Two-dimensional spatial patterning in developmental systems. Trends in Cell Biology **22**:438-446.

Tucker, G. M. 2008. Apostatic selection by song thrushes (Turdus philomelos) feeding on the snail Cepaea hortensis. Biological Journal of the Linnean Society **43**:149-156.

Turing, A. M. 1952. The Chemical Basis of Morphogenesis. Philosophical Transactions of the Royal Society of London Series B-Biological Sciences **237**:37-72.

Ueshima, R., and T. Asami. 2003. Evolution: single-gene speciation by left-right reversal. Nature **425**:679.

van den Berg, C., J. Troscianko, J. A. Endler, N. J. Marshall, and K. L. Cheney. 2020. Quantitative Colour Pattern Analysis (QCPA): A comprehensive framework for the analysis of colour patterns in nature. Methods in Ecology and Evolution **11**:316-332.

Vercken, E., B. Sinervo, and J. Clobert. 2008. Colour variation in female common lizards: why we should speak of morphs, a reply to Cote et al. Journal of Evolutionary Biology **21**:1160-1164.

Vetter, E. W., C. R. Smith, and F. C. De Leo. 2010. Hawaiian hotspots: enhanced megafaunal abundance and diversity in submarine canyons on the oceanic islands of Hawaii. Marine Ecology: an Evolutionary Perspective **31**:183-199.

Vorobyev, M., and D. Osorio. 1998. Receptor noise as a determinant of colour thresholds. Proceedings of the Royal Society B: Biological Sciences **265**:351-358.

Vorobyev, M., D. Osorio, A. T. D. Bennett, N. J. Marshall, and I. C. Cuthill. 1998. Tetrachromacy, oil droplets and bird plumage colours. Journal of Comparative Physiology A: Neuroethology Sensory Neural and Behavioral Physiology **183**:621-633.

Wada, S., K. Kawakami, and S. Chiba. 2012. Snails can survive passage through a bird's digestive system. Journal of Biogeography **39**:69-73.

Wade, C. M., P. B. Mordan, and B. Clarke. 2001. A phylogeny of the land snails (Gastropoda: Pulmonata). Proc Biol Sci **268**:413-422.

Wagner, W. L., and V. A. Funk. 1995. Hawaiian biogeography: evolution on a hot spot archipelago. Washington :Smithsonian Institution Press,1995.

Wallace, A. R. 1965. Island life. Cambridge University Press, Amherst, New York.

Walton, O. C., and M. Stevens. 2018. Avian vision models and field experiments determine the survival value of peppered moth camouflage. Communications Biology **1**:118.

Warren, B. H., D. Simberloff, R. E. Ricklefs, R. Aguilee, F. L. Condamine, D. Gravel, H. Morlon, N. Mouquet, J. Rosindell, J. Casquet, E. Conti, J. Cornuault, J. M. Fernandez-Palacios, T. Hengl, S. J. Norder, K. F. Rijsdijk, I. Sanmartin, D. Strasberg, K. A. Triantis, L. M. Valente, R. J. Whittaker, R. G. Gillespie, B. C. Emerson, and C. Thebaud. 2015. Islands as model systems in ecology and evolution: prospects fifty years after MacArthur-Wilson. Ecology Letters **18**:200-217.

Weaver, R. J., R. E. Koch, and G. E. Hill. 2017. What maintains signal honesty in animal colour displays used in mate choice? Philosophical Transactions of the Royal Society B: Biological Sciences **372**:20160343.

Webster, N., and A. R. Palmer. 2019. How do gastropods grow synchronized shell sculpture? Effect of experimental varix manipulations on shell growth by *Ceratostoma foliatum* (Muricidae: Ocenebrinae). Invertebrate Biology **138**:74-88.

Wellenreuther, M., E. I. Svensson, and B. Hansson. 2014. Sexual selection and genetic colour polymorphisms in animals. Molecular Ecology **23**:5398-5414.

Wennersten, L., J. Johansson, E. Karpestam, and A. Forsman. 2012. Higher establishment success in more diverse groups of pygmy grasshoppers under seminatural conditions. Ecology **93**:2519-2525.

Wheldale, M. 1907. The inheritance of flower colour in Antirrhinum majus. Proceedings of the Royal Society of London. Series B, Containing Papers of a Biological Character **79**:288-305.

Whisson, D. A., J. H. Quinn, and K. C. Collins. 2007. Home range and movements of roof rats (*Rattus rattus*) in an old-growth riparian forest, California. Journal of Mammalogy **88**:589-594.

Williams, S. T. 2017. Molluscan shell colour. Biological Reviews of the Cambridge Philosophical Society **92**:1039-1058.

Winter, J. E., J. E. Toro, J. M. Navarro, G. S. Valenzuela, and O. R. Chaparro. 1984. Recent developments, status, and prospects of molluscan aquaculture on the Pacific coast of South America. Aquaculture **39**:95-134.

Wittkopp, P. J., and P. Beldade. 2009. Development and evolution of insect pigmentation: genetic mechanisms and the potential consequences of pleiotropy. Seminars in Cell and Developmental Biology **20**:65-71.

Worthington, J. P., J. Silvertown, L. Cook, R. Cameron, M. Dodd, R. M. Greenwood, K. Mcconway, and P. Skelton. 2012. Evolution MegaLab: A case study in citizen science methods. Methods in Ecology and Evolution **3**:303-309.

Wright, S. 1937. The distribution of gene frequencies in populations. Proceedings of the National Academy of Sciences of the United States of America **23**:307-320.

Yeh, S. D., S. R. Liou, and J. R. True. 2006. Genetics of divergence in male wing pigmentation and courtship behavior between *Drosophila elegans* and *D. gunungcola*. Heredity **96**:383-395.

Yeung, N. O. W., D. Chung, D. Sischo, and K. A. Hayes. 2015. Rediscovery of *Auriculella pulchra* Pease, 1868 (Gastropoda: Pulmonata: Achatinellidae). Bishop Museum Occasional Papers **116**:49-51.

Yeung, N. W., and K. A. Hayes. 2018. Biodiversity and extinction of Hawaiian land snails: How many are left now and what must we do to conserve them: A reply to Solem (1990). Integrative and Comparative Biology **58**:1157-1169.

Yeung, N. W., W. M. Meyer, K. A. Hayes, J. R. Kim, T. J. Skelton, and R. H. Cowie. 2019. Non-native gastropods in high elevation horticultural facilities in Hawaii: a threat to native biodiversity. Biological Invasions **21**:1557-1566.

Yeung, N. W., J. Slapcinsky, E. E. Strong, J. R. Kim, and K. A. Hayes. 2020. Overlooked but not forgotten: the first new extant species of Hawaiian land snail described in 60 years, *Auriculella gagneorum* sp. nov. (Achatinellidae, Auriculellinae). Zookeys:1-31.

Zhao, L., Y. P. Li, Y. J. Li, J. C. Yu, H. Liao, S. Y. Wang, J. Lv, J. Liang, X. T. Huang, and Z. M. Bao. 2017. A Genome-Wide Association Study Identifies the Genomic Region Associated with Shell Color in Yesso Scallop, Patinopecten yessoensis. Marine Biotechnology **19**:301-309.

6. Appendices

6.1 Covid-19 Project Impact

From March 2020 onwards there were a number of major disruptions to project plans due to the outbreak of the Covid-19 pandemic. The largest impact was the inability to access the laboratory and several other university facilities for the remainder of 2020, and into 2021. This also caused the impossibility of further trips to Hawaii, or for shells to be posted from Hawaii to the UK for further data collection for **Chapter 4**. Collaborators from other institutions were unable to deliver things previously agreed to, and a lack of access to the lab reduced capacity for data collection for **Chapter 3** in particular. This led to a reduced volume of outputs associated with the project.

6.2 Publications and other significant achievements

I was awarded the Vice Chancellors medal in 2021 for a notable endeavour which mas made a difference to the university, and which has had a noticeably positive impact for students and/or staff. The medal was awarded for my involvement in the University of Nottingham COVID-19 response, in which my role was running antibody tests for the staff and student populations across the University of Nottingham. The antibody testing operation was run by myself and Paddy Tighe, with me taking on a large majority of the required laboratory work – preparing and packing testing kits for distribution, receiving used kits and processing/databasing samples, extracting and preparing samples, running ELISA assays to test for antibody presence, organising and presenting results of tests, and preparing data and test results for sending back out.

Publications

Jackson, H.J., Larsson, J., Davison, A. (2021). Quantitative measures and 3D shell models reveal interactions between bands and their position on growing snail shells. *Ecology and Evolution* 11, 6634-6648.

Urbanowicz, R.A.*, Tsoleridis, T.*, **Jackson, H.J.***, Cusin, L., Duncan, J.D., Chappell, J.G., Tarr, A.W., Nightingale, J., Norrish, A.R., Ikram, A., Mason, B., Craxford, S.J., Kelly, A., Aithal, G.P., Vijay, A., Tighe, P.J., Ball, J.K., Valdes, A.M., Ollivere, B.J. (2021). Antibody Responses to SARS-CoV-2 Variants are Significantly Increased Following BNT162b2 Vaccine Boost in SARS-CoV-2 Exposed and Naïve Individuals. *Science Translational Medicine*.

Davison, A., **Jackson, H.J.**, Murphy, E.W. Reader, T. (2019). Discrete or indiscrete? Redefining the colour polymorphism of the land snail *Cepaea nemoralis*. *Heredity* 123, 162–175.

Dunning, J., Diamond, A.W., Christmas, S.E., Cole, E., Holberton, R.L., **Jackson, H.J.**, Kelly, K.G., Brown, D,. Rivera, I.R., Hanley, D. (2019). Photoluminescence in the bill of the Atlantic Puffin *Fratercula arctica. Bird Study* 65, 570-573.

In review:

Tighe, P.J., Urbanowicz, R.A., Bamber, H., Fairclough, L.C., McClure, C.P., Thompson, B,J, **Jackson, H.J.**, Gomez, N., Tsolerdis, T., Chappell, J.G., Loose, M., Carlile, M., Moore, C., Holmes, N., Sang, F., Hrushikesh, D., Clark, G., Temperton, N., Brooks, T., Ball, J.K., Irving, W.L., Tarr, A.W. (2021). Potent anti-SARS-CoV-2 Antibody Responses are Associated with Better Prognosis in Hospital Inpatient COVID-19 Disease. *Frontiers in Immunology.*

Chappell, H., Patel, R., Driessens, C., Tarr, A.W., Irving, W.L., Tighe, P.J., **Jackson, H.J.**, Harvey-Cowlishaw, T., Mills, L., Shaunak, D., Gbesemete, D., Leahy, A., Lucas, J.S., Faust, S.N., de Graaf, H. (2021). Immunocompromised children and young people are at no increased risk of severe COVID-19. *The Lancet: Child and Adolescent Health.*

Vedhara, K., Ayling, K., Jia, R., Fairclough, L., Morling, J.R., Ball, J.K., Knight, H., Blake, H., Corner, J., Denning, C., Bolton, K., **Jackson, H.**, Coupland, C., Tighe, P.J. (2021). Psychological Factors Associated with SARS-CoV-2 Seropositivity. *Annals of Behavioural Medicine.*

6.3　PIPS Reflective Statement

Placement Outline

From the 1st of October 2020 to the 23rd December 2020, I completed a placement with the University of Nottingham, working as part of the University of Nottingham COVID response team. The mainstay of the placement was performing COVID-19 antibody tests for students, staff, and associates of the University of Nottingham. This was a collaborative project involving immunologists, virologists, and clinicians from across the University and the QMC to deliver rapid asymptomatic saliva PCR and antibody tests to both the student and staff population of the university to determine both current and prior infection status for covid-19. Across the twelve week placement period, I processed, extracted, and ran antibody tests on approximately 5,000 samples, allowing positive/negative results for COVID-19 antibody presence to be delivered within 1 week of the sample being delivered. I was the main point of contact for all laboratory processing of these samples, and was largely solely responsible for the day to day processing, running, and analysis of the samples before the delivery of results to patients.

Aims and outcomes

During the placement, my aims were to:

1. Develop laboratory skills in areas outside of my PhD research

2. Gain an understanding of the processes involved in large scale projects involving the processing of human samples

3. Develop the skills required to aid in the running of projects such as these

4. Assist the University of Nottingham Covid-19 effort by the performance of antibody testing for the asymptomatic testing service.

Personal and professional development

Whilst undertaking the PIPS placement, I aimed to develop several new skills, predominantly focussing on enhancing laboratory skills through the learning and development of new techniques in an area outside of my PhD research interest. I feel I achieved this goal, with both personal and professional skills developing across the three month placement timeframe. I gained several new professional laboratory based skills, including the use and programming of liquid handling robots, learning new immuno-assay techniques such as ELISAs, and gaining an understanding of the processes behind health and safety in a laboratory environment, particularly when extracting and processing human blood samples. I also gained experience of using familiar data analysis techniques in a different way and applying pre-existing skills to new scenarios.

An additional benefit to both personal and professional skills gained from the placement came from interacting with a large cohort of people involved in the project, each with varying roles and specialisms. These interactions included delivering results to clinicians under a tight time pressure deadline, beta-software development talks and meetings with liquid handling robot manufacturers to get software to contain features which would be useful to the specific protocols we were developing in the lab and dealing with the members of the team responsible for the logistics of distributing and collecting antibody tests for safe delivery to the lab for processing. It also involved organising other members of the lab team and student volunteers in the creation and packing of several thousand test kits over the course of several weeks.

The PIPS placement has directly impacted my career plans, in that I have been offered a post-doctoral research associate position in the lab in which I undertook my placement. This position will rely on a combination of skills gained from my PhD, and those gained on PIP which are outside of my PhD research area. I also have been involved in multiple collaborative research projects as a direct result

of the connections made whilst on placement, which have resulted in authorship on several COVID related papers to date, with my involvement in one project warranting joint first authorship on a high impact manuscript submitted to Science Translational Medicine. Several other manuscripts are currently in preparation for submission for publication as a direct result of this work (**See section 6.2**).

6.4 Appendicies and Supplementary materials

Appendix 2.1

Location and numbers of each banding phenotype of each population of *Cepaea* in chapter 2.

Location	Population	1.345	340	10300	10305	10345	12300	12345	00300	00345	Total
Austria	Aus	-	-	-	-	1	-	3	-	-	4
	Aus_1	-	-	-	2	-	-	3	-	-	5
	Austria Total	-	-	-	2	1	-	6	-	-	9
Denmark	Aal_1	1	-	-	-	-	-	5	-	-	6
	Arh1	-	-	-	-	-	-	5	-	-	5
	Den_Aar1	-	-	-	-	-	-	-	1	-	1
	Den_odd_1	-	-	-	-	1	-	2	1	-	4
	Ros_2	1	-	-	-	-	-	5	-	-	6
	Veg1_1	1	-	-	-	4	-	1	-	-	6
	Denmark Total	3	-	-	-	5	-	18	2	-	28
England	Eng_dev_1	-	-	-	-	-	-	6	-	-	6
	Eng_rep_1	6	-	-	-	1	-	20	-	-	27
	PortsT	-	-	-	-	-	-	4	-	-	4
	Upt_upton	-	-	-	-	-	-	2	5	-	7
	Wal_gref_1	-	-	-	-	-	-	5	-	-	5
	Wal_newp_1	1	-	-	-	-	-	3	-	-	4
	England Total	7	-	-	-	1	-	40	5	-	53
France	gite_bretagne	-	-	-	-	-	-	6	5	-	11

Region		C1	C2	C3	C4	C5	C6	C7	C8	C9	Total
	France Total	-	-	-	-	-	-	6	5	-	11
Germany	Ger_grob_1	-	-	-	-	-	-	-	2	3	5
	Germany Total	-	-	-	-	-	-	-	2	3	5
	DRG101	-	-	-	-	1	-	13	8	3	25
	DRG102	-	-	-	-	-	-	7	1	-	8
	DRG11	-	-	-	-	-	-	5	-	-	5
	DRG2	-	-	-	-	1	-	2	-	-	3
	DRG20	-	-	-	-	-	-	1	-	-	1
	DRG22	-	-	-	-	-	-	1	-	-	1
	DRG24	-	-	-	-	-	-	1	1	-	2
Pyrenees	DRG28	-	-	-	-	2	-	11	6	-	19
	DRG42	-	-	-	-	42	1	44	17	-	104
	DRG42B	5	-	-	-	11	-	10	10	-	36
	DRG47	-	-	-	-	1	-	1	1	-	3
	DRG77	-	-	-	-	-	-	6	-	-	6
	DRG79	-	-	-	-	-	-	1	-	-	1
	DRG83	-	-	-	-	-	-	1	-	-	1
	DRG90	-	-	-	1	-	-	14	3	-	18
	Pyrenees Total	5	-	-	1	58	1	118	47	3	233
	Sco_inv_1	-	-	-	-	1	-	22	-	-	23
Scotland	Sco_scal	-	-	-	-	-	-	4	-	-	4
	Scotland Total	-	-	-	-	1	-	26	-	-	27
	Swe_fai1	-	-	-	1	-	-	2	-	-	3
Sweden	UPP1A	-	-	-	-	-	-	14	-	-	14
	Sweden Total	-	-	-	1	-	-	16	-	-	17

	Switz_chur_1	-	-	-	1	-	-	-	-	-	1
	Switz_chur_2	-	1	-	1	-	-	3	1	1	7
	Switz_chur_3	-	-	1	-	1	-	1	1	-	4
Switzerland	Switz_chur_4	-	-	-	1	-	-	3	-	6	10
	Switz_chur_5	-	-	-	-	-	-	1	-	-	1
	Switz_malix_1	-	-	-	1	-	-	15	6	-	22
	Switzerland Total	-	1	1	4	1	-	23	8	7	45
Total		15	1	1	8	67	1	253	69	13	428

Appendix 4.1

Mclust classifications and Euclidean distances between measurement points on individual shells of **A)** *Auriculella auricula*, **B)** *Auriculella crassula*, **C)** *Auriculella pulchra*, and **D)** *Auriculella uniplcata*, given in JND units. A difference of 3 or more JNDs is determined as being distinguishable by an avian predator, and these are represented in bold in the table. Indivduals are denoted as the population which they belong to followed by the individual number. Distances displayed are the Euclidean distances between measurements both in 3-dimensional colour space, and along each of the three PC_{xyz} axes.

A) *Auriculella auricula*

Individual	Apertural Mclust Classification	Apical Mclust Classification	Same classification?	Overall distance	PC1 distance	PC2 distance	PC3 distance
109276_1	2	1	n	**4.37878**	2.209194	**3.763069**	0.363983
109276_2	2	2	y	**3.279494**	**3.074759**	1.087442	0.344103
109276_3	1	1	y	1.106401	0.035172	1.087111	0.202671
109276_4	2	2	y	2.730306	2.717633	0.177343	0.193886
109276_5	2	2	y	**5.783743**	**5.573348**	1.54522	0.042025
109276_6	2	2	y	2.276729	1.484053	1.724484	0.085079
109276_7	2	1	n	**6.571313**	2.718433	**5.971524**	0.364933
109276_8	2	2	y	**3.840335**	**3.597355**	1.343083	0.057784
109276_9	1	1	y	**6.020652**	**5.884052**	0.975862	0.820899
109276_10	2	1	n	**5.019309**	1.428195	**4.766874**	0.656228
109276_11	2	1	n	1.983299	1.106634	1.404869	0.857426
109276_12	2	2	y	**5.101618**	**4.633336**	2.130226	0.144351
109276_13	2	2	y	1.755405	0.199437	1.734939	0.177924
109276_14	2	2	y	**3.236006**	**3.180954**	0.359896	0.473014
109276_15	2	2	y	2.929499	2.91825	0.248243	0.064467
12745_1	2	2	y	2.992909	1.677803	2.432835	0.473069
12745_2	2	2	y	**3.127292**	**3.028961**	0.628459	0.458682
12745_3	1	1	y	**6.706715**	**3.471508**	**5.736612**	0.141215
12745_4	2	2	y	2.728239	0.299315	2.694802	0.302894
12745_5	2	1	n	**6.683405**	**5.833488**	3.251365	0.258725
12745_6	1	1	y	**7.558774**	**6.957629**	2.85573	0.755822
12745_7	2	1	n	**10.2507**	**7.208872**	**7.150008**	1.409368

267

12745_8	2	2	y	**3.134414**	0.636911	**3.066213**	0.131278
12745_9	2	1	n	**6.212**	**5.549704**	2.539469	1.157941
12745_10	1	1	y	**4.813711**	**3.74338**	**3.008618**	0.327314
12745_11	1	1	y	2.764834	0.80704	2.639069	0.168246
12745_12	2	1	n	**3.826647**	2.023117	**3.171253**	0.702413
34020_1	2	2	y	**3.795117**	2.028309	**3.207237**	0.050101
51414_1	2	2	y	2.628877	2.004622	1.614905	0.533446
51414_2	2	2	y	2.200525	0.942878	1.919041	0.520164
51414_3	2	2	y	0.934643	0.649735	0.671842	0.005498
51414_4	2	2	y	**3.54675**	0.127512	**3.523291**	0.386781
51414_5	2	2	y	1.004035	0.070244	0.865637	0.50381
51414_6	2	2	y	2.450906	1.718721	1.745674	0.074551
51414_7	2	2	y	2.817091	2.73358	0.643791	0.221526
51414_8	2	2	y	**6.115864**	**5.442462**	2.784128	0.178952
51414_9	2	2	y	2.178357	1.505409	1.527108	0.383304
51414_10	2	2	y	**3.541334**	**3.122773**	1.655844	0.21799
51414_11	2	2	y	**4.502605**	**3.950074**	2.144606	0.266511
51414_12	2	2	y	**4.936076**	**4.681775**	1.454154	0.575557
51414_13	2	1	n	**5.113522**	**4.685159**	1.729219	1.098723
51414_14	2	2	y	1.619456	1.549949	0.021912	0.468845
51414_15	2	2	y	1.835359	1.246304	1.328574	0.22396
51414_16	2	2	y	2.319989	1.875806	1.364134	0.053262
51414_17	2	2	y	1.77175	1.606398	0.727498	0.171262
51414_18	2	2	y	1.007209	0.626267	0.769107	0.175311
56994_1	2	2	y	0.896008	0.822662	0.349519	0.062409
56994_2	2	2	y	2.464865	0.194679	2.343524	0.738619

56994_3	2	2	y	**5.301655**	1.652156	**5.036548**	0.105384
56994_4	2	2	y	1.669524	1.328691	0.938866	0.374728
56994_5	2	2	y	**4.047211**	**3.430018**	2.137977	0.209652
56994_6	2	2	y	**8.389233**	**7.857554**	2.932467	0.196761
56994_7	2	2	y	**6.779794**	6.76497	0.443098	0.066784
56994_8	1	1	y	0.870474	0.577622	0.635929	0.140259
56994_9	2	2	y	**3.923745**	**3.678522**	1.343873	0.241369
56994_10	2	2	y	2.441585	2.202529	0.687253	0.798677
56994_11	2	2	y	0.829295	0.71882	0.331872	0.246755
56994_12	2	1	n	**3.476255**	2.188095	2.667096	0.428006
56994_13	2	2	y	**3.116247**	1.589423	2.680283	0.028553
56994_14	2	2	y	0.988141	0.818898	0.483075	0.269198
56994_15	2	2	y	**5.083181**	**4.77187**	1.690032	0.460201
57018_1	2	1	n	2.414929	1.570498	1.812904	0.280703
57018_2	2	2	y	**3.138888**	1.28608	2.816809	0.514008
57018_3	2	2	y	2.323843	2.158045	0.695149	0.509759
57018_4	2	2	y	1.475054	0.190484	1.416051	0.366469
57018_5	2	2	y	**8.950244**	**8.87952**	1.091267	0.264829
57018_6	1	1	y	1.247797	0.295958	0.148262	1.20309
57018_7	2	2	y	**5.074797**	**5.051242**	0.373057	0.315186
57018_8	2	2	y	**3.529345**	**3.491797**	0.462438	0.223117
57018_9	2	1	n	**3.047896**	0.674348	2.759674	1.104139
57018_10	2	2	y	1.053969	0.62904	0.81503	0.225576

B) *Auriculella crassula*

Individual	Apertural Mclust Classification	Apical Mclust Classification	Same classification?	Overall distance	PC1 distance	PC2 distance	PC3 distance
12934_1	1	2	n	**7.450874**	**7.014642**	2.499037	0.255214
12934_2	1	3	n	**8.529608**	7.866192	2.847724	1.663642
12934_3	1	2	n	**9.16943**	8.704958	2.868815	0.268422
12934_4	1	3	n	**10.10956**	**9.61209**	**3.006181**	0.879689
12934_5	2	2	y	**7.979487**	6.405486	**4.710004**	0.676627
12934_6	1	3	n	**10.30476**	7.793935	**6.69963**	0.746769
12934_7	1	2	n	**12.46516**	**12.3521**	1.567916	0.589505
12934_8	1	3	n	**11.05254**	10.38489	**3.729742**	0.633848
12934_9	1	2	n	1.990766	1.569671	0.966059	0.752339
12934_10	1	2	n	2.252746	0.426002	2.119666	0.632775
12934_11	1	2	n	**4.319175**	**4.093115**	1.350593	0.27853
12934_12	1	2	n	2.185391	0.873461	1.838111	0.796459
12934_13	1	2	n	**3.487871**	**3.345504**	0.812744	0.558831
12934_14	1	2	n	**7.6179**	**7.570878**	0.454245	0.712644
12934_15	1	1	y	**3.626136**	**3.508643**	0.871475	0.280743
12934_16	1	1	y	**5.994447**	**5.812278**	1.356406	0.557656
12934_17	1	1	y	**3.449633**	**3.396924**	0.108643	0.590819
12934_18	1	2	n	**8.814415**	**8.584389**	1.792225	0.888874
12934_19	1	1	y	**4.494915**	**4.427205**	0.406991	0.662177
12934_20	1	1	y	**3.119512**	**3.108916**	0.143079	0.213368
15850_1	2	3	n	2.414749	0.651956	2.314753	0.218825
15850_2	2	2	y	**3.888045**	2.775397	2.683151	0.463428
15850_3	2	2	y	**3.023587**	1.676688	2.45772	0.53889

15850_4	1	2	n	**7.868237**	**7.69552**	1.620368	0.250081
15850_5	2	2	y	**3.540845**	2.195136	2.672601	0.759054
15850_6	1	2	n	**6.47996**	**6.072479**	2.261595	0.008235
15850_7	2	2	y	**5.380743**	**4.967906**	2.040717	0.328292
15850_8	2	2	y	1.753613	0.180075	1.739834	0.125328
15850_9	1	3	n	**7.318562**	**5.262473**	**4.954088**	1.150971
15850_10	1	2	n	**10.70322**	**10.53416**	1.892482	0.095063
15850_11	1	2	n	**5.554814**	**5.417494**	1.171854	0.365346
15850_12	1	3	n	**8.268684**	**4.765311**	**6.514799**	1.794532
15850_13	1	1	y	2.417432	0.333397	2.360992	0.398169
15850_14	2	2	y	2.415022	2.255768	0.858715	0.080332
15850_15	1	2	n	**8.578747**	**7.790151**	**3.592454**	0.052265
15850_16	2	2	y	2.637931	2.585441	0.490907	0.182179
15850_17	1	2	n	**8.141488**	**8.137206**	0.261211	0.038559
15850_18	1	2	n	**7.016284**	**6.998116**	0.190533	0.467238
15850_19	2	2	y	**4.284283**	**4.096719**	1.16129	0.472635
15850_20	1	2	n	**11.26014**	**10.98455**	2.467785	0.201088
15850_21	1	2	n	**9.348832**	**9.344684**	0.224992	0.164046
15850_22	2	2	y	2.171564	0.10218	2.167424	0.086719
15850_23	2	3	n	**9.108998**	**3.453984**	**7.810356**	**3.16894**
25051_1	2	2	y	**4.427714**	**3.470568**	2.712887	0.447279
25051_2	2	2	y	**4.014515**	**3.400439**	2.121254	0.231577
25051_3	1	2	n	**5.801668**	**5.610238**	1.383503	0.520103
25051_4	1	2	n	**5.43047**	**5.071567**	1.904504	0.376944
25051_5	1	2	n	**9.980948**	**9.97419**	0.083923	0.357527
25051_6	1	2	n	**3.200848**	1.784883	2.651164	0.175925

271

25051_7	1	2	n	**6.788503**	**6.314977**	2.323604	0.897612
25051_8	1	1	y	**7.531594**	**7.518883**	0.420764	0.11939
25051_9	1	2	n	**7.859101**	**7.808771**	0.880802	0.112885
25051_10	1	2	n	1.563419	0.246654	1.540329	0.104052
25051_11	1	2	n	**5.303291**	**5.162214**	1.169066	0.331259
25051_12	1	3	n	**13.70562**	**13.3283**	**3.184399**	0.244984
25051_13	1	2	n	**3.841337**	**3.79014**	0.561159	0.27533
25051_14	2	2	y	2.716107	2.303619	1.427294	0.182775
25051_15	1	2	n	1.929851	1.760135	0.761453	0.215499
25051_16	1	1	y	**3.966813**	**3.581239**	1.685449	0.263805
25051_17	1	2	n	**8.550284**	**8.059942**	2.834802	0.329538
25051_18	2	2	y	1.99467	1.249552	1.546103	0.163997
25051_19	1	2	n	**7.594798**	**7.588817**	0.298541	0.041096
25051_20	1	2	n	**3.180637**	2.283376	2.213873	0.037546
25051_21	1	2	n	2.419086	2.032485	1.223186	0.474131
25051_22	1	2	n	**3.963458**	**3.458145**	1.894664	0.400598
25051_23	2	2	y	**4.519367**	**4.327192**	1.299619	0.105224
25051_24	1	2	n	**5.246597**	**5.235116**	0.222186	0.266393
25051_25	1	2	n	**3.326705**	**3.190156**	0.85781	0.392476
25052_1	1	1	y	2.200363	2.00708	0.84376	0.31827
25052_2	1	1	y	0.761554	0.441227	0.590062	0.192641
25052_3	1	3	n	**6.10153**	**5.162823**	**3.131191**	0.877247
25052_4	2	2	y	**7.291412**	**5.4703**	**4.773902**	0.671094
25052_5	1	1	y	1.706826	0.456038	1.475733	0.72629
25052_6	1	1	y	1.881311	1.663436	0.871171	0.11564
25052_7	2	2	y	1.313717	1.3053	0.105578	0.104391

25052_8	1	1	y	**3.868452**	**3.635184**	1.290049	0.293483
25052_9	1	2	n	2.77103	2.732422	0.055418	0.457609
25052_10	1	3	n	**4.453331**	1.915795	**3.890496**	1.012879
25052_11	2	3	n	**3.519873**	2.856551	1.85867	0.880322
25052_12	1	3	n	**3.093437**	1.491656	2.44219	1.174743
25052_13	3	3	y	**5.896392**	1.834162	**5.601066**	0.177068
25052_14	2	2	y	**3.832557**	0.491881	**3.799615**	0.097344
25052_15	1	1	y	**3.134758**	**3.017904**	0.745527	0.403918
25052_16	1	2	n	**3.554314**	2.192958	2.794765	0.115639
25052_17	1	1	y	2.115793	0.328117	2.071461	0.279234
25052_18	1	3	n	**14.47317**	**11.81819**	**8.351252**	0.244051
25052_19	1	3	n	**20.70753**	**20.63609**	0.543232	1.630503
25052_20	1	1	y	**1.806615**	1.64447	0.742513	0.090831
25053_1	2	3	n	**6.914037**	**6.101658**	**3.197058**	0.593711
25053_2	1	2	n	**8.937055**	**8.796533**	1.488176	0.526586
25053_3	3	3	y	**6.372191**	**4.494624**	**4.132878**	1.822772
25053_4	1	1	y	**5.418447**	**5.174729**	1.588141	0.244061
25053_5	2	2	y	2.992424	1.88898	2.31989	0.066846
25053_6	1	1	y	2.759187	2.682077	0.513289	0.395105
25053_7	1	1	y	1.66722	0.507296	1.588127	0.011154
10001_1	2	2	y	0.954397	0.817555	0.492089	0.018058
10001_2	1	2	n	2.461722	1.991996	1.421855	0.265244
10001_3	2	2	y	**3.669358**	2.818473	2.32736	0.322169
10001_4	2	2	y	0.211131	0.195437	0.058073	0.054848
10001_5	2	2	y	1.634212	1.629134	0.094319	0.08762
10001_6	2	2	y	**4.371344**	**4.362982**	0.251133	0.099832

10001_7	1	2	n	**5.503477**	**5.364815**	1.139514	0.45666
10001_8	2	2	y	1.724798	1.178092	1.259652	0.017531
10001_9	1	1	y	1.506973	1.067036	1.048773	0.180214
10001_10	2	2	y	2.104168	1.072649	1.788849	0.277429
10001_11	1	1	y	2.533231	2.320123	0.953414	0.353965
10001_12	2	2	y	1.317921	0.771872	0.820946	0.683503
10001_13	1	2	n	**5.973391**	**5.760585**	1.394785	0.742725
10001_14	2	2	y	1.320469	1.175828	0.53142	0.280462
10001_15	2	2	y	**5.789836**	**5.585101**	1.467167	0.419849
10001_16	1	1	y	2.861114	2.803485	0.569829	0.041743
10001_17	2	2	y	**4.696299**	**4.175433**	2.07495	0.561747
10001_18	1	2	n	**3.020928**	2.789215	0.839303	0.801158
10001_19	1	1	y	2.5338	2.498829	0.405098	0.109049
10001_20	2	3	n	**4.91885**	**3.37243**	**3.579828**	0.081448
10001_21	3	2	n	**3.277663**	1.629356	2.293021	1.682358
10001_22	2	2	y	**5.2432**	**4.473281**	2.712133	0.353896
10001_23	1	1	y	0.927578	0.837971	0.391099	0.072436

C) *Auriculella pulchra*

Individual	Apertural Mclust Classification	Apical Mclust Classification	Same classification?	Overall distance	PC1 distance	PC2 distance	PC3 distance
120870_1	1	1	y	**5.408033**	2.338349	**4.872516**	0.193745
120870_2	1	2	n	**27.42189**	**27.02258**	**4.60366**	0.739216
120870_3	2	2	y	**3.251677**	2.856242	1.494616	0.425917
120870_4	1	1	y	2.829451	2.285281	1.635603	0.328766
120870_5	1	2	n	**5.453258**	**5.366881**	0.936146	0.241322
120870_6	1	1	y	**3.959525**	**3.662402**	1.493804	0.182219
120870_7	1	1	y	**7.694685**	**7.409181**	2.045941	0.355426
120870_8	1	1	y	2.730555	0.337822	2.456418	1.143599
120870_9	2	2	y	**3.485642**	2.851772	1.974279	0.345428
120870_10	1	2	n	1.663338	0.635997	1.516655	0.248917
120870_11	2	2	y	**3.03707**	2.984896	0.32071	0.459712
120870_12	1	1	y	**5.320783**	**4.925825**	1.998584	0.229437
120870_13	2	2	y	**5.148554**	**5.147346**	0.108035	0.027624
120870_14	1	2	n	**7.972424**	4.627796	**6.470518**	0.524821
120870_15	1	2	n	**3.088153**	2.457452	1.427612	1.208115
121078_1	2	2	y	**5.208439**	**5.196487**	0.019065	0.352124
121078_2	1	2	n	**4.543663**	3.190851	**3.163734**	0.673894
121078_3	1	2	n	**4.505902**	**4.203763**	1.583349	0.352893
121078_4	2	2	y	**6.876417**	**6.862498**	0.083847	0.429184
121078_5	2	2	y	2.580186	2.493086	0.406353	0.526081
121078_6	2	2	y	**5.535681**	**5.181135**	1.889506	0.478928

121078_7	1	1	y	**4.747733**	**4.667822**	0.860356	0.110458
121078_8	1	1	y	**3.78102**	0.887703	**3.64793**	0.448
121078_9	1	2	n	**5.619805**	**4.956901**	2.593046	0.536146
121078_10	1	1	y	**3.169801**	1.569729	2.753186	0.059626
121078_11	2	2	y	0.810047	0.630971	0.495943	0.109968
121078_12	2	2	y	**4.116372**	**4.034031**	0.727342	0.376938
121078_13	1	2	n	**5.901961**	**5.492051**	2.149361	0.225314
121078_14	1	2	n	**4.073464**	1.586526	**3.713776**	0.532829
121078_15	1	2	n	**5.488815**	**3.589457**	**3.050623**	2.817195
128374_1	2	2	y	**3.316825**	**3.311328**	0.111074	0.155241
128374_2	2	2	y	**7.9189**	**7.791508**	1.413603	0.055695
128374_3	2	2	y	2.800081	2.712139	0.696113	0.013443
128374_4	2	2	y	0.701763	0.693487	0.021984	0.105186
128374_5	2	1	n	**9.809105**	**9.498695**	2.444117	0.140111
128374_6	2	2	y	**5.335975**	**5.214356**	1.128549	0.097494
128374_7	2	2	y	0.416802	0.357454	0.194564	0.089977
128374_8	2	2	y	**3.956699**	**3.855097**	0.65481	0.604085
128374_9	2	2	y	2.496801	2.245715	1.082325	0.13912
128374_10	2	2	y	2.394435	2.339695	0.289329	0.418849
128374_11	2	2	y	**5.814184**	**5.756334**	0.539418	0.615132
128374_12	2	2	y	**5.14687**	**5.009412**	1.172702	0.144349
132435_1	2	2	y	**3.639688**	**3.536472**	0.803479	0.308415
132435_2	2	2	y	**5.795036**	**5.436056**	1.987331	0.286803
132435_3	2	2	y	**7.519537**	**7.430845**	1.151504	0.004063
132435_4	2	2	y	**11.31329**	**10.9757**	2.725626	0.309052
132435_5	2	2	y	**4.19166**	**4.107**	0.817093	0.186885

276

132435_6	2	1	n	**6.371669**	**6.191367**	1.409145	0.528624
132435_7	2	2	y	**4.157233**	**3.615937**	2.037049	0.240865
132435_8	2	2	y	2.315683	2.257799	0.435173	0.274515
132435_9	2	2	y	**3.659325**	**3.252462**	1.606913	0.47956
132435_10	2	2	y	**3.050549**	2.946215	0.745539	0.26426
134368_1	1	1	y	**6.370799**	**6.064518**	1.799958	0.754219
134368_2	1	2	n	**3.965159**	1.115799	**3.526542**	1.428629
134368_3	1	1	y	**3.40655**	1.509551	2.864244	1.059219
134368_4	2	1	n	**12.35065**	**11.76163**	**3.366776**	1.693379
134368_5	1	2	n	**7.221975**	**6.871868**	2.184884	0.40079
134368_6	1	1	y	**4.807097**	**4.559897**	0.207402	1.507482
134368_7	1	2	n	**5.370975**	**5.33443**	0.088152	0.619241
134368_8	1	2	n	**7.192358**	2.089884	**6.866369**	0.464082
134368_9	1	1	y	**8.472512**	**6.848651**	**4.944721**	0.655116
134368_10	1	2	n	2.886316	1.590187	2.267865	0.811733
134368_11	1	2	n	1.859645	0.726913	1.564448	0.694538
134368_12	1	1	y	**4.683458**	**4.439263**	1.492546	0.005665
134368_13	1	2	n	**6.808661**	**3.247071**	**5.818883**	1.398212
134368_14	1	2	n	**4.963872**	**3.940713**	2.799148	1.129412
134368_15	1	1	y	**8.016707**	**6.955022**	**3.980283**	0.229366
185302_1	2	2	y	**3.725938**	**3.295932**	1.719201	0.252574
185302_2	1	2	n	0.652444	0.390992	0.159038	0.497509
185302_3	2	2	y	1.86164	1.078065	1.450826	0.44563
185302_4	1	2	n	**5.735891**	1.317427	**5.397736**	1.424526
185302_5	2	2	y	2.540687	2.431722	0.565622	0.471053
185302_6	1	2	n	**3.550359**	**3.184071**	1.462912	0.571519

185302_7	2	2	y	2.42429	2.415593	0.081979	0.188072
185302_8	1	2	n	**3.780889**	**3.463312**	1.474859	0.35409
185302_9	2	2	y	1.4289	0.881592	1.108149	0.191199
185302_10	2	2	y	0.660781	0.356889	0.159538	0.532738
185302_11	2	2	y	2.391367	2.234589	0.803754	0.281471
185302_12	2	2	y	**3.311042**	**3.287196**	0.396615	0.006341
185302_13	1	2	n	2.218612	1.394953	1.412652	0.990333
185302_14	2	2	y	**5.327473**	**5.23024**	0.798674	0.62344
185302_15	1	1	y	**4.890278**	**4.18367**	2.527704	0.149779
19299_1	2	2	y	1.793584	0.161925	1.785823	0.039498
19299_2	1	2	n	**7.339625**	**3.267845**	**6.507012**	0.922002
19299_3	2	2	y	**3.101723**	**3.099478**	0.080953	0.085869
19299_4	2	2	y	**4.752687**	**4.74089**	0.323575	0.085391
19299_5	2	2	y	2.372643	1.955851	0.721975	1.132622
19299_6	1	2	n	2.138032	1.794817	1.011306	0.571901
19299_7	2	2	y	1.044241	0.993725	0.314304	0.064519
19299_8	2	2	y	**4.215548**	**4.157708**	0.694703	0.041186
19299_9	2	2	y	0.769364	0.508111	0.577701	0.002446
19299_10	2	2	y	0.727828	0.433253	0.166459	0.56064
19299_11	2	2	y	1.588431	1.407368	0.695321	0.242809
19299_12	2	2	y	1.727626	1.554295	0.754185	0.0081
19299_13	2	2	y	**5.013822**	**4.774193**	1.336486	0.747859
19299_14	2	2	y	**5.667086**	**5.555833**	1.075118	0.304492
19299_15	2	2	y	2.545393	2.508704	0.393922	0.17394
19343_1	2	2	y	0.407792	0.326623	0.135645	0.203007
19343_2	2	2	y	1.874084	1.713387	0.719565	0.242328

19343_3	2	2	y	**9.909886**	**9.810103**	1.387779	0.204465
19343_4	2	2	y	**5.62078**	**5.568318**	0.755009	0.130247
19343_5	2	2	y	**7.740319**	**7.620326**	1.356683	0.050865
19343_6	2	2	y	**4.51505**	**4.447095**	0.750179	0.215072
19343_7	2	2	y	0.499819	0.079126	0.424646	0.251463
19343_8	2	2	y	1.790979	1.585596	0.792729	0.255093
19343_9	2	2	y	0.930054	0.437565	0.774273	0.272101

D) *Auriculella uniplicata*

Individual	Apertural Mclust Classification	Apical Mclust Classification	Same classification?	Overall distance	PC1 distance	PC2 distance	PC3 distance
49319_1	1	4	n	**5.163214**	**5.053049**	0.014409	1.060789
49319_2	1	4	n	**3.253863**	2.14214	2.330903	0.752165
49319_3	3	1	n	**4.606708**	**4.558155**	0.58399	0.322394
49319_4	2	3	n	**6.040841**	**3.869638**	**4.559488**	0.853664
49319_5	4	1	n	**4.310611**	**4.10973**	1.187072	0.531365
49319_6	1	1	y	1.418628	1.03856	0.922189	0.288905
49319_7	3	2	n	**20.37197**	**19.00961**	**6.897787**	2.464196
49319_8	1	1	y	**4.088511**	**4.019481**	0.717435	0.21209
49319_9	4	4	y	2.048031	1.449685	1.076718	0.96619
49319_10	1	2	n	**8.583004**	**7.55363**	**3.999395**	0.784524
49319_11	2	2	y	**15.67237**	**12.62028**	**9.261683**	0.757027
49319_12	3	3	y	**8.682498**	**8.395686**	2.161976	0.473369
49319_13	1	4	n	2.365851	0.762746	1.546767	1.619562
49319_14	1	1	y	2.034649	1.785854	0.929261	0.294954
49319_15	1	3	n	**5.237647**	**5.223016**	0.368237	0.132091
49319_16	1	1	y	**3.170612**	2.933462	1.066373	0.557161
15851_1	1	1	y	**3.30707**	**3.201208**	0.665733	0.495758
15851_2	3	3	y	**3.087643**	**3.050121**	0.460451	0.135234
15851_3	3	1	n	1.382917	0.552657	1.241807	0.254841
15851_4	1	3	n	**5.985829**	**5.977315**	0.302479	0.101803
15851_5	3	3	y	0.631432	0.565359	0.118619	0.254962
15851_6	1	4	n	**3.295537**	**3.20543**	0.045584	0.764006
15851_7	3	3	y	**4.696875**	**4.599652**	0.914984	0.258157

15851_8	3	3	y	1.773744	1.773013	0.012586	0.049348
15851_9	1	3	n	**4.293851**	**4.214546**	0.75098	0.332844
15851_10	3	3	y	**3.428623**	**3.337995**	0.74064	0.254362
15851_11	3	3	y	2.463369	2.363848	0.677649	0.145608
15851_12	3	1	n	0.873214	0.080648	0.83985	0.225055
15851_13	3	4	n	**6.338486**	**6.21765**	1.070778	0.608826
15851_14	3	1	n	**3.480744**	**3.405442**	0.686022	0.218909
15851_15	1	1	y	1.851961	1.509494	1.072243	0.038508
15851_16	3	3	y	0.357124	0.014342	0.290037	0.207871
15851_17	1	3	n	**3.71356**	**3.685283**	0.157935	0.429272
15851_18	3	1	n	**6.81242**	**6.665759**	1.402997	0.091251
15851_19	3	3	y	1.301529	1.237836	0.401305	0.026327
15853_1	4	4	y	**5.381221**	**5.36103**	0.405789	0.228538
15853_2	4	1	n	**6.517181**	**6.492271**	0.177199	0.540975
15853_3	3	2	n	**7.959982**	1.619597	**7.787489**	0.305337
15853_4	3	3	y	1.500826	0.521407	1.05933	0.926516
15853_5	4	4	y	**3.670642**	**3.54406**	0.670556	0.680885
15853_6	4	4	y	**13.57743**	**13.12913**	**3.445974**	0.313097
15853_7	1	4	n	**4.297346**	**3.172098**	2.895787	0.139251
15853_8	1	1	y	**5.678696**	**5.400244**	1.718719	0.361869
15853_9	1	4	n	**4.051844**	2.437516	**3.221826**	0.309498
15853_10	1	1	y	1.070003	0.97502	0.285529	0.335734
15853_11	3	4	n	**9.075809**	**8.845794**	2.013946	0.257402
15853_12	4	4	y	**5.882791**	**5.829833**	0.174919	0.767909
164399_1	3	2	n	**4.960498**	0.979054	**4.537478**	1.749081
164399_2	1	4	n	**5.659773**	**4.491275**	**3.205017**	1.260695

281

164399_3	4	4	y	**3.746821**	**3.725174**	0.104362	0.388405
164399_4	1	4	n	**5.825349**	**5.534751**	1.656916	0.745555
164399_5	4	4	y	**3.05885**	2.68928	1.450746	0.140266
164399_6	3	4	n	**6.175047**	**5.460359**	2.868196	0.298569
164399_7	1	4	n	**7.347608**	**6.60453**	**3.175669**	0.53166
164399_8	4	4	y	**3.605883**	2.462755	2.612553	0.334364
164399_9	1	2	n	**6.518151**	1.900991	**6.003424**	1.682683
164399_10	3	2	n	**16.11824**	**14.60111**	6.796841	0.639049
164399_11	4	4	y	2.198963	2.066045	0.386617	0.646082
164399_12	3	4	n	**3.187758**	2.485141	1.799414	0.86486
164399_13	4	4	y	1.851386	1.832252	0.257412	0.064974
164399_14	4	4	y	1.124184	0.562223	0.935554	0.269136
164399_15	1	1	y	1.489684	1.259314	0.793867	0.055315
170344_1	3	4	n	**5.847488**	3.495599	**4.470782**	1.40926
170344_2	3	3	y	**5.798474**	**5.656747**	1.036033	0.741723
170344_3	1	4	n	**3.933662**	1.197839	**3.640995**	0.884329
170344_4	4	4	y	**6.327771**	**6.101815**	1.672782	0.101696
170344_5	1	4	n	1.260197	0.580103	1.043859	0.402413
170344_6	1	3	n	**5.086359**	**5.065023**	0.387853	0.257204
170344_7	1	4	n	**8.765476**	**6.925898**	**5.349774**	0.495412
170344_8	1	4	n	2.533169	0.774414	2.211658	0.962184
170344_9	3	3	y	1.658195	1.213832	1.112488	0.196451
170344_10	4	3	n	2.954222	2.416486	1.336879	1.049179
170344_11	3	1	n	2.984328	2.787181	0.815977	0.687035
170344_12	3	1	n	1.213005	0.715654	0.959749	0.195203
23976_1	3	4	n	**5.441773**	2.39083	**4.797126**	0.94043

23976_2	4	4	y	**3.044695**	1.97594	2.241708	0.583589
23976_3	3	2	n	**13.6045**	**11.13705**	**7.764819**	0.869572
23976_4	1	3	n	**4.300029**	**4.252613**	0.633334	0.066518
23976_5	1	1	y	**3.42509**	**3.297852**	0.924118	0.037689
23976_6	1	1	y	2.343438	2.259579	0.39345	0.480833
23976_7	3	1	n	**6.405409**	**6.306412**	1.113879	0.133088
23976_8	1	4	n	0.923569	0.475386	0.788686	0.070449
23976_9	3	4	n	2.401395	1.244288	1.868969	0.851705
23976_10	1	4	n	**7.39919**	**7.376305**	0.522578	0.255075
23976_11	1	1	y	2.947191	2.768667	0.965691	0.296407
23976_12	1	1	y	1.729105	1.669196	0.371342	0.256312
23976_13	4	4	y	1.462012	1.378589	0.439629	0.209038
23976_14	3	4	n	2.923249	0.749476	2.791644	0.436337
49345_1	1	4	n	**4.829831**	1.770203	**4.49357**	0.038416
49345_2	3	4	n	**6.731163**	**6.03725**	2.975694	0.073638
49345_3	1	2	n	**4.159534**	0.03935	**4.144955**	0.345714
49345_4	4	2	n	**10.28632**	**7.332512**	**7.083995**	1.363676
49345_5	4	4	y	1.592072	1.317552	0.816605	0.363191
49345_6	1	4	n	2.435386	2.163609	1.078261	0.295383
49345_7	1	1	y	1.942944	1.86804	0.53158	0.053668
49345_8	1	4	n	**4.106097**	**4.08589**	0.329065	0.239274
49345_9	1	4	n	2.091853	1.486438	1.347345	0.592462
49345_10	1	4	n	**4.641278**	**3.968511**	2.19172	0.994359
49345_11	4	4	y	**4.386478**	**4.379126**	0.178963	0.180051
49345_12	1	1	y	0.896347	0.818942	0.362745	0.034453
49345_13	3	1	n	**4.290713**	**4.26028**	0.474672	0.186869

49345_14	4	2	n	**19.5398**	**18.97022**	2.706386	**3.822276**
49345_15	4	4	y	**3.827623**	**3.799342**	0.426396	0.184079
49345_16	4	4	y	**3.86856**	**3.846313**	0.380158	0.164677
49345_17	1	4	n	1.844774	0.954244	1.577109	0.073057
92421_1	3	4	n	2.626003	0.470601	2.580963	0.114264
92421_2	3	2	n	**9.870638**	**4.413346**	**8.801107**	0.701695
92421_3	3	1	n	2.950389	2.220093	1.943158	0.011213
92421_4	1	1	y	**3.577213**	**3.524994**	0.579996	0.185685
92421_5	1	1	y	2.833566	2.823674	0.024575	0.235276
92421_6	1	3	n	2.705201	2.639467	0.077602	0.587625
92421_7	3	3	y	**3.668897**	**3.266644**	1.538604	0.650031
92421_8	3	3	y	**4.000202**	**3.893679**	0.843587	0.359497
92421_9	3	1	n	2.276139	0.761521	2.009927	0.749057
92421_10	3	3	y	1.662932	0.050796	1.503603	0.708477
92421_11	3	4	n	**5.238696**	2.399071	**4.549013**	0.997432
92421_12	3	1	n	1.755314	0.98053	1.421183	0.316114

Appendix 4.2

Details of populations of *Auriculella* included in **Chapter 4**. Each population is listed with detailed regarded species,island, extinction tatus, chiral variation, year of collection, and number of individuals.

Population	Species	Island	Extinct/ extant	Chirally variable	Collection year	No. of individuals
12745	*A. auricula*	Oahu	Extinct	Y	1904	24
34020	*A. auricula*	Oahu	Extinct	N	1900	2
51414	*A. auricula*	Oahu	Extinct	Y	1919	36
56994	*A. auricula*	Oahu	Extinct	Y	1923	30
57018	*A. auricula*	Oahu	Extinct	Y	1900	20
109276	*A. auricula*	Oahu	Extinct	Y	1900	30
19299	*A. pulchra*	Oahu	Extant	N	1933	30
19343	*A. pulchra*	Oahu	Extant	N	1918	18
120870	*A. pulchra*	Oahu	Extant	Y	1917	30
121078	*A. pulchra*	Oahu	Extant	Y	1900	30
128374	*A. pulchra*	Oahu	Extant	Y	1916	24
132435	*A. pulchra*	Oahu	Extant	Y	1928	20
134368	*A. pulchra*	Oahu	Extant	Y	1943	30
185302	*A. pulchra*	Oahu	Extant	Y	1910	30
12934	*A. crassula*	Maui	Extant	Y	1904	40
15850	*A. crassula*	Maui	Extant	Y	1907	46
25051	*A. crassula*	Maui	Extant	Y	1900	50
25052	*A. crassula*	Maui	Extant	N	1900	40
25053	*A. crassula*	Maui	Extant	N	1900	14
a.c.m	*A. crassula*	Maui	Extant	Y	Unknown	46
15851	*A. uniplicata*	Maui	Extant	Y	1907	38
15853	*A. uniplicata*	Maui	Extant	Y	1907	24
23976	*A. uniplicata*	Maui	Extant	Y	1900	28
49319	*A. uniplicata*	Maui	Extant	Y	1920	32
49345	*A. uniplicata*	Maui	Extant	Y	1920	34
92421	*A. uniplicata*	Maui	Extant	Y	1928	24
164399	*A. uniplicata*	Maui	Extant	Y	1933	30
170344	*A. uniplicata*	Maui	Extant	Y	1935	24